Keywords:
Superconducting cables
HVDC systems
Low voltage
Systems design
Power system networks
Distribution cables

EPRI TR-103636
Project 7911-12
Final Report
April 1994

Superconducting Low Voltage Direct Current (LVDC) Networks

Prepared by
UNIVERSITY OF WISCONSIN—MADISON, Madison, Wisconsin

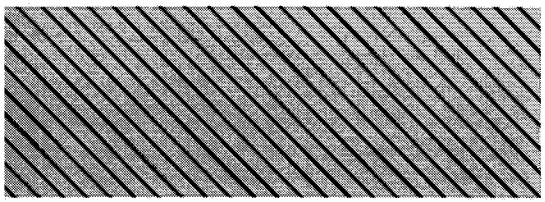

(continued on back cover)

Superconducting Low Voltage Direct Current (LVDC) Networks

A low voltage dc superconducting distribution network is a challenging future opportunity for power distribution. This report presents a scheme for a superconducting, parallel-connected, multiterminal dc transmission system.

INTEREST CATEGORIES

Underground distribution
Advanced delivery system technology
Underground cables
Power system planning and engineering

KEYWORDS

Superconducting cables
HVDC systems
Low voltage
Systems design
Power system networks
Distribution cables

BACKGROUND The discovery of high-temperature superconductivity sparked a great deal of interest in its application to power systems. Past studies of superconducting transmission have concluded that the application of superconducting materials in a power system leads to improved efficiencies and equipment size reduction in some cases. Unfortunately, system costs comparable with conventional technologies are only possible at very high power levels. The major impact of recently discovered high technology superconductors is that energy costs associated with cooling can be significantly lowered at liquid nitrogen temperature instead of liquid helium temperatures. The key question is whether the savings in refrigeration costs is enough to make high-temperature superconductors competitive with other options. The role of superconductors in bulk power transmission is to carry very large currents at relatively low magnetic fields.

OBJECTIVES To develop a scheme to control a superconducting, parallel-connected, multiterminal dc transmission system without the need for fast communication; to investigate different converter topologies for a superconducting LVDC transmission application.

APPROACH The project team reviewed the literature in the areas of advances in superconducting materials, application of superconductors for power transmission, underground cable designs, and dc converter topologies. Assuming that existing superconductors can be used to build a superconducting dc cable, the team developed a conceptual scheme for superconducting dc cable. The team demonstrated the basic concepts with a 10-terminal, mesh-connected study system. They chose a low voltage transmission level (7.5–15 kV) so that the generator could be connected directly to the rectifier without the need for a step-up transformer.

RESULTS Key results include the concept of a superconducting low voltage transmission system, a distributed voltage control scheme for parallel-connected dc systems, and a control scheme for ac systems fed by multiple inverters. The major drawbacks of a mesh-connected LVDC transmission system are additional expense, complexity, and losses in the converter. One problem faced by mesh-connected dc systems is an inability to control the distribution of current within the mesh itself. To solve this problem, a scheme using quenchable superconducting devices for current steering is presented. Fault protection is another important issue for parallel- and mesh-connected dc systems. Some form of circuit breaker is

required. The report also presents a possible design for a superconducting cable. This cable design can be implemented with either thin-film superconductors or bulk superconducting material.

EPRI PERSPECTIVE This scoping study presents a possible transmission application of high-temperature superconductors. Many different ideas are presented, and they are all tied together into a final conceptual design. Near-term applications of superconducting LVDC transmission are likely to be limited initially to simple point-to-point urban in-feeds. Eventually, upgrades would be in the form of parallel transmission paths and additional converter terminals leading to meshed superconducting systems. One of the challenging tasks for the future is development of the superconducting cable itself because the present generation of high-temperature superconductors is inadequate for power transmission.

PROJECT
RP7911-12
Project Manager: Rambabu Adapa
Electrical Systems Division
Contractor: University of Wisconsin—Madison

For further information on EPRI research programs, call EPRI Technical Information Specialists (415) 855-2411.

Superconducting Low Voltage Direct Current (LVDC) Networks

TR-103636
Research Project 7911-12

Final Report, April 1994

Prepared by
UNIVERSITY OF WISCONSIN—MADISON
Department of Electrical and Computer Engineering
Madison, Wisconsin 53706

Principal Investigators
R. H. Lasseter
F. L. Alvarado
D. M. Divan

EPRI LIBRARY

Prepared for
Electric Power Research Institute
3412 Hillview Avenue
Palo Alto, California 94304

EPRI Project Manager
R. Adapa

Power System Planning and Operations Program
Electrical Systems Division

DISCLAIMER OF WARRANTIES AND LIMITATION OF LIABILITIES

ORGANIZATION(S) THAT PREPARED THIS REPORT:

UNIVERSITY OF WISCONSIN—MADISON

Price: $5000.00

ORDERING INFORMATION

Requests for copies of this report should be directed to the EPRI Distribution Center, 207 Coggins Drive, P.O. Box 23205, Pleasant Hill, CA 94523, (510) 934-4212. There is no charge for reports requested by EPRI member utilities.

Abstract

A superconducting transmission line would allow for lossless transmission of electric power. Recently discovered high temperature superconductors can be operated at liquid nitrogen temperatures instead of liquid helium temperatures. These new materials raise the possibility of economically feasible superconducting transmission systems. This report develops a scheme to control superconducting, parallel connected, multiterminal dc transmission systems without the need for fast communication. A ten-terminal, mesh connected study system designed to run at a voltage level of 7.5-15 kV is used to demonstrate the basic concepts. The low voltage level allows the generator to be connected directly to the rectifier without the need for a step-up transformer. The report proposes using quenchable superconducting devices for current steering. A possible design for a superconducting cable is also presented that can be implemented with either thin film superconductors or bulk superconducting material.

Acknowledgements

The research project described in this report was sponsored jointly by the Electrical Power System Planning and Operations Program of the Electrical Systems Division of EPRI and the National Science Foundation.

The University of Wisconsin wishes to extend its appreciation to Dr. R. Adapa, Project Manager, EPRI. The University also wishes to acknowledge the technical guidance provided by John B. Nesbitt of Wisconsin Electric Power Co. and Kellie Peterson of Los Angeles Department of Water & Power. Their comments and suggestions during this project were important to the final outcome.

The principal investigator for this project would like to acknowledge the graduate students that spent many hours during this project to ensure its successful completion. Professor Brian Johnson, now with the University of Idaho, did most of the research related to the DC system, its control and the generator-rectifier interface. Mukul Chandorkar's research was focused on the inverter and their interface to the ac systems. Harry Singh's research was directed to the ac distribution system and the economics of the total system, Eduardo Batalla contributed in the early stages toward the cable concept and its initial design.

Contents

Illustrations

Figure **Page**

Figure **Page**

Figure **Page**

Tables

Summary

Superconducting Power Transmission

The discovery of high temperature superconductivity [1] sparked a great deal of interest in its application to the power area. A superconducting transmission line would allow for lossless transmission of electric power. Lossless transmission would help keep operating costs and thus electricity costs low. A reduction in losses will also limit fuel use by utilities and reduce air pollution. There is no need to limit transmission currents to limit resistive energy losses in the lines, allowing a superconducting transmission system could operate at low voltage levels, yielding a reduction in transformer and insulation costs for the power systems.

Past studies of superconducting transmission have concluded that the application of superconducting materials in a power system leads to improved efficiencies and equipment size reduction in some cases. Unfortunately system costs comparable with conventional technologies are only possible at very high power levels [9, 12, 25]. The major impact of the recently discovered high temperature superconductors is that energy costs associated with cooling can be significantly lowered if the cables can be operated at liquid nitrogen temperatures instead of liquid helium temperatures. The key question is whether the savings in refrigeration costs is enough to make high temperature superconductors competitive with other options [8]. The role of superconductors in bulk power transmission is to carry very large currents at relatively low magnetic fields [11].

A ten terminal, mesh connected study system is used to demonstrate the basic concepts. However, the concepts introduced can be extended to an arbitrarily large number of converter terminals. The system is be fed by three rectifiers supplying seven inverter terminals, at a voltage level of 7.5-15 kV. The low transmission voltage level allows the generator to be connected directly to the rectifier without the need for a step-up transformer. The output waveforms of the generator can be optimized to the rectifier bridge, to increase the efficiency of energy transfer. Superconducting current diverters are explored for possible applications for current steering and

circuit breaker operation. These devices are based on building a small section of the dc line with an external system to force them to quench, or cease to be superconducting.

Any implementation of an LVDC transmission system depends on the development of suitable superconducting cables. Great strides have been made in recent years. There are several different ways to utilize superconducting cables for power transmission. The first is to use bulk superconductors, extruded or deposited as a wire [26]. Much of the research in superconducting transmission systems has concentrated in this area. The present high temperature bulk superconductors suffer from one or more of the following problems: insufficient current density, the inability to carry significant current, or inability to operate at or above liquid nitrogen temperatures. Recent developments in superconducting technology are gradually working away at each of these difficulties [4]. Several processes for constructing conductors from bulk superconductors are under investigation. The powder-in-tube (PIT) process is showing good progress for superconducting cable applications. Cables capable of operating at transmission levels of magnetic fields have been constructed in 30-100 meter lengths [4], and current densities are approaching useful levels. However, fabrication costs are rather high, and the process is quite slow. Other processes are under exploration. Solid state diffusion, though limited to low current densities at present, suggests possibilities for a fast, inexpensive fabrication process that is scalable to longer lengths.

Thin film superconductor technology is closer to providing a realistic possibility of designing high power cables to operate at liquid nitrogen temperatures. Such cables are able to achieve high current levels by having several layers of thin film superconductors arranged in a cylindrical fashion. This results in a rigid, though possibly fragile cable. Recent work with thin film superconductors continues to show promise [4], although abrication costs are still high. Thin film and thick film superconductors continue to have the ability to carry higher currents in high magnetic fields than bulk superconductors [4]. This advantage continues to make them desirable for transmission applications. Depositing thin film superconductors over a large area is still difficult. However, inexpensive techniques have recently been demonstrated [4], although these are still limited to small areas. It may prove easier to deposit films for power transmission cables than it will be to improve the performance of bulk superconductors.

One advantage of the use of thin film superconductors is the ability to design coaxial superconducting cables. The radiated electric and magnetic fields would then cancel, minimizing the affects of the transmission line of the surrounding area. This design would provide for easy cooling. Coaxial cables are at a disadvantage for retrofitting present day ac systems, but would work well for long distance, high-capacity dc infeeds into urban areas using LVDC transmission through

existing corridors [4].

This report presents a design for a superconducting cable. The choice of cable design and type was made only to produce a model to use for system development. This report concentrated on system design and scoping studies. The system results do not depend on a specific type of superconducting cable.

Significant Results

This report develops a scheme to control superconducting, parallel connected, multiterminal dc transmission systems without the need for fast communication. The lossless nature of the superconducting transmission lines results in a single steady-state voltage level across the dc system. Thus dc voltage can be treated as a system-wide quantity in much the same manner as frequency is in conventional ac systems. Control can be based on dc voltage droop, similar to the way frequency droop is used in ac systems. This work presents a voltage droop scheme allowing *all* rectifier terminals to share voltage regulation, while controlling the distribution of current between them. This scheme allows each of the inverter terminals to control local power through current regulation. It also imposes current limits on the inverters to allow them to decrease demand on the dc system as the rectifier terminals approach their operational limits. The ability of this scheme to respond to disturbances is demonstrated.

One problem faced by mesh connected dc systems is the inability to control the distribution of current within the mesh itself. This is especially important for a superconducting transmission system, where it is important to keep the cables away from their current limits. A line that is restored to a superconducting state will carry no current until there is a voltage change across it, since all of the terminals on the system will have equal steady-state voltages. A scheme utilizing quenchable superconducting devices for current steering is presented. This scheme is able to transfer small blocks of current out of a line through the alternate pulsing of parallel devices in a single line. The diverter limits the section of superconductor that quenches to a small area, making it easier to have increased refrigeration at that location. This scheme will result in energy dissipation whenever the device is activated, but this is very small compared to the total energy transferred.

Fault protection is another important issue for parallel and mesh connected dc systems. Some form of circuit breaker is required, ideally one that is superconducting when not in use. A superconducting circuit breaker based on a current diverter is explored.

The LVDC transmission system developed here is capable of supplying passive ac systems, as well as both strong and weak ac systems. This requires and inverter that is capable of controlling both the magnitude and phase of the ac voltage or current injection into the ac system. Controlling these two quantities is analogous to controlling real and reactive power. The ability to provide both a leading or a lagging phase angle on the injection requires a self-commutated inverter. The low voltage level (in the 10 to 15 kV range) would allow for inverters based on six-pulse bridges without the need for series connected devices. The typical inverter station could have two of these bridges in series, and several of these modules connected in parallel to meet the current loading. Controlling the magnitude of the injection mandates either a pulse width modulation scheme or a system with multiple inverter modules phase shifted with respect to each other. The multi-inverter module scheme has the advantage of substantially lower switching losses than would be present with a pulse-width modulated systems. A large ac system may have multiple inverter terminals supplying it from distant locations. It then becomes important for these inverters to be able to share the real and reactive power loading between them. A control scheme based on frequency and voltage droop has been developed for this purpose.

The low dc voltage levels allow a much simpler connection at the rectifier terminals. The basic rectifier terminal will consist of a set of parallel connected modules, with each module needing to have only a single thyristor on each leg. The low voltage level eliminates the need to connect devices in series to achieve high voltages. The transformer connection from the ac system is also much simpler. Generator stations that supply no local ac load, and only supply the rectifier can be connected directly to the rectifier bridge, without any added transformer. Such a generator could be optimized to rectifier operation to improve the efficiency. This optimization is achieved through matching the voltage waveshapes to the current waveforms, thus transferring useful energy via the harmonics.

Near term applications

The complete LVDC transmission system described here is a possible end result after decades of growth. Superconducting power transmission will be added gradually to work in concert with the present ac transmission grid. A likely near term application would be a high capacity infeed into an urban area. The infeed may initially be a point to point dc system. The infeed could follow an existing transmission corridor. However, the dc line could have much greater capacity than the conventional ac line it would replace. The system will be upgraded through the addition of parallel

inverter taps along the line, and possibly additional rectifier taps. The control scheme introduced in this report does not suffer from control problems with these parallel taps as present systems do. Other lines would be added to the system, and eventually a multiterminal dc system would be constructed. The LVDC system will then eventually replace the conventional ac transmission as it replaces ac lines by following the same corridors.

Spin off's

The goal of the work presented in this report was to develop a conceptual design for a superconducting power transmission system. Some of the issues that came up in this process suggested solutions for other problems in the power distribution area.

The LVDC system is capable of supplying passive ac systems. These systems have no local power generation for line commutated inverters, requiring the use of self-commutated inverters. Particularly large passive systems may be supplied by several inverter stations connected at different points in the system. The inverters must be able to coordinate the sharing of real and reactive power without needing to depend on fast communication, similar to the generator stations on a conventional ac power system. The control scheme developed here, based on frequency and voltage droop, can also be applied to paralleling of uninterruptible power supply (UPS) systems for commercial and industrial applications.

The overall control scheme developed for the dc transmission system can also be extended to other applications as well. Control is based on a distributed voltage regulation scheme using the concept of droop. The scheme used for LVDC systems benefits from the lack of resistive voltage drops across the transmission lines. However, this concept can be extended to other cases as well. The voltage droop scheme needs to be modified to operate in a conventional transmission or distribution system, since compensation for resistive voltage drops requires the knowledge of the approximate voltages at the other terminals. Knowledge of the voltage at the other terminals requires either communication, or a system of observers. Large, geographically spread out HVDC systems would require observers to allow operation without dependence on communication in emergency situations. The voltage droop scheme can be applied to industrial power systems where the converters are be close together, allowing reliable communication. It may also be possible to apply the voltage droop scheme to light rail transit systems where the load is not only variable, but also moving around the system.

Conclusions

The key results of this project include: the concept of a superconducting low voltage transmission system, a distributed voltage control scheme for parallel connected dc systems, and a control scheme for ac systems fed by multiple inverters. A possible design for a superconducting cable was also presented. The design utilizes one conductor of a coaxial cable for each pole of a bipolar dc system. This will reduce the radiated fields, and result in a simple easy to cool cable design. The cable design presented here can be implemented with either thin film superconductors or bulk superconducting material.

The major draw backs of a mesh connected LVDC transmission system comes in the form of additional expense, complexity, and losses in the converters. There will also be harmonics on both the ac and dc sides of the converters. The dc side harmonic currents will result in some hysteresis losses in the superconducting material. In contrast, ac superconductors suffer from hysteretic losses at the fundamental frequency that could be large enough to make dc transmission cost effective for longer distances and higher power levels.

This report presents a scoping study a possible transmission application of high temperature superconductors. Many different ideas are presented, and they are all tied together into a final conceptual system design. Near term applications of superconducting LVDC transmission transmission are likely to be limited initially to simple point to point urban infeeds. Once this occurs, it is likely that these systems would then be upgraded by the addition of parallel rectifier and inverter taps. Eventually, upgrades would be in the form of parallel transmission paths and additional converter terminals. This leads directly and naturally to the meshed superconducting systems that are the subject of this report.

Chapter 1

Introduction

The discovery of high temperature superconductivity [1] sparked a great deal of interest in its application to the power area. One such application, low voltage power transmission, is likely to yield a major reduction in system costs. There is no need to transmit power at high voltage levels to reduce currents to minimize resistive losses when superconductors are used. The transmission system can then operate at a single voltage level from generation to distribution systems. This eliminates the need for high voltage insulation and large transformers, in addition to the removal of I^2R losses from the transmission system.

The use of ac transmission with high temperature superconductors involves hysteretic losses in the superconductor and eddy current losses in the copper or aluminum matrix surrounding the superconducting material. This restricts the ac current levels to one-tenth the critical current densities for acceptable levels of ac losses. In addition, the superconducting cables would be restricted to the same kind of length restrictions that apply to conventional ac cables.

The use of a low voltage dc (LVDC) superconducting transmission system eliminates the problem of ac losses, but replaces it with other system issues. These relate primarily to the distribution of steady state and transient currents in the dc mesh [33], system protection, and power conversion issues.

The ac system views the dc mesh as a system capable of delivering power from the generation site to the distribution substation without transmission losses. All nodes in the dc system are at the same voltage due to the lossless transmission lines. The dc voltage level is maintained by

voltage control at one or more of the rectifier terminals. Thus voltage on the dc mesh is a system-wide quantity in much the same way as frequency is in conventional ac systems. Control can be based on the dc voltage droop in the same manner as ac systems are controlled using frequency droop.

Interfacing the superconducting LVDC system with the ac system involves some interesting issues relating to the choice and control of converters. Direct connection of the unit connected generators to the rectifier bridges allows for interesting options in the design of both generators and rectifier bridges.

The study of superconducting LVDC power transmission systems can be broken down into three basic areas: 1) the dc mesh with unit-connected generators, 2) the ac load system, and 3) the dc/ac inverter interface.

1.1 The Study System

The small system used for scoping studies on superconducting LVDC systems [33] does not have sufficient complexity for developing an overall operating scheme scheme for general LVDC systems. This section provides an overview of the study system used throughout this report. The basic design concepts used here can be generalized for use with any LVDC system. A ten terminal study system has been developed that incorporates generator models, a mesh with multiple rectifiers, and multiple ac load systems. The study system will operate with a dc voltage level of ± 7.5 kV, with generation totalling 360 MVA.

The superconducting cables used for the study system are been based upon a coaxial cable constructed using thin film high temperature superconductors. Section 2 provides a general discussion on superconducting cables. Thin film superconductors are utilized for this preliminary study due to their greater current densities compared to bulk superconductors at the outset of the project. However, the concept introduced here can be applied to a transmission system using either bulk or thin film superconductors. The coaxial cable design shown in Figure 2.3 was chosen for its current carrying capability, low external fields, and ease of cooling. The low voltage levels possible with superconducting transmission allow bipolar operation using a coaxial cable to provide the two poles. This essentially eliminates the radiated fields from the cables.

1.1.1 Generator Configurations

The presence of the dc transmission system allows freedom in the design and connection of ac supply systems to the dc mesh. The use of the dc system to replace the ac transmission and subtransmission systems will result in generating stations that do not supply local loads. This is often true since many generating stations are distant from the load centers on the ac grid. This will result in unit-connected generators that feed only the rectifier station, and no other load [47, 48].

The low transmission voltage eliminates the need for step-up transformers to interconnect the generator to the mesh. The dc voltage level is kept at a level compatible with generator output voltages. The generators will be connected directly to the rectifier bridges, without any interconnecting transformer. The direct unit-connection of the generator to the rectifier allows a great deal of freedom in the design and operation of the generator. The generator output will not need to be synchronized to an ac system, making generator control somewhat easier, and also allowing the generator to operate at the optimal speed of the prime mover. This asynchronous connection allows the possibility of variable speed operation.

Direct generator-rectifier connection requires a six-phase generator to implement a twelve-pulse converter bridge for harmonic reduction. A six-phase generator can be implemented by placing two three-phase sets of windings on the generator stator [52, 53]. These two sets are then offset by 30° for twelve pulse operation. The direct connection of a single generator to a bipolar rectifier terminal also poses some problems. The neutral points of the winding sets feeding positive pole of the bipole will experience a dc offset equal to one-half of the dc voltage. The negative pole will experience a similar offset of negative one-half the dc voltage. This offset requires isolation of the winding sets for each pole of the rectifier, even if they are in phase with each other. A double six-phase generator with no phase shift between the two six-phase sets is needed to prevent difficulties from this offset. The neutrals of the two six-phase sets can only be interconnected via a large resistance to prevent large dc current flows between them. Initial examination of the study system will utilize six-pulse bridges to simplify the simulations. The rectifier terminal will consist of bipolar modules connected in parallel to increase the current supplied by the terminal. Figure 1.1 shows the configuration for a six-phase generator with four six-pulse modules connected in parallel. The three-phase sets supplying each pole are in phase with each other.

The output waveforms of the generator can also be optimized to the rectifier. The bridge will

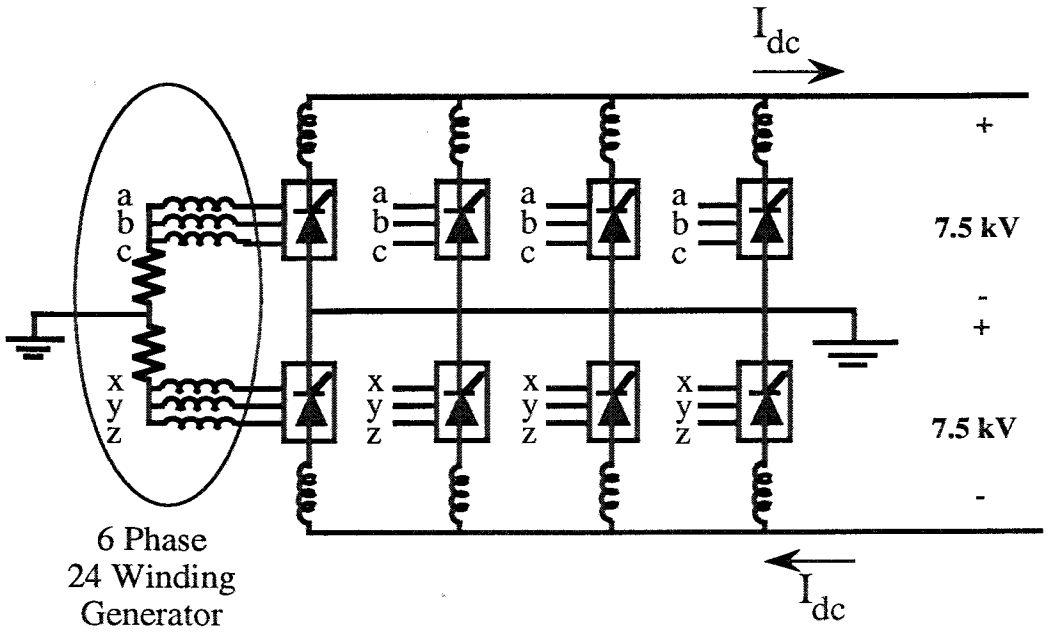

Figure 1.1: Direct Connected Six-Phase Generator-Rectifier Pair

draw trapezoidal current waveforms from the generator, which when coupled with the sinusoidal output voltage waveforms of the conventional generator result in substantial harmonic losses in the power transfer. However, a generator supplying trapezoidal voltage waveforms would be able to increase the efficiency of the power transfer up to 15% [63, 64]. This will require modification of the generator stator and rotor configuration. This converter optimization of the output waveforms is only possible in the case with direct unit-connection of generators.

1.1.2 The DC Mesh

A typical LVDC transmission system will consist of tens of rectifiers feeding perhaps hundreds of inverter terminals. The study system used to test the operation and control concepts for LVDC transmission should consist of multiple rectifier terminals feeding a meshed system to provide sufficient complexity. The system will in turn supply a large number inverter terminals, possibly hundreds. The ten terminal system shown in Figure 1.2 was designed to serve as a testbed for the concepts of the LVDC mesh. The figure shows the positive pole of the dc system.

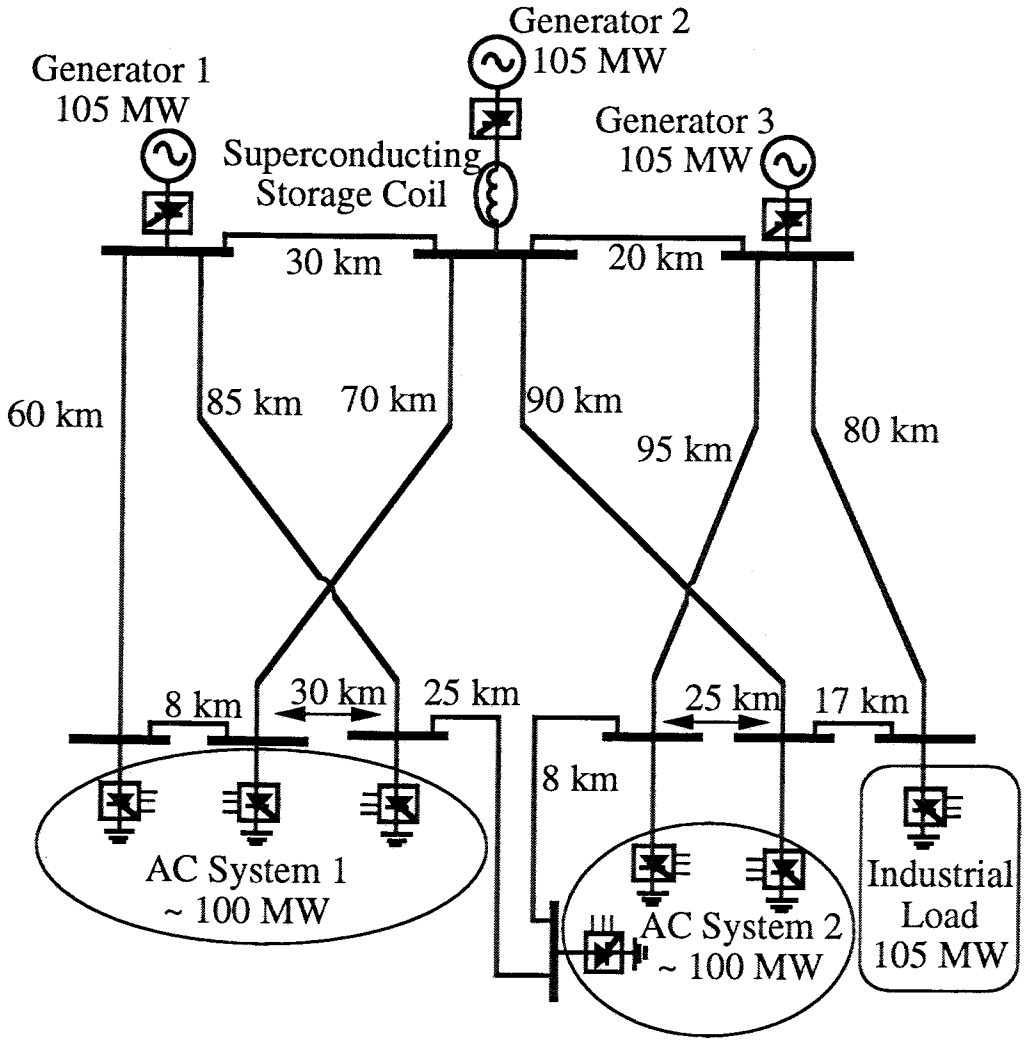

Figure 1.2: Ten Bus LVDC Test System, with SMES Coil

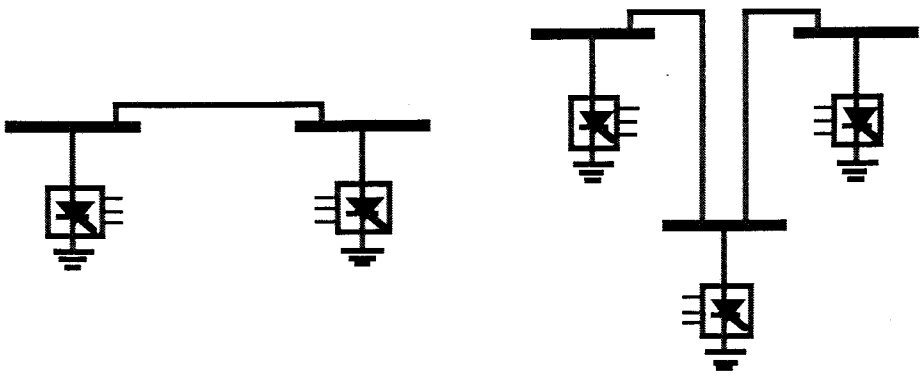

Figure 1.3: Scheme for creating a new inverter node on the mesh

This system is supplied by three rectifier terminals, each fed by a 120 MVA unit-connected generator. The mesh feeds seven inverter terminals, ranging from 30 MW to 105 MW. The largest inverter feeds a large industrial load, while the smaller inverter terminals feed ac distribution systems. Each of the inverter terminals features a modular design allowing for simple design and construction of the inverter terminals.

This system is designed so that each inverter terminal will have two connections to the dc mesh, one of which will be a long line connecting to one of the rectifier terminals. The second connection at each inverter will serve to interconnect the station with another inverter terminal. The limited number of connections reduces the total number of superconducting lines that need to be built while maintaining adequate reliability through redundant paths. The interconnection of small sets of inverter terminal, rather that large groups serves to isolate the inverters in one set from a disturbance on the other set. Further terminals can be interfaced to the mesh by tapping off of the mesh at some point on the existing system as shown in Figure 1.3. Each of the rectifier terminals will have several connections feeding inverter terminals, as well as lines that interconnect the rectifier terminals for added reliability.

1.1.3 AC System and Loads

The mesh connected LVDC system will be capable of supplying a large number of isolated, asynchronous ac loads. The study system utilized here will supply power to two small ac systems. Each system will have roughly the same topology, with a total load of around 100 MW. Both are

urban distribution systems, but will have a few motor loads. The mesh will also feed a 105 MW industrial load. This load will consist primarily of motors, but the details of the individual motors and any static power conversion devices will not be modeled at this time.

Several different variations will be considered for the ac systems. One configuration will have each inverter feeding a passive ac distribution system. This system will have a radial connection. Each of the two ac systems will be divided into three radial systems that can be interconnected under emergency conditions. Figure 1.4, shows the layout for the ac study system. The inverters are located at buses 660, 661, and 662. A second option features radial ac distribution systems, but also has a 69 kV ac bus connected interconnecting the ac systems with a larger ac power grid. This will be a strong ac system. The radial systems can be connected to this bus via ac breakers. It will then be necessary to synchronize the distribution system to the ac bus before the breaker is closed.

1.1.4 The Inverter Interface

The inverter terminals for the study system will have a power ratings ranging from 30 MW to 105 MW. The inverters will utilize self commutating switches to provide the ability to supply passive ac systems. A current capacity of one thousand amps is assumed for the self-commutating switches. Ideally, these converters could be implemented without the need to connect devices in series. The low dc voltage levels already make this possible with thyristors, and this may soon be true with self-commutating switches. Coupling this with the line to line dc voltage of 15 kV limits the module rating to 15 MW.

Each inverter terminal will require at least three of these modules connected in parallel for added reliability. Each of the modules should have a 50% over current rating to allow the terminal to operate at full power with one of the modules off-line. The design for these modules should be standardized, so these could be thought of as low cost, 'off the shelf modules.' Therefore, the 30 MW converter stations, will have three 10 MW modules present, while a 45 MW converter terminal will have three 15 MW modules.

Two major families of inverter types will be considered. First will be dc voltage source inverters. This inverter will be seen be the ac system as a voltage source with a controllable phase angle. The inverter designs considered here will also be able to control the magnitude of the ac voltage

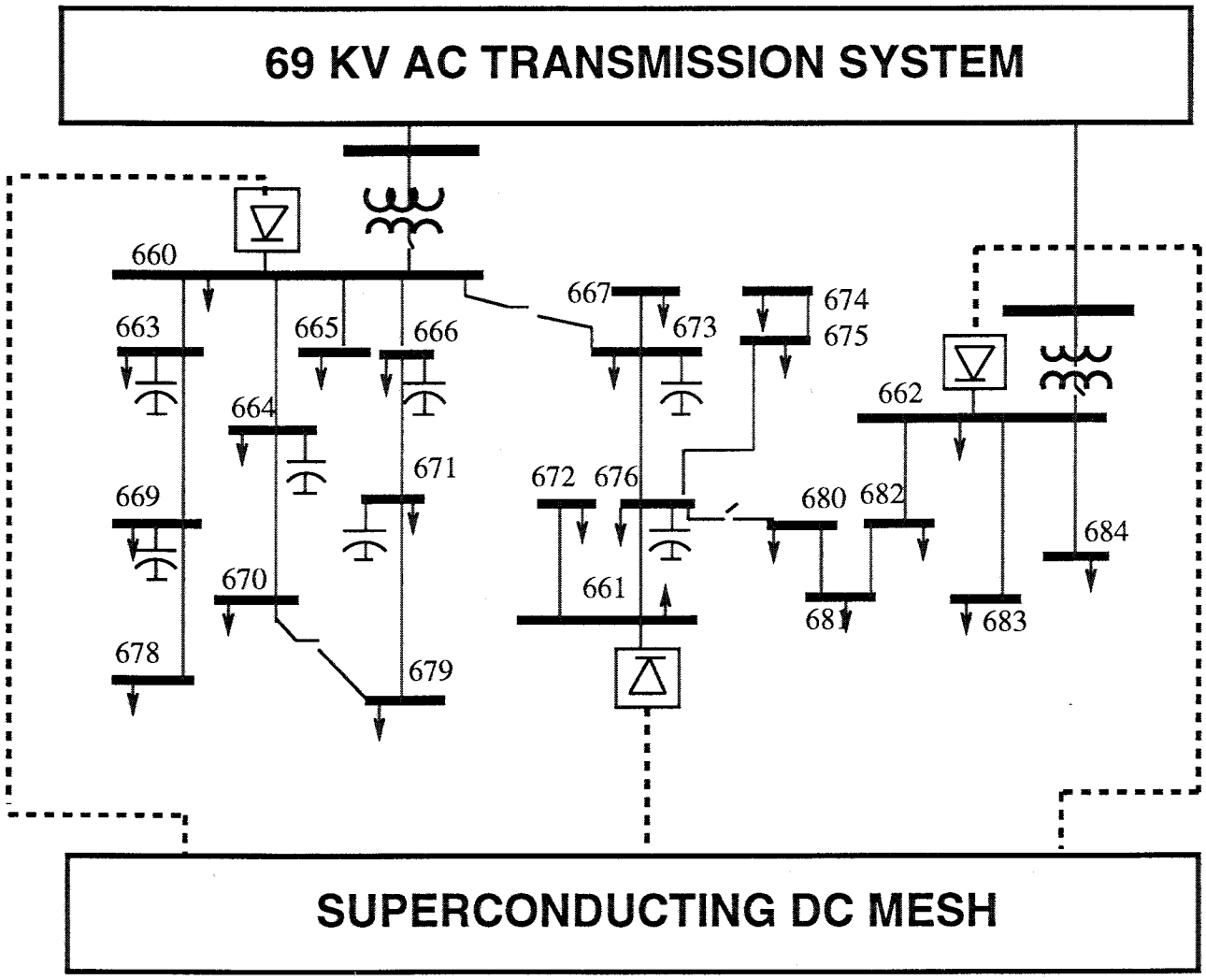

Figure 1.4: AC system layout, includes 69 kV ac bus.

either through the control scheme used, or by the inverter topology. The second converter family consists of dc current source inverters. A current source inverter appears to the ac system as a controlled current injection that is able to regulate its phase angle relative to the ac system. Again, it is possible to develop topologies and/or control scheme that are able to control the magnitude of the current as well. The inverter designs will be tested with the system to see which performs the best from the point of view of the ac system and the dc system.

Chapter 2

Superconductors For Power Transmission

Past studies of superconducting transmission have concluded that the application of superconducting materials in a power system leads to improved efficiencies and equipment size reduction in some cases. Unfortunately system costs comparable with conventional technologies are only possible at very high power levels [9, 12, 25]. The major impact of the recently discovered high temperature superconductors is that energy costs associated with cooling can be significantly lowered if the cables can be operated at liquid nitrogen temperatures instead of liquid helium temperatures. The key question is whether the savings in refrigeration costs is enough to make high temperature superconductors competitive with other options [8]. The role of superconductors in bulk power transmission is to carry very large currents at relatively low magnetic fields [11].

2.1 Properties of Superconductors

Superconductivity is a phenomenon that causes certain metals or alloys to suddenly lose all electrical resistance when their temperature is lowered to near absolute zero. An essentially perpetual current can be induced in a loop of such material. This phenomenon is accompanied by marked changes in the magnetic properties of the material. There are two types of superconductors, which differ in their conduction properties.

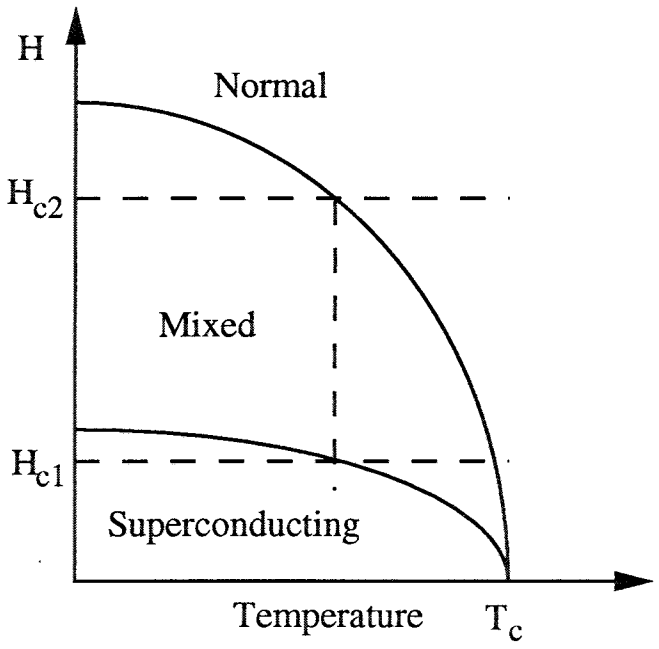

Figure 2.1: Superconductor Phase Characteristics

Type I superconductors operate at low magnetic fields, below their bulk critical field (H_{c1}), as shown in Figure 2.1. All magnetic flux is excluded from the interior of the superconductor at low fields, exhibiting perfect diamagnetism. This is called the Meissner effect. Not only do superconductors exhibit zero resistance, but they spontaneously expel all magnetic flux when cooled through the superconducting state transition [6]. This condition persists until the field, H, is increased (at constant temperature) to the bulk critical field, where flux penetrates into the bulk material [14]. Type I superconductors pass into the normal state at this critical field. This is also known as quenching. Type I superconductors are not attractive for most power applications due to their low current densities and low critical fields [24].

Type II superconductors exhibit the Meissner effect in a range of field strengths. This range does not extend to the bulk critical field. These materials tend to remain superconducting in high fields, even those above their bulk critical field. They are completely diamagnetic up to the lower critical field, H_{c1}, above which its magnetism rapidly diminishes [24]. The quenching of superconductivity in Type II material at T_c is associated with the magnetic field H, which can arise from the magnetic field induced by the current, can be produced by an applied field, or can result from a combination of self and applied fields [14].

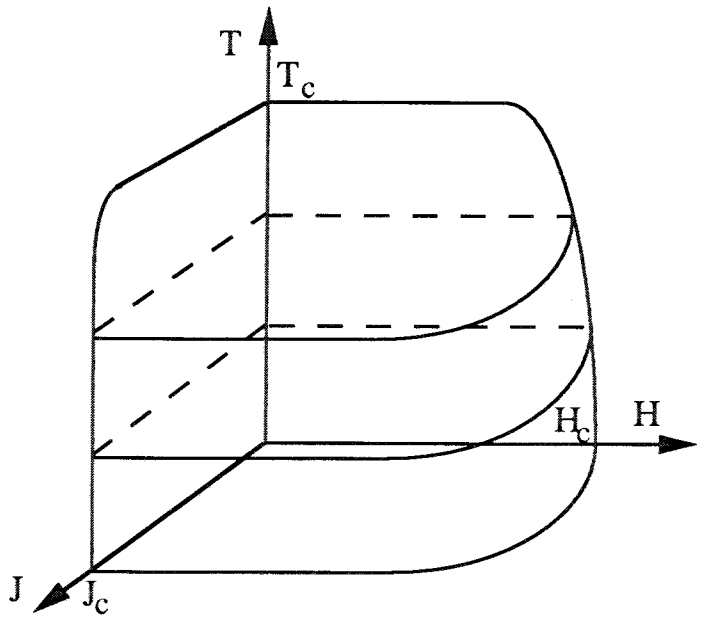

Figure 2.2: Superconducting Phase Transition Diagram

Type II superconductors operate between H_{c1} and H_{c2} in what is called the mixed region, where flux enters the superconductor. Non-oscillatory transport currents continue to flow without resistance in the mixed region [14]. The current density, J_c, is not an intrinsic property of the superconductor like T_c and H_c, instead it is a structurally dependent parameter [18].

Superconductors differ from ordinary or normal conductors in having zero resistivity under certain conditions of magnetic field, temperature and current density. A phase diagram for superconducting state transitions showing relationships between current density (J), temperature (T), and magnetic field (H), is shown in Figure 2.2. Notice the tradeoffs in temperature and field needed to operate with high currents densities. The critical current density can be taken as a single valued function of temperature and applied field for most superconductors of practical interest.

2.2 Liquid Nitrogen Coolant

Widespread use of large-scale superconducting devices is unlikely to be based on refrigeration with liquid helium due to refrigeration and insulation costs [12]. Technical developments allowing

delivery of helium at prices low enough to make superconducting devices economically attractive are not likely to occur in the near future. However, many large-scale superconducting applications could become cost effective using liquid nitrogen, which is more abundant and easier to handle than helium.

The present applications of superconductivity utilize liquid helium superconducting technology. A switch to liquid nitrogen temperature operation would not represent a revolutionary benefit but rather an incremental one. Liquid nitrogen operation lowers capital costs, decreases complexity, and increases reliability. The largest savings are expected for those applications where helium cooling is the main expense [18].

Temperature increases due to resistive losses limit the capacity of conventional underground cables. Low voltage-high, current transmission is not a problem using superconducting cables, since there are no resistive losses. Liquid nitrogen-cooled cables can be made smaller than conventional cables. Smaller cable sizes will significantly reduce construction costs, since tunnel and duct construction account for a large share of construction cost in an underground cable [16]. The higher heat capacities possible with liquid nitrogen cooled cables also will limit the spreading of normal sections in a cable [4]. However, this also means that the heat dissipated in a normal section will be concentrated in a smaller area, increasing the possibility of damage.

2.3 Comparison of DC and AC Cables

Type II superconductors are used in cable design because of their high current and flux density capabilities. However, these superconductors have losses in the presence of time varying fields. The electrical losses are not zero in a superconductor in ac operation. These losses amount to a refrigeration load roughly equal to the heat leak from the outside environment to the superconductor, doubling the refrigeration load. The electric power required to operate the cryogenic refrigerators should be considered as a system loss.

The cost per unit length of a superconducting dc cable (including enclosure and refrigerator) is generally less than the cost per unit length for an equivalent ac cable [15]. A dc system has added costs due to the power converter costs and losses. The converter cost is independent of line length for HVDC transmission systems [36]. HVDC system costs are equal to the costs for

equivalent ac systems for lines about 300 miles in length (and cables about 30 miles in length) using conventional conductors. The costs of ac systems are greater than those for HVDC beyond this point due to the need for compensation [36]. This breakeven distance will probably decrease for superconducting transmission systems.

2.3.1 Operational AC Losses

Losses in ac superconducting cables are due to hysteresis in the superconductor, heat leak, and dielectric losses. Although superconductors are loss-free under dc currents and fields, time-varying magnetic fields will set up an electric field within the superconductor which dissipates heat when it is in phase with the current [19].

An electric field within the material tends to drive the superconductor above its critical current. The superconductor responds by developing a resistance (called the flux flow resistance) which exactly offsets the electric field and maintains the current density at just above its critical value. The loss mechanism is resistive in nature. This resistance is highly nonlinear and the losses are hysteretic in nature. This results in a constant loss per cycle independent of the cycle time [19]. The critical current density is quite low for the new high temperature superconductors so the AC power loss in these materials are higher than those with low temperature superconductors [3].

2.3.2 Operational DC Losses

Although there are no losses due to pure dc currents, harmonic currents produced by the converters will cause steady-state power losses in the conductor, requiring the refrigeration system to supply additional cooling power to compensate for these losses. The dc side harmonics may impose some restrictions on a dc system because of their effects on the hysteresis losses in the superconductor. These harmonic losses are lower than those with ac transmission [7]. The dc system also experiences additional losses due to losses within power converter.

2.4 Low Voltage DC Transmission Systems

The use of superconducting cables provides opportunity for radical departures from the norm in the design of power transmission systems. There is no longer a need for high voltage, low current transmission to reduce resistive energy losses on the transmission system. The transmitted current levels are instead limited by the capacity of the cables. The elimination of resistive losses permits the use of low voltage, high current transmission. Table 2.1 compares different options for the superconducting transmission systems. Note that ac losses are significant with high temperature superconductors. These results suggest that low voltage dc (LVDC) transmission is the most promising option for superconducting power transmission.

The use of LVDC transmission provides flexibility in the design of a superconducting transmission system. The dc voltage level can be chosen to allow the generators to be connected directly to the rectifier bridges, without an intermediate transformer stage. The voltage level can also be chosen to minimize or eliminate the need to connect power electronic devices, or even converter bridges in series. This results in clean, simple converters. The system can then feed directly into ac distribution systems, with small transformers to help isolate the loads from the inverters.

Initial applications of superconducting transmission systems will probably be in the form of point to point dc systems entering an urban area that has insufficient transmission capacity, and is this transmission limited. This system can later be expanded by adding parallel taps to this system. Parallel taps are preferred over series connections due to the high current levels, and thus higher converter losses that result. Later expansions of this scheme would involve adding parallel transmission paths to form a mesh connected system. A mesh connected system has the advantage of having parallel transmission paths, so the system does not need to shut down due the loss of a single line.

2.5 Superconducting Cable Options

There are several different ways to utilize superconducting cables for power transmission. The first is to use bulk superconductors, extruded or deposited as a wire, perhaps on a substrate [26]. Much of the research in superconducting transmission systems has concentrated in this area. The present high temperature bulk superconductors suffer from one or more of the following problems:

ADVANTAGES	DISADVANTAGES
Alternating Current	
Generators and load designed for ac	Higher losses than dc (Excluding conversion loss)
Transformers and circuit breakers available	Less efficient use of conductor volume compared to dc
Wide familiarity in the utility industry	Cable length restrictions
Superconducting cables can be designed for surge impedance loading	
Direct Current	
More efficient use of conductor	Cost and losses of AC-DC-AC conversion
Low cable losses	Limited availability of circuit breakers
Asynchronous tie provides more control of power flow	
LVDC (typically 15 kV and 50 kA)	
Transmission line connects directly to generator	High fault currents
Converter optimized generators possible	High heat in-leak at the terminations
Savings in electrical insulation	Limited availability of circuit breakers
Elimination of transformer stages	
Coaxial cables possible	

Table 2.1: Electrical Options with Superconducting Cables [10, 27]

insufficient current density, the inability to carry significant current, or inability to operate at or above liquid nitrogen temperatures. Recent developments in superconducting technology are gradually working away at each of these difficulties [4]. Several processes for constructing conductors from bulk superconductors are under investigation. The powder-in-tube (PIT) process is showing good progress for superconducting cable applications. Cables capable of operating at transmission levels of magnetic fields have been constructed in 30-100 meter lengths [4], and current densities are approaching useful levels. However, fabrication costs are rather high, and the process is quite slow. Other processes are under exploration. Solid state diffusion, though limited to low current densities at present, suggest the possibilities for a fast, inexpensive fabrication process that is scalable to longer lengths.

Thin film superconductor technology is closer to providing a realistic possibility of designing high power cables to operate at liquid nitrogen temperatures. Such cables are able to achieve high current levels by having several layers of thin film superconductors arranged in a cylindrical fashion, as will be described below. This results in a rigid, though possibly fragile cable. Recent work with thin film superconductors continues to show promise [4], although fabrication costs are still high. Thin film and thick film superconductors continue to have the ability to carry higher currents in high magnetic fields than bulk superconductors [4]. This advantage continues to make them desirable for transmission applications. Depositing thin film superconductors over a large area is still difficult. However, inexpensive techniques have recently been demonstrated [4], although these are still limited to small areas. It may prove easier to deposit films for power transmission cables than it will be to improve the performance of bulk superconductors.

One advantage of the use of thin film superconductors is the ability to design coaxial superconducting cables. The radiated electric and magnetic fields would then cancel, minimizing the affects of the transmission line of the surrounding area. This design would provide for easy cooling as is discussed with the designs presented below. Coaxial cables are at a disadvantage for retrofitting present day ac systems, but would work well for long distance, high-capacity dc infeeds into urban areas [4] using LVDC transmission through existing corridors.

2.5.1 Conceptual Designs for Superconducting DC Cables

Thin film superconductors show promise for near-term application of high temperature superconductors for bulk power transmission. A cable made up of superconductors used in the form of

thin surface layers will need a layer copper acting as a substrate and as a parallel conductor. This arrangement is needed for structural reinforcement and electrical stabilization. A superconducting thin film can be fabricated by sputtering or by plasma plating. The copper substrate must be able to carry the total current if the superconductor quenches, this including high fault currents if quenching occurs under fault conditions.

The cable structure will feature a coaxial geometry, with one pipe acting as the return conductor. External electromagnetic fields can be eliminated from the cable by this arrangement, and using one conductor for each pole of the LVDC bipole. Cylindrical symmetry also minimizes surface current densities in the superconducting layers [21]. A rigid coaxial conductor configuration is chosen for the conceptual design.

There is a factor-of-ten increase in the electrical conductivity of electrical wire grade copper at liquid nitrogen temperature. This permits operation of these cryostabilizers at high current density with small electrical losses [22].

2.5.2 A Superconducting Transmission Line Using Liquid Nitrogen as a Coolant and a Dielectric

Liquid nitrogen has potential for use as a dielectric in cable and other types of apparatus. The voltage breakdown level is relatively high for liquid nitrogen when compared to liquid helium. A high voltage breakdown level is essential for dc transmission applications.

The refrigeration system must be able to cool the conductor down after it has quenched. This is important for having a stable superconducting cable. The recovery process is a thermodynamic process and depends on the following [11]:

- The excess cooling capacity available in the cooling medium
- The heat transfer coefficients
- The total amount of current
- The resistivity of the normal conductor (which is copper for our case)

Outer radius inner conductor	5.505 cm
Inner radius outer conductor	6.005 cm
Outer radius outer conductor	6.010 cm
Insulation dielectric constant	2.1518
Cable current rating	50 kA
Inductance per unit length	17.4 $\mu H/km$
Capacitance per unit length	13.6 $\mu F/km$
Propagation velocity	2.042 x $10^8 m/s$
Characteristic impedance	3.556 Ω
Self magnetic field (B)	0.18 T

Table 2.2: Cable Parameters for the Cable Shown in Figure 2.3, computed in [27]

The copper substrate also prevents burnout of the superconductor from transient effects (current spikes, sudden changes in flux), [14]. Use of liquid nitrogen as an insulator shows promise. Its breakdown strength is comparable with those of insulating liquids. However, it may be susceptible to bubble formation, which could lead to inconsistent insulation properties [22].

A conceptual design using liquid nitrogen as both coolant and dielectric is shown in Figure 2.3 [27]. It will be necessary to install bellows and use materials with low thermal contraction coefficients to accommodate cable contraction during cool-down. The superconductor is in the form of thin surface layers, 25-50 microns thick with a normal metal acting as a substrate. The cable is designed to operate at 50 kA at 5 GW. The inner conductor has an inner diameter of 10 cm, with a 0.5 cm copper substrate. The outer conductor has a 2 mm-thick copper substrate. There is also a 1 cm open annulus for the refrigerant flow. The return path of the refrigeration and pumping station is through the innermost pipe. The electrical parameters for the cable shown in Figure 2.3 are described in Table 2.2.

Figure 2.4 shows system startup for a simple dc system using this cable design. The figure shows the results when detailed distributed parameter cable models are used. The system was driven to a steady-state with each of the three lines carrying 4 kA. Figure 2.4(a) shows the bus voltages during the start up. There are a lot of voltage fluctuations initially due to traveling voltage waves. These are eventually damped out by the terminating impedances at the buses. There are no losses in the cables themselves to help damp out transients due to the superconductors. The ac losses

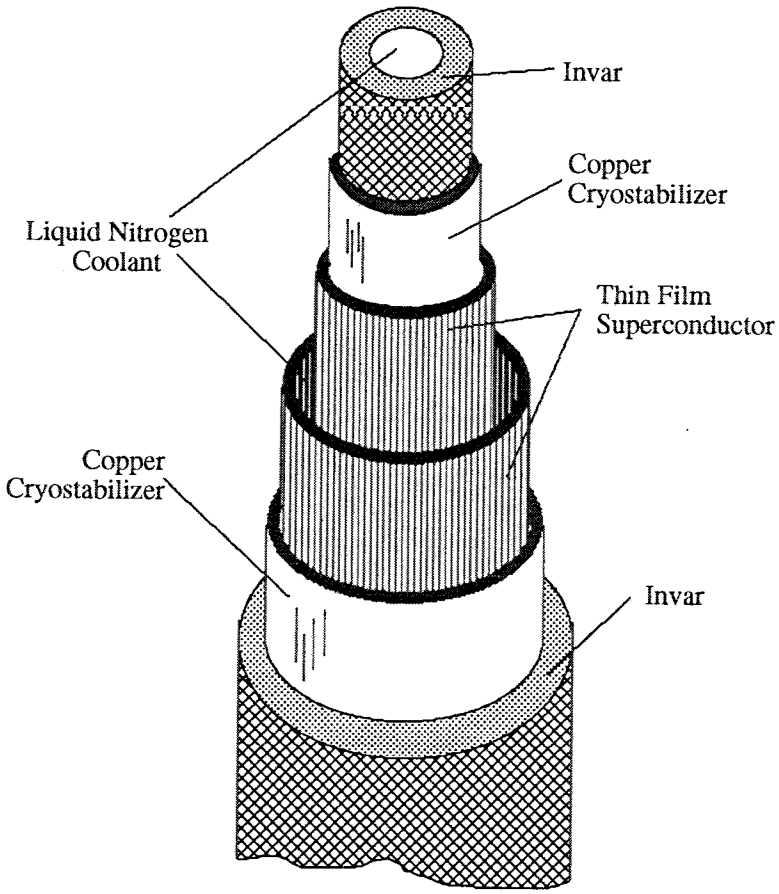

Figure 2.3: Coaxial Superconducting Cable with Liquid Nitrogen Coolant

and the frequency dependence of the superconductors are not modeled here. Figure 2.4(b) shows the line currents. There are some traveling waves on the current initially, but these are quickly damped out. The variations in the inverter currents are due to both the voltage fluctuations at the inverter buses and the changes in the branch currents. Figure 2.5 show the terminal voltages and line currents when a simple lumped inductor model is used. Figure 2.5(a) shows the terminal voltages, while the part (b) of the figure shows the line currents. These results demonstrate that the simple lumped inductor model is adequate for the studies that are performed in this thesis.

2.5.3 DC Superconducting Transmission Line Using a Polymide Film Dielectric and Liquid Nitrogen as Coolant

Instead of using liquid nitrogen as a dielectric, the superconducting shell in now covered with about 3 mm of Kapton (tradename for polymide film). Polymide film possesses a unique combination of properties. It does not melt. It maintains its electrical and mechanical properties over a wide temperature range. It has been used from 4 K to 127 K, making it suitable for operation liquid nitrogen temperatures. No organic solvents are known. As the temperature is increased or decreased, the polymide film characteristics are less affected than those of polyester films [17]. The dc breakdown strength of polymide-Kapton is about 2.4 MV/cm [22].

The conceptual design for the second dc SPTL is shown in Figure 2.6. The inner conductor is nominally a 10-cm (inner diameter) copper tube of about 0.5-cm wall thickness. There is about a 50 micron layer of sputtered superconducting film on the outside surface of the copper cryostabilizer. This superconducting shell is covered with about 3 mm of Kapton, which is surrounded by another copper cylinder of 2-mm thickness, this being coated with a second 50 micron layer of sputtered superconducting film. An open annulus of about 1 cm is then allowed for cryostat (liquid nitrogen) flow. Subcooled liquid nitrogen is pumped through this annulus. The return path of the refrigeration and pumping station is through the innermost pipe. The whole configuration is wrapped with a 5-cm layer of superinsulation to serve as a cryogenic enclosure.

The cable is designed to operate at 50 kA at 5 GW. The inductance per unit length of the proposed configuration is computed to be at $17.41\mu H/km$. The dielectric constant for polymide film at liquid nitrogen temperature is 2.92 to 3.15. This leads to a computation of a capacitance per unit length of $1.38\mu F/km$.

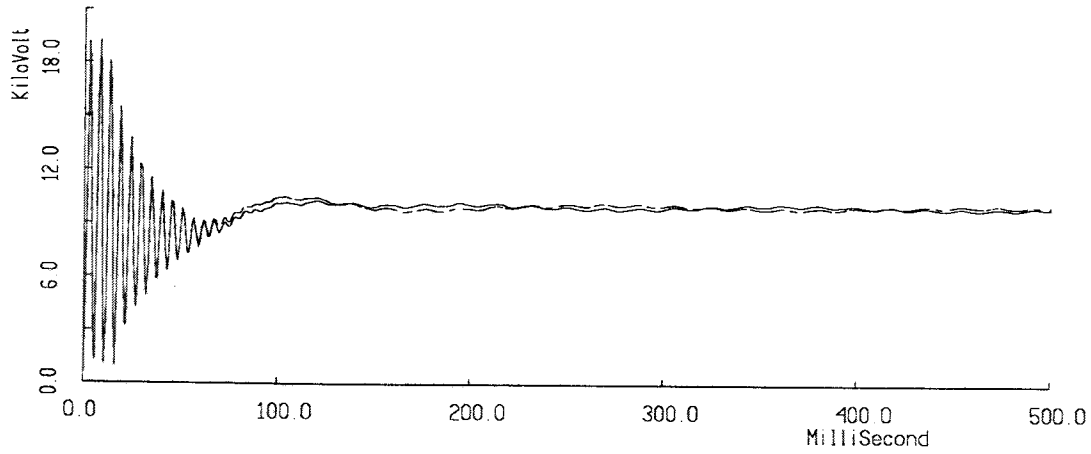

(a) DC Voltage at Converter Terminals

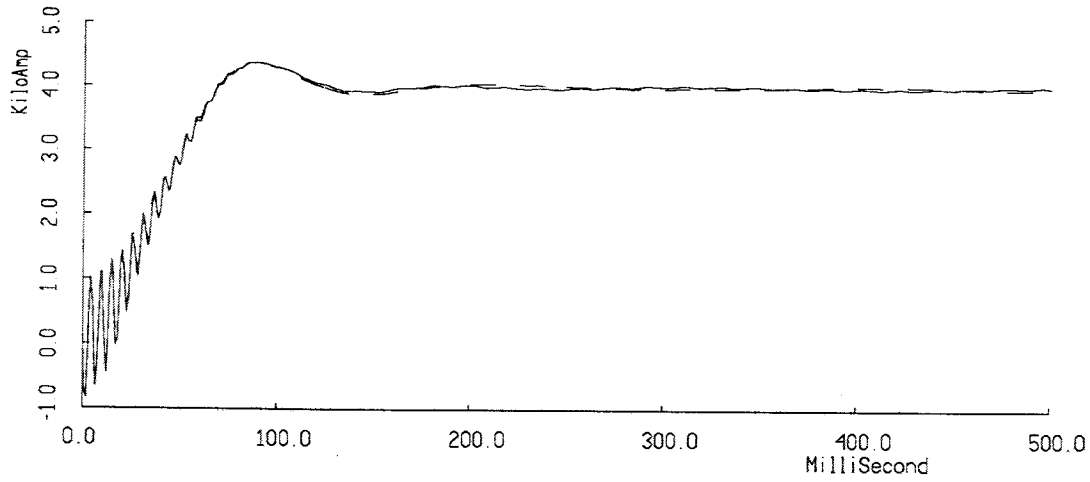

(b) DC Currents in Mesh Lines

Figure 2.4: System Startup with Detailed Superconducting Cable Models

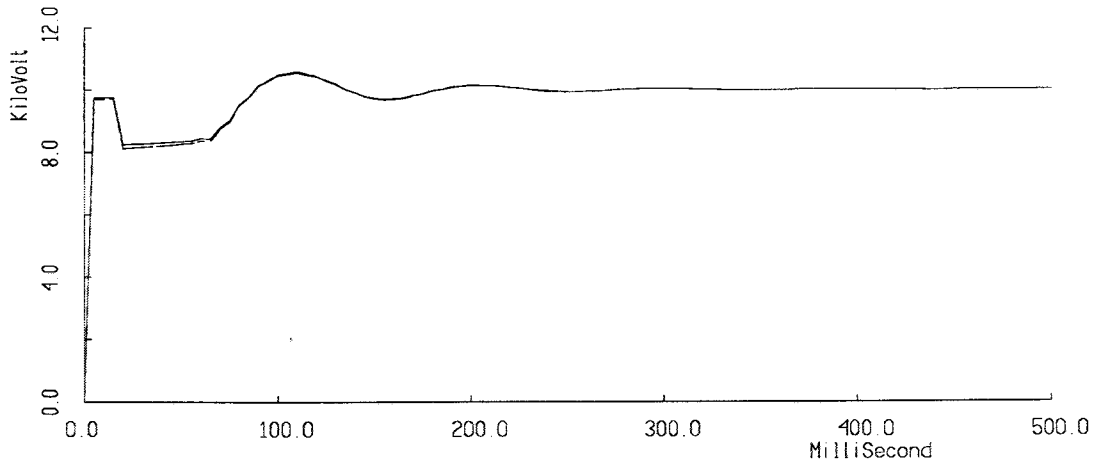

(a) DC Voltage at Converter Terminals

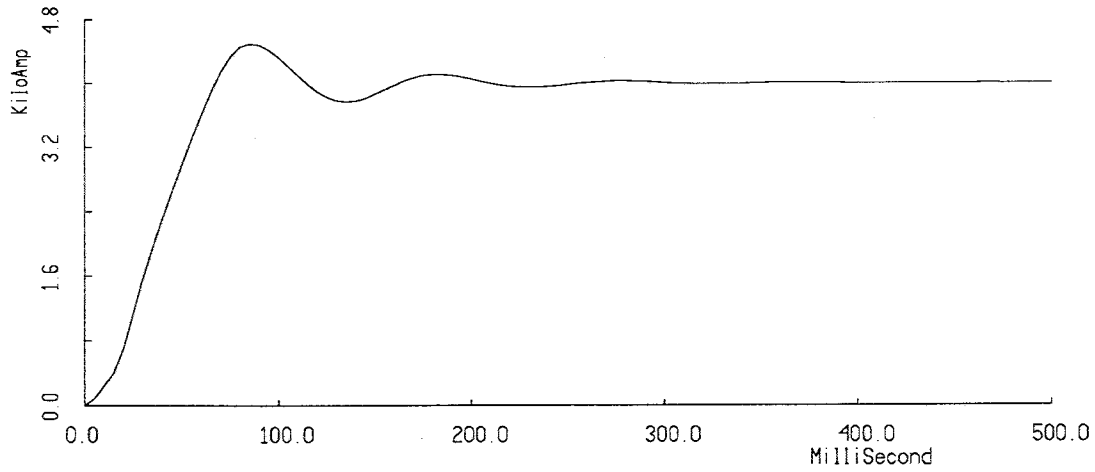

(b) DC Currents in Mesh Lines

Figure 2.5: System Startup with Lumped Inductor Superconducting Cable Models

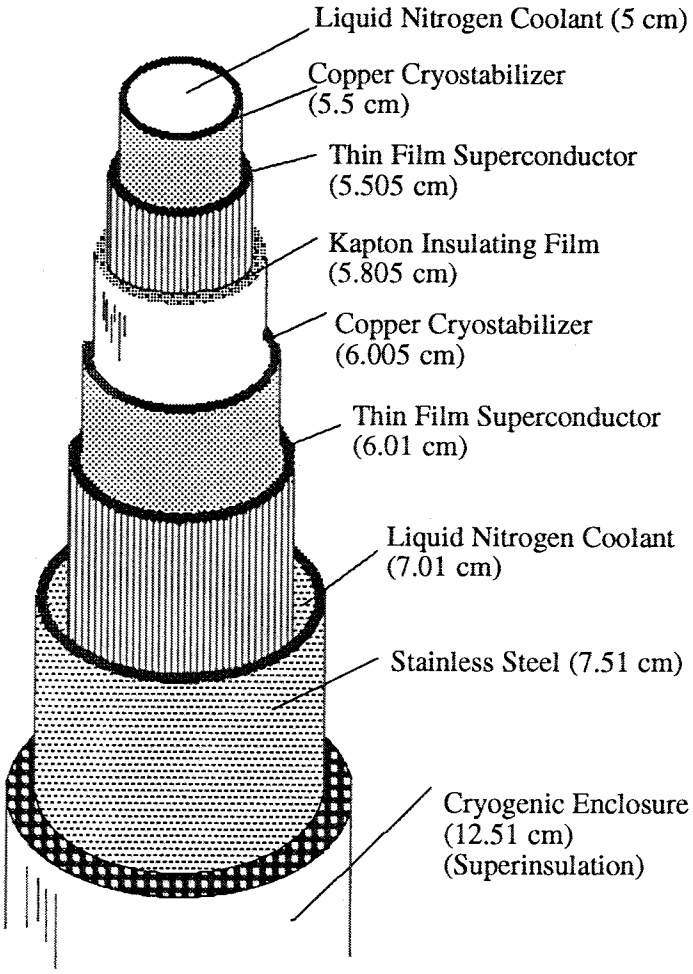

Figure 2.6: Coaxial Superconducting Cable with Liquid Nitrogen Coolant and Kapton as a dielectric

2.6 A Final Word About Superconducting Cables

With the discovery of new high temperature superconducting materials, prospects for power system applications are stronger than ever. This is largely due to the availability of liquid nitrogen as a coolant compared to the use of helium.

It must be understood that all studies of the costs of superconducting systems are subject to large errors. Many technical problems still have to be solved, making cost factors impossible to determine. When calculating the specific cost (cost per MVA per unit length), the rating used must properly reflect the ability of the cable to carry an average load with wide daily variations at a given refrigerator output. The economics of refrigeration will play a important role in the design of the cable. AC losses caused by harmonics will constitute the major heat load in many cases. This makes the the ability to predict and minimize ac losses with reasonable accuracy an important factor in conductor design. The feasibility of this design depends on: the fabrication of thin film superconductors, efficient refrigeration systems, and economic installation. Many technical problems have to be solved before viable dc superconducting cables can be presented to the system planners. The design of liquid nitrogen cryostats is a formidable problem, but it is one that will hopefully be solved in the future. Great progress has been made recently in the design and fabrication of superconducting cable materials, showing promise for transmission applications in the not too distant future.

While this report presents a design for a superconducting cable, this is only to produce a model to use for system development. The key results from this report are system design and studies. The system results do not depend on a specific type of superconducting cable.

Chapter 3

The DC System

The proposed superconducting power system replaces the high voltage transmission and subtransmission portions of the ac power grid with a low voltage direct current system (LVDC). The system incorporates direct current transmission to avoid ac losses associated with superconductors. The use of superconductors allows for the use of high current transmission rather than high voltage transmission, since their is no current dependent penalty from resistive losses. The dc transmission system will also benefit from the fast control available with the converter terminals and their controls [36, 37] along with some of the characteristics of superconducting cables.

3.1 Mesh Connected DC Systems

Multiterminal HVDC transmission systems have been studied for over twenty years. Few multiterminal systems have actually been constructed, but they are likely to be more common in the future. Figure 3.1 shows basic configurations for multiterminal systems. Figure 3.1a shows a series connected system. Each of the converter terminals is connected directly in series with the transmission line. Thus, it always has the full system current flowing through the converters. This is an extension of the common point to point HVDC system. The five terminal Hydro-Quebec system is an example of such a system. This scheme is a promising solution for conventional conductor based systems with low current levels. But this scheme is at a severe disadvantage for low voltage, high current systems due to the large current loading of the converters.

The second multiterminal configuration is the parallel connection. The converter terminals are

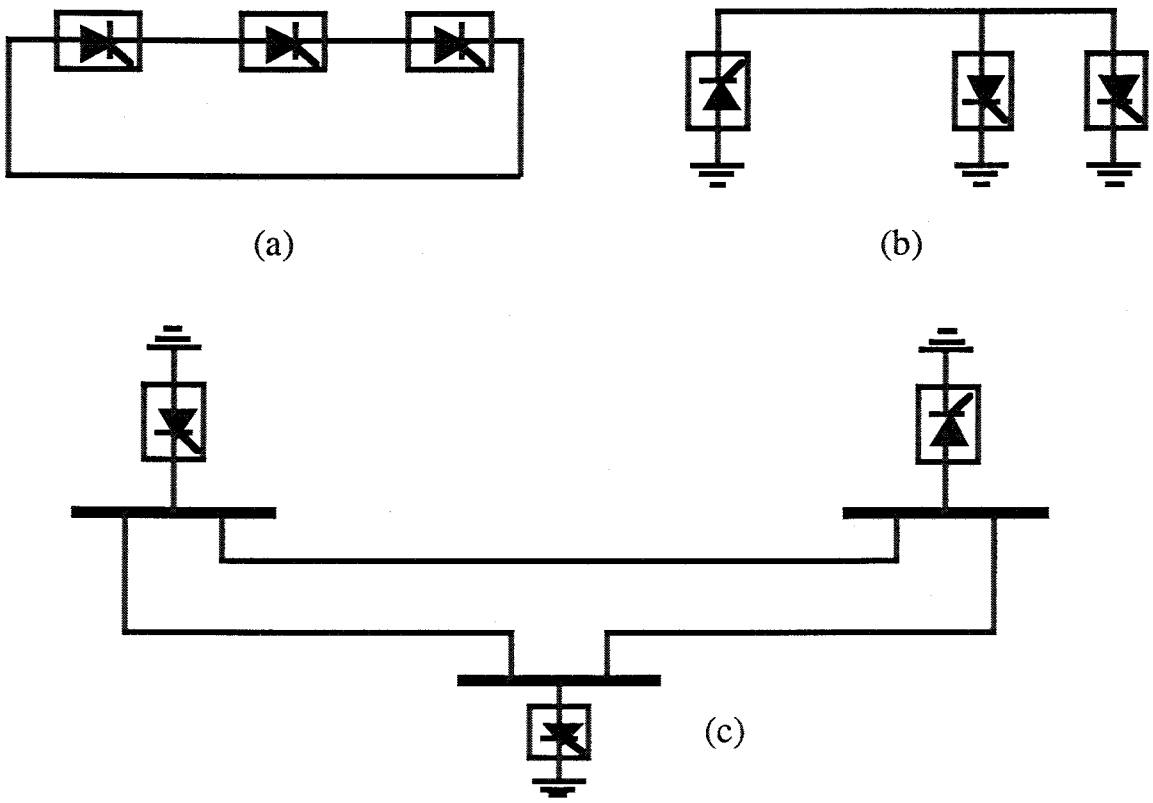

Figure 3.1: Multiterminal DC System Connections

shunt connected to the transmission line. The parallel connection can be utilized in two ways. The first is implemented by adding a parallel tap to an existing point to point system. This results in two converters connected in parallel on the dc side as shown in Figure 3.1b. This is an alternative to adding another converter in series with the line. The parallel converter terminals are all rated for the mesh operating voltage, and have their current ratings set according to the desired output power ratings. Each converter station is rated for the common system current level for a series system, and the voltage rating is determined by the desired power rating. A more extensive parallel system is a meshed system. An example of such a system is shown in Figure 3.1c. The system has several parallel transmission paths between the rectifiers and inverters, increasing the reliability of the system. Parallel systems work very well in low voltage transmission systems. There will be little need to connect switching devices in series to withstand high voltages. Each of the converter terminals will only need to be rated for the local current, and will not need to carry the full system current.

The design and control of mesh connected HVDC transmission systems has been studied extensively in the HVDC transmission literature [38, 39, 40]. The mesh connected LVDC system has a great deal in common with normal conductor based, mesh connected, HVDC transmission systems. The major difference occurring when superconductors are utilized is in the natural distribution of dc line currents. The natural dc load flow attains minimum line losses for a normal system [40], while the natural line flows for a LVDC system result in minimum stored energy in the cable inductances in the mesh [33]. This is the result of maintaining a volt-second balance across inductances of parallel paths when the system is energized, and for any subsequent change in current entering or leaving the system as well.

There are many issues of concern with mesh connected HVDC systems [36, 40] that are unique to such systems. A meshed configuration allows for a flexible flow of power through the branches in the mesh, based upon the interaction of line resistances, inductances, and capacitances with the converter voltages. The presence of parallel dc paths increases operational reliability. This configuration requires two or more dc connections to each of the terminals. The can also be connected in a bipolar configuration.

One of the most serious problems faced by meshed systems is in the detection and neutralization of dc faults [38, 39, 40]. But this system also has the potential to recover quickly from a disturbance since the faulted line can switched out of the system. Detecting the location of the fault will be more difficult for a meshed system, as it will draw current from all of the other branches in the mesh and from each of the converter stations. This requires the presence of relaying equipment on the mesh, and communications between them. A meshed system requires some form of dc circuit breaker to remove a line from service during a fault [38]. Otherwise the mesh voltage will fall to the fault voltage and the rectifier will continue to feed the fault. DC circuit breakers will be discussed more thoroughly later in this chapter. Meshed multiterminal HVDC systems also have different control requirements than conventional point to point systems. Control schemes for parallel systems will be discussed in Appendix A.

3.2 DC Transmission Systems Using Self-Commutated Inverters

All existing HVDC transmission systems use line commutated converters, which are also referred to as naturally commutated converters. Furthermore, each system also uses essentially the same converter configuration. The converters work under the assumption of an ac system with a strong voltage source, and a dc system with a stiff current source. This is referred to as a line commutated current source inverter (LCCSI, or simply CSI). The dc current source is strengthened by adding a large inductance in series with the converter to connect it to the dc line. This is referred to as a smoothing reactor. The reactor also filters the harmonic content of the dc current.

These are thyristor based converters. A thyristor is turned on when it has a forward voltage across it and receives an external firing pulse. However, it cannot be turned off to transfer current to another switch (commutation) until the voltage reverses and the current through the device goes to zero. The voltage reversal necessary to drive current commutation for a line commutated converter is provided by the sinusoidal variation of the ac voltage source connected to the converter. A weak ac system, where the voltage magnitude and frequency can be strongly affected by the operation of the converter, will be unpredictable in its commutations. This can result in switches failing to turn off and keeping subsequent switchings from occurring.

The line commutated inverter topology works well for many of power systems applications. The rectifier terminal is invariably connected to an ac system that has excess power generation, and generally has strong ac voltage sources. There is often more difficulty at the inverter terminal. The total amount of power transmitted over the HVDC links now in existence is gradually increasing as systems are upgraded. This results in inverters feeding weaker systems. An extreme example of such a case is a passive ac system, where there is no ac generation present.

A weak or passive ac system can be supplied by force- or self-commutated inverters. An external circuit, made up of either series or parallel capacitors, forces the proper thyristor to turn off at the correct instant in time in a force-commutated converter. The force-commutated converters that have been considered for HVDC systems have been based on current source inverter (CSI) topologies. Tam and Lasseter [87, 88] compared the most promising configurations for force-commutated inverters.

A self-commutated converter uses switches that are able to stop current flow by the application of a gate pulse. Examples of such devices are transistors, gate turn off thyristors (GTO's), and MOS controlled thyristors (MCT's). Self-commutating inverters see extensive application in relatively low power, low voltage applications, such as motor drives [89]. They have not been considered seriously for HVDC transmission systems until recently. This is due to the higher on-state and switching losses present in such devices. Another major problem with such devices has also been their low voltage and current ratings. Voltage and current ratings of self-commutating switches have increased recently, making them more appealing to HVDC system designers. There are two fundamentally different types of inverters that can be implemented using self-commutating switches. Once again, CSI based topologies can be utilized. This style of inverter would behave in a fashion similar to the force commutated inverters discussed above. Several authors have explored the design of GTO current source inverters for HVDC transmission [84, 90, 91, 95]. The advantage of such a scheme is its similarity to the present state of the art in HVDC converters. Self-commutated inverters can be configured and controlled in such a manner as to be able to control both the real and the reactive power that they supply to the ac system.

The second inverter topology is the dual of the current source inverter. This converter sees the dc system as a stiff voltage source, and sees the ac system as a current source. The transformer leakage reactance from the transformer connecting the inverter to the balance of the ac system is sufficient to make the ac system appear as a current source. The dc system is made to appear as a stiff voltage source through the addition of a shunt capacitor (the dual of the series inductor). This capacitor is sized to absorb voltage harmonics on the dc system. This converter is commonly referred to as a dc voltage source inverter (VSI). Voltage source inverters using self-commutating switches are the workhorses of the motor drives industry. The application of self-commutated, dc voltage source inverters in multiterminal HVDC systems has been discussed in [84, 85, 92, 93]. Parallel connection of voltage source inverters on the dc side is possible. The inverter can control the magnitude, phase, and frequency of the voltage it presents to the ac system if pulse width modulation is used. Voltage source inverters appear to the ac system much the same as a generator would. They appear as an ac voltage source controlling the magnitude and phase of the output voltage. The biggest disadvantage of VSI's for HVDC transmission is the relatively high losses associated with their operation, especially in a PWM mode. A VSI is prone to severe problems during dc faults due to the shorting of the bus capacitors as well as the bidirectional current capacity of the converter itself.

3.3 Properties of Superconducting Cables

The LVDC system studied here will incorporate high temperature superconducting cables. More information about superconducting cables is provided in Chapter 2. Several important differences arise with the use of superconducting cables. There is no longer a current dependent dc voltage drop over the length of a transmission line, so a voltage regulation scheme sets a single voltage level for each of the terminals. This simplifies the overall control of a dc system.

The second key difference is that the cables will have a self-protective nature in the face of fault currents. Large overcurrents cause the superconducting cables to quench, so they will no longer operate in a zero resistance, superconducting state. This will result in a sudden influx of heat due to the energy dissipated in the resistance. The heat will be transferred to nearby sections of the superconductor, possibly causing other sections to also go normal. This could result in a wavefront of normal conductance traveling down the cable [2]. This can be thought of as a time-varying nonlinear resistance. The presence of this normal zone will result in the insertion of large back voltage into the line due to the resistive voltage drop. The superconducting cable will have a high quality aluminum or copper conductor connected in parallel with it. This conductor will pick up the current when the superconductor quenches to minimize damage to the cable itself.

The resistance of the quenched superconductor will rise rapidly, perhaps in several microseconds, so it will essentially appear as a step increase in resistance. Thus, a quenched superconductor can be represented as a inductance in series with a resistance as shown in Figure 3.2. This resistance will actually consist of the normal state resistance of the superconductor in parallel with the resistance of the copper matrix. A well designed cable will have a much smaller resistance in the copper so the current will transfer out of the superconductor and into the copper. This is done to minimize heat damage to the superconductor.

A mesh connected transmission system will not need to shut down if a line quenches. The added resistance will be restricted to a single line in many cases. The remaining superconducting lines will have no resistance, and will be largely inductive, as shown in Figure 3.2. There resistive voltage in the quenched line will cause current to transfer out of this line, and into the parallel superconducting lines. This speed of this transfer will depend on the initial current in the line, and the inductance of the line relative to that of the parallel paths. The behavior is used to advantage for current diverters which will be introduced later in this chapter.

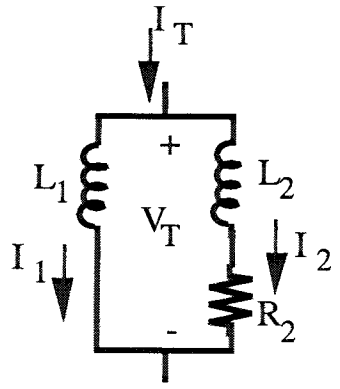

Figure 3.2: The Quenching of a Superconducting Cable

A properly designed cable will resume superconducting operation after the heat produced by the normal zone has been transferred away from the line [2]. However, this will be a slow process. Recovery takes place through a thermodynamic process, and could take several seconds, or even minutes depending on the refrigeration system. The restoration of superconducting operation can result in a wavefront of decreasing resistance that follows the wave of increasing resistance down the line. The end result of this would be a system that is self correcting. There are several potential problems that could arise in this scenario.

- The conductor could stabilize just below its current limit, where a slight increase in current will force it to quench. Then it would be necessary to have some form of branch current control to steer the system away from this danger zone and increase the current margins. One way to do this would would be to use the current steering devices.
- The current transfer could be permanent. This could be because the conductor did not resume its superconducting state due to damage from the heating of the fault or has even opened up. But the overall system would remain in operation due to parallel paths until the the damaged conductor could be repaired. This is especially important for dc faults where the fault current could burn up a section of superconductor.
- The current transfer could cause the current to become large enough in another conductor to make it also go normal leading to a situation where all of the conductors in a section of the system going normal, and could take down part of if not all of the mesh. Such an occurrence is much more likely on a heavily loaded system.

There are several very important differences that arise from the use of superconducting cables. There is no longer a current dependent dc voltage drop over the length of the transmission line. This allows a voltage regulation system to set a single voltage level for each of the terminals. This simplifies the overall control of the dc system. The second key difference is that the cables will have a self-protective nature in the face of fault currents. Large overcurrents will quench the superconducting cables, so they will no longer operate in a zero resistance, superconducting state. This will result in the sudden insertion of large back voltage due to the resistive voltage drop, which will cause the current in the line to transfer to the parallel paths in the mesh. A properly designed cable will resume superconducting operation after the heat resulting from the resistive energy produced by the normal zone has been transferred away from the line [2].

3.4 System Layout

The dc transmission system will utilize a mesh connection to increase operational reliability by providing alternate transmission paths. This will allow the transmission system to supply the loads despite the loss of one of more of the lines or generator stations. This also makes this system compatible with present power grids supplied by a number of generation sources spread over a geographic area. This concept is also compatible with distributed generation systems. The transmission system will then supply hundreds of inverter terminals which are located at what would be distribution substations in a conventional power system.

The design and control of mesh connected HVDC transmission systems has been studied in the literature [38, 39, 40]. The mesh connected LVDC system has a great deal in common with normal conductor based, mesh connected HVDC transmission systems. One big difference is that the natural dc load flow attains minimum line losses for a normal system [40], while the natural line flows for a LVDC system result in minimum stored energy in the mesh. The basic control ideas normally associated with mesh connected dc systems [41, 42] can also be implemented with a superconducting LVDC transmission system [33]. However, there are additional options for the control of the system that will be discussed below.

The LVDC system will utilize a mesh connection similar to that shown in Figure 1.2. This system has an a number of rectifier terminals feeding a large number via a meshed dc system. Each of the inverter terminals will feature a self-commutated inverter that is seen by its load

system as controlling real and reactive power either directly or indirectly via voltage magnitude and frequency control depending on the requirements of the specific system. The large number of terminals forming the meshed system make system layout an important issue. It is important to limit the number of lines to minimize cost and complexity, while still maintaining adequate reliability. A possible configuration rule is to limit each inverter to two connections to the mesh. This will result in small groups of inverter with each group fed by two separate connections to rectifier terminals. The rectifier terminals will also have interconnections to increase reliability. However, each rectifier terminal will be limited four or five connections to the mesh.

3.5 Overall Control

An overall scheme for controlling the converters on the LVDC system is needed for effective operation. The large number of terminals present on the dc mesh make coordination of the converters an important issue. The control scheme must allow the inverters to have local control over the current drawn off of the mesh. Allowing them to meet the demands of the ac systems they supply. The scheme must also have the ability to regulate the mesh voltage level. A reliable scheme must have the ability to respond to disturbances on the dc system without the use of fast communication between the converters so the system can still operate without the communication links.

Classical schemes for controlling mesh connected multiterminal HVDC transmission systems depend on fast communication to operate the system during transients [41]. The mesh voltage level is regulated at one terminal, and the remainder of the terminals are each operated in a current regulation mode. Fast communication is needed to coordinate the current orders of each of the current controlled converters to stay within the current limits of the voltage regulating converter. This type of control scheme was used in [33] to demonstrate the ability to control power flow on a superconducting LVDC mesh. This is an area where the zero resistance to dc current is beneficial. The entire dc mesh will settle to a single voltage level since the lines do not have a voltage drop. Therefore, it is very simple for the inverters to regulate their dc output power levels by simply regulating local current levels.

This basic scheme can be improved by designing the control characteristics such that another converter will be able to assume voltage regulation when the converter regulating voltage reaches

a current limit, or shuts down. This method of mode switching for parallel connected systems was demonstrated in [42], and does quite well for small multiterminal systems. Such a scheme will run into difficulty for very large multiterminal systems, where there could be a very large number of modes of operation.

3.5.1 Distributed Voltage Control Via Voltage Droop

A better control scheme for a large system would operate all of the rectifiers terminals in a joint voltage regulation scheme, and have each of the inverters regulate local dc current. It is not practical to send each of the rectifiers a voltage setpoint, since the system would again require fast communications for consistent operation during transients. However, a system where each of rectifiers is operated in a constant α mode (maintain the firing angle of the rectifier as a constant) could provide a stable voltage regulation scheme. The lack of a resistive voltage with superconducting cables can again be used to advantage in this situation. Each of the line commutated rectifier bridges has a current dependent voltage drop due to commutation overlap. This can be modeled as a resistance in steady-state converter models [36]. Combining this with rectifier operation in a constant α mode results in a constant voltage source connecting to the mesh through a resistance. Any change in the current drawn off of the rectifiers will change the voltage drop across the resistance. The change in current will divide between several rectifier terminals according to the equivalent resistances and current division. The system will settle into a new voltage steady-state, although there will be a change in the voltage level. The system will response to changes in current demand is similar to frequency droop on ac systems. The voltage droop control scheme is discussed further in Appendix A.

3.6 Inverter Issues

The choice of inverter topology and control scheme used for inverters connected to the dc system will have some effect on the behavior of the system. Therefore, it is necessary to consider some issues relative to interactions between the inverter and the dc system.

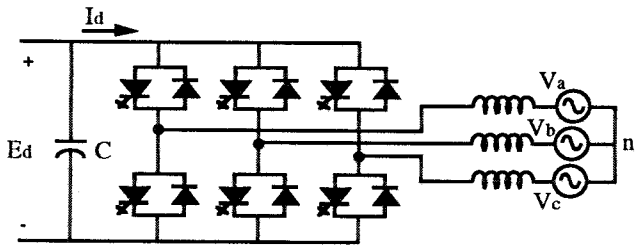

Figure 3.3: Three Phase Voltage Source Inverter

3.6.1 Voltage Source Inverter Issues

There are several issues that need to be faced when utilizing dc voltage source inverters (VSI's) that are quite different than those that arise with dc current source inverters (CSI's). A VSI requires switches with bidirectional current carrying abilities. Implementing the converter with gate-turn-off thyristors (GTO's) requires the presence of a diode connected antiparallel with each switch. These diodes provide a path for the ac system to feed a dc side fault, and this current cannot be blocked by control action [85]. This will require some form of dc circuit breaker to disconnect the faulted line from the mesh. Otherwise all of the VSI's will feed the fault until ac side breakers trip.

The use of VSI's also has the potential to cause voltage instabilities on the dc mesh. The inverter increases its power demand by discharging the capacitor. This depresses the mesh voltage and increases the current drawn from the mesh. This lowered voltage will pull energy out of the capacitors on other VSI's which are electrically closer to the inverter than the rectifier terminals are in most cases. Lowering the voltage at the other inverters will cause them to try and draw more current to maintain their power demand. This will result in a lightly damped oscillation as the inverters fight for the available energy. This results in a ringing between the inverter filter capacitors and the line inductances. The VSI can be controlled to damp this oscillation by using the derivative of the mesh voltage (the capacitor current) as a damping input to the phase control loop [86].

3.6.2 Current Source Inverter Issues

A self-commutated CSI will be needed to supply a passive ac system. The voltage magnitude and frequency power can again be controlled by utilizing either a pulse width modulation scheme or by operating two parallel bridges with a controlled phase difference on the ac side [44]. Pulse width modulation is not a very effective way to control the magnitude of the fundamental component of the ac current injected by the inverter. This is due to the relatively low switching frequencies that can be achieved. However, a dual CSI, consisting of two bridges connected in parallel on the ac side is able to this effectively. These then sum to form a single vector with a controlled magnitude and phase. The CSI will not cause difficulties during dc side faults as a VSI does and connecting several CSI's in parallel does not cause dc system instabilities. However, a CSI requires a more complicated control loop to be able to control ac voltage magnitude and frequency.

3.6.3 DC System Imposed Inverter Control Constraints

The overall control scheme for the dc system will place additional demands on the inverter controls. Implementing decentralized mesh voltage control without mode switching will require some means of preventing the inverter controllers from causing the system to crash during an emergency. The droop scheme will cause the mesh voltage to decrease as the rectifier loading increases. The inverters will need to have some form of voltage dependent current limit to cause them to back off when the mesh voltage falls below a set level. This is especially true when VSI's are implemented, since the ability to control ac voltage magnitude is lost when the dc voltage falls. Essential loads can back off on their loading more slowly than other loads. This voltage dependent current limit will need to be incorporated into the inverter loops for controlling ac frequency and voltage magnitudes.

3.7 Near Term LVDC Applications

The mesh connected system discussed in the previous section represents a final generation of LVDC systems. This type of system will be the end result of many years of development and incremental changes. Near term applications of LVDC systems will obviously be implemented as much simpler systems. Such a system will have rectifier terminals supplied by conventional

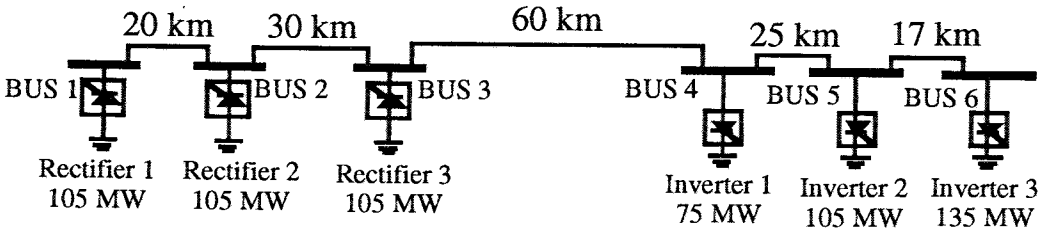

Figure 3.4: Superconducting Point to Point System with Parallel Taps

ac systems. Therefore the rectifier will be connected to the ac system or generator through a transformer. In addition, the system can have a much simpler configuration. An early system could be a simple point to point system entering an urban area. The inverter terminals will supply relatively strong ac systems, and could be implemented using line commutated CSI's as present day HVDC systems do. This will still be a low voltage, high current dc system. Therefore, and expansion of the system should be in the form of parallel taps rather than series connections.

A logical extension of this system would be to add a second superconducting line into the urban area. This would follow an existing transmission corridor, perhaps replacing the existing line eventually. This would provide a parallel path for the current to follow. The LVDC system could continue to grow though the addition of additional terminals and lines.

3.7.1 Point to Point MTDC Systems

An early expansion of this system would be to add parallel taps to the system, adding more inverter and rectifier terminals. The control scheme developed in Appendix A for the mesh will work in the same manner for this system. This is because the lack of current dependent voltage drops on the transmission lines eliminates the effects of system configuration on the sharing of load between rectifier terminals. Figure 3.4 shows the configuration of such a system. The system is build around a 152 km dc line, with parallel rectifier taps at 20 km and 50 km. There are also two parallel inverter taps at 110km and 135 km. Table 3.1 provides the details about each of the converter terminals on the dc system. This scheme allows the smaller inverter terminals to still have complete control of their output power, unlike the case with conventional transmission lines. This is because the entire mesh consistently reaches a single steady-state voltage level.

Converter	Power Rating	Current Rating	Normal Firing Angle
Rectifier 1	105 MW	7 kA	$\alpha = 5°$
Rectifier 2	105 MW	7 kA	$\alpha = 5°$
Rectifier 3	105 MW	7 kA	$\alpha = 5°$
Inverter 1	75 MW	5 kA	$\gamma = 25°$
Inverter 2	105 MW	7 kA	$\gamma = 25°$
Inverter 3	135 MW	9 kA	$\gamma = 25°$

Table 3.1: Converter Terminal Ratings for 6 Terminal DC System

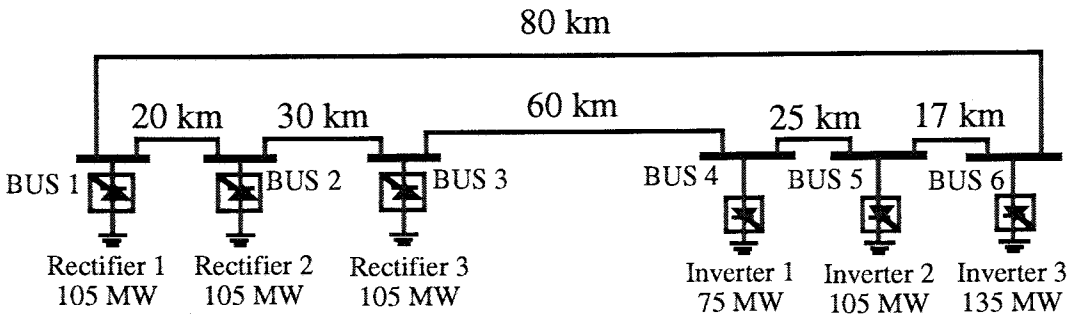

Figure 3.5: Loop Connected Superconducting Transmission System

3.7.2 Looped Systems

Another logical extension of this system would be to add a second superconducting line into the urban area. This would follow an existing transmission corridor, perhaps replacing the existing line eventually. This would provide a parallel path for the current to follow. It could also be used to later increase the total current carrying capacity of the system. Figure 3.5 shows an example of such an extension of a point to point system with parallel taps. This is the result of adding an 80km line connecting rectifier 1 to inverter 3 in the system shown in Figure 3.4. The system parameters are the same as those shown in Table 3.1. Subsequent additions would then move towards a mesh connected system.

3.8 System Protection

There are several issues to consider for the protection of any transmission system. These all apply to superconducting LVDC meshed systems, too. However, there are a few areas of special concern for such systems. The biggest concern with a superconducting cable is how the cable will respond to situations where is ceases to be a superconductor. This is referred to as quenching, or 'going normal,' as was discussed earlier. The response of the system and the superconductors to dc faults is another issue. Protective schemes built into the converter controls have also been discussed and demonstrated in earlier chapters.

Mesh and parallel connected dc systems have difficulties with dc faults, and will need some form of dc circuit breakers for added protection. These can work in tandem with the control actions of the dc system. These circuit breakers can take the form of conventional HVDC breakers, or it may be possible to take advantage of the properties of superconductors for a simpler breaker.

The direct connection of unit-connected generators can cause problems with the grounding of the generator and the rectifier bridge. The grounding of the dc system is also an issue that needs consideration.

3.9 DC Circuit Breakers

Fault protection is an important issue, especially for a mesh connected system. One possible solution would be to simply let the current increase until the line quenches. This has the drawback of needing to wait for the entire line to resume a superconducting state before reinserting it, and could also increase the possibility of damage to the line. The quenched line will still carry current to the fault unless the current decreases enough to clear the fault.

3.9.1 Conventional DC Breakers

It is important to be able to remove one of the lines from the dc mesh in response to faults and other disturbances. It is very easy to implement breakers in ac systems. However, it is much more difficult to apply circuit breakers to dc systems. AC systems have current zeros 120

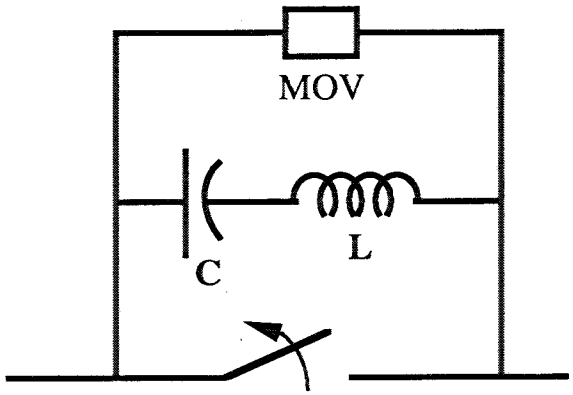

Figure 3.6: Conventional DC Circuit Breaker

times per second to aid in the clearing of the resulting arc. But dc systems do not have current zeroes readily available. Point to point HVDC systems do not need circuit breakers, they use the converter controls to bring the line current to zero instead. Since the type of control action necessary for this is generally not available with multiterminal dc systems, it becomes necessary to have some sort of current interruption device, such as a circuit breaker. To operate a circuit breaker in a dc circuit it is necessary to force an artificial current zero to allow the arc and its ionization path to be cleared. DC circuit breakers that induce a current zero have been developed for HVDC transmission [78, 80, 79]. These breakers force a current zero by creating an unstable resonance in an LC circuit connected across an ordinary breaker. The arc that results from the parting of the contacts triggers the resonance, which in turn forces a current zero in the arc. Figure 3.6 shows the general configuration of a dc circuit breaker. This breaker also has a metal-oxide varistor (MOV) connected across the LC circuit as shown in the figure. The energy in the dc line would be dissipated in this resistance and the resistance of the line to damp out the resonant oscillations and clear the line.

3.9.2 Superconducting Line Current Diverters

Adding a circuit breaker to a superconducting system may not be wise, or even needed. It is difficult to add a mechanical circuit breaker to a superconducting transmission system. Any resistance in the contacts, or in the breaker itself will transfer the current out of the line into parallel paths, as well as resulting in local heating. The presence of mechanical breakers in each

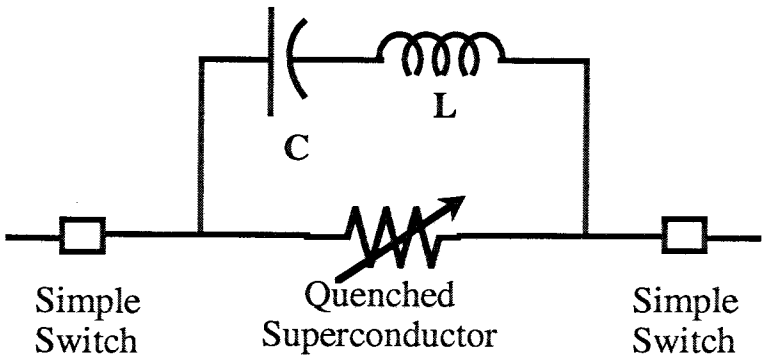

Figure 3.7: Superconducting Current Diverter with LC Tank to Initiate Current Zero

of the lines will negate any current transfer problems that result from the added resistance by balancing the resistances. But it may be possible to do better by using superconductors.

A circuit breaker that forces a current zero in a simple contact switch, allowing that switch to open is preferable to a breaker that operates with an arc between two contacts. One possible way to create a breaker in a superconducting line is to force a section of line to quench, as is done with superconducting current limiters [81, 82]. This inserts a resistance into the line, with the resistance increasing in a a period of microseconds. The resulting back voltage across the resistance triggers a LC resonant circuit. The resonance creates a current zero in the line, allowing a simple mechanical switch to be opened without arcing. The energy of the LC tank would be absorbed by the ac resistance of the superconducting line. It may be necessary to supplement this resistance with a fixed resistance in the LC circuit to damp the oscillations more quickly. Figure 3.7 shows a superconducting circuit breaker with a section of line that triggers an LC resonance when the superconductor quenches.

Figure 3.8 shows an example with a superconducting breaker opening a transmission line. This example has two parallel transmission lines, each initially carrying $1000A$. Then a resistive fault occurs in one of the lines, triggering a circuit breaker. The breaker has a normal resistance of $R_n = 11\Omega$, and an RLC network with: $R = 0.5\Omega, L = 1.8mH$, and $C = 450\mu F$. Figure 3.8(a) shows the current in the faulted circuit. The current increases, and then goes to zero after the breaker acts. This is the current in the switch that opens when the current crosses zero. Figure 3.8(b) shows the receiving end current for the faulted line (solid line), and the current in the parallel line (dash-dotted line). The current at the receiving end decreases when the fault occurs,

and then a switch opens to prevent current reversal. The other line picks up the current that was originally carried in the faulted line. Figure 3.8(c) shows the current in the LC network. This is the current that causes the current zero in the contact switch.

There are several design parameters to consider with the superconducting breakers. The first is the resistance of the normal section. It is possible to tune this through varying the length of the section of conductor that is quenched, as well as other parameters in the material itself. The next important items are the sizes of the inductor and capacitor in the resonant network. These must be chosen so the current rings through zero in the contact switch for any initial currents in the design range of the breaker. The full energy stored in the line will be dissipated in either the normal zone when the switch is first quenched, or else in the resistance seen by the LC network. The necessary refrigeration arrangements must be made.

There are several different rules to consider for the placement of these switches in the dc system. The line carrying current from the rectifier terminals to the inverters will normally only carry current in a single direction. Therefore, it will only be necessary to put breakers at the sending end of the line. Simple switches can open when the current at the receiving end of the line reverses. Any line that can normally carry bidirectional current must have breakers at both ends of the line.

3.9.3 System Grounding

There are several interesting issues that arise with the grounding of the LVDC system. The main issue in grounding the dc mesh is deciding whether or not to ground the neutral points of all of the converters. Leaving the neutral points of the converters floating could result in the neutral voltage rising up to the level of one side of the bipole during a line-to-line or line-to-ground fault [106]. This can be limited through the use of zinc oxide arrestors as is done with some HVDC systems.

Grounding the bipole at each of the converter terminals to provide a system reference will not create any new problems. There is little need for monopolar operation since the parallel paths in the mesh provide the needed redundancy. This is important since it is unlikely that the system could be operated in a monopolar fashion due to the superconducting lines. There will be some harmonic currents flowing along the ground path, which will probably be the sheath of the cable.

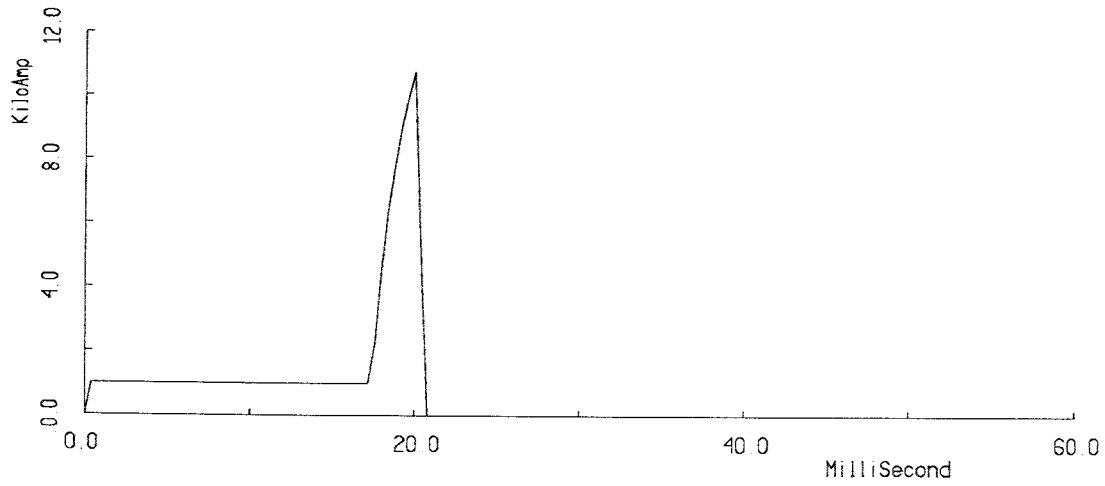

(a) Current in the Circuit Breaker

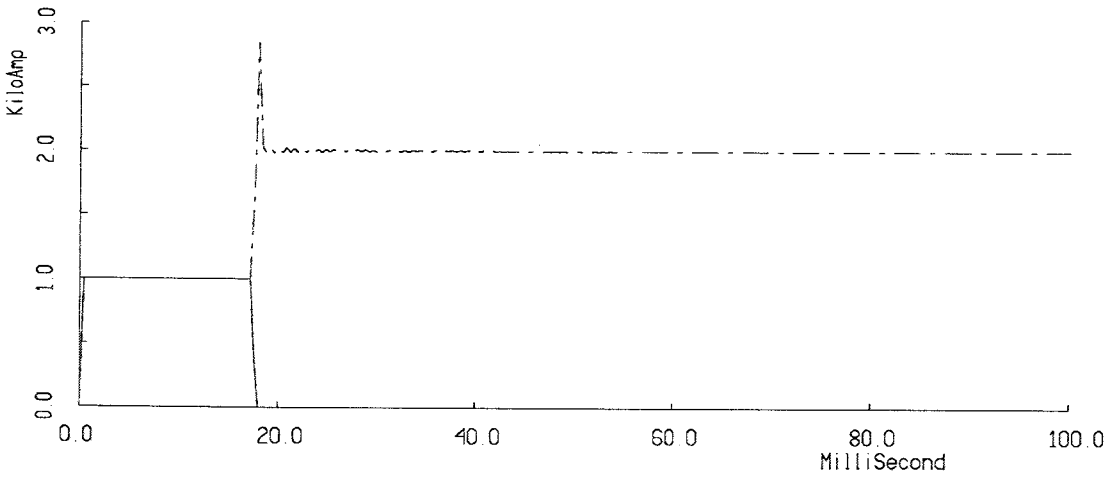

(b) Current at Receiving End of Faulted Line (Solid Line), and Current in Parallel Line (Dashed Line)

Figure 3.8: Operation of Superconducting Breaker During DC Fault

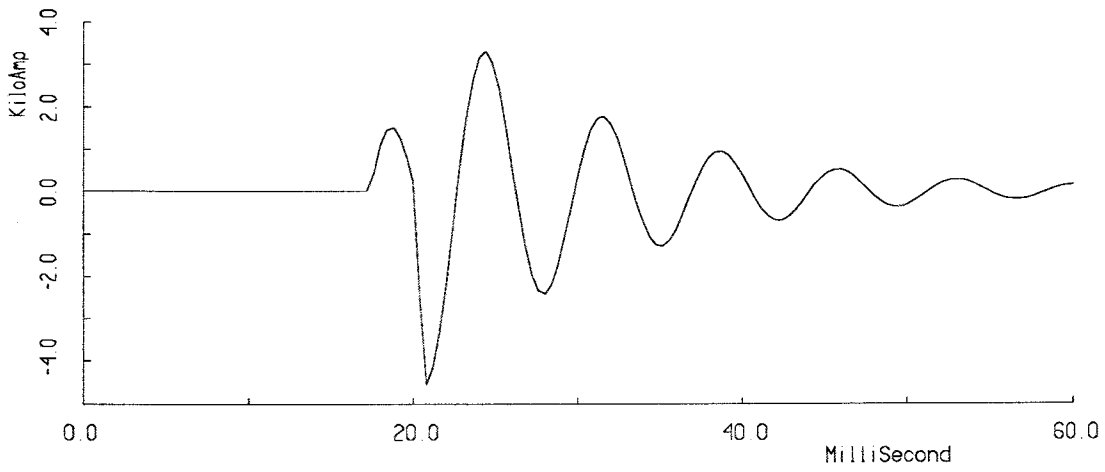

(c) Current in LC Network

Figure 3.8: (cont.) Operation of Superconducting Breaker During DC Fault

This is due to the non-zero harmonic impedance of cables. This could be a fairly large current if the harmonic impedance of the ground path is lower than the harmonic impedance of the cable. There will be harmonic currents passing through the ground if that path has a lower harmonic impedance than the cables, so filtering on the neutral points of each converter may be needed.

Generator and rectifier grounding is an important issue when direct connected generators are used. Generators feeding ac systems are grounded through a high impedance ground or a resonant ground [107, 108, 109, 110, 111]. This is done provide the ability to detect ground faults within the generator while still limiting their magnitude. The generators are then isolated from each other by connecting them to the ac system through $\Delta - Y$ transformers. This prevents ground loop currents between generators. This type of protection is not available for a generator connected directly to a rectifier. The rectifier does not isolate the generator ground from the ground of the dc system. There could also be a problem if more than one generator is present at the same site. The rectifier does not isolate the generators from each other, so there is a potential for currents circulating between the grounded neutrals of different generators. In addition the neutral point of the generator will have an average voltage equal to one-half of the dc transmission voltage as

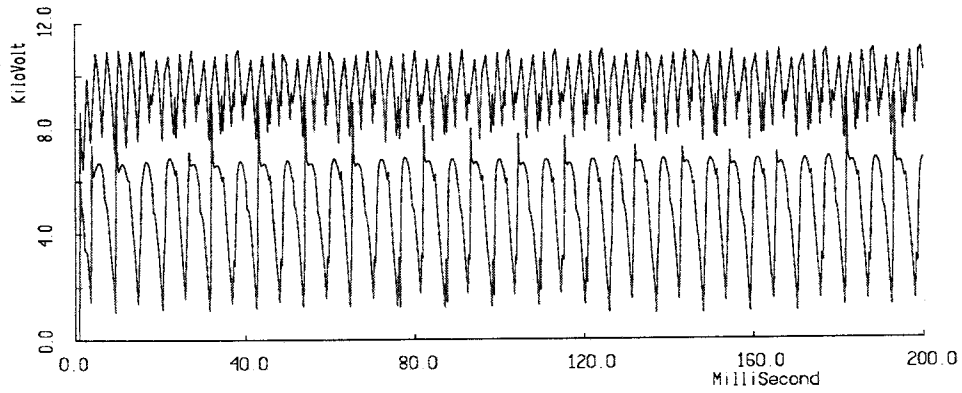

Figure 3.9: DC Voltage Offset on Generator Neutral with Direct Connection

will be demonstrated in Figure 3.9. The top trace in the plot shows the dc voltage on the positive pole, while the lower trace is the voltage at the neutral point of the grounded three phase source. It is important to have ground connections with large resistance to prevent large neutral currents.

The generators will be grounded through a large resistance. This resistance will be sized to limit the ground current to 1-5% of the rated stator current under normal operating conditions. The neutral points for the windings feeding each pole of the bipole will have separate resistances connecting them to ground as shown in Figure 3.10 to prevent current loops between the poles.

3.9.4 Differential Current Protection of Bipolar Systems

Another concern that results in grounded systems is the presence of dc currents flowing along the ground return path, since this will result in corrosion of the sheath of the cable. There will be temporary dc currents on the neutral due to disturbances, but it will be important to make sure that the currents delivered to both sides of the bipole are balanced. This will require a control loop on the converters to balance dc currents on each pole.

It is also be useful to be able to limit the rise of a fault current on one pole of the bipole before the relays activate the breaker. This could even eliminate the need for activating the breaker in some cases. One such scheme is discussed in [82]. Here the section of line making up the superconducting breaker, or near the breaker, is wound around an iron transformer core such that the flux from each pole of the bipole cancels the flux from the other pole. The reaction to

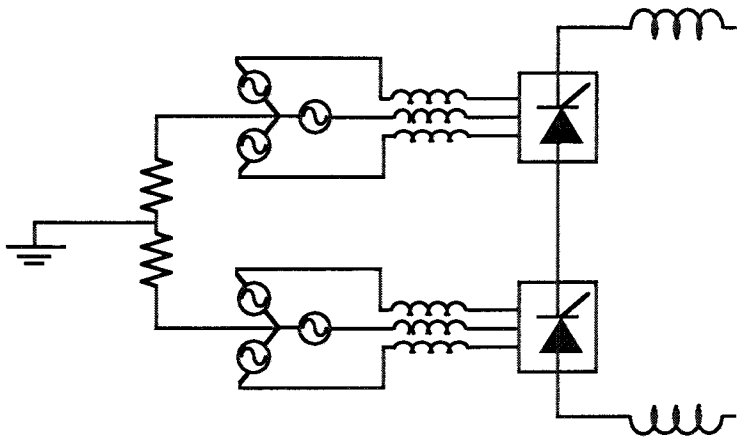

Figure 3.10: Grounding a Direct-Connected Generator

an increase in current in one pole will result in an increase in the inductance seen by that pole, and will limit the current increase. Figure 3.11 shows a differential current limiter. This can be implemented in systems with normal conductors as well.

3.10 Controlling Current Flows Within a DC Mesh

The current flows within a mesh connected system are determined by the resistances and inductances of the branches. The steady-state currents for a conventional dc system are dominated by the effects of the voltage drops of the resistances. However, each of the nodes in a superconducting mesh will reach equal voltage levels. The changes in the branch currents are determined by the changes in the voltages across each line as the system moves to a new state as was discussed earlier. The current division during a transient maintains volt-second balance between each of the branch voltages, and results in a minimum change in system stored energy. Therefore, the relative changes in branch currents in a superconducting system are dominated by the effects of the line inductances, and are difficult to control with converters connected at the nodes of the mesh. One way to have partial control of mesh currents using controllability theory, but this scheme is very system topology dependent, and is not flexible enough to control all of the lines in a mesh. Some form of active control within the branches of the mesh is needed, rather than trying to control current from the nodes.

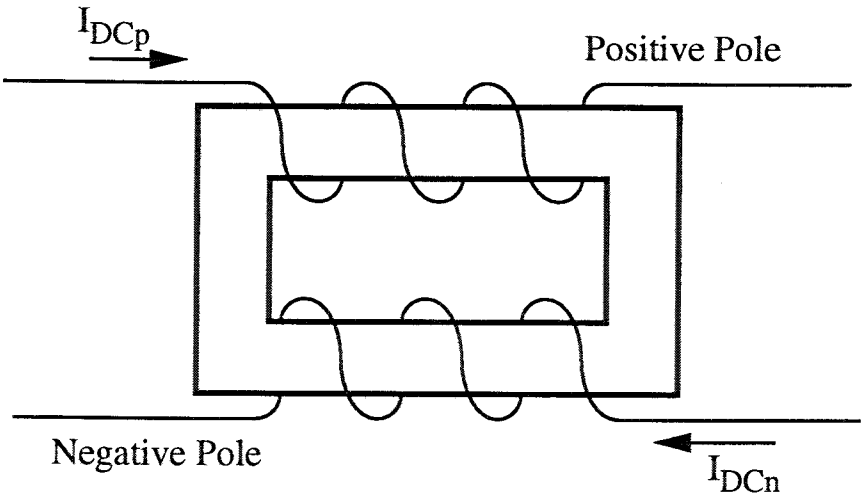

Figure 3.11: Superconducting Differential Current Limiter

There are certain situations where it is desirable to have some control over the branch current distributions. It is important to keep the current in any superconducting line below the level where it will quench and cease to be a superconductor. The sudden increase in resistance when the line quenches will cause a voltage to appear across the line that will drive all of the current into the parallel paths in the mesh, leaving the line carrying no current. This transfer happens over a period of milliseconds depending of the resulting RL time constant of the line. The recovery of the line is a thermodynamic process that could take place over several seconds. The energy dissipated from the quench must be transferred away by the cooling system before any damage occurs. This quenching will not damage well designed cables, but it is still better to avoid quenching lines at unexpected times and locations. An active current steering system could move the threatened line away from its current limit to ward off this possibility.

Another case where current steering is useful is the re-insertion of a line. A line that has been removed from the dc system will carry no current when it is initially reinserted. This is because the mesh reaches a steady-state with all terminals at equal voltages. Reclosing a line into the mesh will not cause a substantial voltage transient so the mesh will stay in the same state until a load current change occurs [33]. Repeated removals and re-insertions over time could lead to a case where a few lines operate close to their limits while other paths carry almost no current. This can be avoided by having a current steering system balance the mesh currents when the new line is reinserted.

A global current steering system will require a centralized communication system. Such a scheme can be slow, so it can operate without fast communication. All that should be necessary is to communicate setpoints to the various controllers on the mesh. There are several ways a current steering scheme can be implemented for a mesh connected system. However, economic constraints eliminate many of these. The following is a brief discussion of the possible schemes for controlling mesh currents.

3.10.1 Series Converters

The simplest scheme would be to add some form of series dc to dc converters to the system. Some of these could actually be in the form of series taps on dc lines. This scheme suffers from the drawback that the series converter carry high currents, and the switching devices must always carry current even when current steering is not needed. This scheme would suffer from the need for complicated, high current converters, and high converter losses. It will also require additional junctions between switches and superconductors.

3.10.2 Magnetic Transfer

A second option would be to initiate the current transfer magnetically. This is based on adding 'dc' transformers to the mesh. The primary of this transformer would be supplied by a dc current source. This transformer can be implemented with a set of coupled reactors. The secondary voltage impressed on the dc mesh will vary during changes in the primary current, and will remain constant when the primary current does so. These current controlled voltage sources can be placed near the rectifier terminals on the dc system so they are able to pull the energy they need to operate from the ac supply feeding the rectifier.

This scheme has the advantage of providing a low loss scheme to transfer current, with the only losses present in the converters. However, the converters will have substantial energy storage requirements in order to maintain fixed injections to the dc system. This could result in a very large, costly converter system.

3.11 Superconducting Current Diverters

Recent work with superconducting current limiters for both ac and dc systems [81, 82] suggests another means for transferring current within between branches in the mesh. A fault current limiter whose operation is based upon a superconductor going normal would work as a current transfer device on a meshed superconducting transmission system. Inserting any resistance into a superconducting line will cause all of the current to transfer into the parallel paths in the dc mesh. The energy of the line will still be dissipated in this resistive section, but it will be localized to a known section of the line, so that section of the line can have a stronger cooling system. This device could also be triggered by an externally generated electric or magnetic field imposed upon it as is discussed with proposals for superconducting power electronic switches [83]. This provides the ability to control when a section of the line quenches. This section can then be built with sufficient cooling ability to handle to normal currents it would see.

This device will work with a resistance of a few Ohms or less. There is no need, nor even a desire for larger resistances, as they would result in large voltage spikes when the conductor goes normal. The magnitude of the induced overvoltages from the quenching operation is directly proportional to the resistance inserted into the line. A smaller quenched resistance will decrease the overvoltages, although it will increase the time it takes to transfer the current. The resistance of the quenched superconductor will rise rapidly, perhaps in several microseconds, several orders of magnitude faster than the current will transfer out of the line, which is based on the the RL time constant of the quenched resistance and the equivalent inductance seen looking at the mesh from this point. Therefore, the transition will appear essentially as a step increase in resistance.

3.11.1 Cryogenically Stable Superconductor Method

The goal of the current transfer device is to be able to transfer part of the current out of the line. One possible way to do this would be to quench a section of superconducting line briefly, and then reset it before the current has gone to zero. This would require a section of superconductor that is cryogenically stable, with sufficient refrigeration to remove the heat rapidly when the quench occurs. Ideally, such a process would happen quickly enough to limit the line current without decreasing it to zero. However, a resistance of a few Ohms will be able to transfer all of the current out a line in less than 10 milliseconds in many cases. Since the recovery of the

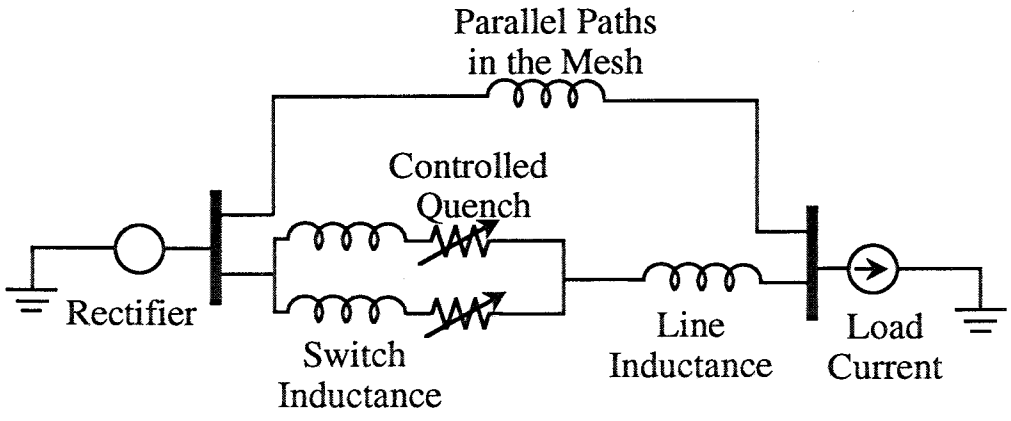

Figure 3.12: Superconducting Current Transfer Device with Parallel Legs

superconductor from a quench is a thermodynamic process, with large energies involved, it is unlikely to occur within such a short time span.

3.11.2 Parallel Resistive Transfer

One possible way to initiate partial current transfer out of a line through the quenching of a device would be to have two identical superconducting devices connected in parallel. Figure 3.12 shows a simple case where a line with a parallel connected current transfer device is connected in a simple system with two parallel lines. Part of the line current could be transferred out of the line by quenching one of the devices, without quenching the other. The current in the quenched portion of the line would divide between all of the possible parallel paths in the system, including the other leg of the device. The current will re-distribute among the paths to maintain volt-second balance over the mesh. The amount of current transferred depends on the size of the inductance added to the transfer device compared to the equivalent inductance of the remainder of the system. However, a larger inductance also increases the amount of energy dissipated when the device is activated. Additional current can be transferred out of the line by quenching the second leg of the device after the first leg has resumed its superconducting state. This process can be repeated to continue this transfer.

These devices can be located in each of the transmission lines connecting the rectifier terminals to the inverter terminals. These are the most important branches to have control over. The

currents in the lines interconnecting inverter terminals and in the line interconnecting rectifier terminals are dependent on the currents in the long lines. These devices should be placed at the sending end of the transmission lines so the energy needed to quench the devices can be provided by the ac system supplying the rectifiers.

There are several concerns in the design of these steering devices. The values of the normal state resistance of the device, and the inductance added to the line with the devices play a very important role in their performance. The resistive voltage of the normal zone divides over the length of the line based on the relative inductances. This will cause the voltage at the sending end to rise, while the voltage at the receiving end of the line will fall. So a larger resistance will cause a larger overvoltage at the sending end of the line.

The size of the inductance determines the amount of current transferred out of the line each time the device is pulsed. The size of the resistance has no effect on this. The size of the inductance in the device, and its interaction with the equivalent inductance seen looking at the mesh is the key. Figure 3.13 shows the how to determine this equivalent inductance for the circuit shown in Figure 3.12. Note that L_{eq} is the equivalent inductance of the balance of the system. The amount of current transferred out of the line by pulsing one leg of the device is shown in equation 3.1, where I_o is the initial current. The value of the inductance in the second leg relative to the inductance of the balance of the mesh is the key to the amount of transfer.

$$\Delta I_{11} = \frac{L_{11} * I_o}{L_{12} + L_{eq} + L_1} \tag{3.1}$$

The energy dissipation each time one leg of the device is pulsed is also dependent on the inductance added to the steering device. Equation 3.2 gives a relationship for this. This is for each time the device is activated, so if the device is pulsed repeatedly with many small jumps, more energy will be dissipated. Again, I_o is the initial current. Larger values of added inductance increase the amount of current transfer, as well as increasing the energy dissipation each time the device is used. Therefore, a design tradeoff needs to be made to choose this value. A smaller inductance will also allow for a more precise transfer if repeated quenchings are used. This will cause additional energy to be dissipated each time the device is used, however, the energy will decline in each subsequent step since the initial current will be smaller.

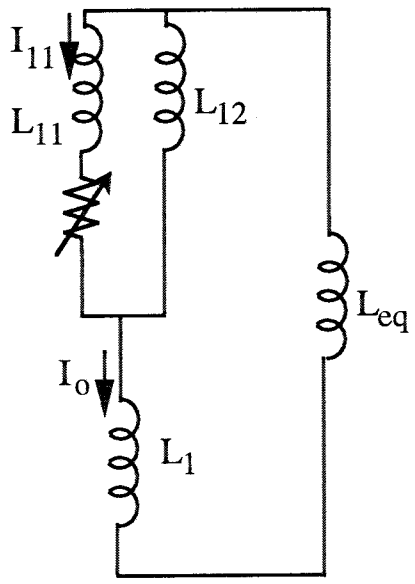

Figure 3.13: Equivalent Circuit for Determining Current Transfer

$$\begin{aligned} E_{diss} &= \frac{1}{2} L_{fic} I^2 \\ L_{fic} &= L_{11} + L_{12} \| (L_1 + L_{eq}) \end{aligned} \tag{3.2}$$

This result can be used to speed the operation of this device. A quenched leg will need to stay out of the circuit until it has resumed a superconducting state. This is a thermodynamic process, and will take longer if more energy has been dissipated. The other leg of the switch can not be quenched until the previous one has resumed superconducting operation, or all of the current will transfer out of the line. Since the total current in the line is smaller in each step, there will be less energy dissipated. The quenched section will recover faster, so it will be possible to decrease the time between subsequent pulsing, allowing for a faster convergence on the setpoint.

The configuration of the test system shown in Figure 1.2 results in pairings of the six long transmission lines. Two lines supply current to inverters 4 and 5 (lines c and e), lines f and i supply current to inverters 6, 7 and 8, and lines j and l supply current to inverters 9 and 10. This pairing is useful to help localize the effects of transients to smaller parts of the system. It results in simpler constraints for the set-points of the current steering devices. The set-points of the current steering devices must always be compatible with the inverter current orders. Figure

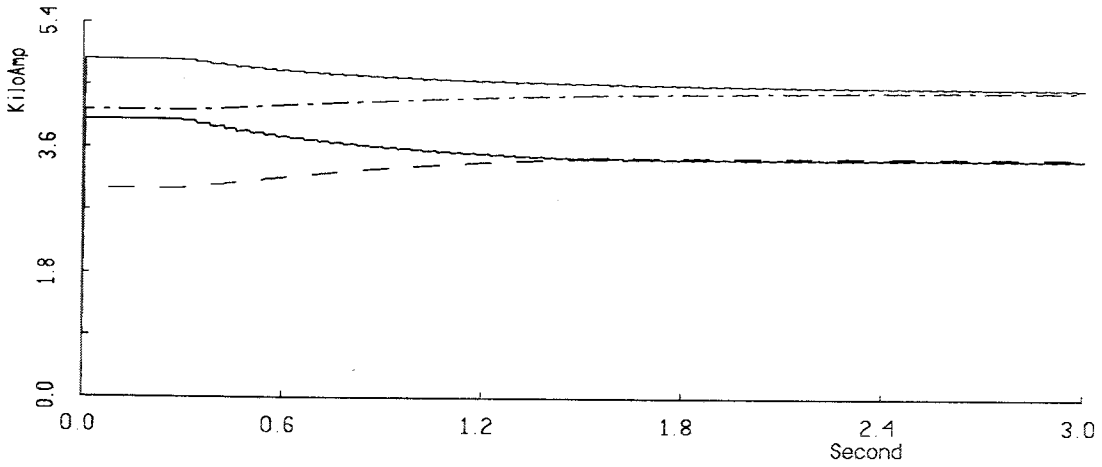

Figure 3.14: Using Current Steering to Set Current Levels

3.14 shows a case where the system initially has some imbalances between parallel sets of lines. The current steering devices are then activated to get each complementary pair of lines carrying equal currents.

Figure 3.15 shows a case where one of the two lines feeding inverters 4 and 5 is re-closed. Figure 3.15(a) shows the line currents. One line carries the full load, and the other carries no current. The other line is reinserted after 200 milliseconds, but does not carry current until the current steering device is activated after 500 milliseconds. The current rapidly moves toward the desired point, and then gradually moves towards a steady state. Figure 3.15(b) shows the dc voltage at the sending end of the lines. The voltage experiences small spikes whenever the devices are fired. Figure 3.15(c) shows that the inverter currents are not affected by the operation of the current diverters. Figure 3.15(d) shows the energy dissipation in the resistances of the normal zones. The energy dissipation increases in a stairstep fashion every time one of the legs quenches.

The total energy transferred through these two lines in this time period was $48MJ$. The diverter was pulsed 33 times (17 times for one leg, and 16 for the other) to bring the currents to the desired levels. The current diverter dissipated $26.6kJ$ during this time, resulting in a 0.055% energy loss. The initial pulse begins with the full line current of $4999A$. The device transfers about $93A$, or little less than 2% of the current out of the leg. It dissipates about $1.4kJ$ in the first step. The energy losses are small, but limit current steering to essential situations.

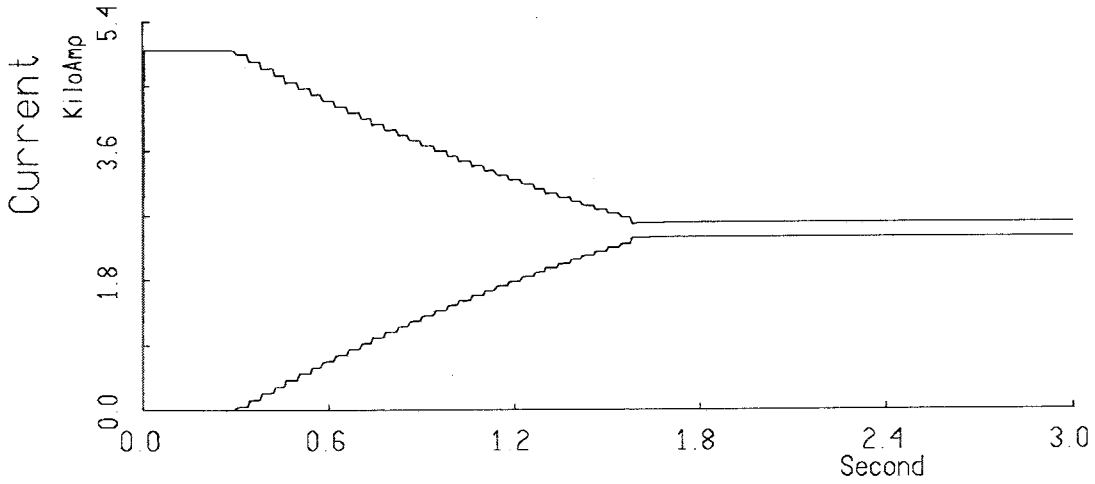

(a) Currents in Lines Connecting Rectifier 2 and Inverter 5 (top), and Rectifier 1 to Inverter 4 (bottom)

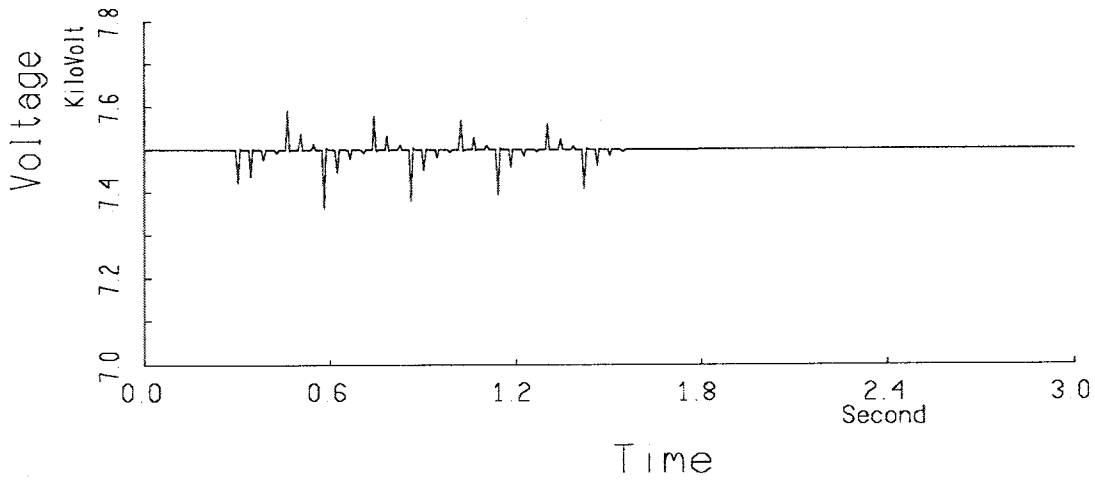

(b) DC Voltage at Rectifier 1

Figure 3.15: Current Steering with the Line from Rectifier 1 to Inverter 4 Restored

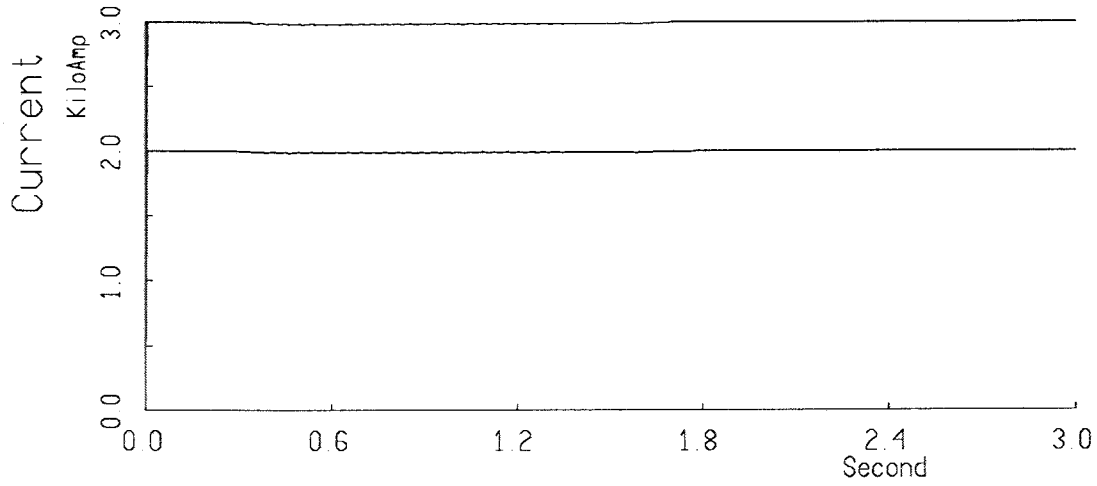

(c) Current at Inverter 4 (Top), and Inverter 5 (Bottom)

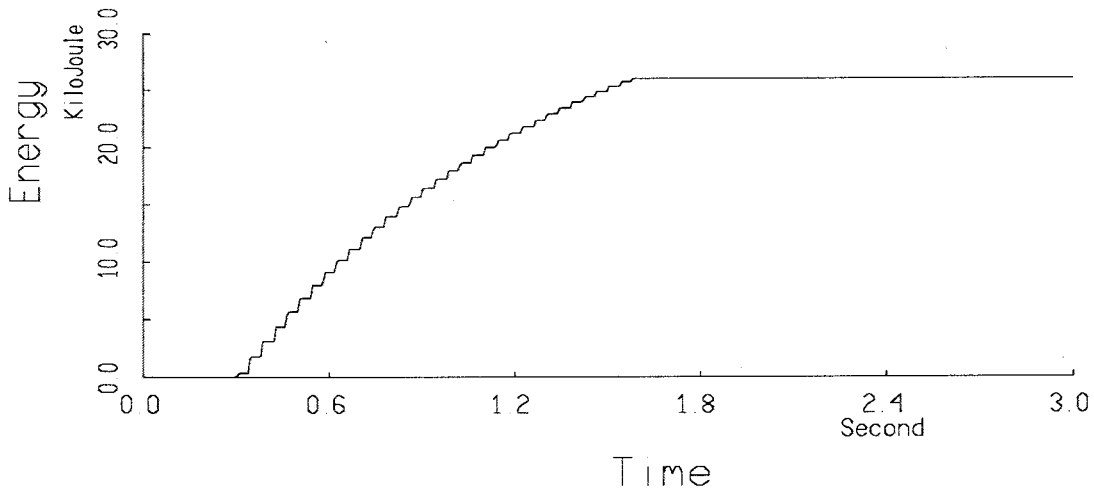

(d) Energy Dissipated in Line Between Rectifier 2 and Inverter 5

Figure 3.15: (cont.) Current Steering with the Line from Rectifier 1 to Inverter 4 Restored

3.11.3 Triggering the Devices

Methods for activating the superconducting breaker are also needed. The breakers could be designed to quench whenever the current rises above a preset level. However, this does not provide any control for activating the current transfer device. A superconductor can also be quenched by increasing its temperature, applying an external magnetic field, or applying an external electric field. Increasing the temperature is not an efficient way to operate the limiter. However, it is feasible to apply either electric [83] or magnetic fields [81]. Both schemes will require an external energy source, which suggests that the diverter should be located in close proximity to a converter terminal. The energy stored in the line must also be dissipated in the resistance when the conductor goes normal. This device will need to have a more powerful cooling system than the remainder of the line to remove the extra heat without damaging the conductor. Proximity to strong refrigeration is another reason to connect the device close to a converter terminal where it is easier to put in the extra cooling. This will also be needed to allow for quick resetting of the device for restoring the line. The refrigeration needs of the rest of the line will decrease due to the decreased probability of the line itself quenching. This type of device can be modified to act as a circuit breaker, as shown in the next chapter.

3.12 Incorporating Alternative Energy Systems

It is not as difficult to interface many alternative energy generation systems to a LVDC mesh as it is to an ac transmission system. Similarly, the power conversion and controls needed to interface dc based storage systems with the mesh is fairly simple as well.

3.12.1 Incorporation of a SMES Coil

It is possible to add a superconducting magnetic energy storage coil (SMES) in series with a rectifier. The other end of the coil would then be connected to the dc mesh. The power conversion equipment necessary for connecting a SMES coil to a dc system is much simpler and easier to control than the interface needed to connect a SMES coil to an ac system [44, 45, 74, 75]. The SMES coil could then be used for load levelling on the transmission system. Previous studies have looked at the possibilities of adding a SMES coil with this configuration to an LVDC system [33].

Figure 1.2 shows how the SMES coil could be interfaced with the LVDC system. This connection allows the generator supplying to coil to supply a more or less average power level to the system. to act as a for a SMES coil in the study system discussed earlier.

The SMES coil is easiest to control if there is a stiff voltage source on each side of the coil. The rectifier is fed by a unit-connected generator, so it can be operated as a stiff dc voltage source. The rectifier feeding the coil can also be implemented using a diode bridge. This arrangement does not suffer from two of the major problems that limit the usefulness of diode bridges for HVDC transmission: the coil will limit the rate of rise of the rectifier current during dc faults and the coil does not require fast voltage magnitude control at the rectifier [33]. Therefore the slower voltage control circuits in the generator and the inability to create a bypass pair will not hurt system performance. The other rectifier terminals on the mesh will regulate the voltage on the mesh side of the SMES coil.

The coil is then charged by either decreasing the mesh voltage level or by increasing the voltage on the rectifier side of the coil. Both of these result in voltage difference across the coil that will increase its current, and thus the energy stored in it. Increasing the mesh voltage will increase the energy drawn off of the coil by the mesh until the coil current begins to drop.

No extra converters are needed to add a SMES coil to a LVDC system, and few modifications in the controls are needed. The details of the control and operation of the system with the coil present will not be discussed further at this time.

The addition of battery storage to the dc mesh is also a possibility. A battery storage system could be interfaced with the dc system through a dc/dc converter that could then control charging and discharging of the battery.

3.12.2 Interfacing to Non-Traditional Generation

It will also be fairly simple to interface alternative energy generation sources to the dc system. Many of these sources, such as photovoltaics [67, 68, 69, 70], MHD generators [66], and wind power [71, 72, 73, 76, 77] often require a solid state power conditioning step prior to their connection to an ac system. These systems can easily be connected to a LVDC mesh. Sources with dc outputs, such as photovoltaics and MHD, could be connected to the mesh via dc-dc boost converters, and then

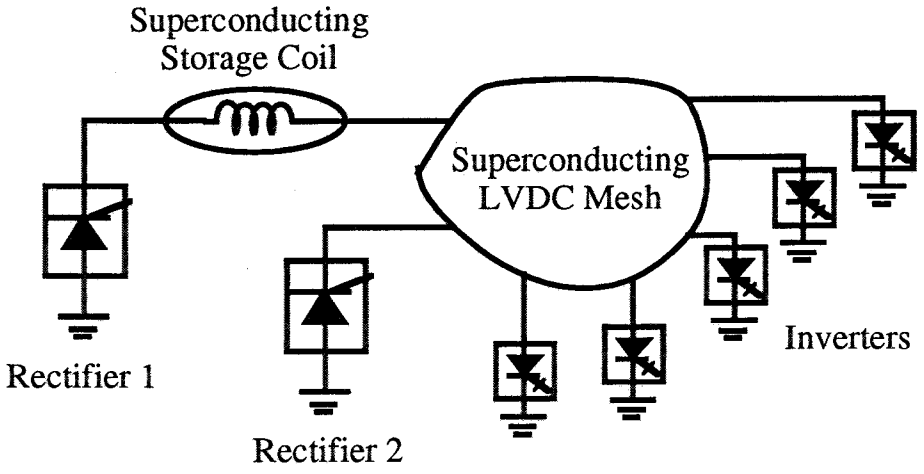

Figure 3.16: Interfacing a SMES Coil with the LVDC Mesh

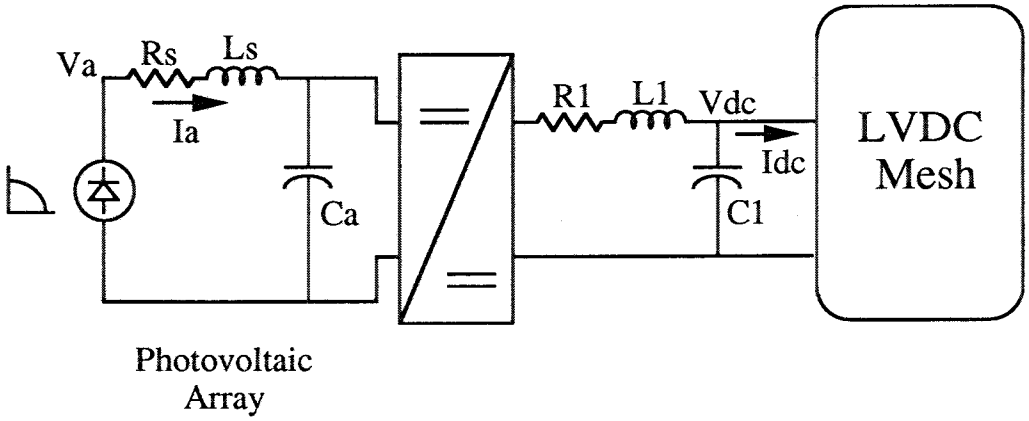

Figure 3.17: Interfacing a Photovoltaic Array with the LVDC Mesh

operated as either constant voltage or current sources feeding the mesh. Wind generators could be rectified and interfaced with the dc system. The low transmission losses of the superconducting transmission system could help make these sources more appealing to add to the utility generation base.

3.13 Conclusions

This chapter has introduced several topics of concern for the design of the dc portion of the LVDC transmission system. This system can be a multiterminal system with either a parallel or mesh connection. Such a system will have several rectifier terminals feeding a large number of inverter terminals. Future systems will utilize self-commutated inverters, but near term applications can also utilize line commutated inverters like those used in present dc transmission systems.

Fault protection is an important issue, especially for parallel connected dc systems. It will be necessary to have some form of circuit breaker to supplement the control actions of the converters. One way to do this is to utilize conventional dc circuit breakers, a proven technology, at the ends of the lines. Another possibility is to use quenched superconducting current diverters. Issues related to the grounding of the dc system and the generators were discussed.

This chapter has discussed situations where the ability to control current flows within the dc mesh is important, as well as several schemes for doing so. Each scheme has its drawbacks. The addition of active series devices to the dc system is impractical due to the very high current loads and losses these converter would incur. Another possibly is to use coupled reactors to implement an external current controlled voltage source. This scheme has the advantage of low losses within the dc system, but results in a converter that requires substantial energy storage and possibly high converter losses. The possibilities of using quenched superconductors based on superconducting fault current limiters presently under development for ac systems provides another possibility.

A scheme based on having a device with two parallel legs provides a way to initiate a partial transfer of current out of the line. This provides a way to gradually adjust the mesh current flows without affecting the inverter power flows. This scheme does have several drawbacks. The first is the losses incurred whenever the device is activated. These losses go into heating a section of the line, which therefore need a much stronger cooling system. A fairly large pulse of energy may be needed to quench the superconductor. However, if the device is used when the line is heavily loaded, less energy will be needed. The energy losses incurred through the use of these devices are a very small fraction of the total energy transfer in the dc system, making them appealing for limited use.

Chapter 4

The Generator-Rectifier Interface

The use of LVDC transmission allows for several changes in the generator-rectifier interface. The generator stations will often supply only the rectifier terminal, and no additional ac load. This is referred to as the unit-connection of the generators. The low voltage level eliminates the need for high voltage step-up transformers, and results in the direct connection of the generators to the rectifier bridge. The generator design will need to be modified to allow twelve pulse and bipolar operation. Parallel connected twelve pulse bridges will be used rather than the more common series connection.

4.1 Rectifier Design Issues

The rectifier terminals will be connected to either strong ac systems or to unit-connected generators. Therefore, the rectifier terminals can be constructed using line-commutated bridges. There is no need for self-commutated converters, since the generators can be operated to provide the reactive power needed by the converter terminal [47, 48].

4.1.1 Twelve-Pulse Rectifiers

Conventional HVDC bridges commonly operate with two six-pulse bridges connected in series for twelve pulse operation. The firing commands and the voltage waveforms supplied to the two bridges are offset by 30°. This results in the cancellation of the 6th harmonic component of the

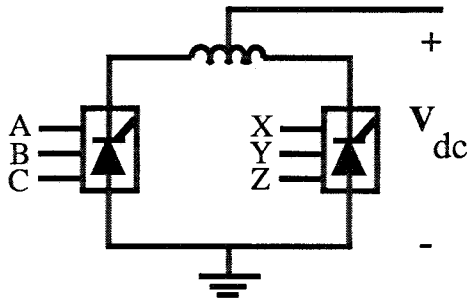

Figure 4.1: Parallel Connections for Twelve-Pulse Bridges

dc voltage, since they will be 180° out of phase [36]. The series connection of the six-pulse bridges is also useful for producing the required high voltage levels.

The low dc transmission voltage changes several aspect in the design of the joint generator-rectifier station. The most important change is the elimination of the transformer connection between the generator and the rectifier. The implications of this will be discussed below. Another important result of the low dc voltage is elimination of the need to connect bridges or even devices in series within the rectifier bridge. The rectifier could then be configured with parallel connected twelve pulse bridge rather than a series connection. Parallel connection has been utilized for some time in the electric rail industry [59, 60, 61], but is relatively new in the power transmission field [62]. Balanced current sharing between the parallel bridges poses a difficulty for this configuration. It is common practice to utilize either coupled ac transformers or current equalizing transformers (CET) to aid in this balance [59, 60, 61]. It is also possible to add an interphase reactor on the dc side of the converter bridges [60, 61, 62]. However this scheme will suffer from 300 hertz acoustical noise. Hall et al discuss a scheme for operating a parallel rectifier without an added ac or dc device through the use of modified operating mode [61]. This scheme also requires a modified transformer design where the added leakage acts in a fashion similar to the CET. Figure 4.1 looks at a connection utilizing an interphase reactor.

4.1.2 The Utilization of Diode Bridges

The use of unit-connected generators provides an opportunity to simplify the converter used at the rectifier terminal. Further simplification is possible if a diode rectifier bridge is used rather

than a controlled thyristor bridge. This scheme was proposed for use with multiterminal HVDC systems by Bowles, [46].

The rectifier terminal can still be used to regulate the mesh voltage level, but now the voltage is varied by adjusting the generator field excitation rather than the firing angle of the converter. Varying the field excitation changes the magnitude of the ac voltage seen by the bridge. This scheme results in cost savings by using diodes instead of thyristors, and also eliminates the need for a converter control scheme. The generator excitation control loop is still needed even if a controlled bridge is used. However, the excitation control allows only slow control of the voltage magnitude, with time constants on the order of 500 milliseconds to one second due to the large inductance of the field winding. This is much slower than the available voltage control with a thyristor bridge. This could present problems for a mesh connected system when the power demanded by the inverters changes. Figure A.9 shows a simplified representation of a unit connected generator and its excitation control loop.

The use of diode bridge rectifiers also presents some problems for fault protection. A thyristor bridge can be controlled to form a by-pass pair in case of a fault on the dc system. The firing angle can also be increased to 90° to bring the dc voltage to zero. This will prevent the ac system or generator from supplying additional energy to the fault. This is not possible with a diode bridge. Additional ac or dc side circuit breakers are required instead. AC circuit breakers could be placed between the generator and the rectifier. However, this case will require breakers with a high current clearing capability. The use of dc current interruption or limitation devices has also been considered for this project, and is discussed in Chapter 3.

The use of a diode bridge does not pose serious problems for the voltage droop scheme, since the rectifier is always operated in a constant firing angle mode. However, it will not be able to enter any of the protective modes, and must instead depend on generator controls when it approaches its limits, rather the cleaner rectifier firing controls discussed earlier. The diode rectifier-unit generator arrangement can also be used with converter optimized generators.

4.2 Direct Connection of Generators

4.2.1 Unit-Connected Generators

The replacement of the ac transmission system with a superconducting dc transmission system makes it possible for many, or possibly all of the generator stations to be unit-connected. Generating stations located within some ac systems will be present as well, but many generating stations are located away from local loads. These generators will feed only rectifier terminals, with no additional connections to ac transmission systems or loads.

ADVANTAGES OF UNIT-CONNECTION

Little or no harmonic filtering The generator will absorb the harmonics from the rectifier, so it designed must be specifically for connection to a rectifier.

Little or no capacitive support The generator can supply the reactive power needed to support the firing delay of the converter, so it will not be necessary to have large banks of capacitors present. It may be preferable to have some capacitors present to be able to operate the generator at an optimal level, without the constraints of supplying leading VArs.

Diode bridge at the rectifiers There is less of a need for fast voltage control or current control at the rectifier end of the system. This would save the cost of setting up thyristor valves and their firing controls.

Fewer transformer stages are needed There is no longer a need for a transformer to connect the generator to the ac system.

Less ac switch gear is needed Fewer ac circuit breakers and associated protective devices are needed when unit-connection is used.

Optimal frequency operation The generator is no longer required to operate in synchronization with the ac system. It is only supplying a rectifier, so it can change its frequency over an operating band to keep the generator operating at its optimal level. This is especially valuable for hydro-electric plants and wind power plants.

DISADVANTAGES OF UNIT-CONNECTION

Slow response time of generator controls The voltage control loop of the generator is dominated by the dynamics of the field control loop, which has a large inductance, resulting in a large RL time constant. This limits the rate of change of the voltage supplied to the bridge.

Controlling faults on the mesh The generator itself will be affected by the faults, without having an ac system to help isolate it. This is less of a problem for a superconducting dc system.

Larger commutation overlap angle The commutating reactance for a unit-connected generator rectifier pair will be much larger than that of an ordinary rectifier. This is due to the addition of the machine transient reactance to the transformer leakage reactance. This results in a larger overlap angle for rectifier and lowers its power factor further (for a controlled bridge). This also increases the likelihood of double commutations in each cycle [37].

Generator harmonic de-rating Converter harmonics are normally absorbed by filters. However, the unit-connected generator is designed to absorb the harmonics in the stator and rotor. The harmonics will cause additional electrical losses in the generator requiring de-rating of the generator. To supply a twelve pulse bridge the generator will need to be de-rated to 96.5% for 100 MW machine [49, 50].

Generator current limit The MVA limit of the generator will be seen by the rectifier as a current limit. The behavior of the generator-rectifier pair changes drastically as the generator approaches is limits [51].

Supplying the LVDC system with a unit-connected generator provides additional savings that are not possible with normal unit-connection. The low dc transmission voltage eliminates the need for a converter transformer to step-up the generator voltage to the transmission voltage level. The allows for the direct connection of the generator to the rectifier bridge. The implications of this option will be considered in more detail below.

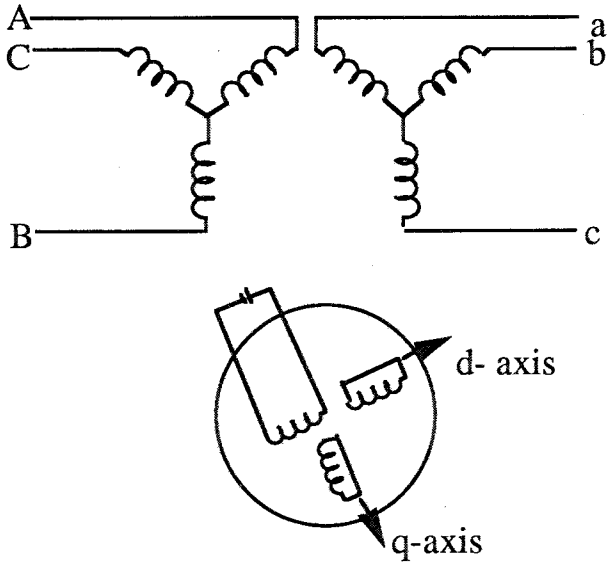

Figure 4.2: Six-Phase Generator

4.2.2 Twelve-Pulse Operation

The direct connection of the generator to the stator eliminates the possibility of using the transformer connection to create the 30° necessary for twelve-pulse operation of the rectifier. Another means of doing so is necessary since twelve-pulse operation is desirable. One possible solution is to utilize a six-phase generator to achieve the necessary phase shift. This is achieved with a six-phase stator made up of two three-phase winding sets [52, 53]. These winding sets are normally offset by 30° for twelve pulse operation [54, 56]. Such machines are presently utilized in industrial applications [55]. Figure 4.2 shows the equivalent circuit for this generator design. The six phases are designed with two sets of wye-connected three phase windings offset by 30°.

4.2.3 Bipolar DC Systems

The superconducting network will be connected in a bipole. This brings up additional questions about the design of the generator. Will it be necessary to have separate generators for each pole of the bipole, as shown in Figure 4.3(a)? This may result in the need for rather small generators in some cases, and this may not be economical. The study system considered in Section 3 contained 120 MVA generators. The other option is to connect both poles to the same generator as shown

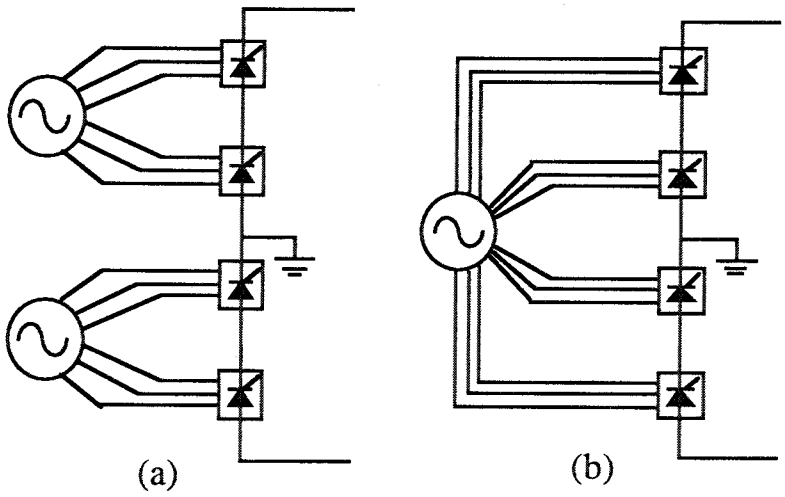

Figure 4.3: Options for Connecting Unit-Connected Generators to a Bipole

in Figure 4.3(b).

Connecting both poles of the dc system to the same generator poses some difficulties in the design and protection of the generator. It will be necessary to insulate the windings that feed the two poles from each other due to the voltage difference across the poles. The neutral points of the winding sets that feed each pole will also be at different potentials. Figure 3.9 shows how the neutral point of an ungrounded wye-connected supply feeding a rectifier bridge floats to an average voltage of one-half of the dc transmission voltage. Therefore the neutral points of the windings feeding the two halves of the bipole cannot be connected directly together. The implications of this are explored further in the section on grounding in Chapter 3. A bipolar system can still use either six-pulse or twelve-pulse bridges. However, the need for separate windings for each side of the bipole will require a six-phase generator to feed a six-pulse bridges, and a twelve-phase generator to supply a twelve pulse bridge. The stator windings feeding each pole of the bipole must also be in phase with those of the other pole to minimize harmonic currents on the neutral. Figure 4.4 shows the configuration for a twelve-phase generator feeding a parallel connected twelve-pulse in a bipole. The parallel connection of modules is needed to supply high current levels to the dc system.

It is very important to operate generator-rectifier combination shown in Figure 4.3(b) with balanced currents on both poles of the bipole. The two poles are now coupled magnetically

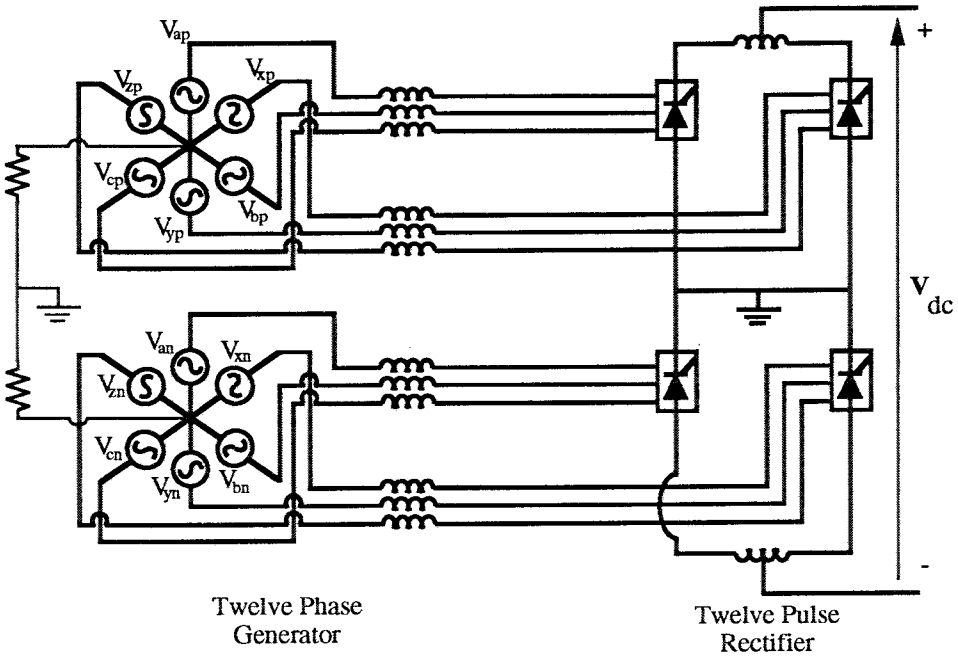

Figure 4.4: Twelve Phase Generator Supplying a Twelve-Pulse Bridge

through the generator. Monopolar operation would be very inefficient in this case. However, monopolar operation is not needed to provide additional redundancy since the mesh connection provides alternate current paths. Therefore, the rectifier should be controlled to maintain balanced currents on each pole of the bipole. This will also minimize the dc component of the neutral current on the dc system.

Another possible way to implement a twelve pulse bridge is two put a 30° between the inputs for six pulse bridges on opposite poles of the bipole. This could eliminate the need for parallel twelve pulse connections of bridges. The dc current and voltage would still see twelve pulse bridge. This scheme will have some problems in a system with grounded neutral points on the dc system. Figure 4.5 compares the neutral currents for cases with and without phase shifts across the poles. Figure 4.5(a) shows a case with no phase shift between the poles. There are simply six-pulse bridges on each pole. The neutral current is fairly small, and is dominated by sixth harmonic. Figure 4.5(b) shows a case where there is a 30° phase shift between the six pulse bridges on each pole. Now the neutral current has a 30 hertz component, and a magnitude much larger than in the previous case. This is still small compared to the dc line current ($6000A$). So this is feasible in some case, and may not be desirable in other cases. It can also be filtered if necessary.

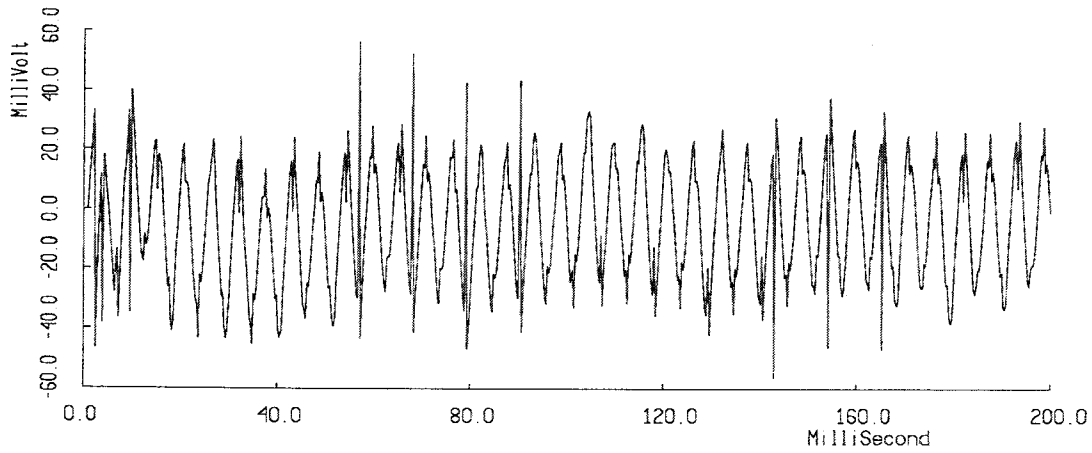

(a) Ground Current with No Phase Shift Across Bipole

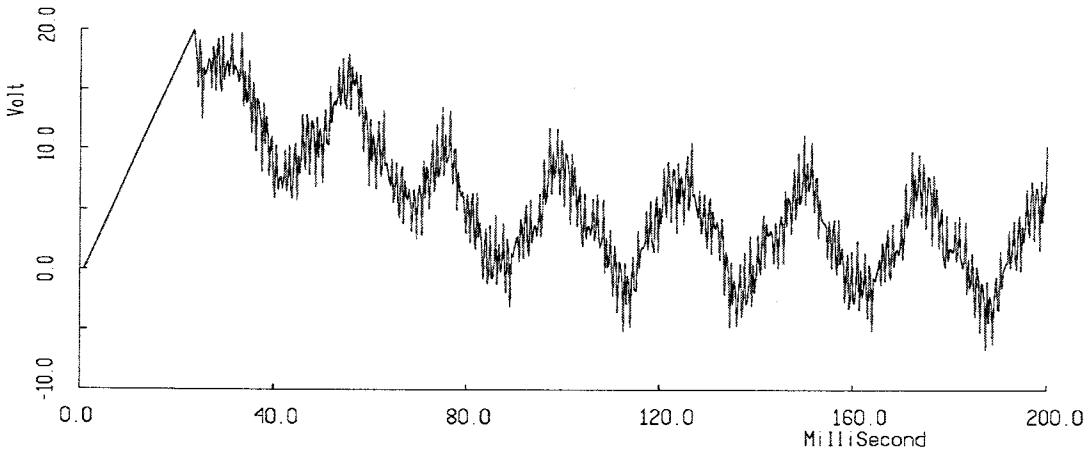

(b) Ground Current with 30° Phase Shift Between Poles

Figure 4.5: Comparing Six and Twelve-Pulse Operation Across Bipole

4.2.4 Converter Optimization

Conventional synchronous generators are designed to provide an ac power system with a sinusoidal voltage source. This is done by designing the generator with a sinusoidally distributed stator winding for each phase. This results in a sinusoidal flux distribution in the air gap. This design leads to fairly high levels of harmonic distortion when the generator is connected to six-pulse rectifier. The rectifier draws rectangular current pulses, each with a duration of 120°. A generator that is designed to supply rectangular voltage and current waveforms will be much more efficient, and will have decreased current current harmonics on the dc side. The converter connected to this machine can use a smaller dc smoothing reactor as a result.

The stator of the generator can be designed to supply optimal waveforms to minimize harmonics and switching losses. This design is feasible here due to the direct connection of the generator. The basic ideas behind converter optimized machines were discussed in [63, 64, 65] for low power synchronous machines. The optimal generator would be designed to have rectangular magneto-motive force (mmf) waves crossing the air gap. This causes quasi-rectangular voltage waveforms. The current waveforms will also be rectangular if the machine is connected to a rectifier. This should allow up to a 15% gain in overall efficiency [63]. This is called a concentrated winding machine (CWM), since each phase winding will be concentrated with one phase per slot. It will not be difficult to parallel windings within the slots or between sets of slots.

Figure 4.6 shows the general topology for a two pole, six-phase generator. The stator windings will be placed in discrete slots with the distribution shown. This will create quasi-rectangular mmf waveforms. But this only occurs during open-circuit operation of the machine. The mmf waveform will have a peak at one end when the machine is loaded. This can be corrected if the generator has a salient pole rotor with a tapered pole face. Figure 4.7 shows the rectangular equivalent of the salient pole CWM. Salient pole rotors are not practical for high speed turbogenerators, although they would work for lower speed hydrogenerators. Some of the effects of the tapered pole faces can be mimicked in a round rotor machine. McLean [65] discusses a scheme for accomplishing this through the distribution of the rotor windings.

Figure 4.8 shows a simulation where a rectifier bridge is fed by voltage source with six-step voltage waveforms (line-neutral, square wave line-lin). Figure 4.8(a) shows the dc voltage. Notice that dc voltage is much smoother than would happen with sinusoidal sources, with much smaller

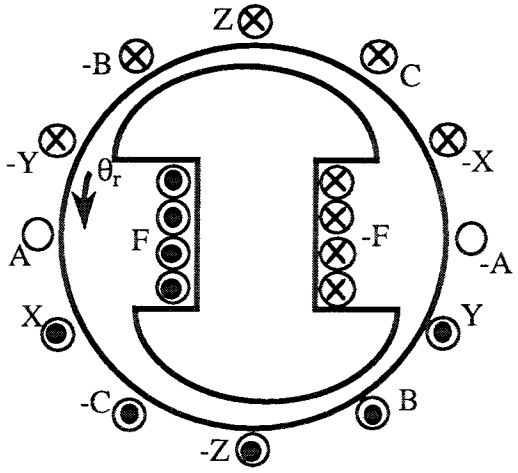

Figure 4.6: Converter Optimized Salient Pole Generator

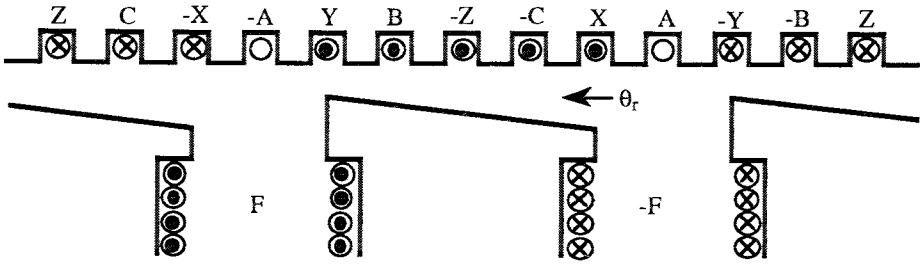

Figure 4.7: Rectangular View of Converter Optimized Salient Pole Generator

Parameter	Rating	Parameter	Rating
Apparent Power	120 MVA	x_d	1.1 p.u.
Real Power	108 MW	x'_d	0.3 p.u.
Reactive Power	52.31 MVAr	x_d"	0.145 p.u.
Power Factor	0.9	x_q	1.1 p.u.
De-Rating Factor	0.97	x_q"	0.145 p.u.
V_{ll}	7 kV	T'_{do}	5.9 sec.
Frequency	60 Hz.	T_{do}"	0.042 sec.
Poles	2	R_n	700 Ω

Table 4.1: Generator Parameters

ripple. The voltage still has dips due to commutations. Figure 4.8(b) shows the dc current. This current has a much smaller ripple content than would be present with sinusoidal sources.

4.3 Generator-Rectifier Models Used for LVDC Studies

4.3.1 Generator Models

The simulation studies used in this thesis are all based on the use of the same basic generator model. This model comes roughly from a sample generator in the appendix of [57], with some modification. Table 4.1 gives the generator parameters. A three phase generator model is used for simplicity. All three of the generators connected to the mesh use this model.

The generator is connected directly to the rectifier without an intermediate transformer stage. The generator is also de-rated by 3% to represent the effects of the converter harmonics [49]. The generator is not represented in detail. A generator supplying a converter is constantly operating in a subtransient state [51, 58] Therefore, a simpler model of the generator using a subtransient voltage source behind the subtransient voltage source is adequate if generator dynamics are not of concern. Figure 4.9 shows this representation.

The rectifier terminals assume the use of thyristor bridges, with the thyristors rated for $3000A$. Larger rectifier terminals have several modules connected in parallel. These could also be parallel connected twelve pulse bridges. Figure 4.10 shows the layout for a typical rectifier bridge. The

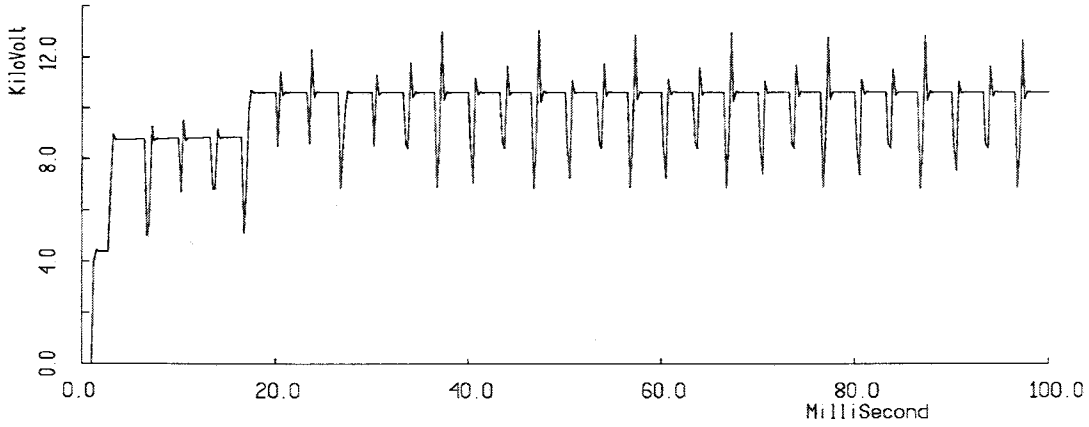

(a) DC Voltage

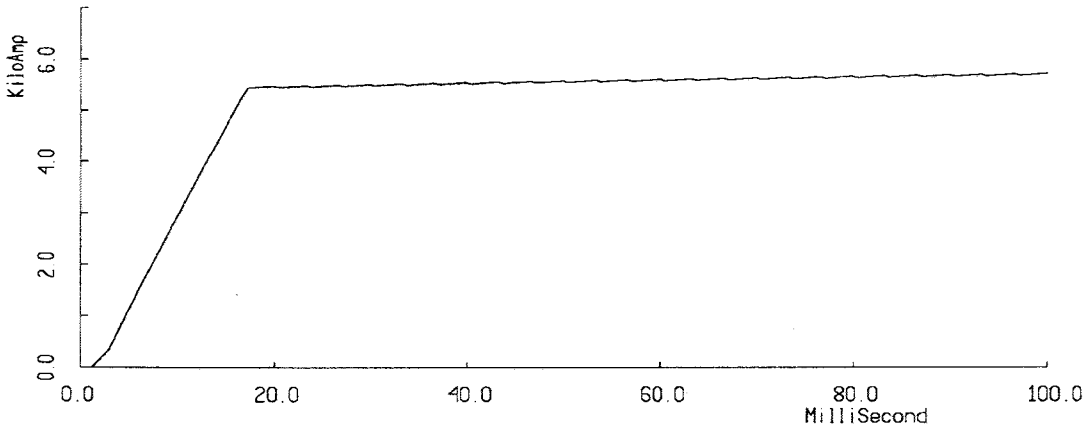

(b) DC Current

Figure 4.8: DC Waveforms for a Rectifier Fed by a Converter Optimized Source

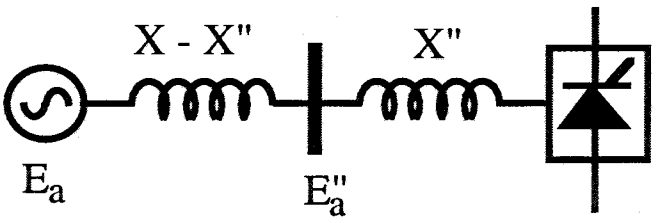

Figure 4.9: Representation of Direct Unit Connected Generator

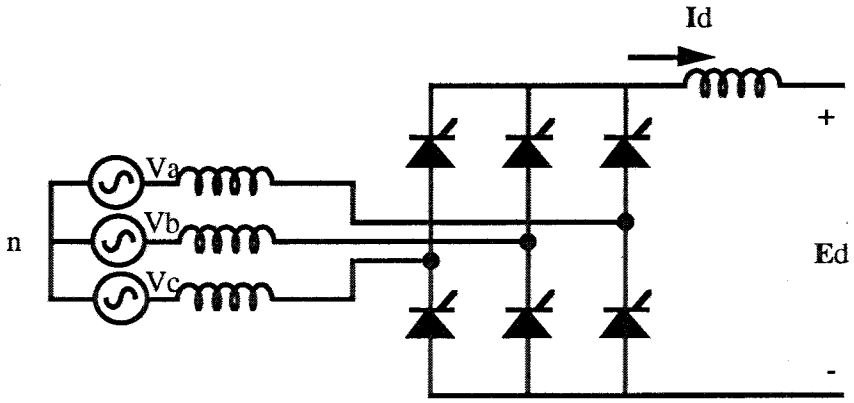

Figure 4.10: Line Commutated Rectifier Bridge

ac side inductance is assumed to be the subtransient reactance of the generator. The dc side smoothing reactance is chosen to filter the current ripple. It is designed to limit the twelfth harmonic current ripple to 5% of the rated dc current.

4.4 Conclusion

Basic concepts for the generator-rectifier interface for a superconducting LVDC transmission system have been introduced. The first generation of LVDC transmission systems would simply have a rectifier terminal connected to a strong ac system. Future upgrades of the system would see the addition of unit-connected generators, and could eventually see 12 phase converter optimized generators.

Chapter 5

The AC Distribution System

5.1 Introduction

This section of the report is concerned with AC distribution systems fed by converters from LVdc superconducting networks. A 13 kV prototype ac distribution system was selected as a basis for conducting studies and is described here. Unlike conventional distribution systems, this system is fed by inverters from a superconducting dc mesh. Also, unlike transmission systems, a distribution system is a largely passive system. This means that the inverters used in the interface with the dc mesh will be GTO based self commutated inverters instead of SCR based line commutated inverters which are more common in high power utility applications.

The operational problems in the ac system that are of interest here are closely related to the choice and proper operation of inverters. The operational problems include steady state considerations such as the ability of the inverters to provide the real and reactive power requirements of the ac system. The inverters used are capable of delivering reactive power to the ac system, thus reducing the size of capacitors for reactive power compensation. Another issue of interest is the ability of the system to operate under different line and inverter outages. These problems were studied by conducting power flow studies on the ac system. The operation of the system under faults was also studied and is discussed in this report. An important feature of this system is that fault currents are lower than those in conventional systems.

Dynamic considerations involve problems related to the ability of the inverters to supply the

required real and reactive power by following the continuous load variations in the ac system. Moreover, this is done without communications between the different inverters by using a frequency droop in a manner similar to load-frequency control in conventional ac systems. A control scheme that was developed for this purpose is discussed in another part of the report. The ability of the control scheme to function properly in the presence of abnormal situations in the ac system is important. EMTP simulations are the basis for such studies. The stability of the ac system as influenced by the inverter model is another area of concern.

This part of the report concentrates on the steady state aspects of the operation of the system.

5.2 The AC System

We see a trend in power systems for the increased use of power electronics and alternative methods for the transmission of power that differ from the conventional ac system. FACTS (Flexible AC Transmission Systems) is an example of this trend. The technology proposed here is another, perhaps more radical example. In order to conduct studies on a typical ac distribution system which may use such a technology in the future, a test system was selected. The system is based on the one described in [101], modified to represent an urban area operating at 13 kV. The system consists of 23 buses and 24 lines and cables which form three essentially radial networks. Each of these radial networks is fed by a bank of inverters connected to the superconducting dc mesh. The rating of each converter module is 10-15 MW. The total system load is 100 MW. The load model consists of industrial and commercial components operating at a power factor of 0.9 after compensation. In order to consider the possibility of a parallel supply from the backbone 69 kV ac system, transformers are available at two of the three substations. This gives an opportunity to model both active and passive ac systems.

5.3 Steady State Operation

An ac system with an embedded dc system can be described by adding additional equations to the power flow model. From the ac system side, the interface with the dc system can be represented by three converter banks which can supply the real and reactive power requirements. The results of the power flow studies conducted on the system are summarized in Table 3.

The power flow studies give an idea of the power ratings required at each inverter bank. However, these are not used to decide the set-points for inverter real and reactive power outputs which vary according to the instantaneous changes in load.

For the prototype ac distribution system considered, the settings for the inverters were optimized manually using repeated power flows and engineering judgment. However, for a larger system, this will not be practical. Our results with the 13 kV prototype system used in a networked configuration, indicated that the real power losses were minimum when each inverter bank supplied the load in its own subsystem. Some tradeoff was involved between loss minimization and minimizing loadings on critical feeders. Similarly, the reactive power losses were minimized by adjusting the voltage magnitudes at the inverters. For radial operation of the system, the problem becomes even simpler. The optimal settings for radial operation were close to those obtained for networked operation of the system.

The entire transmission network has been represented by a superconducting dc mesh in this project. However, conventional ac transmission network will always be available as an alternative path for transmission of power. An obvious question is how to dispatch the power so that the total operating losses are minimized. With the inclusion of detailed converter models incorporating losses, an Optimal Power Flow (OPF) can be formulated which will include, in addition to the ac system power flow equations, the fundamental frequency converter equations and the dc system constraints. The OPF would have to consider losses associated with the dc system which are described in an earlier section on economics of superconducting transmission.

From	To	kV	miles	Circuits	MVA	R(pu)	X(pu)	B(pu)
660	663	12	1	2	16	0.09	0.200	0.000
660	664	12	2	2	16	0.180	0.390	0.000
660	665	12	0.5	1	4	0.170	0.230	0.000
660	666	12	0.5	2	16	0.045	0.100	0.000
660	673	12	2.5	2	16	0.224	0.500	0.000
661	672	12	3	1	8	0.540	1.070	0.000
661	676	12	2	3	21	0.135	0.292	0.000
662	682	12	1	2	16	0.090	0.195	0.000
662	683	12	5	2	8	0.900	1.950	0.000
662	684	12	4	2	16	0.360	0.780	0.000
663	669	12	3	2	16	0.270	0.590	0.000
664	670	12	2	1	8	0.360	0.780	0.000
666	671	12	3.5	2	8	0.600	0.810	0.000
667	673	12	1	2c	20*	0.020	0.012	0.008
667	674	12	0.5	1c	10	0.005	0.003	0.008
669	678	12	2	1	4	0.679	0.920	0.000
670	679	12	1.5	1	4	0.510	0.690	0.000
671	679	12	2	1	4	0.679	0.920	0.000
673	676	12	1	2	16	0.090	0.195	0.000
674	675	12	0.5	1c	10	0.010	0.006	0.004
675	676	12	2	2	16	0.180	0.390	0.000
676	680	12	1	2	8	0.169	0.229	0.000
680	681	12	1	2	8	0.170	0.230	0.000
681	682	12	1	2	16	0.090	0.195	0.000

Table 5.1: Line and Cable Data for the Prototype AC System

Bus	Section	p.f.	MW	MVAR	Q_c(MVAR)
660	I	0.9	15.62	7.56	
663	I	0.9	4.37	2.71	-0.61
664	I	0.9	5.00	3.09	-0.67
665	I	0.9	2.50	1.21	
666	I	0.9	1.25	0.77	-0.17
669	I	0.9	2.50	1.54	-0.33
670	I	0.9	1.25	0.60	
671	I	0.9	3.75	2.32	-0.51
678	I	0.9	1.25	0.60	
679	I	0.9	3.79	1.63	
661	II	0.9	12.5	6.05	
667	II	0.9	3.75	1.81	
672	II	0.9	2.5	1.21	
673	II	0.9	6.87	4.26	-0.93
674	II	0.9	1.25	0.60	
675	II	0.9	1.87	0.90	
676	II	0.9	1.25	0.77	-0.17
662	III	0.95	12.5	3.90	
680	III	0.9	3.75	1.63	
681	III	0.95	1.87	0.58	
682	III	0.95	1.87	0.58	
683	III	0.95	2.50	1.08	
684	III	0.95	6.25	1.95	

Table 5.2: Load Levels in the Prototype AC System

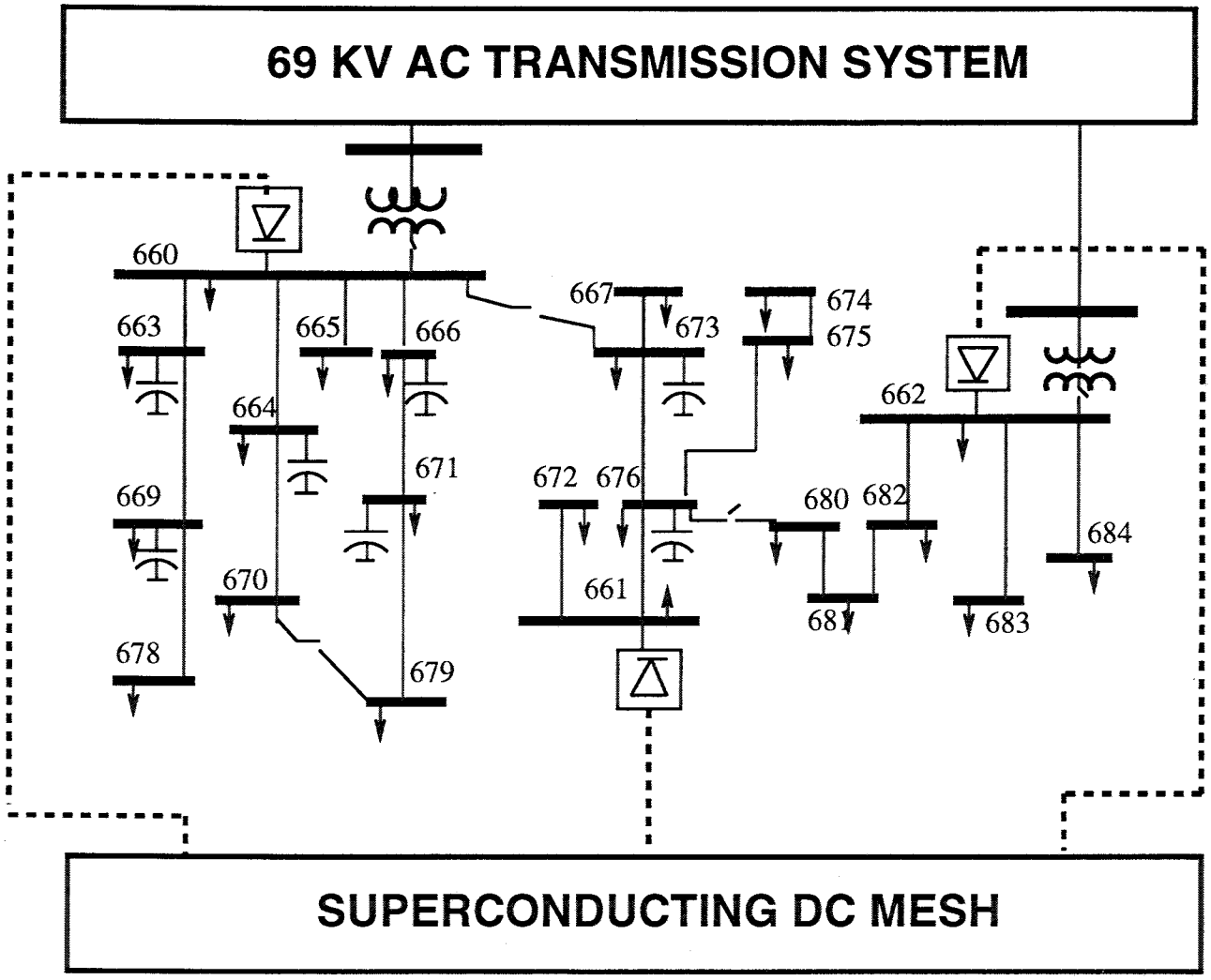

Figure 5.1: The 13 kV AC System

Bus	P_G MW	Q_G MVAR	P_L MW	Q_L MVAR	V(pu)
660	41.76	18.82	15.62	6.80	1.05
661	30.32	10.59	12.50	5.44	1.04
662	29.04	16.24	12.50	5.44	1.04

Table 5.3: Power Flow Results for AC System: Peak Load

5.3.1 Operation Under Inverter Outages

Unlike conventional systems where a single large transformer may feed a radial distribution system, this system has multiple inverter units operating at a substation. In the event that one of them fails, others can be switched on. Depending on how critical it is to maintain uninterrupted supply, sufficient overload capacity can be built into the inverter banks. In the event of the loss of a complete substation it would become necessary to connect two radial subsystems and supply both from one inverter bank. A consequence of this kind of scenario is that the system may no longer be radial and bidirectional power flow is possible. This complicates the design of protection schemes which are usually based on a radial design in which abnormal conditions are isolated by interrupting service at a point nearest to the fault.

5.4 Operation Under Faults

The representation of the primary ac supply by converters results in some differences from conventional distribution systems. Under fault conditions, the converters as seen by the ac system are best modeled as current sources instead of the usual voltage behind transient reactance model used for conventional systems. Current levels in the self-commutated inverters to be used in this system are limited by control action and device limits to levels not too far in excess of the rated load currents. Typical values range from 1.5pu to 2.0pu although currents of 3.0pu may be permissible momentarily. Therefore, fault current levels are lower and make the task of detecting faults on the ac side more difficult. Conventional overcurrent relays would not be sufficient in the design of a protection system. Moreover, the fault behavior is different for networked and radial operation of the ac system.

Although lower fault currents would force changes in present protection schemes, they provide advantages such as the reduction of current stresses on equipment and the elimination of current limiting fuses.

Faults could also occur inside the converter itself. This possibility makes the task of limiting currents to below a critical level more difficult. To prevent the GTOs from being destroyed while attempting to turn-off higher than critical currents, it is necessary to override the gate signals when such a condition occurs [96]. Under such situations, the converter may switch to an externally

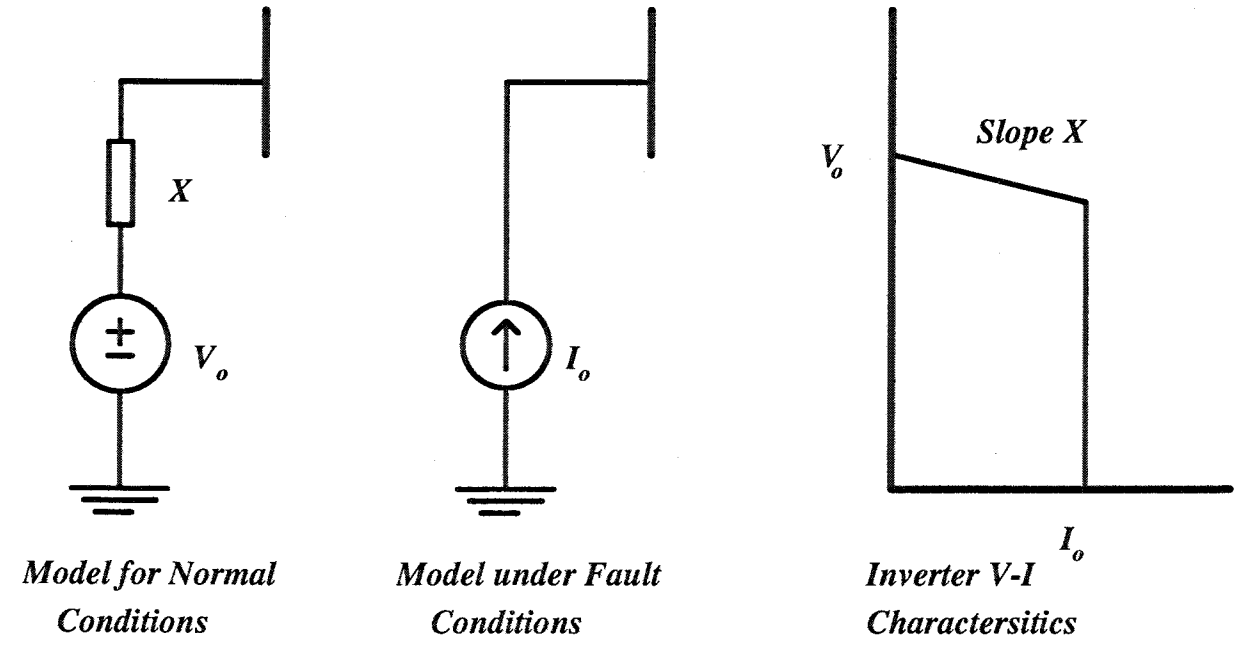

Figure 5.2: Inverter Representation

commutated mode, thus absorbing reactive power instead of supplying it, and cause a disturbance on the ac system. Strategies for protection of voltage source inverters have been discussed in [97].

5.4.1 Voltage Sags on Unfaulted Feeders

One consequence of low fault currents that has not been considered so far is the issue of voltage sags on unfaulted portions of the network. To understand the problem, consider the substation and two feeders shown in figure 5.3. Let us assume for the moment that the system is a conventional one and the substation at bus 662 is fed by a generator. If a fault is applied at bus 684, the voltage at bus 662 drops and as a result, the voltage on the unfaulted portion of the network (bus 683) also drops.

It is easy to see that the voltage sag at bus 683 is a direct consequence of the high fault current in 662-684. The voltage sag can be improved if the fault current is limited to a lower value by using a fault current limiter (FCL). FCLs have been used successfully in distribution systems to reduce currents of 3900 A to 2140 A and improve voltage sags from .33 to .9 per unit [102]. However, to realize any benefit from the FCL as far as voltage sags are concerned, the location of the FCL

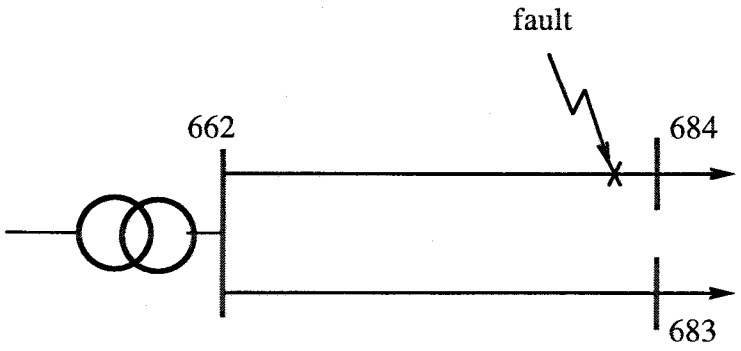

Figure 5.3: Fault applied at bus 684

is extremely important. Figure 5.4 shows two possible configurations for applying the FCLs. In the first case, the current in the faulted feeder is reduced while the current in the unfaulted feeder is unaffected. This configuration is desirable for improving the voltage sag. In the second case, the current in both feeders is affected hence this is not a desirable configuration. However, it is precisely this configuration that exists in inverter fed systems that are fed from superconducting LVdc systems. Recall, that these systems were modeled as being fed by voltage sources under normal conditions. Under fault conditions, the model was switched to a current source of around 2 per unit. Therefore, a parallel can be drawn with systems operating with FCLs.

In order to improve voltage sags in inverter fed systems, a number of things can be done. An obvious question is to ask what kind of current levels would be required to ensure satisfactory operation. Note that although individual GTOs are constrained by device limits there is no reason why they cannot be hooked up in configurations which will provide the necessary current. In addition, an FCL can be used (possibly superconducting) in the faulted circuit. However, a better solution would be to have multiple small inverter modules at the substation, each connected to a single feeder as shown in figure 5.5. The different modules would have interconnection capability and the cost of the back up or redundant units within the substation would remain unaffected. However, one would require individual controllers on each module. This might raise costs but would improve reliability of the system. The different modules would of course have to be synchronized before any interconnection. Such interconnection would be needed if more than one feeder is to be supplied by one converter module. This could be required under low load conditions when only one converter module needs to be kept on. It could also be required if one of the modules fails.

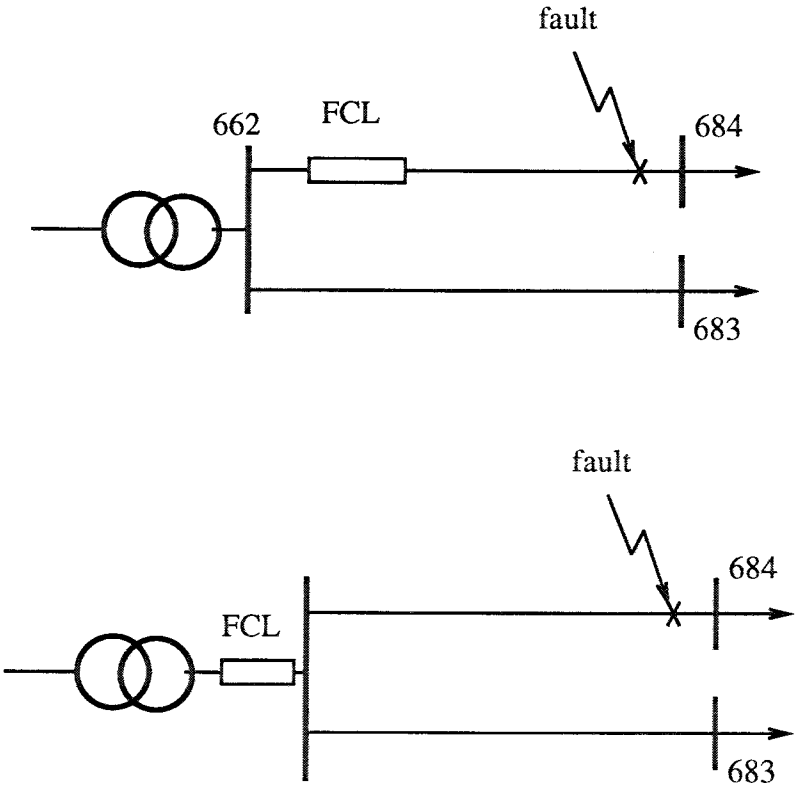

Figure 5.4: Configurations for applying FCLs

5.4.2 Operation of Faulted Feeders

Another issue of concern is the operation of the faulted feeder. This would depend on the type of feeder. If we assume that the feeder would be the similar to a typical feeder today, i.e. with a breaker at the substation and overcurrent fuses at the loads with perhaps a recloser somewhere between the two, there could be some problems. If a fault occurs at the load, the fuse would require a longer time to operate. This might require the recloser operation to be modified. The relay at the substation could be replaced by the inverter which would sense the changes in currents under faults and then clamp the current at its limit. It could operate the breaker if needed. So the inverter would limit fault currents by its operation. One concern would be the inverter switching to its current limiting mode under transients caused by induction motor starting etc. This may infact be desirable from the ac distribution point of view. One of the concerns in distribution systems is avoiding transient overvoltages and voltage sags. Inverter fed systems would naturally help in this. The issue of voltage sags is however, not as simple. If the inverter at the substation is operating at its current limit under a fault and the breaker has not been tripped, the fault will

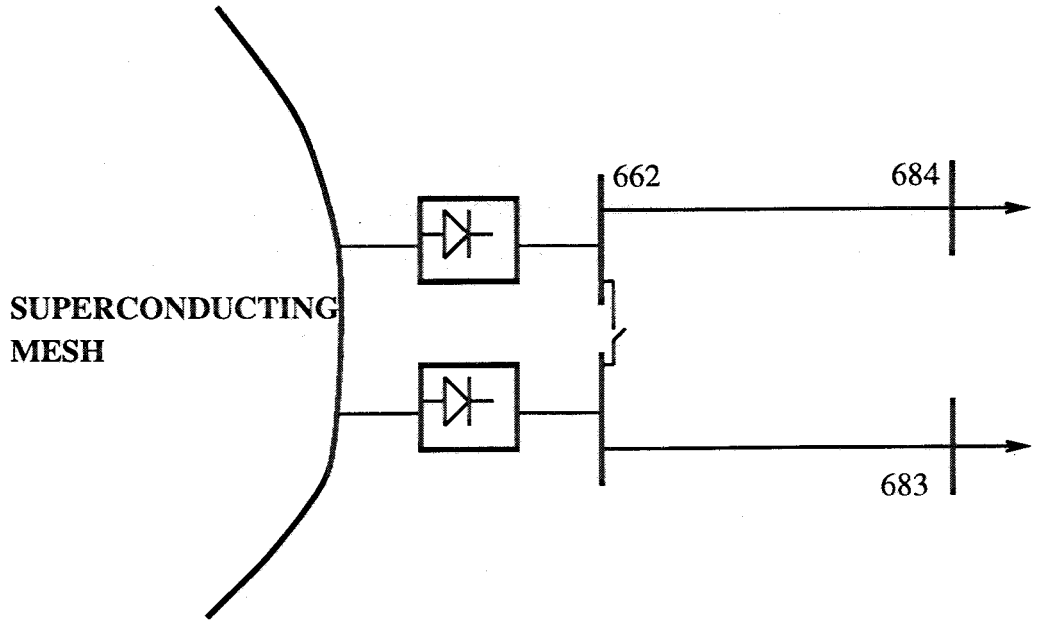

Figure 5.5: Proposed feeder configuration for increased fault isolation

be cleared by the operation of a fuse after some time which is longer than usual due to the lower current. This would mean that the voltage sags at buses between the fault and the substation are not only higher but also longer. If the breaker at the substation is opened, it means disrupting the operation of the entire feeder. High impedance faults could also pose problems. The protection scheme would have to consider all these factors in detail. The operation would become much simpler if microprocessor relays were available down the feeder, and the characteristics of the relays could be tailored to meet the requirements. Perhaps, this may not be an unreasonable assumption when such technologies are finally put to use.

5.4.3 Load Contributions to Fault Current

The other question of interest is the contributions of loads to the fault current. Besides the inverters, induction motors, which form a significant portion of the load, can also feed the fault.

The difference between the response of induction motors as compared to a synchronous machine during a fault lies in its method of excitation. In a synchronous machine the separate dc excitation is unaffected during a fault and is able to deliver large transient currents during towards the fault. Induction motors on the other hand are excited by the line voltage which drops drastically during

a fault, perhaps even to zero if a three phase fault occurs at the motor terminals. However, the machine's residual excitation continues to force currents into the fault for a few cycles. These currents are limited only by the impedance of the machine. The initial ac component of this current is usually represented by the motor sub-transient reactance (it is accepted practice to use the locked-rotor reactance). The initial frequency of the ac component differs from the system frequency only by the slip and then drops as the motor slows down. This change in frequency can be neglected for the first few cycles. The magnitude of the ac component is considered to be significant only for the first four cycles after which it is neglected. Its decay during this period can be accounted for by using appropriate multiplying factors [103]. If sufficient information about the motors is not available, the short circuit contribution may be estimated as the sum of four times the rated currents of the motors comprising the group. This corresponds to a reactance of 0.25pu based on the kVA rating of the load at rated voltage. The 'four times rated current' approximation is based on the assumption that the group of motors consists of 75% induction motors and 25% synchronous motors. It is however acceptable for an all induction motor load also. Zero sequence currents are neglected as most induction motors are wound in the open delta configuration.

Traditionally, protection engineers neglect load currents by assuming that they are much lower than the fault currents. Short circuit studies conducted on the test system reveal that the level of fault currents from the load side (induction and synchronous motors) are non-negligible. In view of the reduced current contributions from the inverters their consideration in the design of a protection scheme becomes important. One argument against, consideration of load contributions to fault currents is that their short duration. This should not pose a problem for the extremely fast operation of the protective equipment available. For example, fault current limiters can operate at the first current zero. Moreover, the inverters are capable of extremely fast response.

5.5 Interconnection of Radial Systems

Although the ac systems considered are radial, there can be occasions when it may be necessary to interconnect two or more of these radial subsystems. Such a situation may arise, for example, if a fault occurs in one subsystem which isolates a part of the system from the inverters in that system. It may also occur if some of the inverters are inoperable and the load in one system has to be fed from inverters in the neighboring subsystem. The latter scenario results in a situation

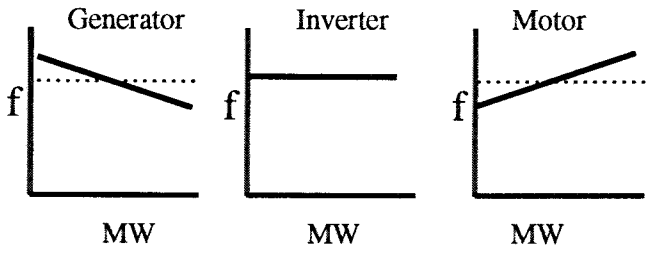

Figure 5.6: Natural Droop Characteristics

where inverters separated by some distance have to operate in parallel to supply a geographically distributed load. In a conventional system, frequency synchronization at the distribution level is assured by the HV system. However, in the proposed system this is done according to the "frequency droop characteristic" of the inverters which must be built into the control scheme. As shown in figure 5.6, inverters do not have any natural frequency droop unlike generators and induction motor loads. Frequency droops have been used before in ac systems fed largely by inverters. An example is the island of Gotland in Sweden [36, 37] which is fed by a single HVdc link. The sharing of power between two inverters according to their droop characteristics is illustrated in figure 5.7. Assume that the inverters are operating at output P_1 and P_2 represented by position 1 in the figure. A load increase in the system will be shared by the two inverters according to their droop characteristics. This is a result of the fact that the two inverters must settle to operate at the same frequency which is a system wide parameter. This process is referred to as natural generation governing. Since this is a result of artificially built in droops, distribution of power between the two inverters as a result of natural generation governing action can be controlled to some degree. However, the system frequency drops and has to be restored to its nominal value. This can be done by shifting the power-frequency characteristic for each inverter by means of supplementary regulation. A more important function of supplementary regulation is that it allows a desired sharing of power to be obtained between the two inverters as indicated by position 2. One factor that we have not mentioned is the load governing characteristic which is positive. In effect, the governing characteristic is the algebraic sum of the generation governing characteristic and the load governing characteristic. This combined curve is also negative like the generation governing characteristic. We note two important differences between the operation of this scheme from the manner in which it operates in conventional systems. First, the load sharing can be influenced by building desired natural governing characteristics. Secondly, in conventional

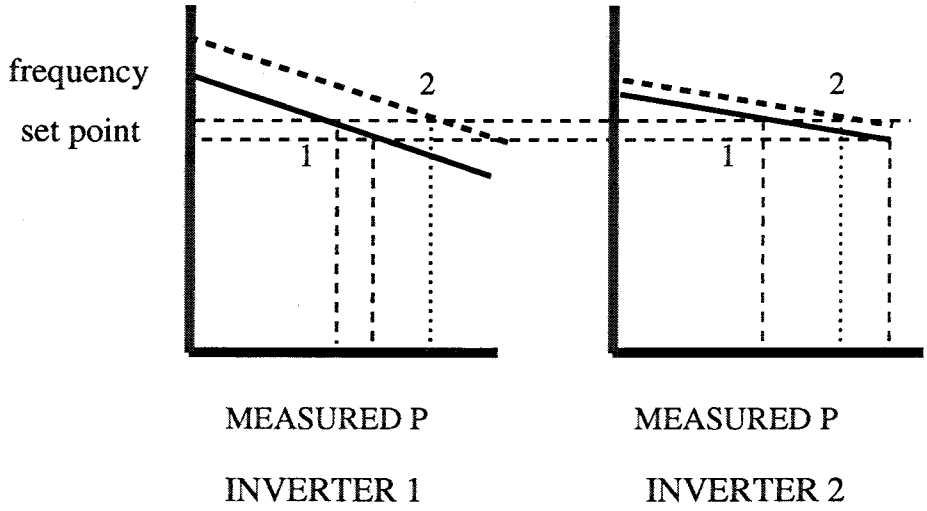

Figure 5.7: Parallel operation of two inverters with droop

systems supplementary regulation is a much slower process than governing regulation. This need not necessarily be the case with inverters. Moreover, the amount of supplementary regulation needed would be less. These facts suggest that with proper control settings, such systems may hold promise over conventional ones.

A similar scheme can be used for voltage droop and reactive power sharing. However, the voltage is not a system wide quantity due to voltage drop in the lines. Hence there are differences between the operation of frequency droops and voltage droops. The parallel operation of inverters feeding a passive ac system is discussed further in a later section.

5.6 Synchronization with AC Systems

It is possible that a radial distribution feeder may already be connected to the 69 kV ac subtransmission network before it is interfaced to the dc mesh by the inverters. Under such a scenario and also under interconnection of two radial feeders connected to inverters, one has to deal with the issue of inverter voltage synchronization. The output voltage of the inverter (or rather its time-integral) must be matched both in magnitude and frequency to that of the ac system that it is to be connected to. Simulations performed using ACSL and EMTP to study the synchronization process indicate no difficulties with proper control settings.

5.7 Conclusion

This part of the report discussed issues related to the operation of ac distribution systems fed by a superconducting dc mesh. Studies done on a prototype 13 kV distribution system revealed that such inverter fed ac systems would have lower fault currents requiring changes in present protection schemes. The configuration of the inverter banks was found to have an effect on voltage sags on unfaulted feeders. It was observed that building small modules, each feeding a separate feeder would help solve the problem of voltage sags. In addition, a detailed EMTP model of a PWM voltage source inverter was implemented using switches. Results from tests conducted with this model matched those obtained from ACSL simulations conducted independently. The model provides a basis for conducting studies on inverter response to faults in the AC network.

Chapter 6

The Inverter Interface

6.1 Introduction - The Inverter Interface

The interface between the DC superconducting transmission mesh and the AC system loads forms a very important part of the overall transmission system. The economics, reliability and stable performance of the transmission system are critically dependent on the operation of the inverter interface. For this reason, it is very essential that the issues pertaining to the inverter interface be understood in detail. Most of these issues can be conveniently treated under two headings: the inverter topology, and the inverter control scheme. The total inverter interface scheme can then be evaluated on the basis of pre-determined performance and cost criteria. Some of the considerations regarding the inverter interface have been presented in previous project reports [1, 2]. It must be mentioned here that some features of the inverter control scheme are dependent on the inverter topology. However, others are dictated by performance requirements, and it is useful to make a distinction between the two.

There is no dearth in the technical literature of different inverter topologies suitable for applications in the ranges of watts to the megawatts (as in HVDC transmission applications). The obvious choice of an inverter topology for application in the superconducting meshed DC transmission system would lie in the high power range, and the topology would preferably be a proven one. HVDC transmission is one such proven technology. However, to this day, the vast majority of HVDC transmission systems are either back-to-back converters, or point-to- point transmission systems. These systems typically have AC systems, either strong or weak, at both the sending and

the receiving end. This permits the use of line-commutated current- source rectifiers and inverters which draw reactive power from the AC systems. In the absence of any active AC generation on the receiving end (a "stand-alone system"), one may be required to use a force-commutated inverter topology which employs gate control switches like Gate Turn Off (GTO) thyristors.

For the purpose of inverter selection, the emphasis of the present project is on force- commutated inverters, which allow interconnection to weak AC systems and to passive, stand- alone loads in an AC system which has no active power generation from synchronous alternators.

In addition to HVDC transmission, another utility application which uses high power inverter interfaces is Photovoltaic (PV) power generation. PV power plants are connected to the utility grid through inverter interfaces. However, at the present time, the penetration of PV generation into the transmission system remains at a very small percentage of the total system generation, and experience with central station PV systems rated above 10 MW is either small or not well documented. Since present-day large scale PV plants do not supply stand-alone loads, the inverter topology of choice has been the line-commutated thyristor inverter. In recent years, however, there has been a tendency to consider the use of force-commutated inverters for PV applications [3]. In addition, some theoretical studies have been done regarding the modelling and control of force-commutated inverters in a large scale PV environment [4].

Yet another area employing high power force commutated converters is Superconducting Magnetic Energy Storage (SMES). For this application, there is a need to charge up the SMES coil when there is excess power generation, and to discharge it into the utility transmission system during peak demand. The converter interface connecting the SMES coil to the utility grid has to be capable of handling power bi-directionally. An extensive theoretical study of force-commutated converters for SMES applications has been done in [5]. One more area of current interest is battery storage, and the interface between the battery bank and the utility grid.

The major body of work on force-commutated converters has so far been in the electric drives area, typically for traction and mill drives. Moreover, drive power ratings have been constantly increasing, and it is no longer out of place to talk of applications in the megawatt ratings for drives. It therefore proves useful to consider work done in high power drives, in addition to considering the work done in the utility environment, when coming up with a topology and control methodology for use in the superconducting DC transmission mesh. However, for such a consideration, the differences between the requirements of a drive application and an utility application must be

borne in mind. This is especially true from the viewpoint of control. A major difference is with respect to the frequency. While a drive application may require a large range of frequency and voltage variation, an utility application needs a much smaller range. In fact, the control on frequency and voltage in an utility application needs to be much tighter than for a drives application.

This project has addressed both, the topological and the control issues for the inverter interface between the superconducting DC transmission mesh and the AC system. Specific inverter topologies have been considered and evaluated. Control issues have been considered in substantial detail. The modelling of the DC mesh, the inverters and the AC system has been done using the Electro-Magnetic Transients Program (EMTP). Extensive simulations have been performed for the inverter topologies and the results are presented.

6.1.1 Overview

As indicated in Section 1.0, the issues pertaining to the inverter interface between the superconducting DC transmission mesh and the AC system can be conveniently treated under two headings: the inverter circuit topology, and the inverter control scheme. Both of these have been considered in detail in this report.

Concerning the inverter topology, there are two main classes of circuit configuration: Voltage Sourced Inverters (VSI's) and Current Sourced Inverters (CSI's). As the name suggests, the VSI ideally sees a stiff DC voltage source at its input, and the output is an AC voltage source synthesized from the DC source. In a similar manner, the CSI ideally sees a stiff DC current source at its input, and the basic output is an alternating current source synthesized from the DC source. This report will make a short review of the basic VSI and CSI circuit principles, and will then present the detailed operating principles of certain VSI and CSI topologies considered suitable for application to the superconducting DC mesh. The pros and cons of each topology will be discussed.

Concerning the inverter control methodology, the basic requirements of the control system will be established first. This will be followed by a detailed description of a control scheme suitable for the control of inverters connected to the AC system. The specifics of the control schemes for VSIs and CSIs have been considered in their respective sections.

6.1.2 Inverter Topologies

As indicated in the previous section, there are two main configurations of inverter topologies, the VSI and the CSI. The VSI sees a stiff DC voltage source at its input, and dually, the CSI sees a stiff DC current source at its input. Both topologies have been extensively used for various applications. The VSI has traditionally been used in low and medium power applications requiring very fast dynamic response. The CSI has been used predominantly in high power applications with low switching frequencies and a slower dynamic response. However, there is no well defined power range for the two, and there is a considerable amount of overlap in the applications of the two types of inverters. The present trend has been towards increased power ratings for the VSI, and increasingly the VSI's are cutting into the applications traditionally performed by the CSI. The preference of one topology over the other for use in a superconducting DC transmission mesh is far from obvious, given the current level of inverter and device technology.

Given that there is no obvious preference of one topology over the other, it is useful to define some criteria on which to base the evaluation of any candidate topology for the superconducting DC mesh. This would serve the purpose of bringing the trade-offs involving the circuit configurations into focus. The criteria chosen for this purpose could be as follows:

1: Response to abnormal operating conditions. This is one of the most important points to be considered in a utility environment. The abnormal conditions to be considered include: a) Short circuit and open circuit faults on the AC and DC sides. b) Operation with unbalanced loads on the AC side. c) Start-up of large loads on the AC side. d) Load rejection. e) Overvoltages and voltage surges on the AC system. f) Errors in firing the inverter valves.

2: Circuit Complexity. It is desirable to have a simple topology for high power applications. This not only reduces the cost, but also provides for greater reliability of the inverter interface.

3: Controllability. The inverter interface needs to address the control issues relating to both, the superconducting DC mesh, and the AC system. There could be a need to provide active damping on the DC superconducting mesh, since natural damping is not present in the resistance-less mesh. On the AC side, there is a need to control the voltage magnitude and the frequency in order to supply passive loads. The inverter topology should be such as to permit such a control.

5: Filter requirements. The voltage demanded by the AC system is ideally a set of balanced

three phase sine-waves with a constant frequency (60 Hz) and a constant magnitude of specified value. To achieve this voltage from the switching action of the inverters, the harmonics have to be removed from the voltage derived from the inverter output. This is typically done by means of filters. It is obviously desirable to have as simple a filter configuration as possible and to minimize the size of the filter components while still achieving the desired filter action.

The VSI and CSI topologies have different control and interface requirements for both the AC and DC system interconnections. These have been considered in their respective sections.

6.1.3 The Inverter Control Scheme

This section considers the general requirements of the control system for the inverter interface. Of special interest are the control issues that arise when the inverters are feeding power into a weak AC system, or a system composed entirely of loads, with no active generation. One of the most significant requirements of the control system is that due to the large distances involved, the inverter control should not depend critically on signal communication between the various sources feeding the AC system. Signal communication may be used to enhance system performance, but must not be critical to the stable operation of the system.

As a first approximation, the AC behavior of the inverter could be modeled by an equivalent circuit composed of an AC voltage source in series with a reactance. The magnitude and the frequency of the voltage source would correspond to the fundamental component of the inverter output voltage. Such a model would be similar to the low-frequency model of a synchronous alternator. This model is adequate for a macroscopic study of the system. However, it neglects the fact that the inverter output voltage could contain substantial harmonics, and the presence of harmonics could have a major impact on the behavior of the filters in the system. Moreover, unlike the synchronous alternator, the solid-state inverter has the ability to change its output quantities with extremely low time constants. If used judiciously, this fact can be used to great advantage in achieving very tight control over the AC system behavior. However, if adequate care is not taken, the fast response of the power electronic converter could be a potential source of instability for the AC system.

This section describes the basic requirements of the control system for an inverter feeding power into the AC system. It is assumed that the inverter has the ability to feed both real and

reactive power into the system independently. The main cases of interest are:

1): An inverter feeding an isolated passive load

2): An inverter feeding a passive load in the presence of a stiff power system, as from a synchronous alternator of large capacity.

3): An inverter feeding passive load in parallel with a weak power system.

4): An inverter feeding distributed passive loads in the presence of other inverters connected to the passive system.

Inverter feeding an isolated passive load

The situation of an inverter feeding an isolated passive load is shown schematically in Figure 6.1a. In many respects this is the simplest of the three cases from the control viewpoint. The inverter supplies whatever real power P and reactive power Q that the load demands. The set-points for the overall control scheme could be chosen as the frequency and the magnitude of the inverter output voltage. The inverter could then supply the load till its maximum Volt- Ampere rating is reached. If the load increases beyond this rating, then the typical strategy is to decrease the inverter output voltage magnitude or frequency, and supply the load in a pre- determined manner which is considered adequate for the load. This is similar to the case where an inverter is used to feed a single load like an induction motor. A higher level of control may be required to control the interaction of the filter with the load, especially if the load has a dependence on frequency. However, the interaction of the inverter with other power sources is not a valid consideration for this system, because of its isolated nature.

Inverter feeding AC system with stiff AC source.

The situation of an inverter feeding an AC system with a stiff AC voltage source is shown schematically in Figure 6.1b. In this case, the source impedance Ls is small. For this reason, the voltage source is stiff enough so that the magnitude and frequency of its voltage can be considered to be constant regardless of the load or the power supplied by the inverter. Thus, the inverter does not affect the system stability, and the loads are decoupled from the inverter by the presence of the

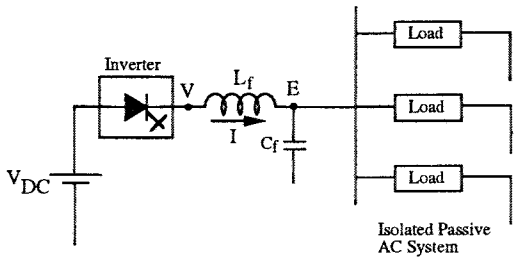

a: Inverter Feeding Isolated Passive AC System

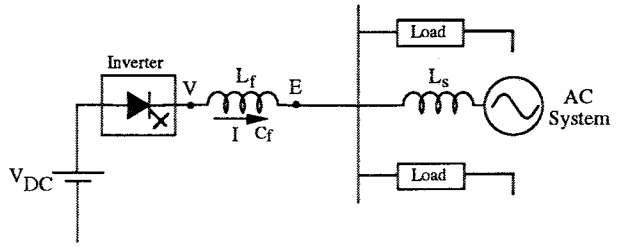

b: Inverter Feeding AC System with Stiff AC Source

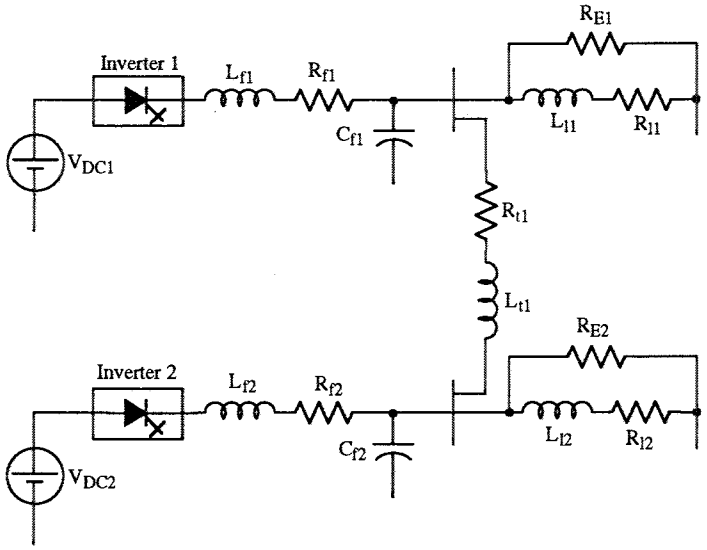

c: Two Inverters Feeding Distributed Passive Load System

Figure 6.1: Inverter Interconnections to AC System

AC source. In practice, such a situation arises for example in the case of an intermediate rating photovoltaic (PV) power plant connected to a large power grid, where the PV penetration is a small fraction of the total power carried by the power system.

In such a case, the inverter frequency is constrained to exactly equal the frequency of the AC source. The two control set-points can be chosen directly to be on the real power P and the reactive power Q fed by the inverter into the AC system. The P and Q set-points can be chosen to satisfy DC system constraints. For example, in an intermediate range PV plant, these could be chosen to satisfy peak power tracking constraints of the DC photovoltaic array.

It is well known that the real power P and the reactive power Q are decoupled to a good extent in a typical power system. The real power depends predominantly on the angular difference between the positions of the inverter voltage vector and the AC source voltage vector. These voltages are marked as V and E respectively in Figure 6.1b. The reactive power depends predominantly on the voltage magnitude difference between V and E. The P and Q set- points for the inverter can thus be translated into set-points for the angular difference and voltage magnitude difference respectively. Moreover, decoupling between the P and the Q control loops can be achieved by closed-loop control of P and Q. As regards the angle difference, it must be recognized that the inverter can have only certain specified output voltage vectors. Thus, it may be necessary to consider an average output voltage vector, which rotates continuously in the complex plane.

Inverter feeding passive loads in parallel with weak AC system

Figure 6.1b is also representative of an inverter connected to a load bus in parallel with a weak AC system. In this case, the source impedance Ls is large. This situation typically arises when the sinusoidal source (generator) is connected to the load bus by a long transmission line. The load bus voltage is now affected by both, the inverter and the sinusoidal source. The degree to which each affects the load bus voltage depends on the series impedance present in the respective interconnection to the load bus. For operation with a weak AC system, it is preferable to control the load bus voltage magnitude by means of the inverter. Since the remote sinusoidal source sets the frequency, it is not possible to have a frequency loop for the inverter. Instead, it is preferable to have closed loop control on the real power P delivered by the inverter. Thus, the inverter has P and V control at the load bus. Control of the load bus voltage magnitude by the inverter implies that the inverter supplies a large part of the reactive power demanded by the load.

Multiple inverters feeding distributed passive loads

Figure 6.1c shows two inverters feeding a distributed AC system composed of passive loads. There is no sinusoidal voltage source in the system, as was the case with the system of Figure 6.1b. The absence of a voltage which could be used as a reference for control makes the stand-alone system of Figure 6.1c rather difficult to control. The difficulty is increased by the fact that the two inverters could be separated by large distances, making communication of control signals between the inverters impractical.

Multiple inverters connected to a common AC system essentially act in parallel, and need to be controlled in a manner which ensures stable operation and prevents inverter overloads. An essential constraint is that the inverter control should be based on the feedback of signals measurable locally at the inverter, and should not depend on signal communication between inverters. Communication may be used to enhance system performance, but must not be critical to the operation of the system.

In a stand-alone system like the one shown in Figure 6.1c, the operation of the inverters directly affects the stability of the AC system. It is well known that stable operation of a power system needs good control of the real power P and the reactive power Q in the system. As indicated previously, the real power P is predominantly dependent on the power angle, and the reactive power Q is predominantly dependent on the voltage magnitude difference. It is thus apparent that the frequency of the inverter dynamically controls the the real power, since it dynamically changes the power angle. In the stand-alone system, both the frequency and the voltage magnitude are controllable. The basic control could thus be on the magnitude of the filtered inverter voltage (across the capacitors in Figure 6.1c), and on its frequency.

The inverter control scheme must ensure that arbitrary changes in the loads are taken up by the different inverters in a reasonable manner, which avoids overloading one inverter at the expense of another. This action must also be done without communication of control signals. In conventional power systems, this action is achieved by introducing a droop characteristic of the frequency with P in the control systems of the various synchronous alternators. The system frequency is thus effectively used as a communication link between the various components of the power system. A similar scheme could be applied to the inverter fed system of Figure 6.1c.

The filters used to remove the harmonics from the respective inverter output voltages present

control problems that could become rather severe in a large system with many filters. Interactions between different filters could lead to instability.

The following sections consider the details of the VSI and CSI topologies and the associated control systems.

6.2 Current Source Inverter Interface

The current source inverter (CSI) has a DC current source at its input, and specified AC currents at its output. Figure 6.2 gives the basic CSI topology. Traditionally, CSIs have been used in high power applications, including High Voltage DC (HVDC) power transmission. To date, most CSI circuits have used thyristors, and so rely on external means for commutation. Inverters used in HVDC power transmission rely on the AC power system to provide the reactive power needed to commutate the current between thyristor valves. CSI circuits using thyristors are therefore unable to provide reactive power to the AC system.

When Gate Turn Off (GTO) thyristors are used as the main switches in the CSI topology, as shown in Figure 6.2, the CSI can provide reactive power (Q) to the AC system, in addition to real power (P). In effect, the CSI is capable of four quadrant operation when GTOs are used. The operation quadrant is defined by the angle α, which is the delay angle between the AC system voltage and the firing of the CSI switches. A thyristor CSI can operate only in two quadrants:

$0 < \alpha \leq \pi/2$	1st Quadrant: Receive P, Receive Q
$\pi/2 < \alpha \leq \pi$	2nd Quadrant: Deliver P, Receive Q

In these expressions, the direction of the power flows is with reference to the AC system. In addition to these two quadrants, the use of GTOs as switches in the CSI topology permits operation in the third and fourth quadrants.

$\pi < \alpha \leq 3\pi/2$	3rd Quadrant: Deliver P, Deliver Q
$3\pi/2 < \alpha \leq 2\pi$	4th Quadrant: Receive P, Deliver Q

The expressions of P and Q and the DC bus voltage are given by:

$$P = \sqrt{3} V_{ll} I_{lf} cos(\alpha) \tag{6.1}$$

$$Q = \sqrt{3} V_{ll} I_{lf} sin(\alpha) \tag{6.2}$$

$$V_{dc} = 1.3504 V_{ll} cos(\alpha) \tag{6.3}$$

In these Equations, V_{ll} is the rms line-to-line voltage of the AC system, I_{lf} is the fundamental AC line current, and α is the delay angle. For inverter operation, α should be chosen in the second or third quadrants. In this case, from the basic theory of phase controlled converters, the DC voltage of the inverter is negative. This agrees with the interconnection to the superconducting DC mesh as shown in Figure 6.2. Also with this convention, it is to be noted that P and Q delivered by the inverter are negative.

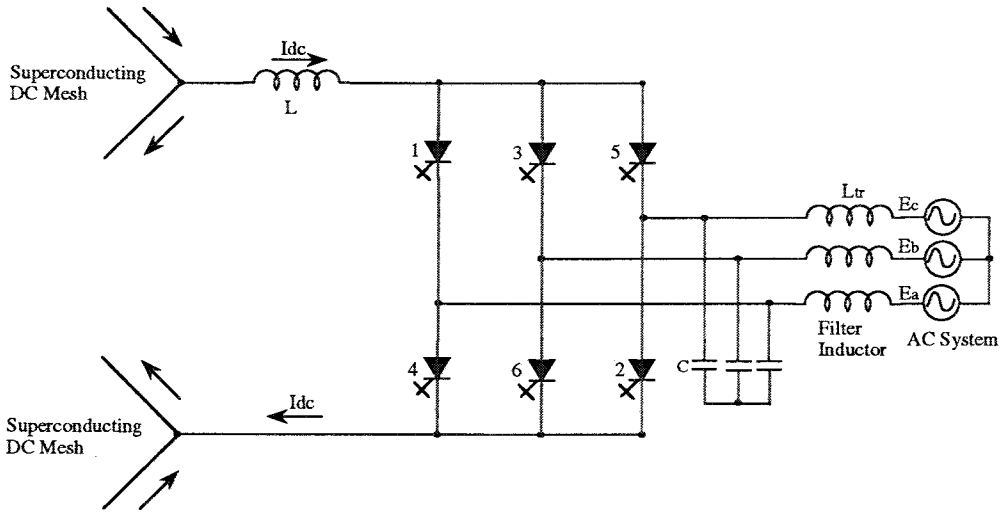

Figure 6.2: CSI Topology

In the topology of Figure 6.2, it is apparent that the phase of the CSI output currents with respect to the AC voltage can be controlled by controlling the delay angle α. If Pulse Width Modulation (PWM) is not used, the magnitude of the fundamental AC line current I_{lf} is solely determined by the value of the DC current. The DC current then needs to be controlled to control the magnitude of the AC line current. Since the DC mesh voltage and the AC system voltage are fixed, the value of the delay angle α in Equation 6.3 is fixed. The phase of the AC current relative to the AC voltage is thus fixed. Equations 6.1 and 6.2 indicate that both P and Q can be varied by varying I_{lf} but independent control of these two quantities is not possible without PWM. P and Q are related by the expression $Q/P = tan(\alpha)$.

Another problem with the CSI topology of Figure 6.2 is that the output current has substantial 5th and 7th harmonics, which are injected into the utility. The harmonic spectrum is the same regardless of the value of α. PWM can be used to reduce harmonics, but this increases losses in the inverter switches, and is not practical for high power applications.

The problems described above can be solved to a good extent by the use of a dual CSI (DCSI) topology which has been proposed by earlier researchers for use with high current applications, typically as an interface between a Superconducting Magnetic Energy Storage (SMES) coil and the utility system. This topology has the ability to control large currents, and also to control independently the P and the Q fed into the utility system without resorting to PWM. A description of this topology, its control aspects and trade-offs are described in detail in this section. EMTP simulations performed on this interface are presented and discussed.

6.2.1 Dual Current Source Inverter

The topology of the Dual Current Source Inverter (DCSI) is given in Figure 6.3. From this figure, it is readily apparent that the circuit essentially consists of two CSI circuits connected in parallel on both the DC and AC sides. This parallel connection enables the circuit to handle high currents, since each bridge is required to handle only half the total DC current. The magnitude of the AC current can be controlled by controlling the relative phase difference between the firing patterns of the two CSIs. The phase of the AC current can be controlled by controlling the firing of both bridges relative to the utility voltage. The control of magnitude and phase of the total AC current provides the ability to independently control the real power P and the reactive power Q delivered to the utility. The range of independent control is dependent on the nature of the DC source, and this issue is discussed in the section on inverter control.

An important feature of the DCSI topology is the requirement to control the sharing of the DC current between the bridges. This means that the average DC bus voltage for both the CSI bridges must be equal. In case of unequal average DC bus voltages, the DC currents in the two bridges tend to drift, and eventually, one bridge would carry all the DC current, and the other bridge would carry no current at all. The control system needs to consider this.

It is possible to get stepped waveforms by appropriate phase shifting of the two bridges. This leads to reduction of harmonics in the AC line currents without the use of PWM. The filtering

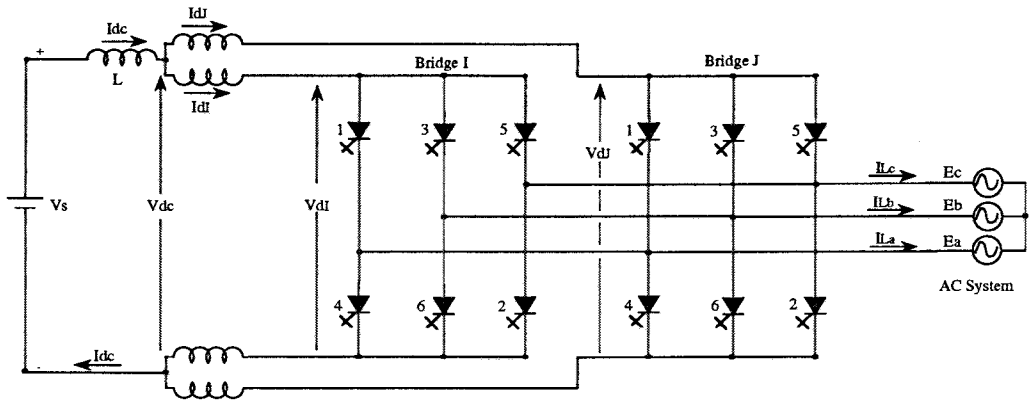

Figure 6.3: Dual CSI Topology

requirements on the AC side are reduced as a consequence.

The following sections discuss the DCSI topology and control, and present EMTP simulations on the interface of a DCSI circuit between the superconducting DC mesh, and the AC system.

DCSI Topology

As seen in Figure 6.3, the DCSI topology consists of 12 switches, effectively forming two CSI bridges. Each bridge carries half the total DC current. This current division is not inherent to the circuit, and must be achieved by appropriate control, to be described in the next section. However, for the present discussion, it is assumed that current is shared equally between the two bridges. This section develops the vector diagram of the DCSI output current vectors, and presents output current waveforms for different phase angle differences in the firing of the two CSI bridges.

The CSI topology must ensure that no two output lines are shorted and that the input does not see an open circuit at any given time. This implies that exactly one switch from the upper three switches of a CSI bridge, and exactly one from the lower three, should be on at any time. This means that each switch must conduct for 120 degrees of the output current cycle. It can be shown that there are 36 different conduction combinations possible for the DCSI switches. There exist sets of switch combinations which give the same distribution of AC line currents, and this

fact can be used to achieve flexible control of the DC bus voltage, and hence of the DC current balance between the inverter bridges. It can be shown that there are 19 such sets.

The total AC current is the sum of the individual inverter currents. It is possible to control the magnitude of the fundamental component of the total AC line current by introducing a relative phase shift between the firing of the two bridges. For example, if the firing is exactly in phase, the output AC current will be maximum. If a slight phase shift is introduced, the magnitude of the AC current will decrease, since for part of the cycle, the current circulates in the bridges, and does not appear at the output.

A very convenient method to represent the possible switch combinations and the resulting AC line currents is to effect a transformation from the a-b-c (natural) reference frame to the stationary d-q-n reference frame. This transformation is detailed in Appendix 1, and is summarized below.

$$i_q = i_a$$
$$i_d = (2/3)(i_c - i_b)$$
$$\vec{I}_{d,q} = i_q - j i_d$$

In these equations, i_a, i_b, i_c are the instantaneous values of the three line currents. The current vector in the stationary d-q-n reference frame is denoted by $\vec{I}_{d,q}$. Under the constraint that the sum of the three line currents is zero, the n component of the vector is zero. Figure 6.4 shows all the 19 possible output current vectors and the table of the 36 switch combinations that generate these vectors. The redundancy between the switch combinations is readily apparent from Figure 6.4. The vector representation provides a convenient means for considering the combined action of the two bridges. It enables the analytical description of the output currents, and facilitates the development of control schemes for the inverter.

The method of selection of the vectors determines the output current waveform. Figure 6.4 shows that apart from the zero vector, there are three distinct classes of vectors. Class I consists of the vectors 1 to 6. Class II consists of the vectors 7 to 12. Class III consists of the vectors 13 to 18. When only the vectors 1 to 6 are used in sequence, the output AC current waveform is the standard six-step waveform with a maximum value of $2I_{dc}$. Multi-stepped waveforms are obtained by the use of the other vector classes. It is possible to control the magnitude of the

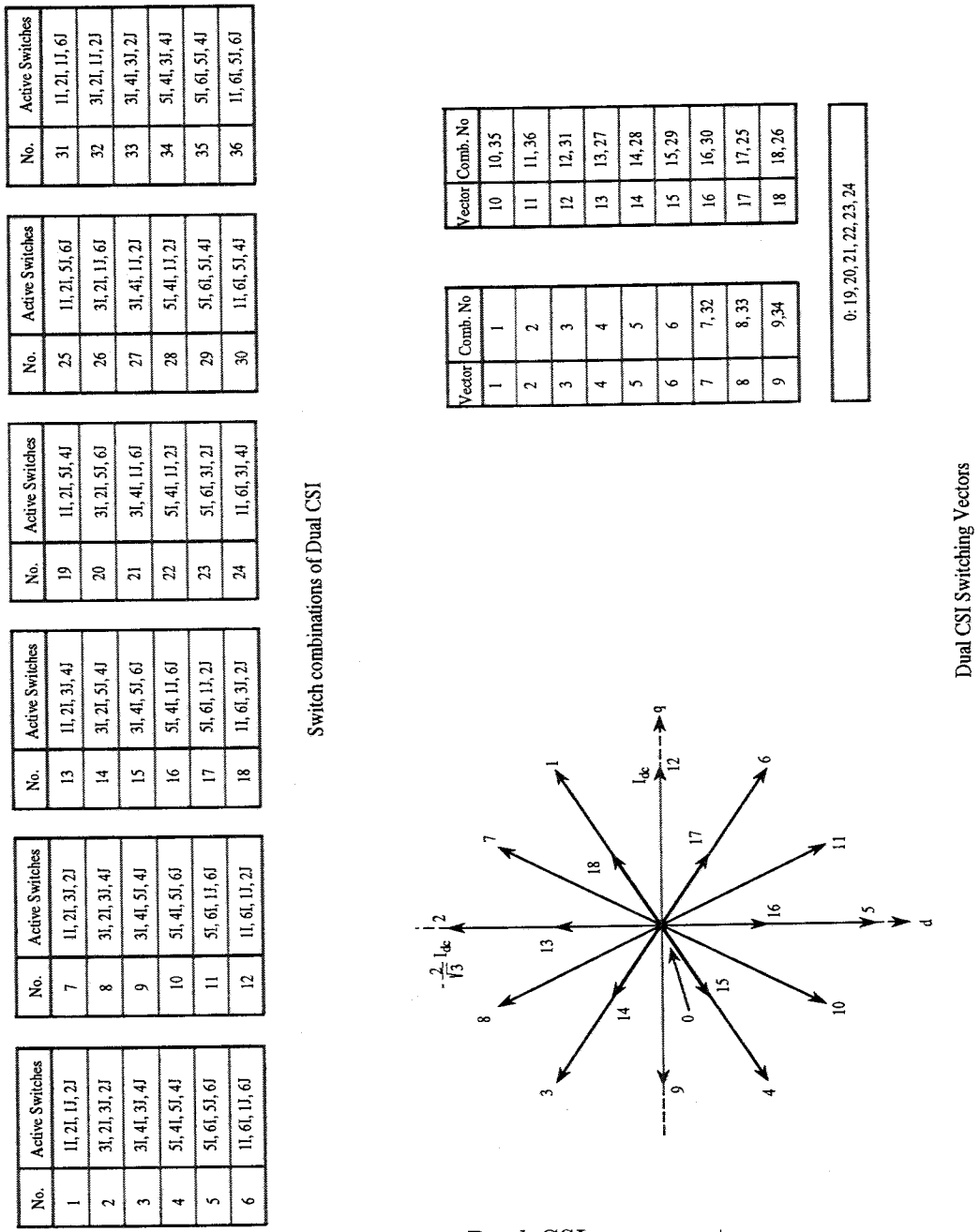

No.	Active Switches
1	1I, 2I, 1J, 2J
2	3I, 2I, 3J, 2J
3	3I, 4I, 3J, 4J
4	5I, 4I, 5J, 4J
5	5I, 6I, 5J, 6J
6	1I, 6I, 1J, 6J

No.	Active Switches
7	1I, 2I, 3I, 2J
8	3I, 2I, 3I, 4J
9	3I, 4I, 5I, 4J
10	5I, 4I, 5I, 6J
11	5I, 6I, 1I, 6J
12	1I, 6I, 1I, 2J

No.	Active Switches
13	1I, 2I, 3I, 4J
14	3I, 2I, 5I, 4J
15	3I, 4I, 5I, 6J
16	5I, 4I, 1I, 6J
17	5I, 6I, 1I, 2J
18	1I, 6I, 3I, 2J

No.	Active Switches
19	1I, 2I, 5I, 4J
20	3I, 2I, 5I, 6J
21	3I, 4I, 1I, 6J
22	5I, 4I, 1I, 2J
23	5I, 6I, 3I, 2J
24	1I, 6I, 3I, 4J

No.	Active Switches
25	1I, 2I, 5I, 6J
26	3I, 2I, 1I, 6J
27	3I, 4I, 1I, 2J
28	5I, 4I, 1I, 2J
29	5I, 6I, 5I, 4J
30	1I, 6I, 5I, 4J

No.	Active Switches
31	1I, 2I, 1I, 6J
32	3I, 2I, 1I, 2J
33	3I, 4I, 3I, 2J
34	5I, 4I, 3I, 4J
35	5I, 6I, 5I, 4J
36	1I, 6I, 5I, 6J

Switch combinations of Dual CSI

Vector	Comb. No
1	1
2	2
3	3
4	4
5	5
6	6
7	7, 32
8	8, 33
9	9, 34

Vector	Comb. No
10	10, 35
11	11, 36
12	12, 31
13	13, 27
14	14, 28
15	15, 29
16	16, 30
17	17, 25
18	18, 26

0: 19, 20, 21, 22, 23, 24

Dual CSI Switching Vectors

Figure 6.4: Dual CSI space vectors

fundamental component of the output current by changing the time for which each vector class is chosen. Control of the position of the output current relative to the AC voltage is also possible.

An added flexibility is provided by the fact that each vector in Classes II and III can be synthesized by two distinct switch combinations. This is apparent in Figure 6.4. This means that the same output current waveform can be produced with different DC bus voltages. This fact can be used very effectively to control the current sharing between the two bridges.

The relative phase shift $\alpha = \alpha_1 - \alpha_2$ determines the output AC current. The relative phase shift α ranges from zero to 180 degrees. The maximum output current is obtained when $\alpha = 0$. The output current is zero when $\alpha = 180$. Figure 6.5 illustrates the output current i_a in phase a when $\alpha = 30$. This figure clearly shows the multi-stepped nature of the output current waveform, and gives an idea of the variation possible with variations in α. Figure 6.6 shows the output current waveforms for the entire range of α:

$$0 \leq \alpha \leq 180$$

Figure 6.6 gives an idea of the variation of the harmonic content in the output current as a function of alpha. The waveform of Figure 6.5 can be represented as a Fourier series. It is convenient to set up the waveform to have odd symmetry, and expand the waveform as a Fourier sine series. Figure 6.5 shows the odd symmetry of the output current. The waveform is then represented as:

$$i_a(t) = \sum_{n=1}^{\infty} b_n sin(n\omega t) \tag{6.4}$$

$$b_n = (8I_{dc}/n\pi)cos(n\pi/6)cos(n\alpha/2) \tag{6.5}$$

$$n = 1, 3, 5, ...$$

In these equations, I_{dc} is the total DC current drawn form the DC source, and ω is the fundamental angular frequency (377 rad/sec for 60 Hz). Although the series for i_a given by equations 6.4 and 6.5 has been derived for the waveform of Figure 6.5, it can be shown that the same representation holds for all waveforms in the entire range.

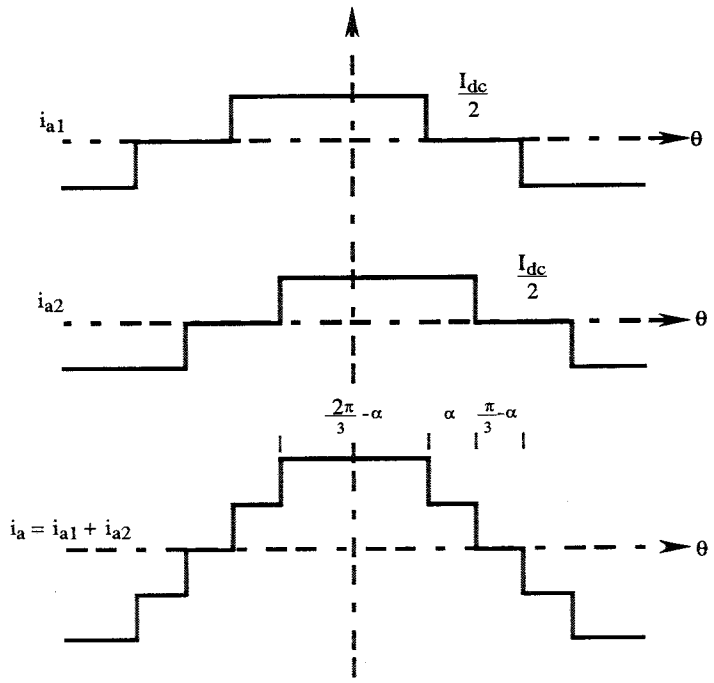

Figure 6.5: DCSI output current waveform for alpha=30

Figure 6.7 gives the variation of the the harmonic content in the AC line current as a function of α, the relative phase shift between the firings of the two CSI bridges. In this figure, the total DC current is taken to be 1pu, and equal sharing of the DC current between the two bridges is assumed. Thus, each bridge has a DC current of 0.5pu.

Figure 6.7 shows that it is possible to control the magnitude of the fundamental component of the AC line current by controlling α. However, α-control alone will not have any control over the current harmonics. In fact, close to $\alpha = 150$, the harmonic content relative to the fundamental is maximum. Selective notching of the output current (PWM) can be employed to eliminate any chosen harmonic (typically the 5th) from the output current, but this scheme leads to added switching losses in the GTOs.

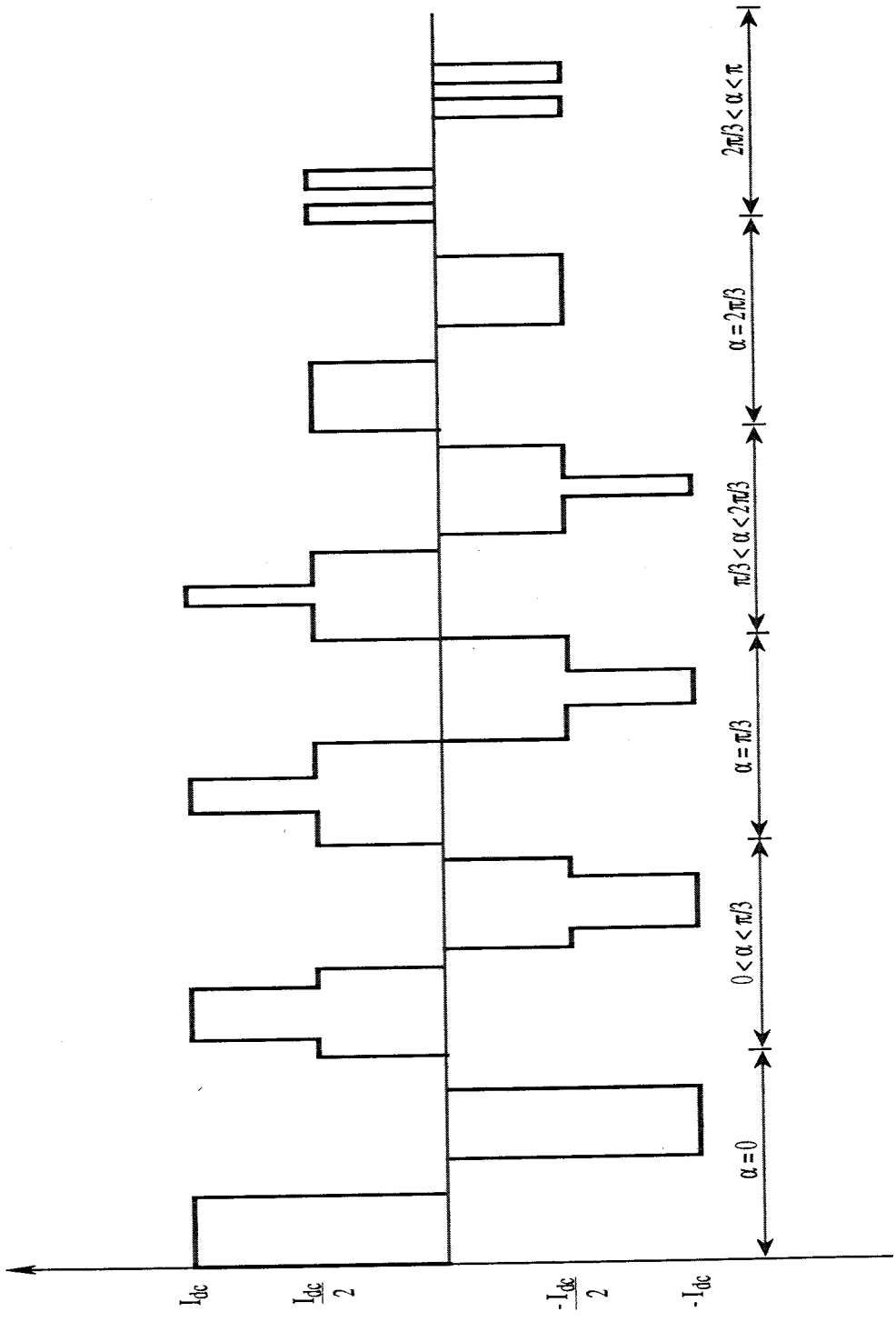

Figure 6.6: DCSI output current waveform for the range $0 \leq \alpha \leq 180$

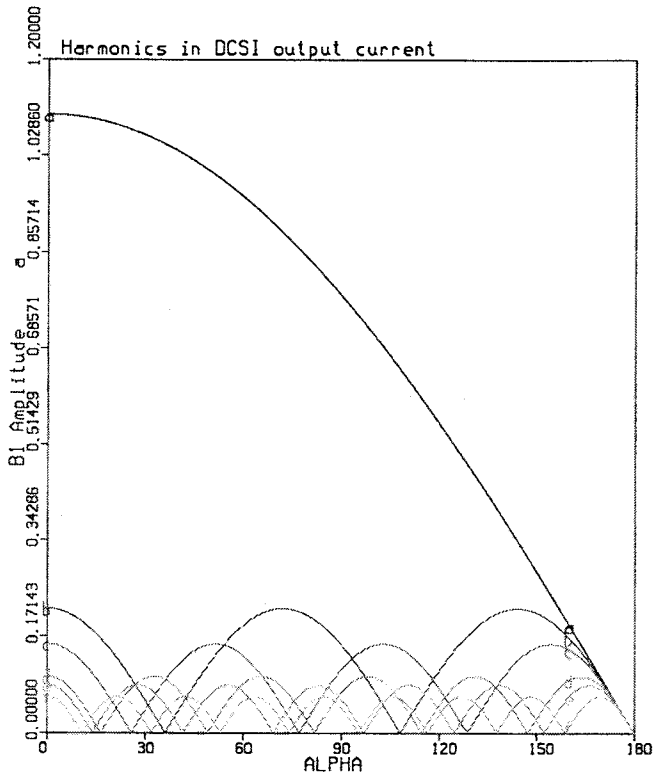

Figure 6.7: DCSI Output Current Harmonics as functions of alpha

DCSI Control

The topological aspects of the DCSI developed in the previous section are considered here to develop effective control mechanisms for the inverter acting as an interface between the utility system and the DC mesh. The essential aim of the control system is to control independently the real and the reactive power (P and Q) fed by the inverter to the utility. The range of independent control of these two quantities is related to the magnitudes of the utility AC voltage and the DC mesh voltage. An additional function of the control system is to achieve equal DC current distribution between the two inverter bridges (Figure 6.3). The dynamics of the control system in controlling the P and Q output from the inverter are also considered in this section.

Figure 6.8 gives the fundamental component vector diagram of the DCSI connected to the utility. This vector diagram represents the utility voltage vector $\vec{E}$, and the output currents of the two bridges, $\vec{I}_{LI}$ and $\vec{I}_{LJ}$ in a synchronously rotating reference frame with an angular rotation

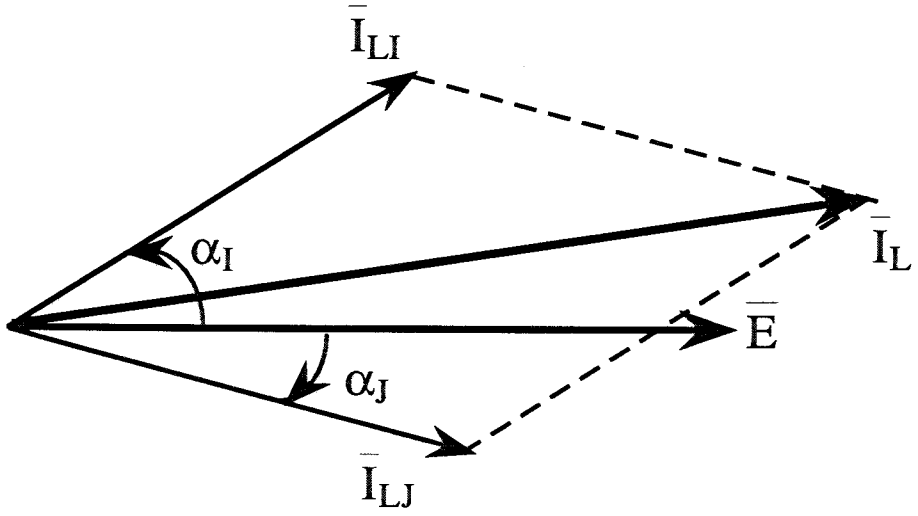

Figure 6.8: DCSI Fundamental Component Vector Diagram

frequency of ω rad/sec. The delay angles α_I and α_J are also shown. Appropriate control of the two delay angles enables the resultant current vector $\vec{I}_L$ to be controlled in both magnitude and phase.

It can be shown that the real and reactive power (P and Q) provided by the inverter are given by:

$$P = \frac{3\sqrt{3}}{2\pi} E I_{dc} [cos(\alpha_I) + cos(\alpha_J)] \tag{6.6}$$

$$Q = \frac{3\sqrt{3}}{2\pi} E I_{dc} [sin(\alpha_I) + sin(\alpha_J)] \tag{6.7}$$

In these equations, E is the magnitude of the utility line-neutral voltage and I_{dc} is the DC current as shown in Figure 6.3. When the DCSI operates with delay angles α_I and α_J, the DC bus voltage (Figure 6.3) is given by:

$$V_{dc} = \frac{3\sqrt{3}}{2\pi} E [cos(\alpha_I) + cos(\alpha_J)] \tag{6.8}$$

It is apparent that equations 6.6 and 6.8 imply that the real power P calculated on both the AC and DC sides is the same. It is convenient to define the following two quantities:

$$a = cos(\alpha_I) + cos(\alpha_J) \tag{6.9}$$

$$b = sin(\alpha_I) + sin(\alpha_J) \tag{6.10}$$

Figure 6.3 indicates that in the steady state, V_{dc} must equal V_s, the DC mesh voltage which is typically set by a remote rectifier terminal. This is in fact a very strong constraint on the operation of the DCSI. Equations 6.8 and 6.9 indicate that for a given AC system voltage magnitude, a must be a constant in steady state. Further, with this constraint, equation 6.6 indicates that for given I_{dc}, the real power P is a constant in steady state. Therefore, Q can be varied by varying the quantity b under the constraint that a is constant in the steady state. This defines the region of steady state independent control of P and Q possible for specified values of I_{dc} and E.

The maximum value of b under the constraint that a is constant can be obtained. Define the constraint and the auxiliary function f as:

$$cos(\alpha_I) + cos(\alpha_J) - a = 0$$

$$f = sin(\alpha_I) + sin(\alpha_J) - \lambda[cos(\alpha_I) + cos(\alpha_J) - a]$$

With this, b can be maximized by letting

$$\frac{\partial f}{\partial \alpha_I} = cos(\alpha_I) + \lambda sin(\alpha_I) = 0$$

$$\frac{\partial f}{\partial \alpha_J} = cos(\alpha_J) + \lambda sin(\alpha_J) = 0$$

This gives:

$$\lambda = \frac{-cos(\alpha_I)}{sin(\alpha_I)} = \frac{-cos(\alpha_J)}{sin(\alpha_J)}$$

$$tan(\alpha_I) = tan(\alpha_J)$$

$$\alpha_I = \alpha_J \pm n\pi \qquad n = 0, 1, 2, 3 \ldots$$

To deliver real power to the utility, both α_I and α_J must be in the second or the third quadrants, giving a negative V_{dc}. This means that in the above equation, for maximum Q at a given P, the angles must satisfy the condition that $\alpha_I = \alpha_J = \alpha$. The actual value of α is determined from E and V_S using equation 6.8. This gives:

$$\begin{aligned} \frac{P}{Q_{max}} &= cot(\alpha) \\ \alpha &= cos^{-1}(a/2) \\ & or \\ \alpha &= 2\pi - cos^{-1}(a/2) \end{aligned}$$

The region of independent control of P and Q in the steady state is shown in Figure 6.9. In this, the power delivered to the utility is *negative*. Two values of α give the same value of a, as shown in the above equations. These correspond to the maximum delivered Q and the maximum received Q. Figure 6.9 shows that a higher value of I_{dc} gives a larger region of Q. The value of P is fixed by V_s and I_{dc}. For a given I_{dc}, Q can have any steady state value on a line parallel to the P-axis (Figure 6.9), bounded by the limits of the region of independent control. Increasing I_{dc} is equivalent to shifting this line down on the Q-axis.

As mentioned earlier, it is essential for the control scheme to achieve equal sharing of the DC current in the two inverter bridges (Figure 6.3). In general, the two bridges would operate such that $\alpha_I \neq \alpha_J$. This implies that $V_{dI} \neq V_{dJ}$. All the DC current would tend to drift to the bridge with the smaller value of DC voltage. Eventually, one bridge would carry all of I_{dc}, and the other bridge would carry no current.

Equal sharing of the DC current can be ensured by periodically swapping the values of the delay angles between the two bridges, thus ensuring that the average value of V_{dI} equals that of V_{dJ}. Figure 6.10 gives the schematic diagram of the control needed to implement the delay angle swapping. The controller of Figure 6.10 essentially maintains the difference between the DC currents of the two bridges within a specified band. If $I_{err} = I_{dI} - I_{dJ}$ goes above a specified

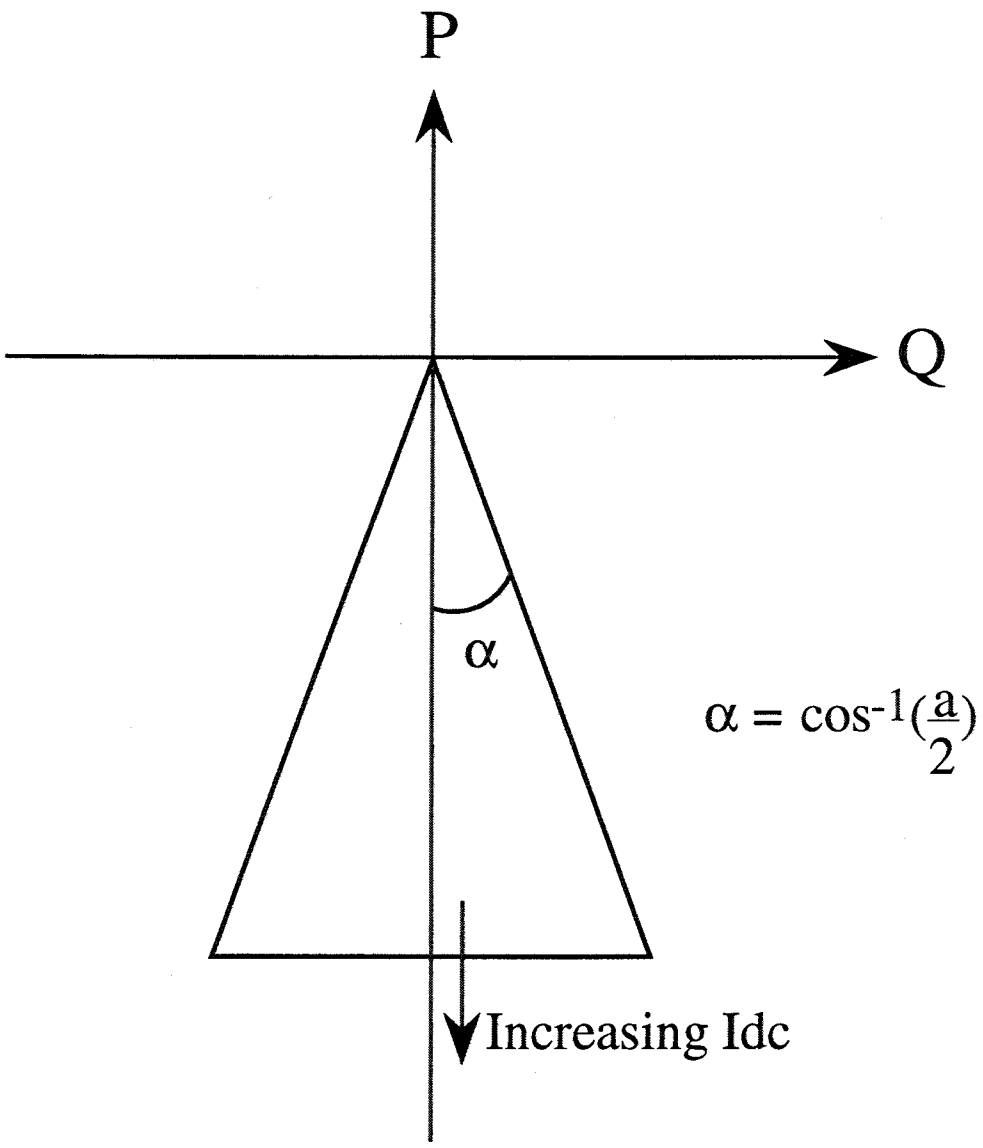

Figure 6.9: Region of Independent P and Q Control

tolerance band, the firing angles are distributed to the bridges such that the DC bus voltage of Bridge I is larger than the DC bus voltage of Bridge J. I_{dI} decreases and I_{dJ} increases, driving the error I_{err} back into the tolerance band.

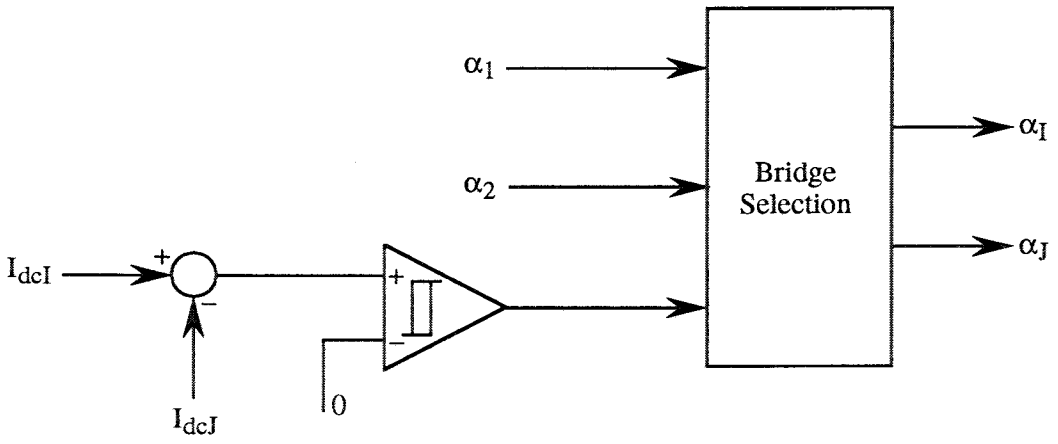

Figure 6.10: Delay Angle Swapping for Current Balancing

It is noted here that unequal DC current sharing would affect the harmonic spectrum of the output AC current. The harmonic amplitudes will not be given by equation 6.5. Further, the ripple on the DC current caused by the action of interchanging the bridge firing angles would modify the spectrum.

The considerations on the independent control of P and Q are used in developing a control mechanism for the DCSI (Figure 6.3). The essential aim of the controller is to produce the values for a and b. Equations 6.9 and 6.10 are then used to compute values for α_I and α_J, which are given to the bridges. The DC current equalizing control is used to provide the correct α to the appropriate bridge.

The value of a is essentially obtained from the set point for the DC current I_{dc}. The controller for a is given in Figure 6.11. The control consists of two sections. The first is a feedback section, which acts on the error between the set point for the DC current, I^*_{dc}, and the actual DC current, I_{dc}. This error is given to a P-I controller, to form the value a_1. The second section is a feed-forward section, which generates the value a_2 on the basis of the actual AC voltage magnitude E and the estimate of the DC source voltage $\hat{V}_s$, using equation 6.8. Thus, a_2 is calculated from:

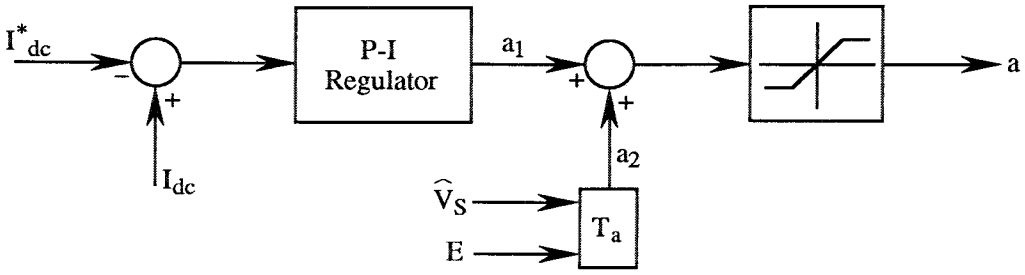

Figure 6.11: Controller for "a"

$$a_2 = \frac{2\pi \hat{V}_s}{3\sqrt{3}E}$$

The value of a is obtained as $a = a_1 + a_2$. The feed-forward serves to speed up the dynamic response of the controller. It computes an approximate value of a, and the P-I regulator compensates for errors in the approximate value. Since the a controller controls the value of the DC current I_{dc}, it effectively controls the real power transfer P. The value of a is limited to be such that $-2 \leq a \leq 2$.

The control scheme of Figure 6.11 indicates the control action for a change in the DC current set-point I^*_{dc}. For an increase in DC current set point, the controller will act to increase a, and thus reduce V_{dc}. This increases the DC current, and then V_{dc} is increased again to maintain the DC current at the new value. Thus, although the steady state power P increases with an increase in the DC current set-point, there is a transient dip in P to enable more current to be drawn from the mesh.

The value of b is obtained from the set-point for reactive power Q. The controller for b is shown in Figure 6.12, and consists of a feedback and a feed-forward section. The feedback section acts on the error between the Q set point, Q^*, and the actual value of Q, calculated from AC current and voltage measurements. The output of the feedback section is b_1. The feed-forward controller computes b_2 on the basis of equation 6.7 as follows:

$$b_2 = \frac{2\pi Q^*}{3\sqrt{3}EI_{dc}}$$

The value of b is then obtained as $b = b_1 + b_2$. This is then passed through a limiter which ensures that the value of b is within the region of independent control. The maximum value of b is given by:

$$b_{max} = 2sin(\alpha)$$
$$\alpha = cos^{-1}(a/2)$$

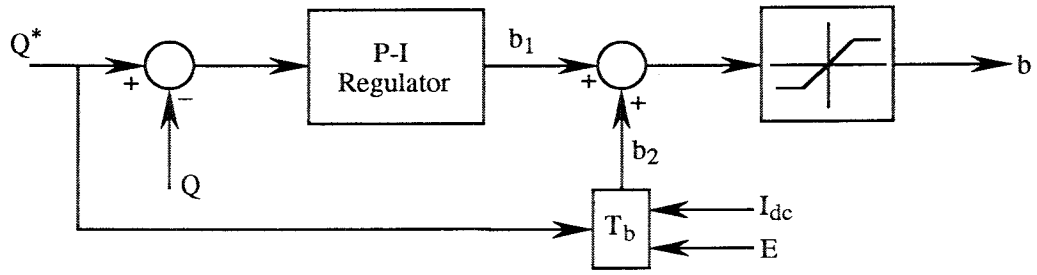

Figure 6.12: Controller for "b"

The values of a and b are used to compute the values of the two firing angles on the basis of equations 6.9 and 6.10. The firing angles are given by:

$$\alpha_1 + \alpha_2 = cos^{-1}\left(\frac{a^2 - b^2}{a^2 + b^2}\right) + 2\pi \quad (6.11)$$

$$\alpha_1 - \alpha_2 = cos^{-1}\left(\frac{a^2 + b^2 - 2}{2}\right) \quad (6.12)$$

The values of α_1 and α_2 are then provided to the bridges by the controller to equalize DC current sharing (Figure 6.10).

EMTP Simulation of the Dual CSI.

The Dual CSI topology is implemented in EMTP, and the associated control system has been implemented using TACS. This section presents EMTP simulation results performed on the topology

and control, and discusses the simulation results. The circuit configuration is shown in Figure 6.3. For the simulations, the DC bus voltage V_{dc} is taken to be 7.5 kV. The AC voltage is taken to be 6.6 kV rms line-line. The nominal DC current I_{dc} is 3 kA, thus giving a nominal power rating of 22.5 MW for the inverter.

Figure 6.13 shows the plots of the real power P and the reactive power Q. The plot shows the response of these variables from startup. The values of P and Q up to 125 milliseconds correspond to set-points of $I_{dc}^{*} = 3kA$ and $Q^{*} = 2MVAr$. The real power P is thus $7.5 \times 3 = 22.5MW$. At 125 milliseconds, the DC current set-point, I_{dc}, is changed from 3 kA to 3.5 kA. The DC current controller responds by lowering the DC bus voltage, thus increasing the DC current. However, the reduced DC voltage results in a reduction in P, until the current controller brings the DC bus voltage back up to 7.5 kV. There is thus an increase in the steady state power, resulting from an increase in I_{dc}, but the power dips transiently to enable the steady state increase. Figure 6.13 shows that during the disturbance accompanying a change in I_{dc}^{*}, the reactive power, Q, remains at 2 MVAr.

Figure 6.13 also shows the response of the inverter to a subsequent change in the reactive power set-point Q^{*} from 2 MVAr to 5 MVAr at 300 milliseconds. In the steady state, this is equivalent to changing $b = sin(\alpha_1) + sin(\alpha_2)$ while maintaining the value of $a = cos(\alpha_1) + cos(\alpha_2)$ at that dictated by the DC source voltage. Thus, there is no change in P, while Q changes from 2 MVAr to 5 MVAr.

Figure 6.14 shows the plot of the DC current I_{dc} in response to a change in the DC current set point I_{dc}^{*} from 3 kA to 3.5 kA. The DC current is increased as desired by the action of the inverter, which lowers its DC bus voltage transiently for this purpose. The "feed-forward" part of the current controller (Figure 6.11) provides a nominal value of a, and the P-I controller acts on the error between the set and actual DC currents.

Figure 6.15 shows the DC current in each inverter bridge. The figure shows that the average DC current is the same in each bridge. This is achieved by swapping the firing angles between the two bridges, thus ensuring that the average DC voltage across each bridge is the same. The α-swapping action of the equalizing controller (Figure 6.10) is readily apparent in Figure 6.15. This Figure also shows the response of the current sharing control to a change in the set-point I_{dc}^{*}. Current sharing is maintained even in the new steady state.

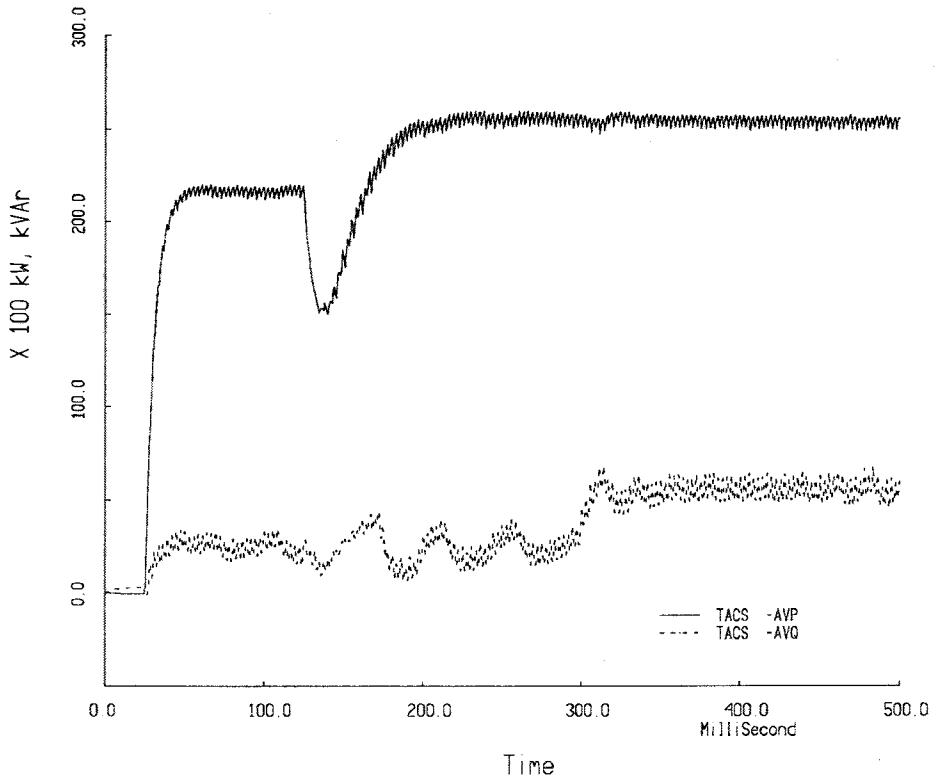

Figure 6.13: Response to change in DC current and Q set-points. Upper Plot: P ; Lower Plot: Q

Figure 6.16 shows the plots of the two delay angles, α_1 and α_2. At 125 milliseconds, there is an increase in I^*_{dc}. The action of the P-I controller for a (Figure 6.11) is readily apparent. In the steady state, both α_1 and α_2 return to their original values. This is because a is a constant, and the set-point Q^* is not changed. Thus, in the steady state, both a and b (equations 6.9 and 6.10) are constant, and hence, α_1 and α_2 are unchanged.

Figure 6.16 also shows the effect of a change in the Q^* set point, which is changed from 2 MVAr to 5 MVAr at 300 milliseconds. Both α_1 and α_2 are changed by the controller (Figure 6.12). However, although b is changed in response to a change in Q set-point, a is unchanged. This can be verified from the fact that in Figure 6.14, the DC current I_{dc} remains unchanged, and thus, the DC bus voltage V_{dc} is unchanged.

Figure 6.17 shows the plot of the DCSI output line current. Comparison of this plot with Figure 6.6 shows that the DCSI operates such that $\alpha_1 - \alpha_2 \approx \pi/3$. This is apparent from the fact that the plot of Figure 6.17, to a large part, has no non-zero interval of zero current. Figure 6.16

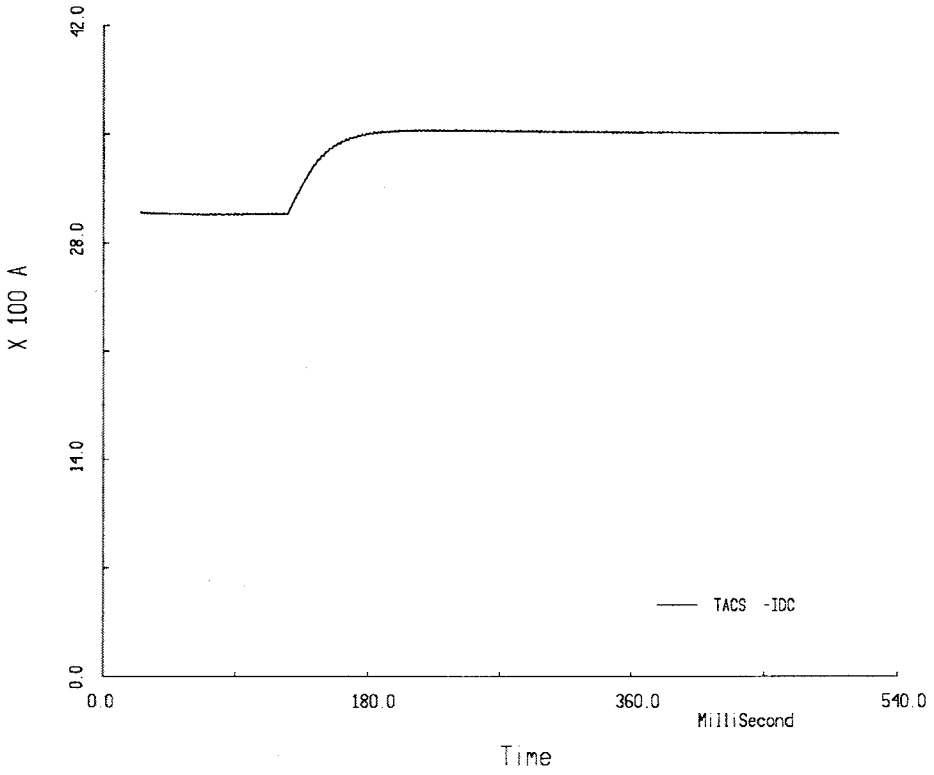

Figure 6.14: Response to change in DC current set-point

also confirms that $\alpha_1 - \alpha_2 \approx \pi/3$.

Figure 6.17 further shows the effects of a changes in the I_{dc} and the Q set-points, at 125 milliseconds and 300 milliseconds respectively. At 125 milliseconds, the I_{dc} set point is changed from 3 kA to 3.5 kA. In response to this, I_{dc} increases, and correspondingly, the amplitude of the DCSI output line current also increases. At 300 milliseconds, the Q set-point is changed from 2 MVAr to 5 MVAr. However, the DC current remains unchanged, and thus, the effect on the AC line current is negligible. Figure 6.17 also shows the effect of α-swapping to equalize DC current sharing. It is noticed that the current waveform is somewhat asymmetric. This reflects the fact that at a given instant in time, the DC currents in both the bridges may not be exactly the same. However, on the average, the DC current is shared equally.

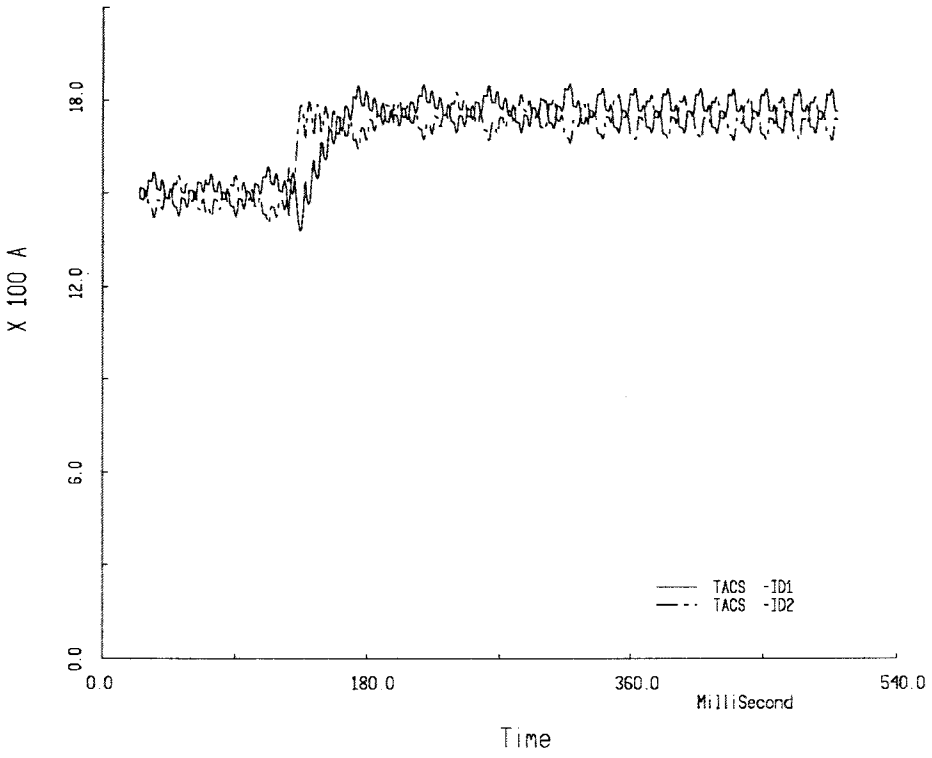

Figure 6.15: DC current sharing between the two bridges of the DCSI

6.3 Voltage Source Inverter Interface

The Voltage Source Inverter (VSI) has a specified stiff DC voltage source at its input, and specifies voltages at its output. The basic topology of the VSI is given in Figure 6.18. Traditionally, VSI's have been used predominantly in low and medium power circuits. An important reason for this has been that semiconductor devices with gate turn-off capability and high current and voltage ratings have not been available. As gate turn-off devices with higher power ratings than previously have been available, there has been substantial interest in investigating their use in VSI topologies for high power applications, including HVDC power transmission.

In Figure 6.18, the DC capacitor at the input of the inverter forms the inverter forms the DC bus for the inverter. The capacitor, along with the isolating inductor, has the ability to shield the inverter against transient disturbances on the superconducting DC mesh. On the AC side, the circuit has the property of achieving independent control over the real and reactive power (P and

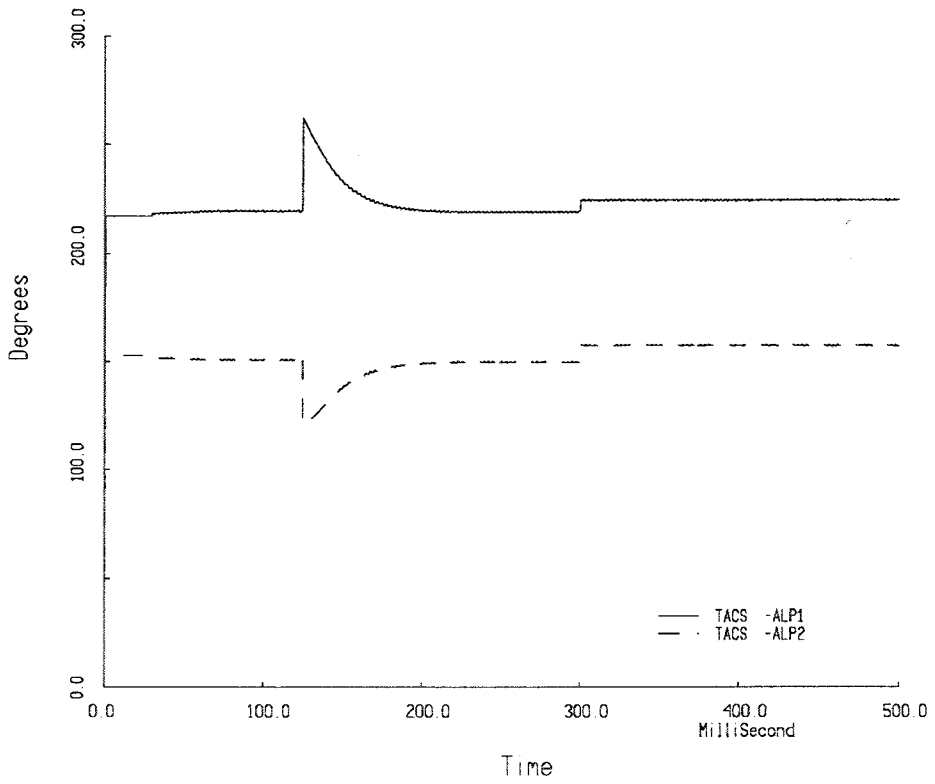

Figure 6.16: Plot of the two delay angles

Q) if controlled appropriately. It is well known that stable operation of a power system needs good control of the P and Q flows in the power system. Typically, the P and Q flows are decoupled to a good extent. P depends predominantly on the power angle, and Q depends predominantly on the voltage magnitudes. Figure 6.19 is used to illustrate this basic power transfer relationship. With reference to Figure 6.19, the following power transfer equations hold:

$$P = \frac{VE}{\omega L_f} sin(\delta) \tag{6.13}$$

$$Q = \frac{V^2}{\omega L_f} - \frac{VE}{\omega L_f} cos(\delta) \tag{6.14}$$

In these equations, ω is the angular frequency of the two voltage sources, δ is the power angle shown in Figure 6.19, and V and E are the magnitudes of the two voltages sources. From these equations, it is apparent that for small δ, P is sensitive to δ and Q is sensitive to the voltage

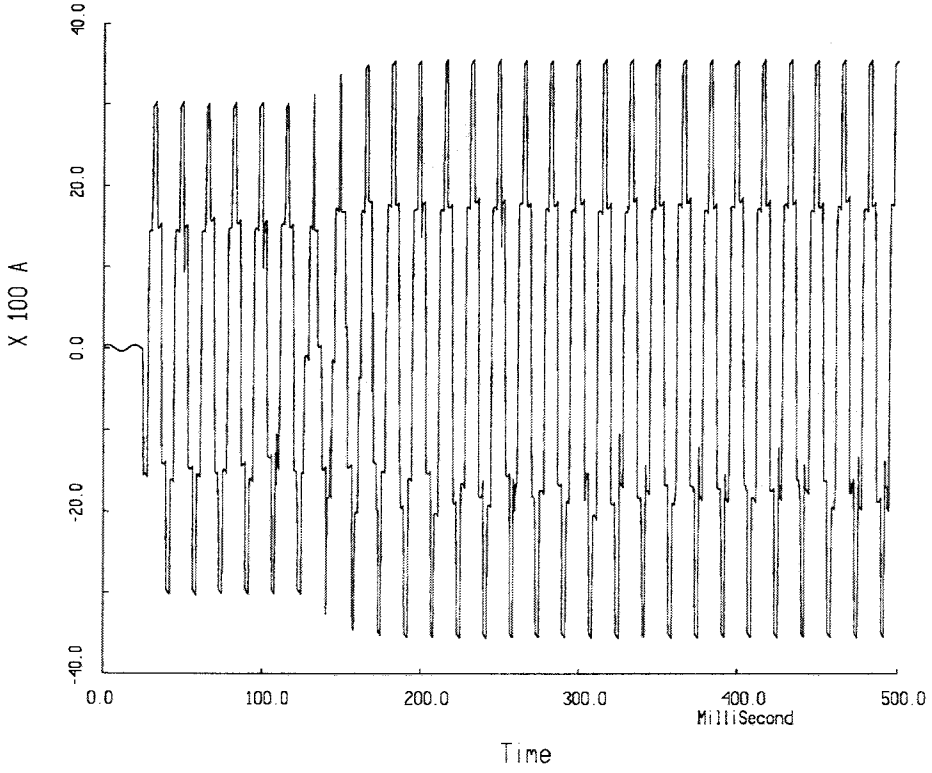

Figure 6.17: DCSI output line current in the "a" phase

magnitude difference. Thus, to control independently the P and Q flows, the inverter must control the power angle δ and the voltage magnitude.

The following sections consider briefly the familiar three phase bridge VSI topology, and proceed to develop a detailed control system suitable for the control of the VSI connected to the AC power system. Simulation results are then presented and discussed.

6.3.1 VSI Topology

The basic VSI topology is shown in Figure 6.18, and essentially consists of six gate controlled switches. These six switches operate under the constraint that no output line is ever open, and no switch combination short-circuits the input DC bus. This essentially means that at least two switches from either the upper half or the lower half of the bridge conduct, and that no two switches from the same leg of the bridge conduct, at any given time. Thus, exactly three switches

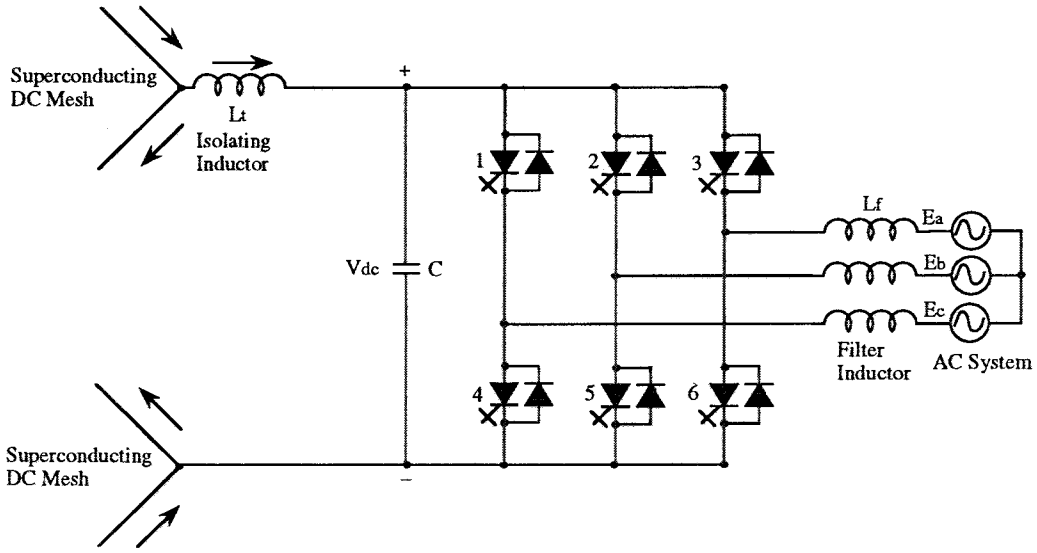

Figure 6.18: VSI Topology

are on at any given time. It can be shown that eight different switch combinations satisfy the constraints detailed above.

A particular combination of conducting switches results in specified output voltages on the AC lines. These output voltages can be mapped from the $a-b-c$ reference frame to the $d-q-n$ reference frame, as detailed in the Appendix. This mapping results in a set of seven output voltage vectors in the $d-q-n$ reference frame. These vectors are shown in Figure 6.20, along with the switch combinations that cause them.

The transformation of the VSI output voltages onto the $d-q-n$ reference provides a very elegant way to effect control. Furthermore, it provides a physical meaning to many steady state quantities even transiently. For example, definition of power factor angle as the angle between a sinusoidal voltage and current in the steady state can be extended to the transient case as well. It could be defined as the instantaneous angle between the voltage and current vectors obtained from the transformation to the $d-q-n$ frame of reference. No assumption need be made regarding the wave shapes of the quantities. It is easy to show that in sinusoidal steady state, this definition reduces to the conventional definition of power factor angle.

In the six-step mode of operation, the six non-zero vectors are chosen sequentially, in the

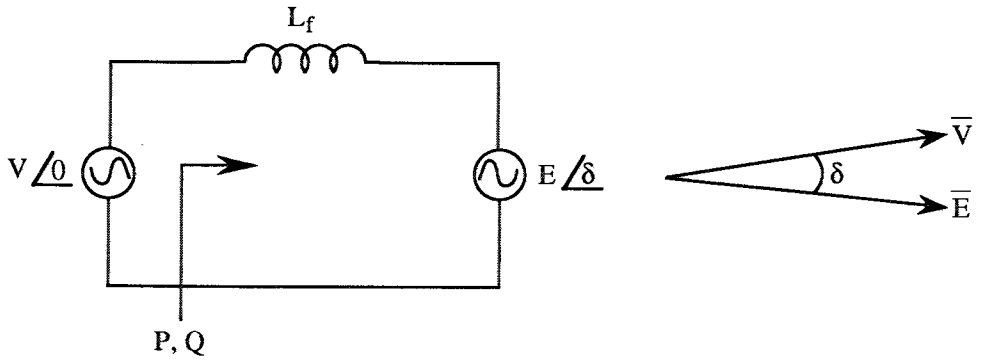

Figure 6.19: Power Transfer in AC System

counter-clockwise direction, each vector being chosen for $\pi/3$ radians. This mode is said to give *one degree of freedom*, since it is possible to control the *frequency* of the output voltage by controlling the rate at which the vectors are chosen. However, for a fixed DC bus voltage, it is not possible to control the *magnitude* of the output voltage.

Pulse Width Modulation (PWM) must be employed to control the magnitude of the output voltage. This is done by choosing a zero vector (Figure 6.20) according to a control law. When the magnitude of the fundamental component of the output voltage can be controlled by the inverter, in addition to the frequency, the control mode is said to provide *two degrees of freedom.* Additional degrees of freedom (by choosing a zero vector a multiple number of times) can be used to eliminate specified harmonics from the output voltage, and still control the magnitude of the fundamental output voltage. However, the resulting increase in switching frequency causes an increase in the switching losses in the devices. The output voltage wave shapes for six step operation are given in Figure 6.21. The wave shapes for PWM operation are given in Figure 6.22.

Figure 6.18 also shows the filter inductor L_f needed to filter the effect of the inverter voltage harmonics on the AC line current. The filtering action can be provided by the leakage inductance of the transformer used to connect the inverter to the utility. The inductance acts as the power transfer element between the VSI and the utility. This is apparent from Equations 6.13 and 6.14.

The VSI is sensitive to short-circuit faults , especially at its output terminals. As can be seen from Figure 6.18, the DC capacitor is short-circuited by the terminal fault through two switches which happen to be conducting at the fault instant. If the fault current is limited only by the

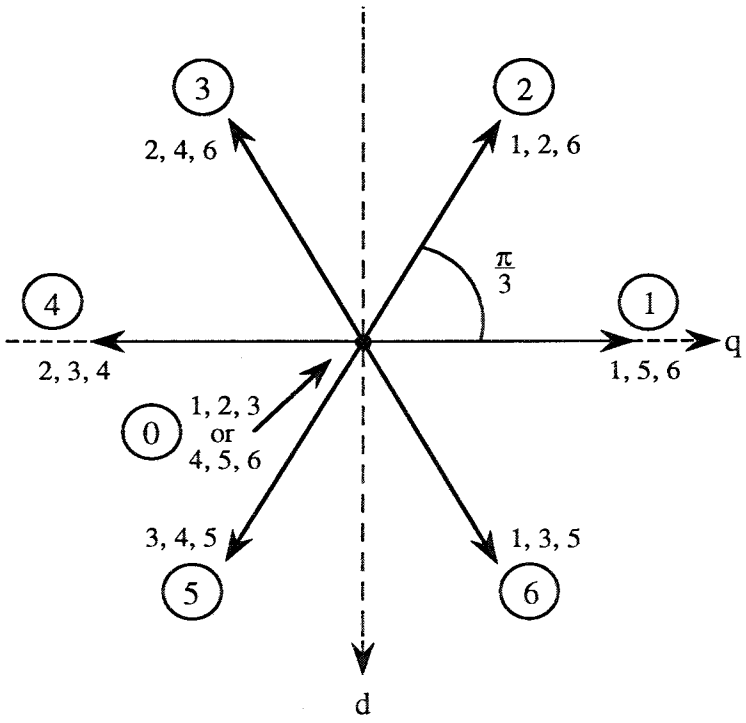

Figure 6.20: VSI Switching Vectors

stray inductance in its path, it can destroy the switches before any protection scheme has time to act, and if the switches are not appropriately oversized. On the DC side, a fault on the mesh could be fed by the AC system voltage through the diodes (Figure 6.18).

6.3.2 VSI Control

This section considers the details of the control scheme needed to control a VSI connected to a utility system. Essentially, two output quantities are controlled: the magnitude of the inverter output fundamental voltage vector, and its position relative to the utility voltage vector. The following two cases will be considered:

(i) VSI connected to stiff utility.

(ii) VSI connected to weak utility and distributed loads.

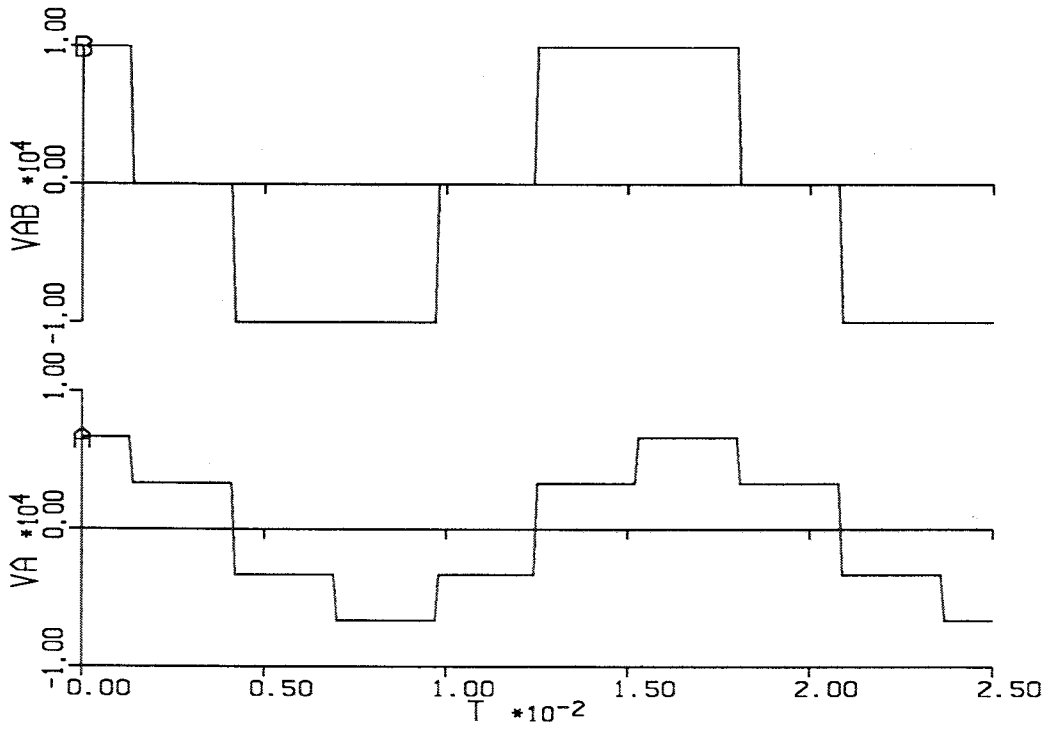

Figure 6.21: VSI Six Step Waveforms. Upper trace: Line-Line voltage. Lower trace: Line-Neutral voltage

The requirements of the control system have been detailed in the Introduction (Section 6.1.3). An important requirement of the control system is that the control should be based mainly on those quantities which can be measured locally at the inverter. This ensures reliable control without signal communication between the various inverters connected to the system. Communication may be used to enhance the performance, but must not be critical to the operation of the inverter.

Figure 6.23 gives the schematic diagram of the interconnection of the VSI with the utility.

Control of VSI connected to stiff utility

The situation of a VSI connected to a stiff utility is represented in Figure 6.23 with the source inductance L_s taken to be practically zero. Thus, the voltage at the AC bus is determined by the utility voltage source, and not by the inverter. The inverter feeds specified amounts of real and

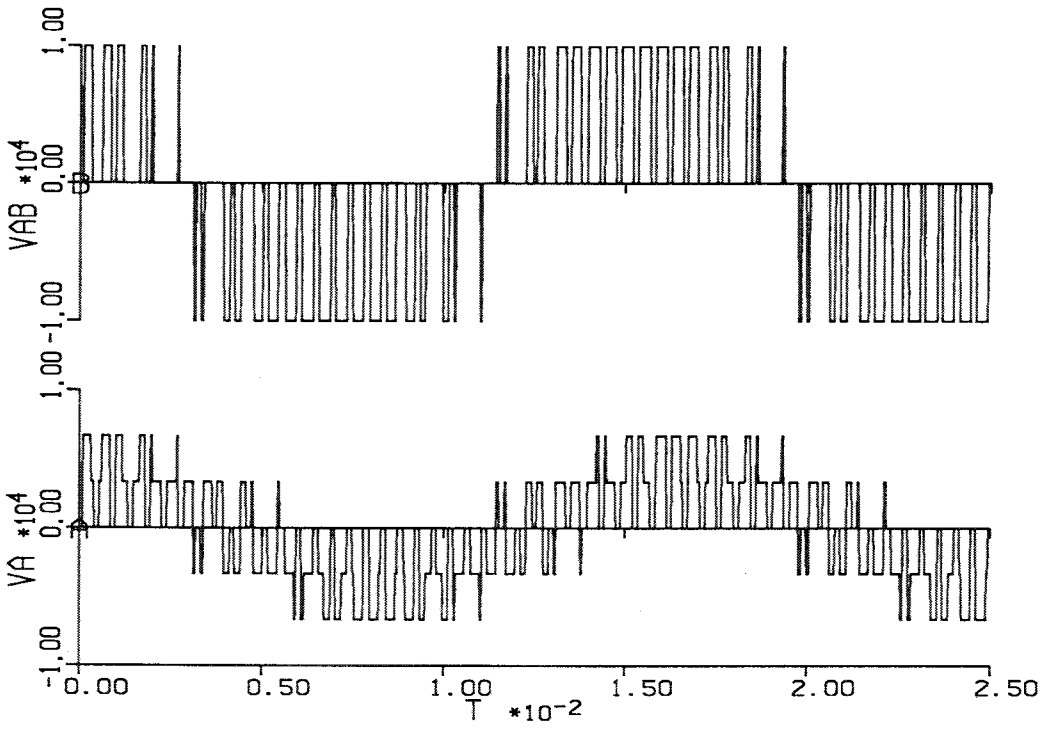

Figure 6.22: VSI PWM Waveforms. Upper trace: Line-Line voltage. Lower trace: Line-Neutral voltage

reactive power (P and Q) into the AC bus. The control scheme developed for this situation forms the basis of the control in the more complex situation (ii) mentioned above.

Since the AC source present in the system is stiff, the frequency of the inverter is constrained to exactly equal the source frequency in the steady state. Independent control of P and Q fed into the AC system by the inverter means that two inverter quantities need to be controlled. For the purpose of the scheme presented here, these two quantities are take to be the *magnitude and position of the time integral of the inverter output voltage vector.* This fact is responsible for the ability to control the inverter based only on locally measured quantities. This scheme has been applied previously to AC drive control under the title of *Direct Self Control.*

The control is in the complex domain. The transformation of the three phase quantities into the complex domain is detailed in the Appendix. The essential equations are reproduced below for convenience.

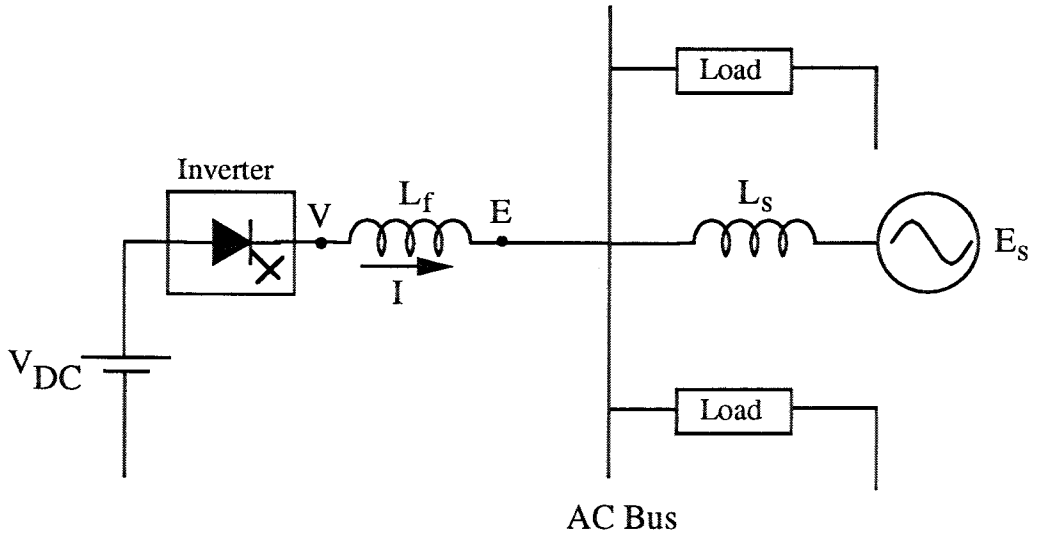

Figure 6.23: Interconnection of VSI with Utility

$$
\begin{aligned}
f_d &= \frac{2}{3}(-\frac{\sqrt{3}}{2}f_b + \frac{\sqrt{3}}{2}f_c) \\
f_q &= \frac{2}{3}(f_a - \frac{1}{2}f_b - \frac{1}{2}f_c) \\
f_n &= \frac{2}{3}(\frac{1}{\sqrt{2}}f_a + \frac{1}{\sqrt{2}}f_b + \frac{1}{\sqrt{2}}f_c)
\end{aligned}
$$

In these equations, f generically denotes a physical quantity, such as a voltage or a current. The subscripts $a, bandc$ are for the three phases and the subscripts $d, qandn$ are for the quantities in the transformed reference frame. In the absence of a neutral connection, the quantity f_n is of no interest. The *dandq* components define a vector in the complex plane.

The inverter output voltage vector can be any of the seven discrete vectors shown in Figure 6.20. The components of the inverter output voltage vector on the d and q axes are denoted by v_d and v_q respectively. The components of the time-integral of the inverter output voltage vector are defined as:

$$\psi_{dv}(t) = \int_{-\infty}^{t} v_d d\tau \tag{6.15}$$

$$\psi_{qv}(t) = \int_{-\infty}^{t} v_q d\tau \tag{6.16}$$

$$\vec{\psi_v} = \psi_{qv} - j\psi_{dv} \tag{6.17}$$

$$\tag{6.18}$$

The quantity $\vec{\psi_v}$ is called the *inverter flux vector.* Its magnitude and position are given by:

$$|\vec{\psi_v}| = \psi_v = \sqrt{\psi_{qv}^2 + \psi_{dv}^2} \tag{6.19}$$

$$\delta_v = tan^{-1}\left(\frac{-\psi_{dv}}{\psi_{qv}}\right) \tag{6.20}$$

The d and q axis components of the AC system voltage flux vector, $\vec{psi_e}$, are defined likewise.

The inverter voltage vector switches between discrete positions, while the AC system voltage vector traces out a smooth circle in the $d-q$ plane. Thus, it is difficult to define a power angle in the same manner as that defined in conventional AC power systems for synchronous generators and transmission lines, where all voltages are sinusoidal, and so trace smooth circles in the $d-q$ plane. The "Fluxes" provide a convenient way to define a power angle, since the inverter flux vector cannot change discretely in position or magnitude. The power angle δ_p may be defined as the angle between the two flux vectors.

$$\delta_p = \delta_v - \delta_e \tag{6.21}$$

The classical P and Q transfer equations can be written in terms of the fluxes as:

$$P = \frac{3}{2L_f}\omega\psi_e\psi_v sin(\delta_p) \tag{6.22}$$

$$Q = \frac{3}{2L_f}\omega\left[\psi_v\psi_e cos(\delta_p) - \psi_e^2\right] \tag{6.23}$$

These expressions show that the real power transfer P is predominantly determined by the power angle δ_p, and the reactive power transfer is predominantly determined by the relative magnitudes of the flux vectors. This provides a convenient method for controlling the inverter.

The control system for the inverter is shown in Figure 6.24. The innermost loop is seen to be the one that controls ψ_v and δ_p. The set-points for this are ψ_v^* and δ_p^*. Hysteresis bands are set up about these two set-points and the actual values of ψ_v and δ_p are confined to the hysteresis bands by the appropriate choice of the inverter switching vector.

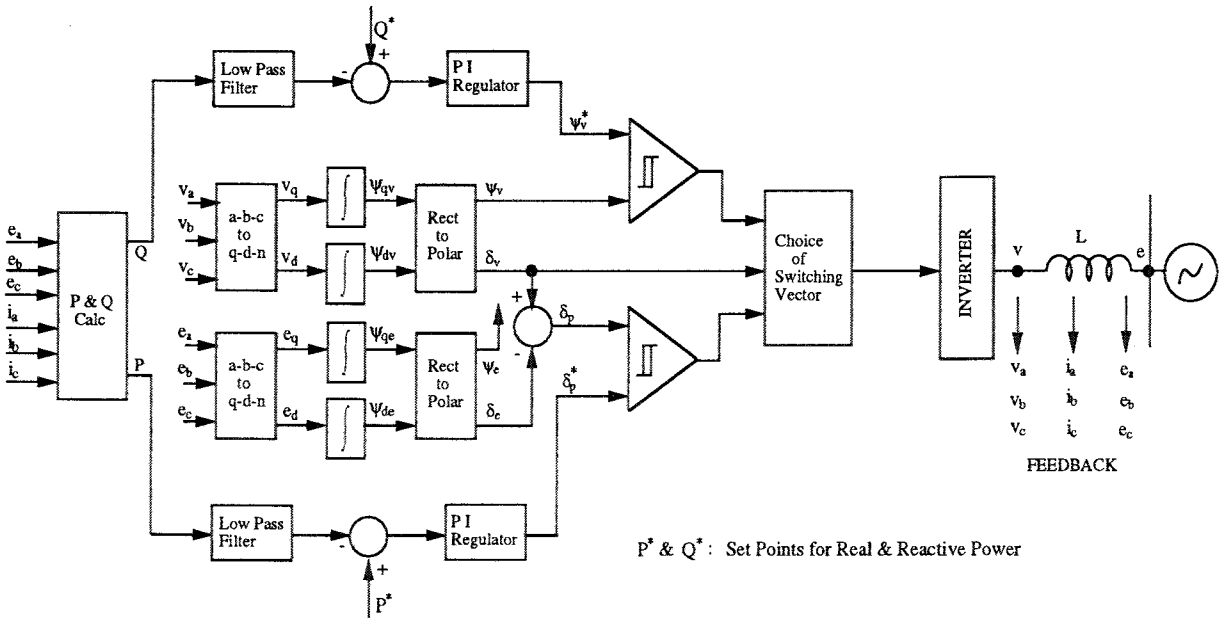

Figure 6.24: Control scheme for strong system interconnection

One of the factors that determine the choice of switching vector is the position of the inverter flux vector. The $d-q$ plane is divided into six sectors for δ_v, as shown in Figure 6.25. The value of δ_v determines the choice of two possible inverter switching vectors, apart from the zero vector. One vector increases ψ_v and the other decreases it.Both vectors increase the power angle δ_p. To decrease δ_p, the zero vector is chosen. To correct the value of ψ_v, one of the two active vectors is chosen depending on the sign of the correction required. Table-1 gives the choices of the active switching vectors for different positions of the inverter flux vector. The magnitude ψ_v and the power angle δ_p thus lie within the specified hysteresis bands.

As shown in Figure 6.24, the set-points ψ_v^* and δ_p^* are computed by P-I regulators from the outer loop set-points P^* and Q^*. The regulators are driven by the errors between the set and actual P and Q. The P-I regulators generate the correct values of ψ_v^* and δ_p^* to achieve the desired values of P and Q respectively. This closed loop control of P and Q nullifies the effect of cross-

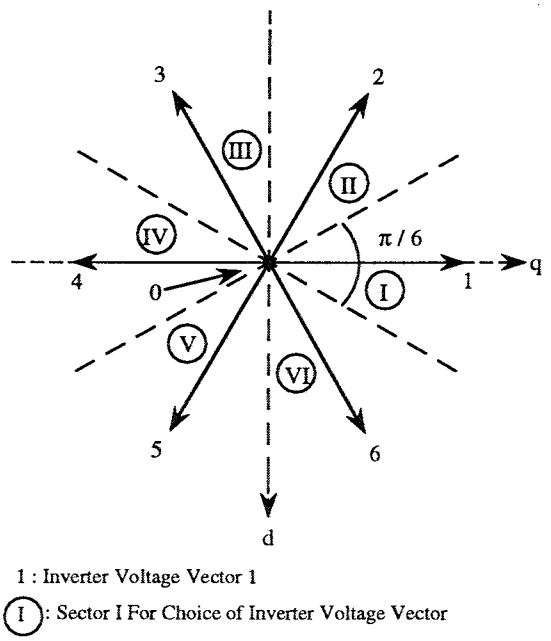

Figure 6.25: Sectors for choice of switching vector

Sector No. →	I	II	III	IV	V	VI
Increase ψ_v	2	3	4	5	6	1
Decrease ψ_v	3	4	5	6	1	2

Table 6.1: Choice of Switching Vector

coupling between P and Q in the AC system. The entire control is based on the measurement of signals available locally to the inverter. The vector control is based on instantaneous quantities and does not need information on the AC system frequency. It uses the instantaneous position of the AC system flux vector, which is easily calculated from the measurement of the AC system phase voltages.

EMTP Simulations: VSI connected to stiff utility system

The control system described in the previous section has been applied to the system shown in Figure 6.23, with the source inductance L_s taken to be zero. The simulation has been carried out

using the Electro-Magnetic Transients Program (EMTP). This section presents the simulations of the control system. In starting the simulations, the initial values of the components of the AC system flux vector must be chosen correctly. Equations 6.15 and 6.16 indicate that the integration of the voltage must start at $t = -\infty$. However, the simulation typically starts at $t = 0$. If the AC system voltage is a balanced three phase voltage with the sequence $a - b - c$ and the a-phase to neutral voltage is $E_a = E_{max}cos(\omega t + \beta)$, then the initial values of the AC system flux vector components are:

$$\psi_q(0) = \frac{E_{max}}{\omega} sin(\beta)$$
$$\psi_d(0) = \frac{E_{max}}{\omega} cos(\beta)$$

Figure 6.26 gives the locus of the tip of the inverter flux vector. For a perfectly sinusoidal set of output voltages, the flux vector would be a circle. The switching action of the inverter produces a locus that deviates from a perfect circle.

Figure 6.27 gives the plots of the real and reactive power, P and Q. The plots show the response of the controller to step changes in the P^* and Q^* set-points. The sequence of events is as follows. Between 0 and 20 milliseconds, the inverter output voltage is synchronized with the utility voltage. At 20 milliseconds, the inverter is connected to the utility, but the set-points P^* and Q^* are kept at zero. At 40 milliseconds, the set-point for real power, P^*, is increased suddenly from 0 MW to 1 MW. The output power increases as a result. At 70 milliseconds, the reactive power set-point, Q^*, is increased suddenly form 0 MVAr to 0.25 MVAr, and this causes a corresponding increase in the output reactive power. Figure 6.27 clearly demonstrates the independent control of P and Q.

Figure 6.28 and Figure 6.29 give the plots of the quantities ψ_v and δ_p respectively. The plots show the changes in these two quantities in response to the set-point changes corresponding to Figure 6.27. The control of ψ_v and δ_p within specified hysteresis bands is readily apparent from Figures 6.28 and 6.29.

Figure 6.30 shows the AC line current fed into the utility. The line current deviates from the perfect sinusoid because of the width of the hysteresis bands. A higher width results in a lower inverter switching frequency. While this results in lower switching losses in the inverter switches, the current deviates from the sinusoidal. This results in a ripple in the P and Q fed to the utility.

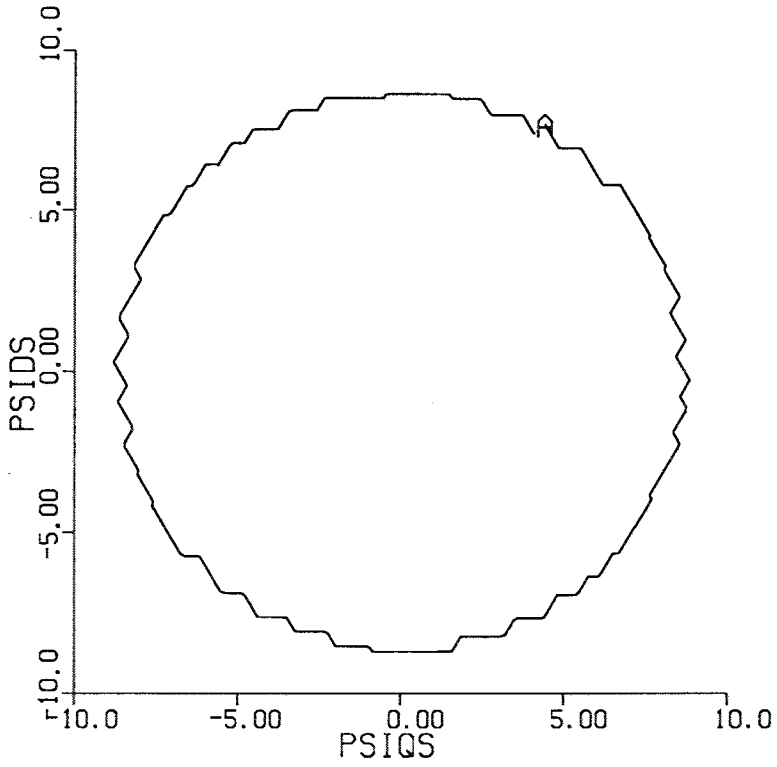

Figure 6.26: Locus of tip of inverter flux vector

The inverter line-line voltage is given in Figure 6.31. The inverter line-line voltage is the result of the switching scheme described in the previous section. With reference to Figure 6.24, the ψ_v controller controls the widths of the pulses in the inverter line-line voltage. The δ_p controller controls the position of the inverter line-line voltage relative to the utility voltage.

Control of VSI connected to weak utility and distributed loads

The control scheme developed for the control of the VSI connected to a strong utility system forms the basis for developing a control scheme for controlling a VSI connected to a weak utility and distributed loads. Thus, the VSI feeds the loads in parallel with the utility. This case is represented by the schematic diagram of Figure 6.23 with the the source inductance L_s taken to be comparable to the inverter system inductance L_f. Thus, the voltage at the load bus is determined by the combined action of the inverter and the utility source voltage. The inverter

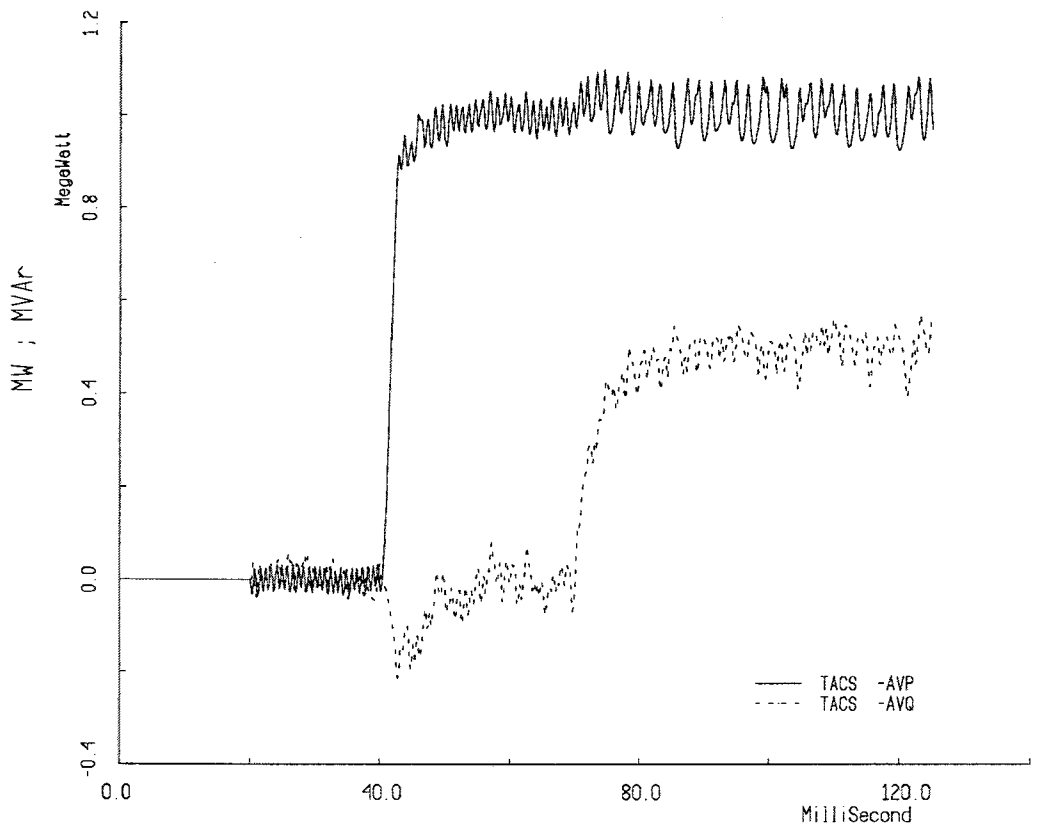

Figure 6.27: P and Q supplied by VSI

output voltage is filtered before the utility interconnection, thus ensuring that the bus voltage distortion is within tolerance limits.

The interconnection of the VSI to a weak utility through a transformer is shown schematically in Figure 6.32. In the EMTP simulation of the system, the AC system is taken to be 69 kV, and the nominal load voltage is 3.3 kV. The filter components are L_f and C_f. The mesh voltage is taken to be 7.5 kV DC.

Figure 6.32 indicates the control methodology needed for the VSI. It is seen that the voltage across the load is not determined by the AC system alone, as was the case when the AC system was strong. Since L_f and L_s are comparable, both the inverter and the AC system would affect the load voltage comparably. Thus, one control loop is on the load voltage. In addition, the position of the inverter flux vector relative to the load voltage determines the real power P delivered by

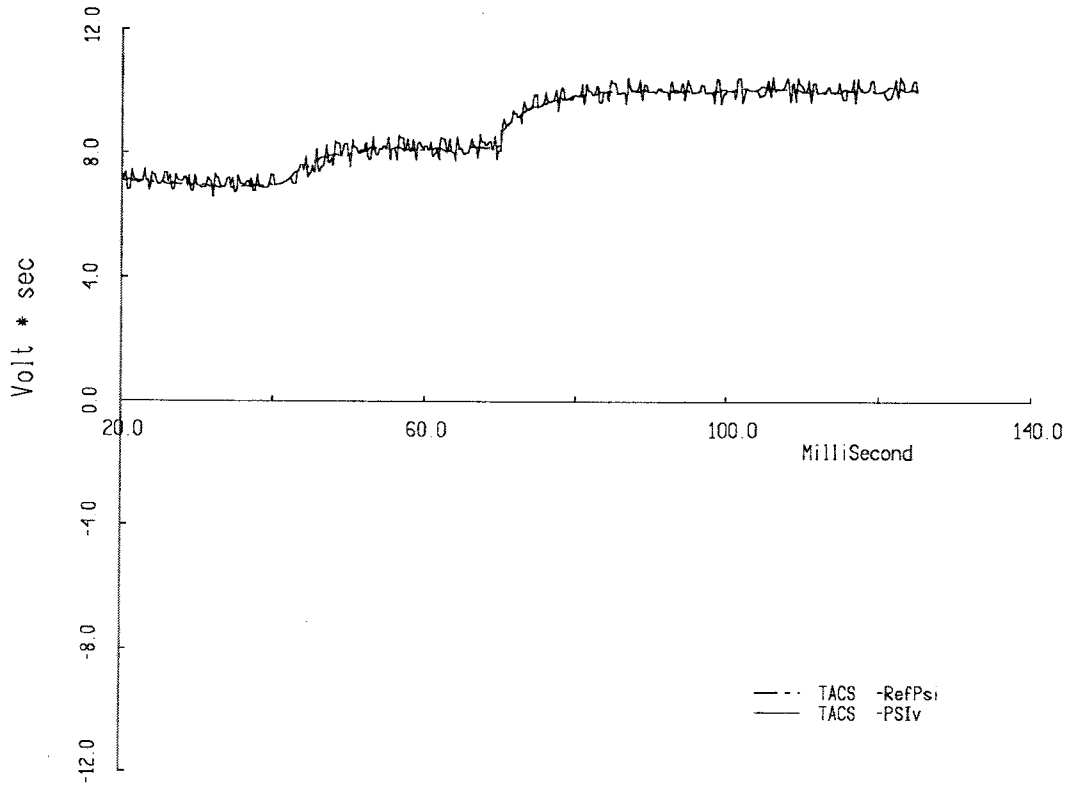

Figure 6.28: Magnitude of Inverter Flux Vector. Set Value: Hatched line ; Actual Value: Solid line

the inverter, and this forms the second control loop.

Figure 6.33 gives the control loop for the load voltage. The controller is seen to be in two parts. The feedback part operates on the error between the voltage set-point and the actual load voltage. The error is driven to zero by the P-I regulator. The second part is the command feed-forward, which generates an estimate of the inverter flux magnitude needed to achieve the set load voltage magnitude. The feed-forward part depends on an estimate of the filter components. The feed-forward transfer function essentially produces the value of the inverter flux needed to achieve the specified load voltage magnitude when the filter is unloaded. The feedback part thus corrects for the effect of the load current, and the errors in the filter component value estimates. The outputs of the two parts are summed to produce the set-point for the inverter flux vector magnitude.

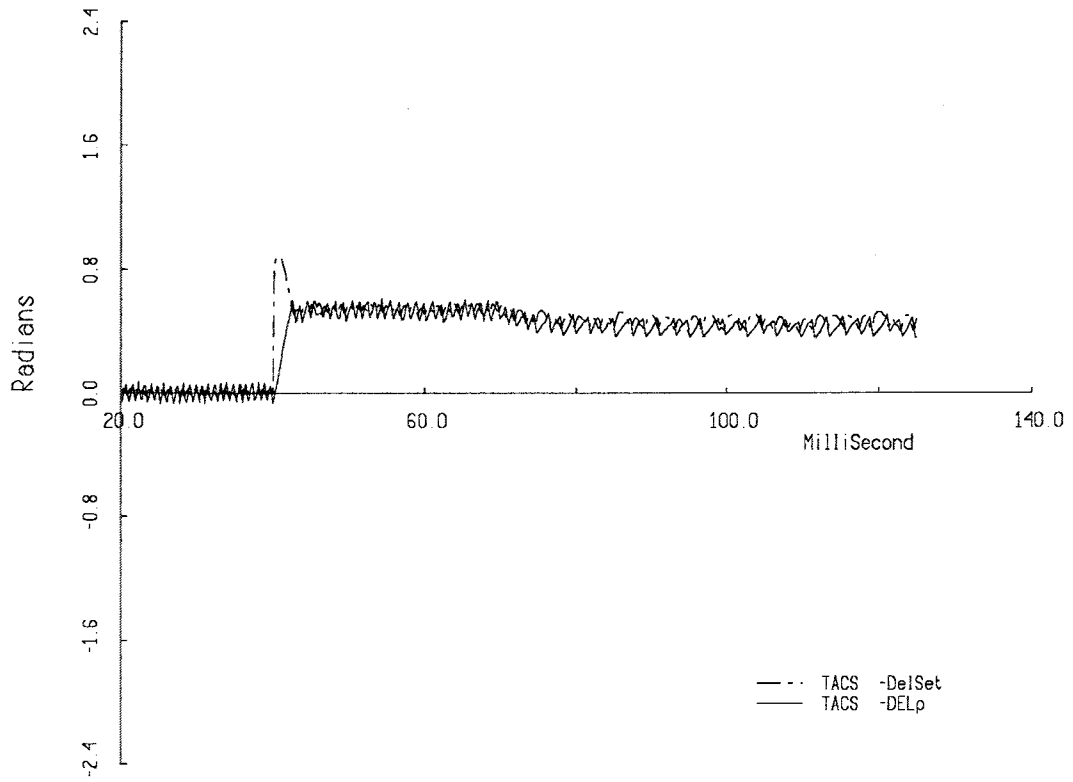

Figure 6.29: Power Angle. Set Value: Hatched line ; Actual Value: Solid line

Figure 6.34 gives the control loop for the real power delivered, P. Similarly to the load voltage controller, the P-controller is also made up of two parts. The feedback portion acts on the error between the set and actual values of P. The feed-forward part computes the power angle δ_p needed to deliver the set power to the AC system, assuming that δ_p is small. The feed-forward transfer function can be deduced from the expression for P, given by equation 6.13. The P-I regulator corrects for errors in the estimate of the value of the filter inductance L_f, and for the fact that the actual relationship between P^* and E^* is non-linear.

The set-points ψ_v^* and δ_p^* are given to the hysteresis controller, which determines the inverter output switching vector. The control for ψ_v and δ_P has been dealt with previously in the discussion of the control scheme for the inverter connected to a strong AC system (Figure 6.24).

The following section presents the simulations obtained from the control scheme described

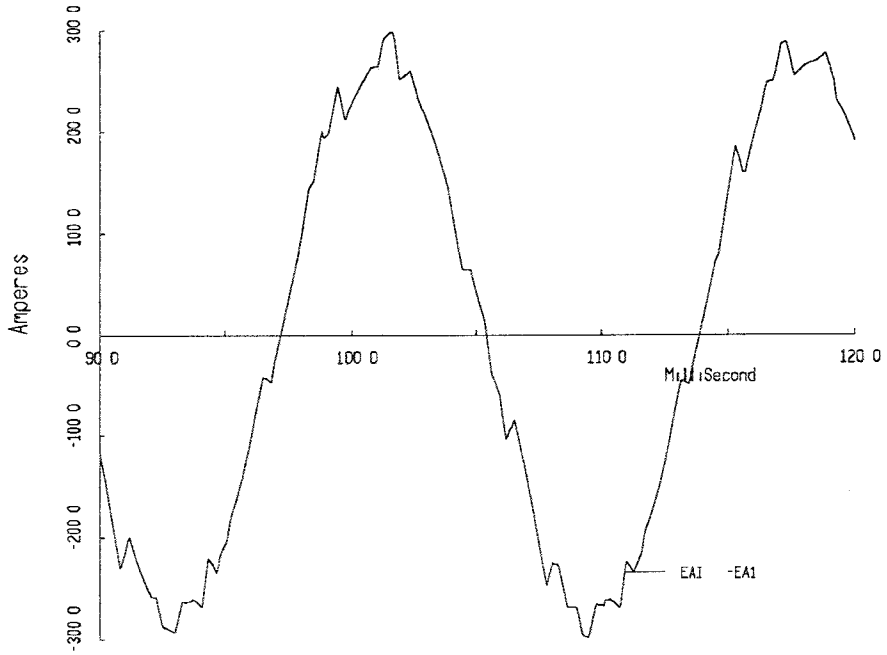

Figure 6.30: AC line current fed to the utility

above.

EMTP Simulations: VSI connected to weak AC system and distributed loads

A detailed computer model of the VSI has been set up using EMTP. The VSI is connected to a weak AC system, as shown in Figure 6.32. The loads are constituted by the 10 bus network of the AC system used for this study. The circuit parameters are: L_f = 10 mH, C_f = 300 μF, $L_s = 10mH$. The nominal DC mesh voltage is 7.5 kV DC. The AC system voltage is 69 kV line-line rms. The loads are rated at nominal voltage of 3.3 kV. The transformer leakage reactance is assumed to be small compared to L_s. The nominal power rating of the inverter is taken to be 1 MW.

Figure 6.35 shows the response of the system power when the load at Bus 684 is changed suddenly at 250 milliseconds. This change causes an increase in the load real power from 0.9 MW to 1.3 MW. Since the inverter set point P^* is maintained at 1 MW, there is no change in the power

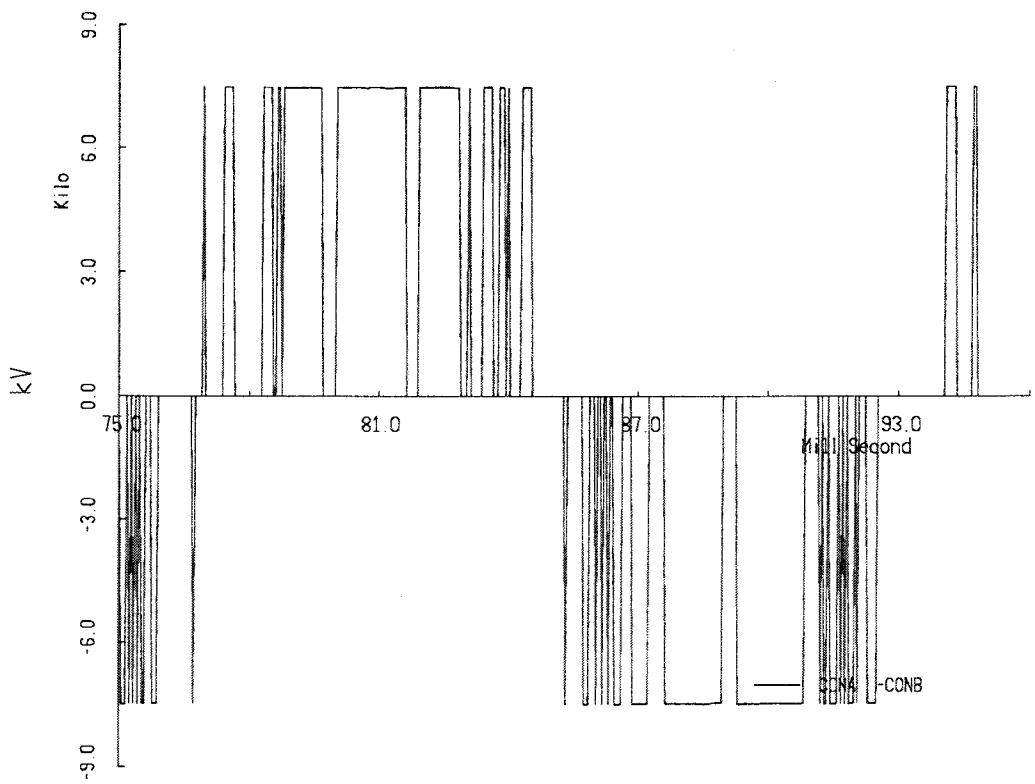

Figure 6.31: Inverter output line-line voltage

delivered by the inverter. The utility bears all the increase in load power. Figure 6.35 indicates that the control system is effective in maintaining a constant power output from the inverter.

Figure 6.36 shows the response of the system reactive power for the same load change as for Figure 6.35. The change causes an increase in the load reactive power from 0.4 MVAr to 0.65 MVAr. This causes the reactive power drawn from the utility to increase transiently. However, this is achieved at the expense of lowering the load bus voltage magnitude. The voltage controller of the inverter then brings the load voltage back to normal. In the process, the reactive power supplied by the inverter increases. As the voltage magnitude rises back to normal, the reactive power drawn from the utility decreases. The inverter thus takes up the reactive power demand of the load.

Figure 6.37 shows the action of the inverter flux magnitude in response to the load change

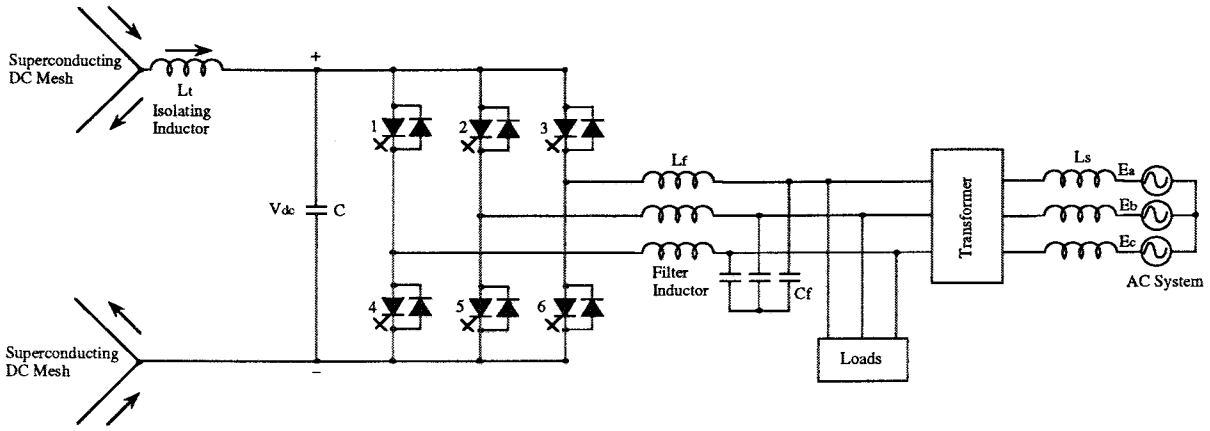

Figure 6.32: VSI interconnection to weak AC system and distributed loads.

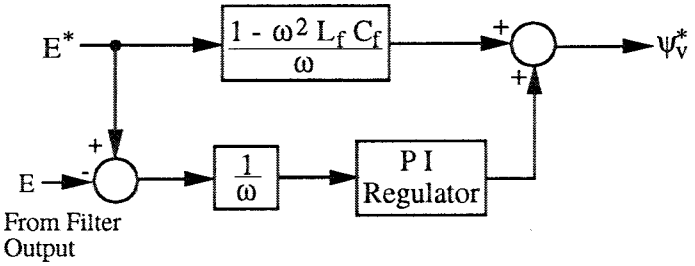

Figure 6.33: Controller for Load Voltage Magnitude.

of Figure 6.35. The voltage controller of the control system causes the inverter flux magnitude to increase so as to restore the load bus voltage to the nominal value. Figure 6.38 shows the corresponding response of the power angle δ_p.

Figure 6.39 shows the action of the load voltage in response to the load change of Figure 6.35. The voltage dips transiently when the load increases, thus causing an increase in the reactive power drawn from the utility (Figure 6.36). However, the inverter voltage controller restores the load voltage to its nominal value, and the utility reactive power decreases. Figure 6.40 gives the load current. Figure 6.41 gives the inverter line-line voltage.

Voltage Source Inverters are very sensitive to over-currents, and an over-current limiting scheme needs to be built into the controller. In the inverter controller described in the previous section, the

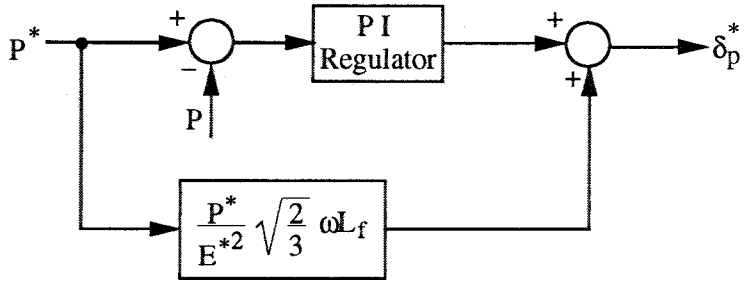

Figure 6.34: Controller for real power delivered (P)

over-current limiting is achieved essentially by lowering the inverter flux set-point ψ_v^* in proportion to the extent that the inverter current exceeds a set over-current limit. This serves to reduce the load bus voltage, and thus the over-current. In the present simulation, the over-current limit has been set at 400 A peak.

Figure 6.42 shows the inverter current for a change in the load that tends to draw more than 400 A peak from the inverter. The inverter current thus increases sharply, and the over-current limiting control reduces the inverter current to the limit value. This is achieved by reducing the inverter flux magnitude set-point ψ_v^*, and thus the load voltage. The plot of the load voltage is given in Figure 6.43. The total load current is shown in Figure 6.44. The excess load current is fed by the utility, since the inverter load current is limited.

Control of multiple inverters feeding distributed passive loads

This section considers the control of parallel connected VSI's feeding distributed loads. This case is represented by the schematic diagram of Figure 6.1. The control requirements for this environment have been detailed in a previous section. The present section details the structure of a specific control scheme to achieve those requirements. Simulation results are also given.

The control is essentially derived from the control scheme used in the case of the VSI connected to a strong AC system. Thus, the two variables controlled directly by the inverters are the inverter flux magnitude, ψ_v, and the power angle, δ_p. Outer loops are then used to control the magnitude and angular frequency of the AC system voltage vector $\vec{E}$. The set-points for the magnitude and angular frequency of $\vec{E}$ are obtained from the outermost loop, which implements specified

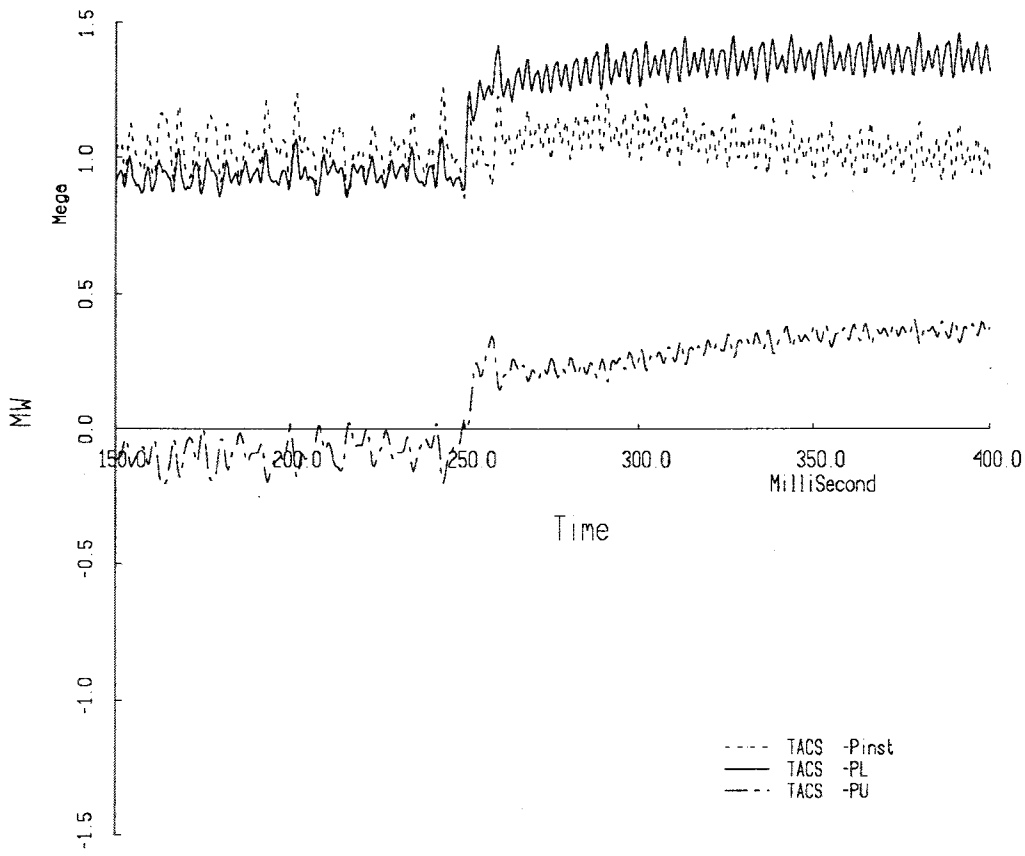

Figure 6.35: The real powers injected by the inverter and the utility, and the load power

droop characteristics for the frequency with P and the magnitude with Q. As in a conventional power system, the droops ensure that arbitrary load changes are taken up by the inverters in a pre-determined manner. The control is thus a three level structure. The innermost level controls ψ_v and δ_p, and is the same as that for control for a strong utility interconnection. The second level controls the AC side frequency and voltage magnitude at each inverter, and provides set points δ_p^* and ψ_v^* for the innermost level. The third level computes the set points for the frequency and voltage for each inverter. The two outermost levels are described below.

Control of Frequency and Voltage

The frequency controller determines the set point δ_p^* that is needed to attain the specified frequency. The structure of the frequency controller is given in Figure 6.45a. The frequency setting, ω^*, is integrated to obtain a position reference δ_{ac}^* for the AC system voltage vector $\vec{E}$

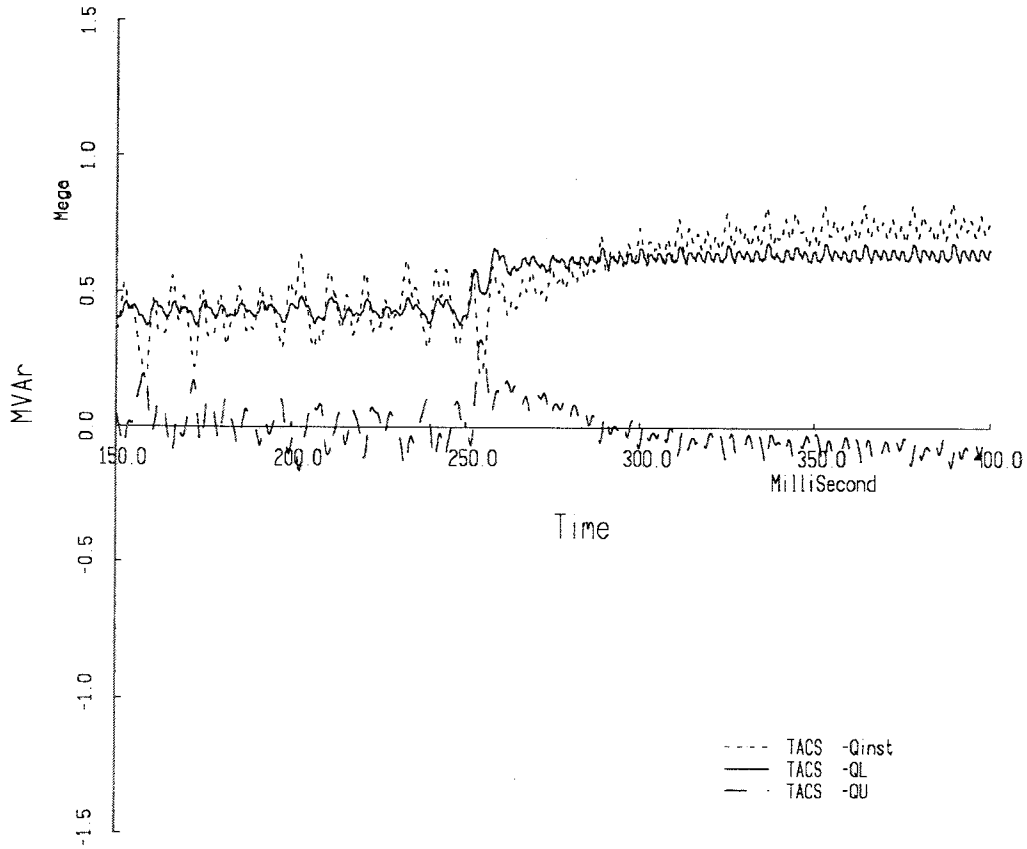

Figure 6.36: The reactive powers injected by the inverter and the utility, and the load power

across the filter capacitor. This is compared with the actual position δ_{ac}, and the error is used to produce the set point δ_p^*. This scheme achieves a very tight control of the output frequency, since the regulator attempts to control the output voltage vector at every instant.

The voltage controller determines the set point ψ_v^*, and its structure is shown in Figure 6.45b. The controller command input is E^*, the specified value of the magnitude of $\vec{E}$. The controller consists of a command feed-forward section and a magnitude feedback section. The feed-forward section gives the value of ψ_V^* needed to obtain the specified E^* with an unloaded filter. The magnitude feedback part essentially compensates for load current. The frequency ω in Figure 6.45b is the actual frequency of the AC system voltage $\vec{E}$.

The set points ω^* and E^* for each inverter system are produced on the basis of the inverter real and reactive power loadings, as described below.

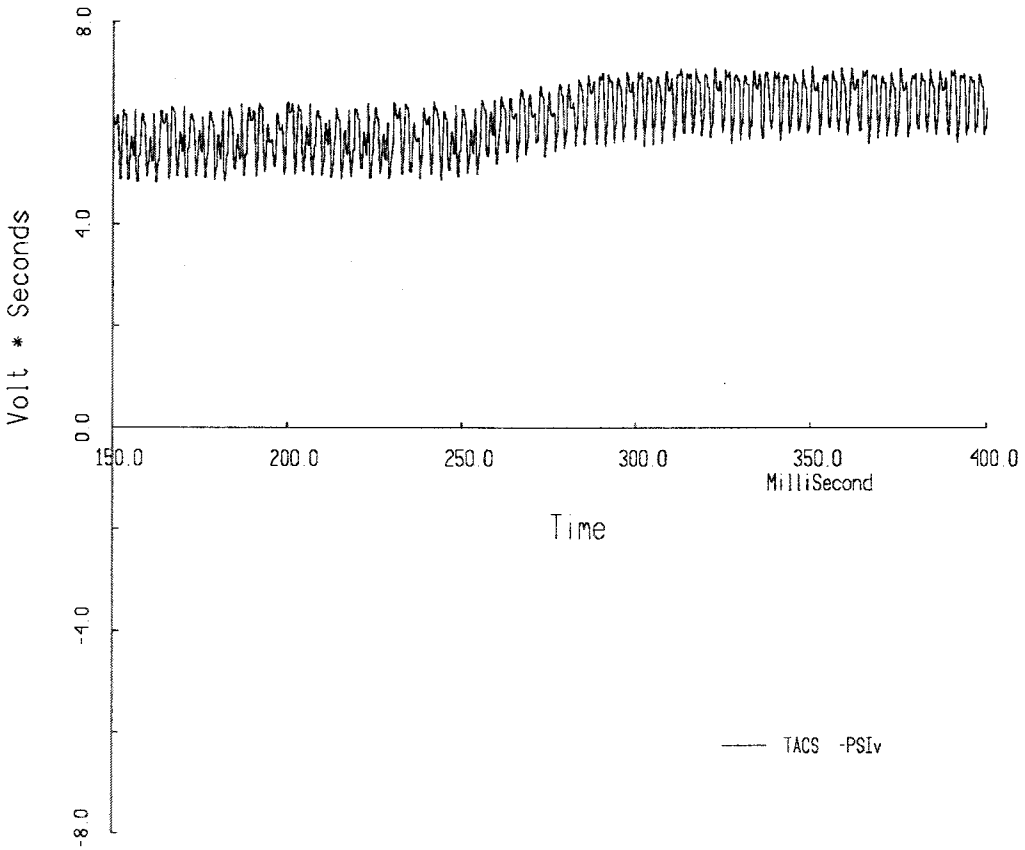

Figure 6.37: Inverter Flux Magnitude change in response to AC load change

Computing ω^* and E^* for Parallel Operation

The set points ω^* and E^* for parallel inverter operation are determined to ensure correct real and reactive power sharing between the parallel connected inverters. This is similar to the power sharing control used in conventional power systems. For the frequency controller, a droop is defined for the $P - \omega^*$ characteristics of each inverter. The droop characteristic is shown in Figure 6.46a. This can be described by:

$$\omega_i^* = \omega_0 - m_i(P_{0i} - P_i)$$

In this expression, i is the index number of the inverter, ω_0 is the nominal operating frequency of the AC system, P_{0i} is the power rating of the ith inverter, and P_i is its actual loading. The slope of the droop characteristic is m_i, and is numerically negative. The values of m for different

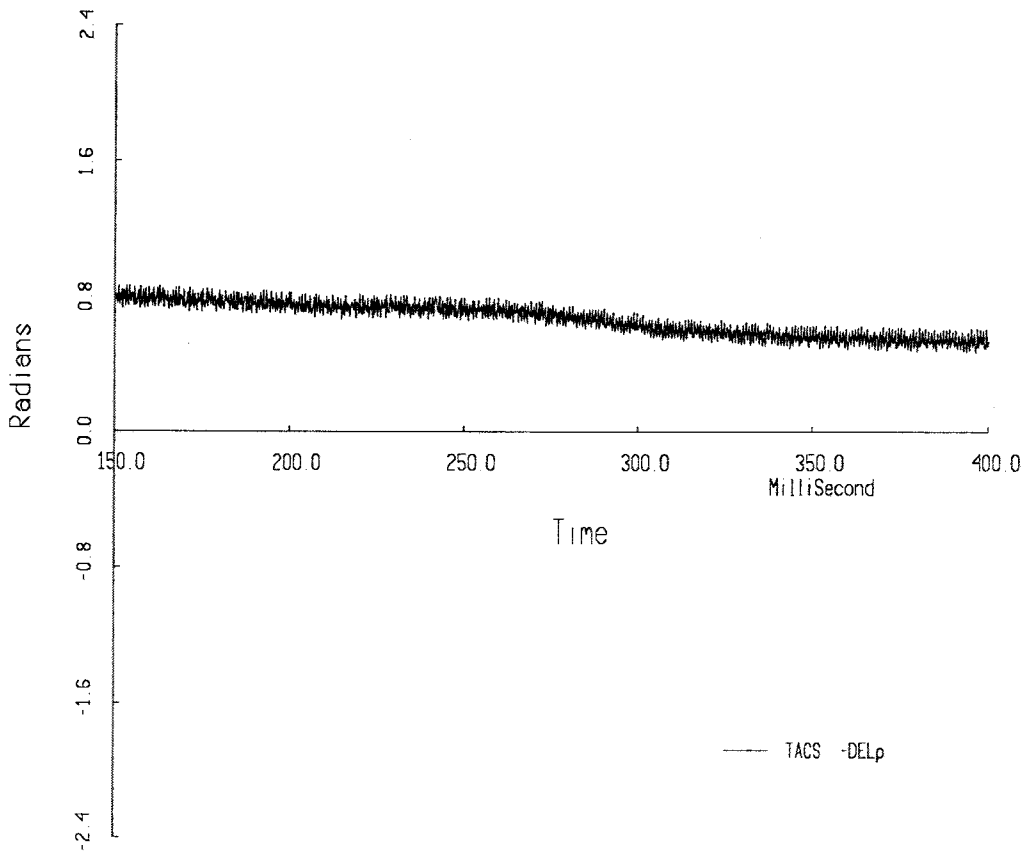

Figure 6.38: Power Angle change in response to AC load change

inverters determine the manner in which the total load power is shared by the inverters. In typical power systems, the droop is very small, and the frequency does not drop substantially with increased load. If the slopes m_i are chosen such that

$$m_1 P_{01} = m_2 P_{02} = ... = m_n P_{0n}$$

then the total power P is distributed between the inverters as follows:

$$m_1 P_1 = m_2 P_2 = ... = m_n P_n$$

$$P_1 + P_2 + ... + P_n = P$$

Thus, by an appropriate choice of slopes, it can be ensured that load changes are taken up

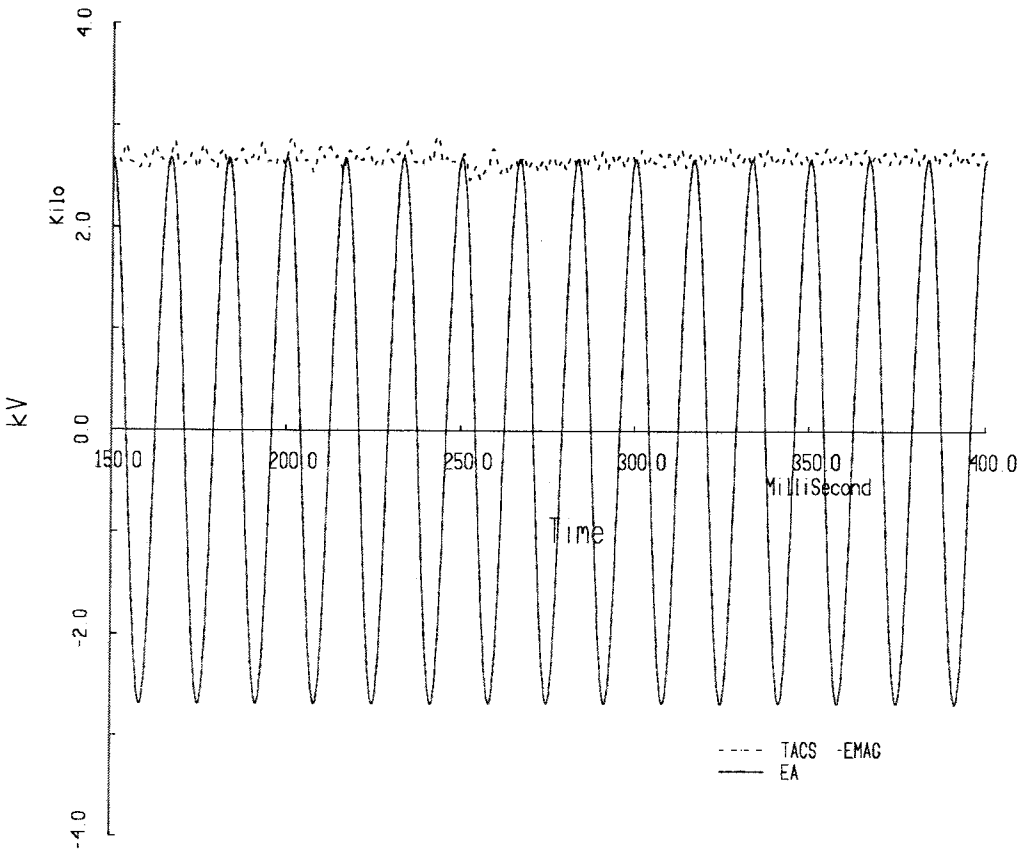

Figure 6.39: Response of the Load Voltage to AC load change

by the inverters in proportion to their power ratings. It is possible to define a composite power-frequency curve for all inverters in the system. The composite load curve is likewise defined. At the steady-state operating point on the composite load-frequency curve, the total power delivered by the inverters matches the total load power. Depending on the stiffness of the composite power-frequency curve, the steady state frequency will change with changing loads. The frequency may then be restored by a slower outer loop. To restore the frequency, the value of P_{0i} has to be modified for the inverters. This is equivalent to shifting the power-frequency curve up or down.

In a similar manner, the set points E_i^* for the voltages can be determined from drooping reactive power - voltage characteristics $(Q - E)$ for the inverters. This droop ensures the desired reactive power sharing between inverters and is described by:

$$E_i^* = E_0 - n_i(Q_{0i} - Q_i)$$

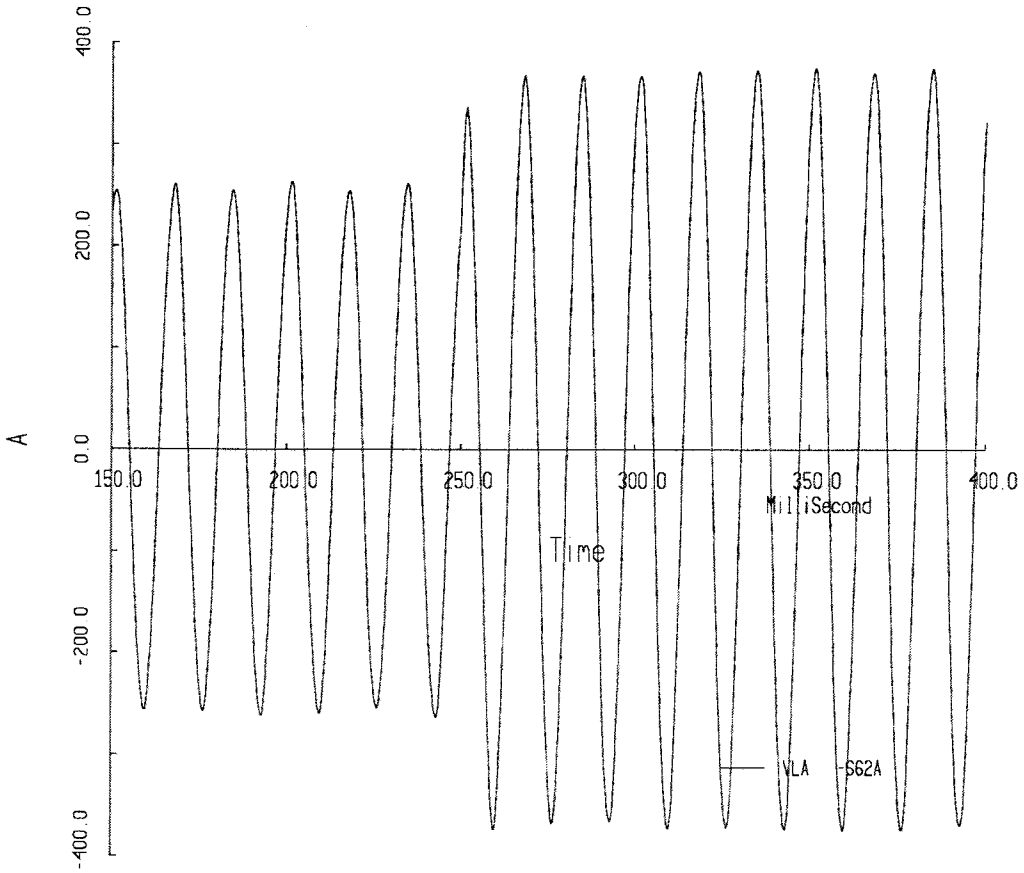

Figure 6.40: Response of Load Current to AC load change

The droop characteristic for the reactive power control is given in Figure 6.46b.

The control system described above has been applied to the stand-alone parallel inverter system of Figure 6.1. The results of the simulations are presented below.

Simulation Results: Multiple Inverters Feeding Distributed Loads

The control system detailed in the previous section has been simulated, along with distributed passive loads, according to the schematic diagram of Figure 6.1. The simulations were meant to verify the control method of the previous section, and were executed using the Advanced Continuous Simulation Language (ACSL). The values of the various parameters were as follows:

The values for the circuit components for both inverters (ref. Figure 6.1) were as follows:

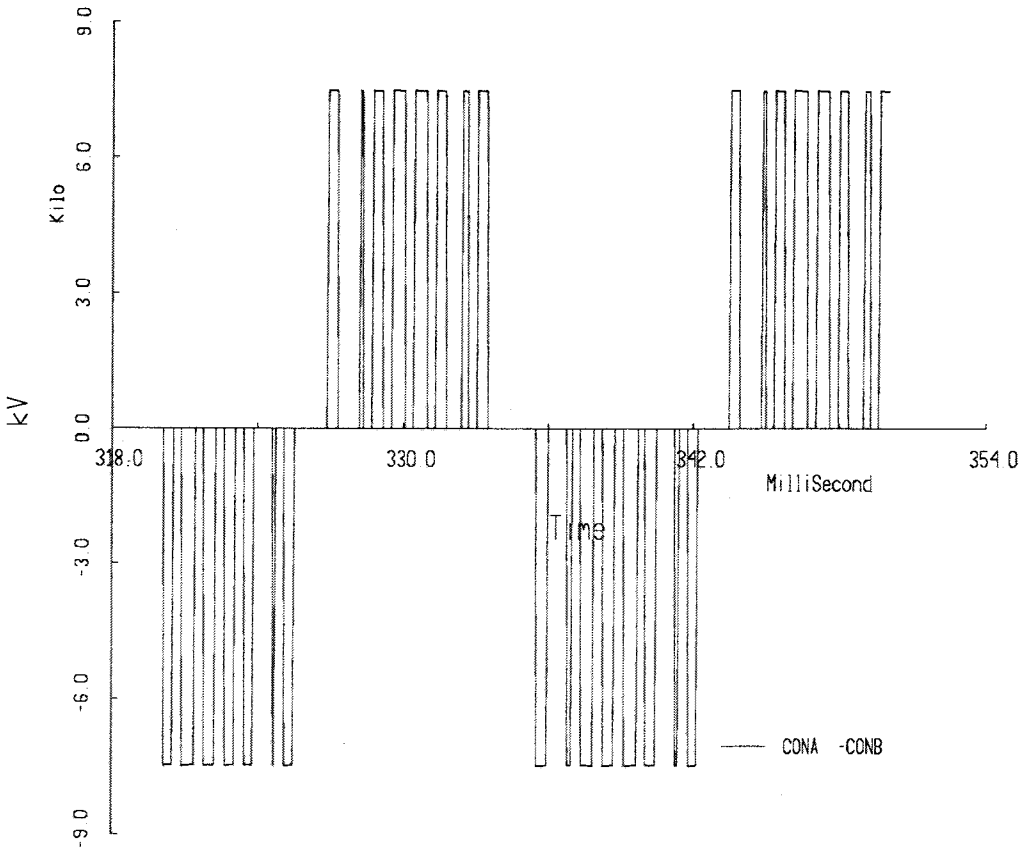

Figure 6.41: Inverter line-line voltage waveshape

The nominal voltage is 3.6 kV line-line and the nominal frequency is 60 Hz.

The following simulations show the response of the control system when the resistance R_{E2} of Figure 6.1 is suddenly reduced to half its value at 0.3 Sec. The information about the load change is not transmitted to either inverter, and the response of the controllers is solely due to measurement of local quantities, which are affected by the load change. The effect of the inverter droop characteristics in determining the load sharing is easily apparent from the simulations.

Figure 6.47 shows the real powers P_1 and P_2 delivered by the two inverters. The figure shows that Inverter 1 carries a larger share of the real power, since it has a stiffer slope.

Figure 6.48 shows the reactive powers Q_1 and Q_2 delivered by the two inverters. As with the real power, Inverter 1 carries a larger share of the load reactive power.

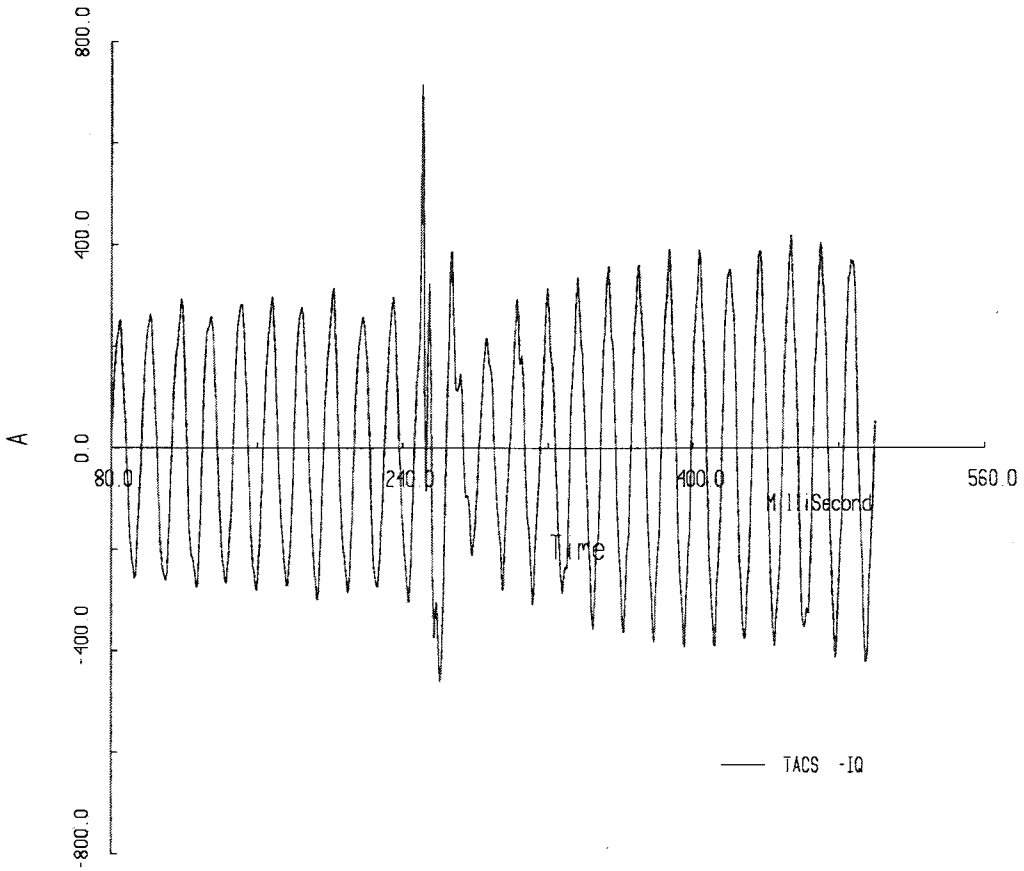

Figure 6.42: Inverter over-current limiting

Figure 6.49 shows the line-line voltage across the inverter filter capacitors. The slight distortion in the voltage waveshapes is apparent at 0.3 Sec.

Figure 6.50 shows the angle difference across the tie line between the inverters. It is seen that since the Inverter 1 carries a larger share of the load, the angle difference increases at 0.3 Sec.

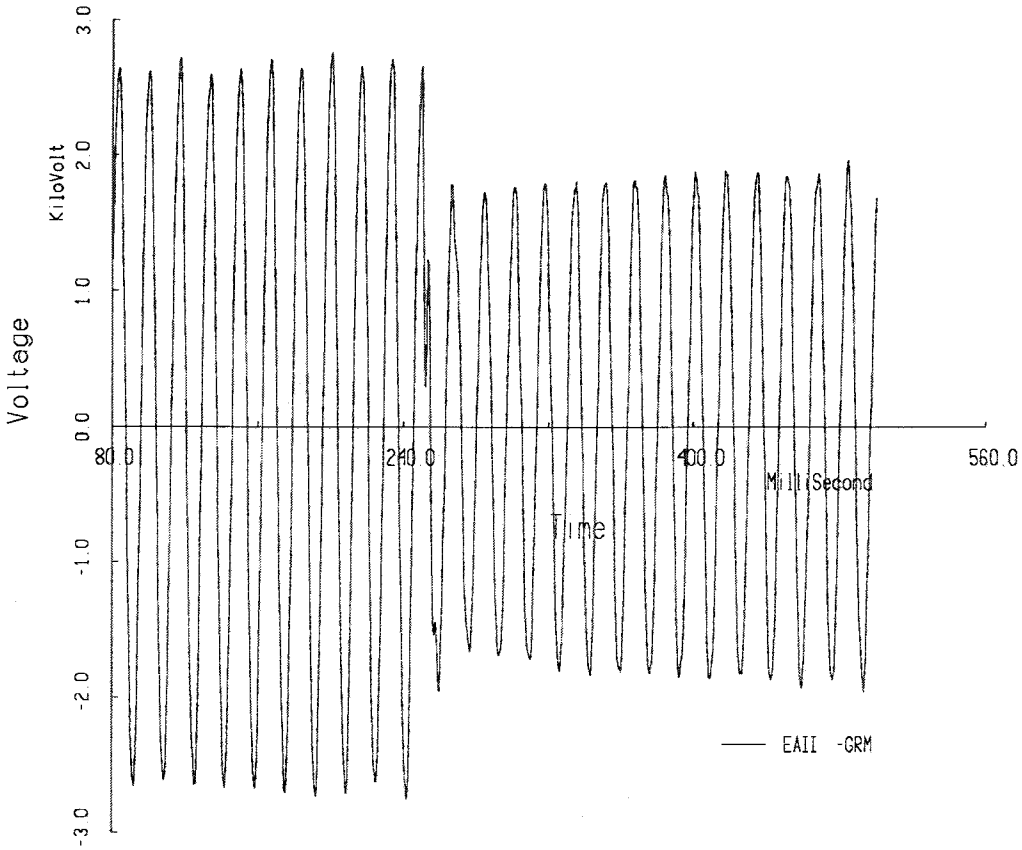

Figure 6.43: Load Voltage for inverter over-current limiting

$$P_{01} = 0.75MW \quad P_{02} = 0.6MW$$
$$m_1 = -1.4 \times 10^{-5} \quad m_2 = -1.75 \times 10^{-5}$$
$$Q_{01} = 0.2MVAr \quad Q_{02} = 0.1MVAr$$
$$n_1 = -1.0 \times 10^{-4} \quad n_2 = -2.0 \times 10^{-4}$$

$$L_{fi} = 8mH \quad R_{fi} = 0.05\Omega \quad C_{fi} = 150\mu F$$
$$L_{t1} = 6mH \quad R_{t1} = 0.4\Omega$$

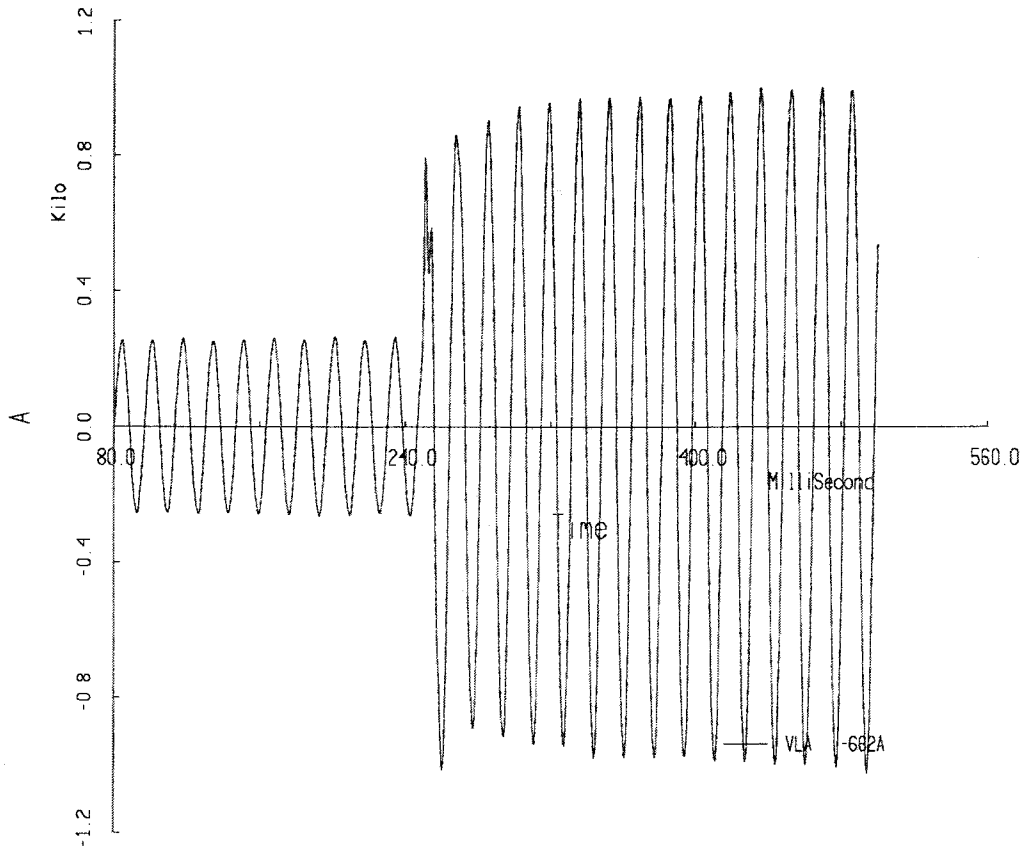

Figure 6.44: Load Current with inverter over-current limiting

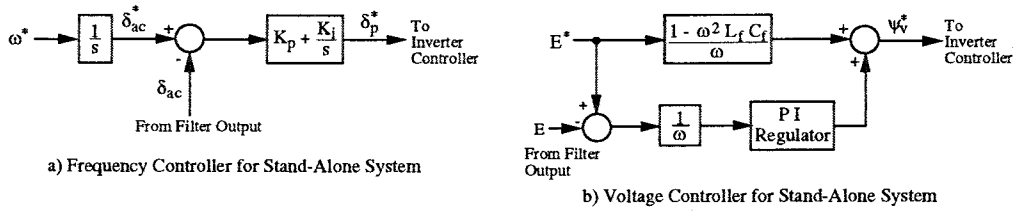

Figure 6.45: Frequency and Voltage Controllers for Stand Alone Parallel Operation

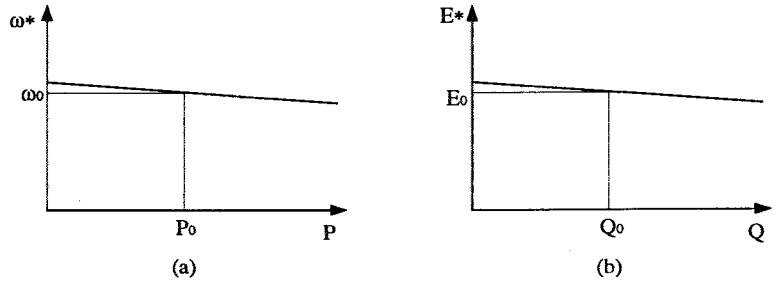

Figure 6.46: Inverter Droop Characteristics

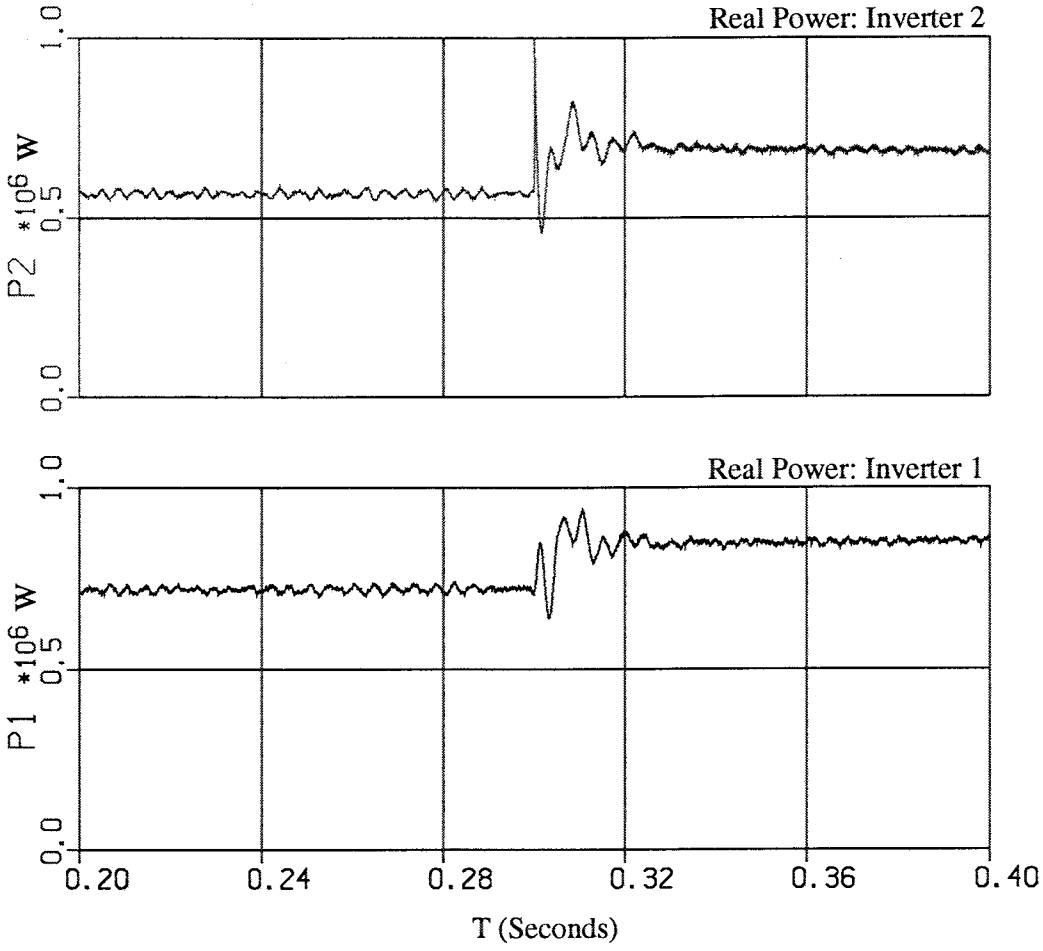

Figure 6.47: Inverter Real Power

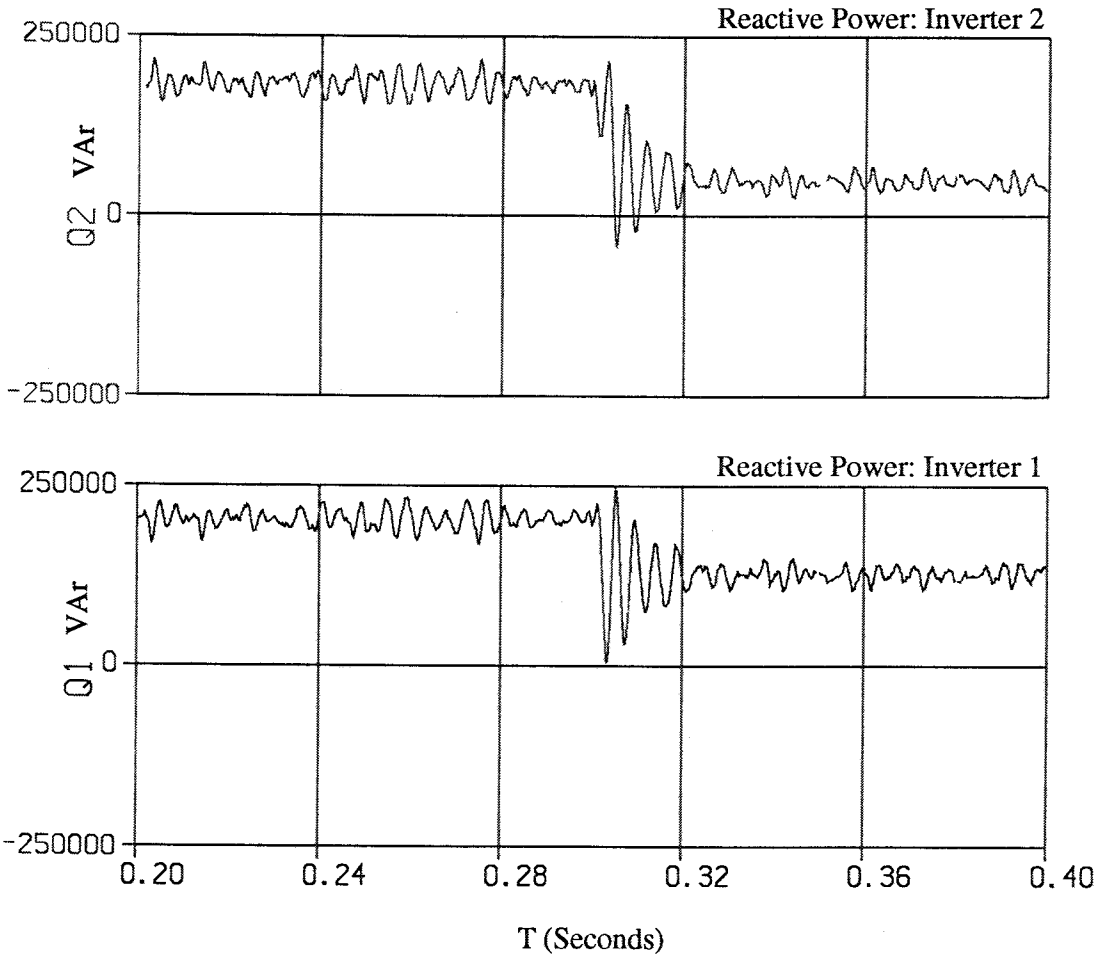

Figure 6.48: Inverter Reactive Power

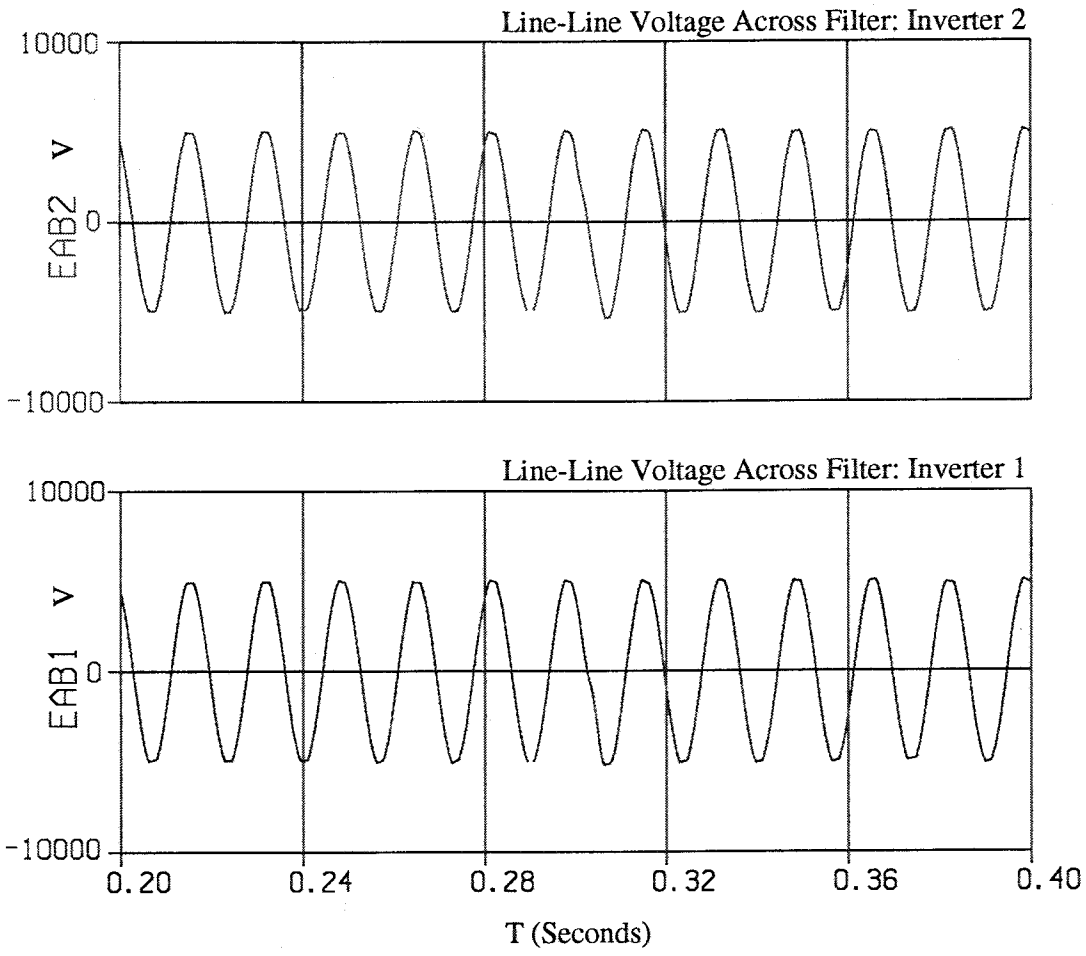

Figure 6.49: AC Syetem Voltage

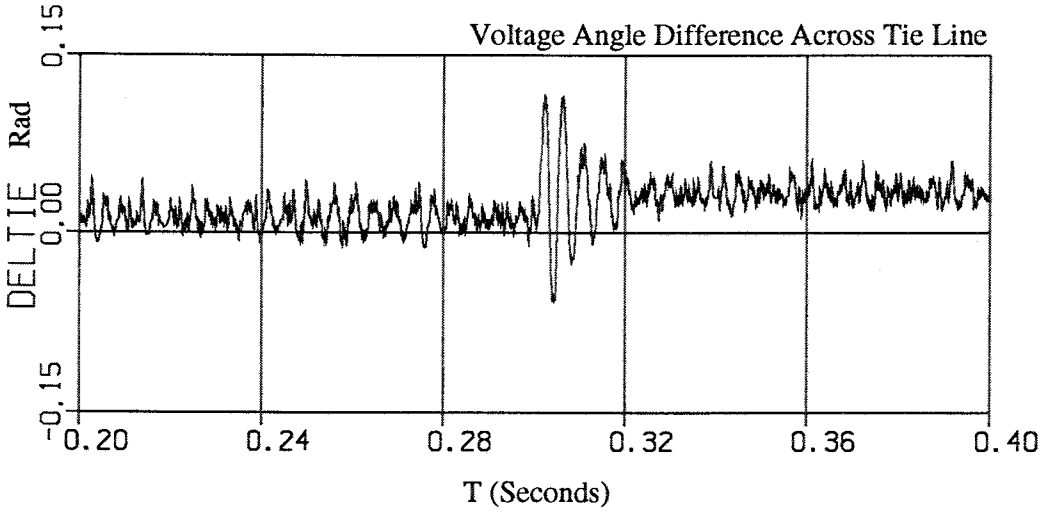

Figure 6.50: Voltage Angle Difference Across Tie Line

Chapter 7

Economics of Superconducting Transmission

7.1 Introduction

This chapter discusses some of the economic considerations involved in superconducting power transmission. A significant portion of the total cost is associated with the installation and construction of the system. This includes right of way costs, refrigerant costs, and substation costs (including converters). Since it is difficult to estimate these costs, we will restrict our attention primarily to operating costs. In particular, we will compare the refrigeration costs of a dc SPTL (superconducting power transmission line) to the I^2R loss in an equivalent three phase ac transmission line. It is of significant importance to point out that the losses in an ac SPTL contribute to a refrigeration load that is about equal to that of the heat leak from the environment. Therefore refrigeration costs in a dc SPTL are about one half of those in an ac SPTL. An ac SPTL would also require a larger enclosure and larger amount of refrigerant leading to higher initial costs [29]. DC SPTLs will also lead to many of the advantages that are associated with HVdc systems. A generic discussion of these, is given in [104].

Although these arguments tend to favor a dc SPTL over an ac SPTL, the most detailed study of such a comparison, conducted by the Philadelphia Electric Company [105] in 1977, found the ac SPTL to be more economical. The principal reason for this was that converter costs associated with the dc SPTL accounted for 60% of the total costs. The particular study was restricted to

a line length of 106 km indicating that for a longer length the dc SPTL may well become more economical. The power levels considered in that study were in the order of 10000 MW. Such high levels were considered necessary at the time to make the superconducting options competitive with the conventional ones. However, much has changed since then. The most important change is the advent of high temperature superconductors [1] which reduces the refrigeration costs considerably. This together with the fact that we are only concerned with the evaluation of the operating costs, allows us to consider power levels which are much lower and are closer to those proposed for a study system designed for examining an LVdc superconducting transmission system.

The various operating losses in a dc SPTL are discussed and results from specific case studies are presented.

7.2 Sources of Losses in a DC SPTL

Although a DC SPTL has zero resistance to pure dc current, it does experience energy losses due to harmonics generated by converters under normal conditions and during transient faults. In either case there will be hysteresis losses in the superconductor and resistive losses in the copper matrix surrounding it. A study was conducted to calculate these harmonic currents and the associated losses [7] for a 100 km, 100 kV, 2.5 GW dc SPTL, assuming a 12 pulse converter. The characteristic harmonics were found to contribute negligible losses compared to the total refrigeration loss. These losses are influenced by the magnitude of the harmonic currents and hence depend on the size of the filter reactor. For a PWM inverter they are expected to be lower due to the lower harmonic levels.

Refrigeration Costs

The heat load for refrigeration is due mainly to the heat transfer by radiation. The power required to run the refrigerator is given by [31]

$$W_r = q(\frac{T_{amb} - T_{op}}{T_{op}})(\frac{1}{\eta}) \tag{7.1}$$

where q is the heat removal rate, η is the efficiency and T_{amb} and T_{op} are the ambient and operating temperatures. The efficiency η varies with temperature [31]. For temperatures around 4K it is

between 0.1 to 0.3 and for temperatures around 80K, it is between 0.4 to 0.5. This indicates that the power required to remove 1W of heat is much less for high temperature superconductors operating at 77K than it is for low temperature superconductors operating at 4K. The numbers quoted at a recent presentation on the subject [30] were 20W and 500W respectively. These are based on using the same efficiency for both cases. If we use an efficiency of 0.4 (a conservative estimate) we arrive at 7.2W instead of 20W and we will use this figure in our calculations.

Next, one must calculate the amount of heat to be removed. For perfect black body radiation this can be calculated using the Stefan-Boltzmann law.

$$q_{300-77} = \sigma[300^4 - 77^4]W/m^2 \tag{7.2}$$

where $\sigma = 5.670E-8\ W/m^2K^4$ is the Boltzmann constant. This amounts to 457 W/m^2. For the low temperature superconductors the number is only slightly different at 458 W/m^2. For some reason, it was suggested [30] that the number would be higher for high temperature superconductors. This is obviously incorrect.

Since we are not dealing with a perfect black body, we must take into account the emissivity of the surface. We chose this value to be 0.01 [31]. The power required for refrigeration is then equal to 32.9 W/m^2. Assuming a radius of 3cm, this translates into 9.9 $kW/mile$. We will use this number in our calculations. It should be noted that the actual loss/mile will be dependent on the exact configuration and design used. Previous studies indicate that this number is reasonable, although perhaps a little higher than what might be expected.

7.3 Converter Losses

A DC SPTL requires converter terminals at its two ends. While these may involve a considerable cost of installation, attention is restricted to operating costs. The primary sources of losses are the following:

- Losses in converter transformers.
- Losses in GTO or thyristor valves.
- Losses in filters.

The losses in the valves are discussed as they are the main concern.

A thyristor valve consists of individual thyristors connected in series. A lower operating voltage such as that in LVdc systems would require a smaller number of series devices. The main component of losses in conventional thyristor valves in the on-state loss of the thyristors. This is likely to be a little higher for GTOs due to a slightly higher forward voltage drop. The *average steady state power loss* is given by

$$P_l = V_{\text{on}} I_{\text{on}} \frac{t_{\text{on}}}{T} + V_{\text{off}} I_{\text{off}} \frac{t_{\text{off}}}{T} \tag{7.3}$$

The offstate loss due to leakage current I_{off} is negligible. Since a semiconductor switch requires a finite time to make the transition from one state to the other, the product of voltage and current during this transition is non-zero. Thus, there is a *switching loss* which includes losses in snubbers. The total energy dissipated in the turn-on and turn-off operation multiplied by the switching frequency gives the net switching loss. The switching loss is typically 3-10% of P_l [95] for normal six pulse operation. This increases with pulse number. For PWM this loss is likely to be considerable. The switching loss is expected to be lower for a VSI compared to a CSI.

For HVdc systems, the total converter losses are typically less than 1% per terminal [32]. We will assume the same figure for our calculations. The actual losses may be higher depending on what type of converters are finally used with the system.

7.4 Comparison with a Conventional System

The system proposed for LVdc superconducting transmission is a networked system. However, for the purposes of comparing the operating losses in a superconducting system with a conventional ac system, we considered a single transmission line. The voltages considered for the ac case were 138 kV and 230 kV. The dc SPTL operates at $\pm$7.5 kV. The resistance per phase per mile for the ac lines was used as 0.259 ohms and 0.12 ohms respectively [99]. The losses in the dc SPTL due to refrigeration and in the converters were based on considerations discussed above i.e. 9.9 kW/mile and 2% respectively. The results from two cases are shown below.

	Conventional ac	dc SPTL
Daily Loss(MW)	300.11	204.96
Annual Cost (M$)	7.5	5.1
Cost/MW-mile	151.16	103.2

Table 7.1: Operating costs of a 100 mi, 500 MW, 230 kV line vs. dc SPTL

	Conventional ac	dc SPTL
Daily Loss(MW)	50.38	52.87
Annual Cost (M$)	1.2	1.3
Cost/MW-mile	181.25	190.22

Table 7.2: Operating costs of a 70 mi, 100 MW, 138 kV line vs. dc SPTL

The detailed results revealed that peak load periods tend to favor the dc SPTL whereas the low load periods tend to favor the ac line, particularly in case of the shorter line with the lower power rating. Thus, load factor is a strong determinant of economic viability. The results also illustrate that for a longer line and higher power ratings, the dc SPTL tends to become more economical.

7.5 Conclusions

The comparisons made in this study are based on a single radial transmission line instead of the networked system that has been proposed for LVdc superconducting transmission. Moreover, the numbers used are rough estimates. For this reason, it would be unwise to draw too many conclusions from the specific case considered here. Nevertheless, the study does bring out some points which are indicators of the operating economics of superconducting transmission.

It was observed for high temperature superconductors that the refrigeration costs are reasonable and considerably lower compared to low temperature superconductors. It was also observed that making the line power rating as high as possible would favor the dc SPTL over an ac line where the I^2R losses would increase with the power rating. The line length and the load factor also play

a significant role in the economic viability of a dc SPTL. The various losses discussed here would be an important part of any integrated AC-DC optimal power flow.

Chapter 8

Conclusion

8.1 Summary

The LVDC transmission system utilizes direct current transmission to avoid losses resulting from time changing flux and currents in the superconducting material. The low transmission voltage reduces the number of transformer stages necessary as well as reducing the need for high voltage insulation. The low voltage level allows for the direct connection of generators to the rectifier bridges, and also suggests the possibility of optimizing the generators to the rectifier. The dc system could have tens of rectifier bridges feeding possibly hundreds of inverter terminals. The low voltage level allows for the use of self-commutated inverters that are capable of feeding very weak, or even passive ac systems.

The lossless nature of the superconducting cables allows new freedom in the control of the dc system as well as placing some additional constraints. The cables no longer have current dependent voltage drops over their length since they have no resistance. The entire dc system reaches the same steady-state voltage, rather than having each terminal at a slightly different voltage. Therefore changes in the dc voltage level to be used as a communication signal for the control system, much as change in frequency is used on an ac system. A voltage droop scheme is used to provide distributed dc voltage regulation, rather than using a scheme where only a single terminal can regulate voltage one time. The distributed voltage regulation scheme can be extended to multiterminal systems of arbitrary size, rather than being limited to four or five terminal systems as traditional schemes are.

Fault protection is another important issue for parallel and mesh connected dc systems. Some form of circuit breaker is required. DC circuit breakers operate by having a back voltage trigger resonant oscillations in the current through a switch. These oscillations are used to force a current zero, and allow a disconnect switch to open. The back voltage can be due to an current arc, as is done in conventional dc breakers or it could also be from the normal resistance of a quenched superconductor. A breaker based on this process was introduced.

One problem faced by mesh connected dc systems is the inability to control the distribution of current within the mesh itself. This is especially important for a superconducting transmission system, where the cables must be kept away from there current limits. A line that is restored to a superconducting system will carry no current until there is a voltage change across it, since all of the terminals on the system will have equal steady-state voltages. A scheme utilizing quenchable superconducting devices for current steering is presented. This scheme is able to transfer small incremental blocks of current out of a line through the alternate pulsing of parallel devices in a single line. This limits the section of superconducting material that quenches to a small, known area, and makes it easier to have increased refrigeration at that location. This scheme will result in energy dissipation, but this is very small compared to the total energy transferred.

The issues pertaining to the inverter interface in a superconducting DC transmission environment have been discussed. These issues can be broadly grouped under two headings: the inverter topology, and the inverter control scheme. The general characteristics of Voltage Source Inverters (VSIs), and those of Current Source Inverters (CSIs) have been reviewed. The essential control requirements of the inverters have been presented for various inverter interconnections with the AC system.

A specific topology of CSI, the Dual Current Source Inverter (DCSI) has been investigated in detail. The topology has been presented and studied. The Space Vector formulation of the DCSI switching has been developed. The control requirements specific to this topology have been discussed. The region of independent control of Real Power (P) and Reactive Power (Q) possible with the DCSI has been identified. An overall control scheme for the DCSI connected to an AC system has been developed. The DCSI, the AC system, and the control have been modeled in the EMTP, and simulation results have been presented. The simulations show the effectiveness of the DCSI control in controlling P and Q delivered to the AC system.

The three phase bridge VSI has been considered for interface with the AC system. The basic

Space Vector formulation of the VSI has been developed. A control scheme has been developed for the control of the VSI connected to a stiff utility system. This control has been developed using the time-integrals of the voltage vectors as the basic control variables. This approach has fast dynamic response, and facilitates the definition of a Power Angle. The control has been developed using only those quantities which can be measured locally by the inverter control scheme. On the basis of the control scheme for an inverter connected to a stiff AC system, the control scheme for an inverter connected to a weak AC system is developed. Next, a control scheme for parallel operation of two VSIs in a stand-alone system (without the presence of a utility voltage) has been developed. This scheme utilizes only locally measured variables, and does not depend on signal communication between the inverters for voltage synchronization. The total load P and Q are shared by the inverters in a pre-determined manner by droops. The topologies and control have been simulated, and simulation results are presented. The effectiveness of the control has been demonstrated.

Studies done on a prototype 13 kV distribution system revealed that such inverter fed ac systems would have lower fault currents requiring changes in present protection schemes. The configuration of the inverter banks was found to have an effect on voltage sags on unfaulted feeders. It was observed that building small modules, each feeding a separate feeder would help solve the problem of voltage sags.

The economic comparisons made in this study are based on a single radial transmission line instead of the networked system that has been proposed for LVDC superconducting transmission. Moreover, the numbers used are rough estimates. Nevertheless, the study does bring out some points which are indicators of the operating economics of superconducting transmission. It was observed for high temperature superconductors that the refrigeration costs are reasonable and considerably lower compared to low temperature superconductors. It was also observed that making the line power rating as high as possible would favor the dc SPTL over an ac line where the I^2R losses would increase with the power rating. The line length and the load factor also play a significant role in the economic viability of a dc SPTL. The various losses discussed here would be an important part of any integrated AC-DC optimal power flow.

8.2 Future Extensions

This work can be extended in several directions. The most important aspect is the further development of superconducting LVDC transmission systems. This can proceed in the following directions:

Cable Development The present generation of high temperature superconductors is inadequate for power transmission. The current densities are still rather low, and the ability to produce long cables is still lacking. All of the present research concentrates on bulk superconductors, with the majority of the emphasis placed on ac transmission.

Near Term Applications The near term applications of LVDC transmission need to be developed further. These would be single point to point lines into urban areas, or simple systems with several parallel taps off a single line. The full requirements of such a system need to be determined. Then the possible economic benefits can be produced to generate interest LVDC transmission. A key to any near term applications must be to demonstrate the superiority of this system over ac transmission.

Inverter Control The control scheme needs to be demonstrated with more complicated load systems connected to the inverters. This includes strong ac systems with detailed load models, weak ac systems, and passive ac systems. It is also useful to look at ac systems fed by more than one inverter, with the inverter interconnected on the dc side as well. The response of the dc system to ac disturbances must be studied as well. The interactions between the ac systems and dc systems, especially in the case of inverter load shedding need to be considered. It may also be useful to look at the effect of feeding large motor loads, especially for possible applications with industrial power systems

Further Consideration of Inverter Topologies The work presented here concentrated on very simple inverter topologies, that do not are inadequate for use with passive ac systems. However, these have not been studied in conjunction with a full dc system at present. It will also be useful to develop simplified representations for these inverters for the simulation of large systems.

Interfacing Alternative Energy Supplies Possible schemes for interfacing the LVDC mesh to alternative energy supplies or storage systems was discussed briefly. This needs to be studied

further to look at the characteristics of each of specific interfaces, whether its a photovoltaic system, or a SMES coil, to see how these will interact with the dc system, and determine any special protection needs.

Application with Normal Conductors The possibilities for using the voltage droop scheme, or a modified form of it for dc systems with normal conductors need to be pursued further. A first task would be to determine whether or not the scheme can be implemented without any additional communications links. There may be system configurations where observers alone will be sufficient. Then the voltage droop scheme can be implemented for HVDC transmission.

Application to Industrial Power Systems This control scheme can be implemented for other types of power systems, not just power transmission. It could be used for space station power systems, or possibly industrial power systems. The requirements to implement the voltage droop scheme for a system using normal conductors, utilizing communication between terminals needs to be considered. A scheme using communication between terminals can still be implemented for industrial power systems, where the short distances between converters eliminates the concerns centered on communications problems.

Several of the topics introduced here are not likely to see near term application to superconducting LVDC systems. However, several of these also warrant further study:

Direct Connection of Generators Direct connected generators have few applications. Therefore, much needs to be learned about the design and behavior of direct connected generators. Especially for application to LVDC systems. Possible areas of study include: generator-rectifier interactions during current changes, generator behavior at MVA limits, twelve pulse bridges, and converter optimizations. These topics were introduced here, but more needs to be known to see if this is actually feasible.

This project was done as part of a scoping study for LVDC transmission systems. This resulted in a large number of topics being introduced, but not pursued to completion. Part of this was due to the lack of concrete information about superconducting cables. While this report presents a design for a superconducting cable, this is only to produce a model to use for system development. The key results from this report are system design and studies. The system results do not depend

on a specific type of superconducting cable. There are many interesting topics that can be studied, several of which do not require further development of superconducting LVDC transmission. These spin-offs, such as application of the voltage droop for industrial power systems could be applied at present.

Appendix A

Voltage Droop on the DC System

An overall control scheme for superconducting, parallel connected, LVDC systems is developed here. This scheme differs from the classical approach for controlling parallel and mesh connected multiterminal dc systems through the use of a distributed voltage control scheme. The voltage control scheme is based on voltage droop. The control characteristics also have built-in limits to allow the system to operate in the face of disturbances.

A.1 Classical Meshed Connected HVDC Control

'Classical' control schemes for parallel or mesh connected multiterminal HVDC systems are basically extensions of the control modes used for point to point HVDC systems. The basic control scheme regulates the mesh voltage level at one converter terminal, and operates the remainder of the converter terminals in a current regulation mode. The converter terminal regulating voltage is unable to control its local current. Its current is determined by the other converter terminals' current demands. Such a situation is undesirable for an inverter that is scheduled to supply a fixed amount of power to a load system. Therefore, voltage control should be limited to rectifiers for normal operation. The current limits of the voltage regulating converter can create problems during transients. Many implementations of this basic scheme depend on the presence of a central controller to balance current orders between the converters. This requires fast communication between the converters to coordinate currents during a disturbance [38, 39, 41, 43]. A scheme with the ability to coordinate control on the mesh without fast communication was proposed by

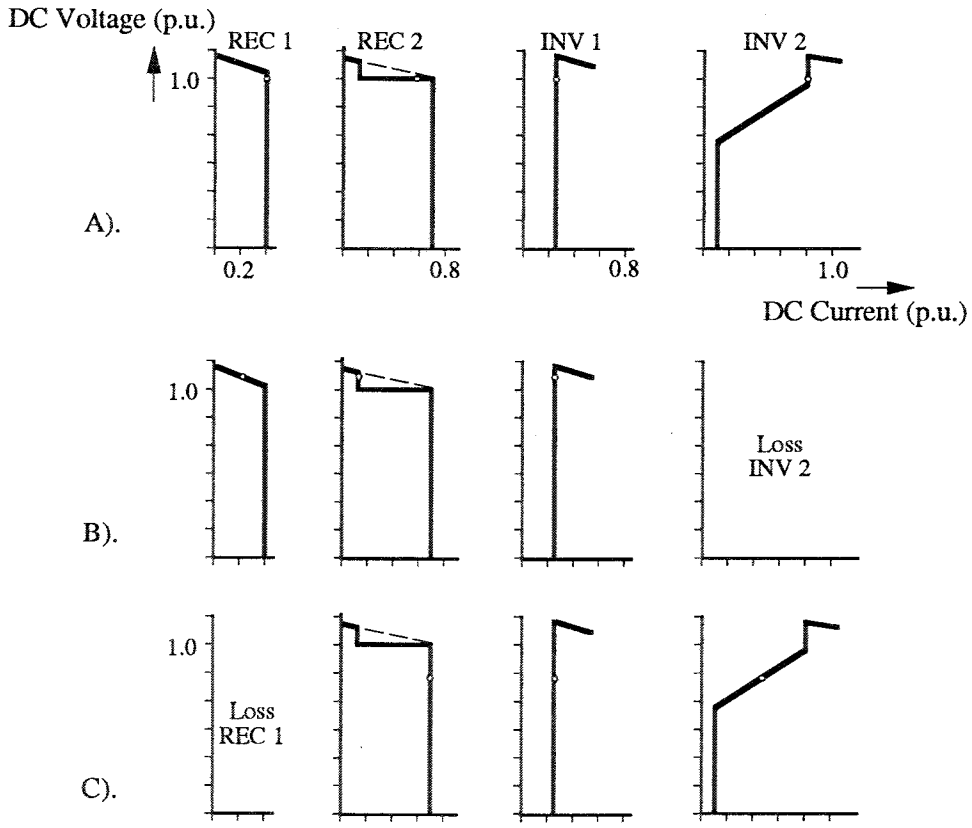

Figure A.1: Classical Multiterminal HVDC Control Characteristics

Lasseter, Krüeger, and Povh [42]. Schemes for controlling a mesh connected multiterminal HVDC systems run into difficulty when one of the converters reaches a current limit. The voltage regulating converter changes to a current regulation mode when it hits a current limit. One of the other converters must then regulate dc voltage. This mode switching between different terminals in the mesh must be coordinated so that one of the converters always operates in a voltage regulation mode, and the others operate in current regulation mode. The scheme described in [42] is able to change modes through an intricate design of the control characteristics, as shown in Figure A.1. This allows the system to respond to contingencies on the dc system without the need for fast communication. The system can then be maneuvered into an optimal state, once it has reached steady-state, with the assistance of communication.

The characteristics shown in part A) of Figure A.1 are the normal steady-state operating characteristics of a four terminal, mesh connected HVDC system. The system has two rectifiers

feeding two inverters. Rectifier 2 is regulating the mesh voltage, while the other three converters each operate in a current regulation mode. Note that rectifier 2 has a broad, flat voltage regulation characteristic, allowing it to keep a constant voltage on the system over a wide range of current levels.

The larger of the two inverters, inverter 2, shuts down in case B). The total current demand of the system decreases, and causes rectifier 2 to enter a constant current mode at its lower current limit. This mode switch causes the dc voltage level to increase and also forces rectifier 1 onto a voltage regulation portion of its characteristic. Part C) of the figure shows rectifier 1 going off line. This causes rectifier 2 to reach its upper current limit, and again assume a constant current mode. This decreases the mesh voltage level causing inverter 2 to assume voltage control. Notice that this type of control scheme requires fairly complicated control characteristics for individual converters. This combination of characteristics is tailored to a specific system, and would need to be changed if a new converter terminal was added. This can result in a complicated overall control scheme for a large system, even one with as few as 5 terminals. It becomes increasingly more difficult to determine which converter should assume voltage regulation following mode changes as system size increases.

A.2 Desired Control Properties

The proposed superconducting, LVDC transmission could have tens of rectifiers feeding hundreds of inverter terminals. The control scheme for such a system must be able handle converter limits without fast communication or the intricate mode switching of Figure A.1. The control scheme should be general in nature, and not tailored to any specific system layout, or to a system with a specific number of terminals. This makes it much simpler to expand the system. Regulating the mesh voltage at a single terminal causes this terminal to act like a slack bus in a power flow. This is an undesirable situation for an inverter terminal, especially one operating in a power control mode. Nor will this allow a rectifier (or the unit-connected generator feeding it), to operate in its optimal operating zones. This will also require frequent mode shifts as one rectifier hits its current limit and another one goes into voltage regulation. A more effective scheme would be to operate all of the rectifier terminals in a joint voltage regulation mode. Then it would be possible to balance of the power loading of the terminals more effectively. The overall control system would also need to respond to faults and disturbances in addition to routine operations. The key is for the system

to be able to maintain some form of stable operation in the face of contingencies. The system can be moved to an optimal operating point with slow communication later. The control system must also be able provide damping to the dc system. The lossless nature of the superconducting cables results in a transmission system with little inherent damping in the cables. However, the cables will have a resistance to any sinusoidal current, which will help to damp any LC resonances that take place as well as harmonic currents. This problem was discussed for ac systems in [28].

A.3 Inverter Control of Real and Reactive Power

One of the features of the superconducting LVDC transmission system is the ability to supply weak and passive ac loads. This requires ability on the part of the inverters to control the real and reactive power supplied to the load system. This can be done by controlling the magnitude and phase of the quantity injected into the ac system. This is a voltage injection for a VSI, and a current injection for a CSI. The reactive portion of the injection to the ac system is provided by internal variations within the converter itself, and does not affect the average dc power drawn off of the mesh by the inverter [89]. The real component of the inverter output power is equal to the dc power drawn by the inverter, minus losses within the inverter. Maintaining a still voltage level on the dc system will allow the inverters to regulate their power by varying the local dc current drawn off of the mesh [33].

A.4 Voltage Droop Control

A.4.1 The Basic Idea

A voltage droop scheme provides a joint voltage regulation scheme for the dc mesh. This allows all of the inverters to operate in a local current or power control mode. The voltage droop scheme does not require fast tracking of the voltage to maintain stability. This results in a system requiring fast communication for consistent operation during transients.

A distributed voltage regulation scheme must be able to maintain a consistent sharing of current between the rectifiers to be successful. A useful analogy to this is the use of frequency droop on the ac system to set an operating frequency, and also regulate the distribution of real

power loading on the generators. Similarly, a voltage droop scheme can be implemented for a dc system. The lack of resistive voltage drops with superconducting cables is used to advantage in this situation. Each of the nodes on the dc system will reach the same steady-state voltage level. Thus it is possible to use the change in voltage on the dc system as a communication signal, without having the system state affect the solution.

Each line commutated rectifier bridge has a current dependent voltage drop due to commutation overlap. This can be modeled as a resistance in steady-state converter models [36]. Rectifier operation in a constant firing angle mode can be modeled as voltage source connecting to the mesh through a resistance. Thus the line commutated rectifier has a 'built-in' droop. Any change in the current drawn off of the rectifiers will change the voltage drop across the resistance. The change in current will divide between several rectifier terminals according to their equivalent resistances via current division. The system will settle into a new steady-state at a different voltage level following a change in total current.

The system response to changes in current demand is similar to that with frequency droop on ac systems. This can be demonstrated for the study system in Figure 1.2, which has three rectifier terminals feeding a dc system. The three rectifiers feature identical droop 'resistances.' Figure A.2 shows a simplified model for these rectifiers feeding a dc system represented as a variable current load. The distribution of a change in current between the rectifiers is based on a simple resistive current divider. This is demonstrated in equations A.1 and A.2. This representation is sufficient for observing steady state operating points. All of the nodes will reach equal steady state operating voltages. This will not be adequate for representing the dynamics of the changes because the dc system isn't included. The 'RL' time constant between the slope of the droop characteristic, and the inductance in the path between a given rectifier and the inverter that changed its current demand would affect the response.

$$\begin{aligned} \Delta I_{tot} &= \Delta I_1 + \Delta I_2 + \Delta I_3 \\ &= \frac{\Delta V}{R_1 \| R_2 \| R_3} \end{aligned} \tag{A.1}$$

$$\Delta I_1 = \Delta I_{tot} * \frac{R_2 \| R_3}{R_1 + R_2 \| R_3}$$

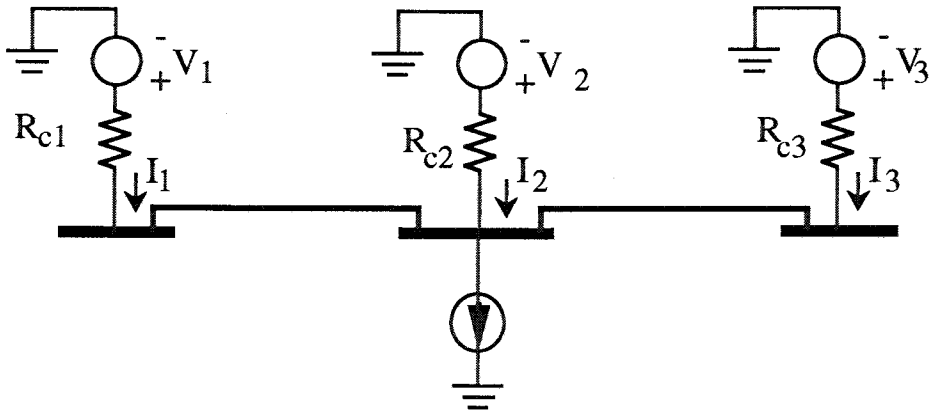

Figure A.2: Simplified Equivalent of DC System Fed by Three Rectifiers

$$\begin{aligned} \Delta I_2 &= \Delta I_{tot} * \frac{R_1 \| R_3}{R_2 + R_1 \| R_3} \\ \Delta I_3 &= \Delta I_{tot} * \frac{R_1 \| R_2}{R_3 + R_1 \| R_2} \end{aligned} \tag{A.2}$$

The system begins in an initial state with each rectifier supplying $7000A$ to the mesh at a voltage of $7500V$, shown at operating point 'A' of Figure A.3. The total current drawn by the dc system is then decreased by $3kA$. This results in the system operating voltage increasing as the current is decreased, shown at point 'B' on the figure, where each of the rectifiers supplies $6kA$.

Operating point 'C' on Figure A.3 shows a case where rectifier 3 has been shut down. The other two rectifiers pick up the load supplied by that rectifier, increasing their currents to $9kA$. Figure A.4 shows a computer simulation of this case. Figure A.4(a) shows the mesh voltage at the three rectifier terminals. The large swings are due to interactions with the current regulators at the inverters. Figure A.4(b) shows the currents supplied by each of the three rectifiers. Notice that one current goes to zero, while the other two increase to maintain the desired total current. A well designed system will have sufficient excess capacity in the rectifier terminals to operate without any one of the terminals. It may not be able to operate at full output power, but it should be able to supply a substantial load. However, the droop scheme will need a way to respond to generator MVA limits or rectifier current limits.

The current distribution between different rectifier terminals depends on the relative droop

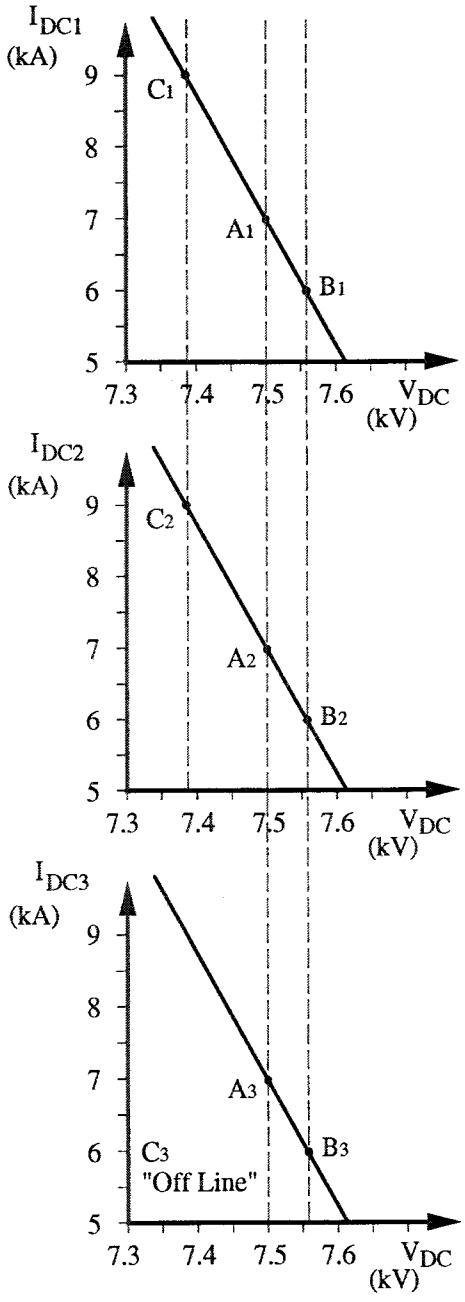

Figure A.3: Example of the DC Droop Scheme for the System of Figure A.2

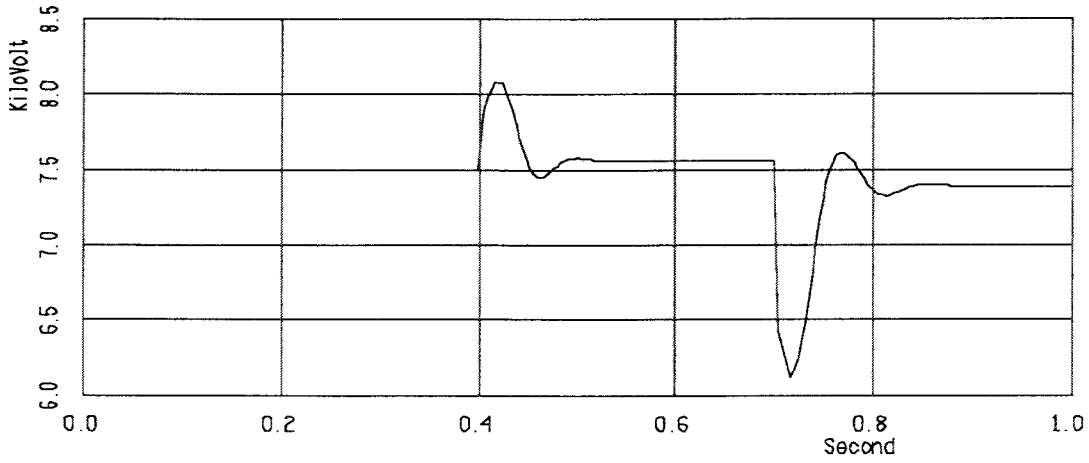

(a) DC Voltage Level

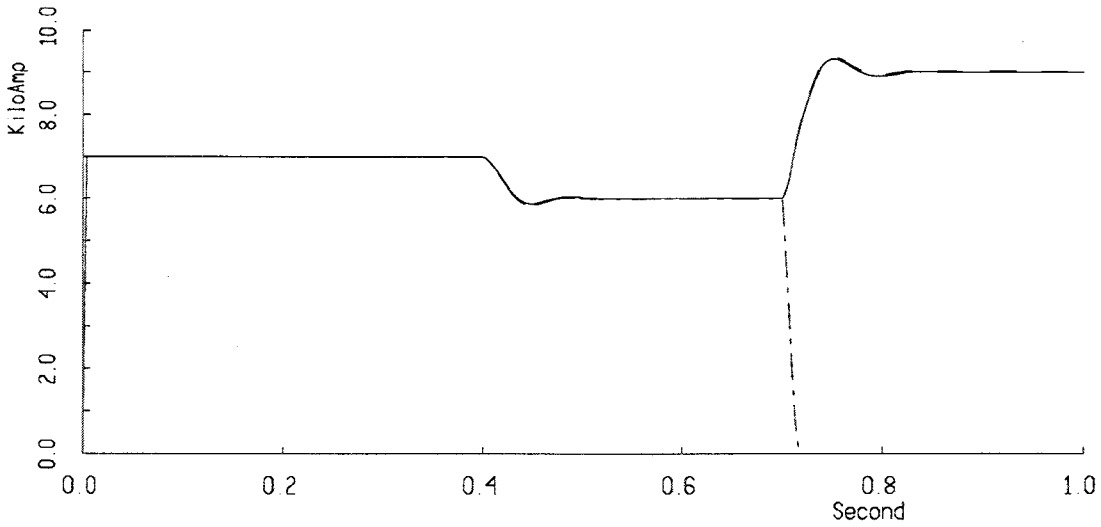

(b) Currents at Rectifiers 1 and 2 (Solid Line), and Rectifier 3 (dash-dotted Line)

Figure A.4: Simulation Demonstrating Voltage Droop for Case in Figure A.3

Rectifier Droop Terms	Current $I_{tot} = 21kA$	Current $I_{tot} = 30kA$
$R_{c1} = 0.29\Omega$	3333.333 A	4774.2 A
$R_{c2} = 0.155\Omega$	6333.333 A	9030.4 A
$R_{c3} = 0.086\Omega$	11333.333 A	16194.3 A

Table A.1: Current Levels for a System with Unbalanced Rectifiers

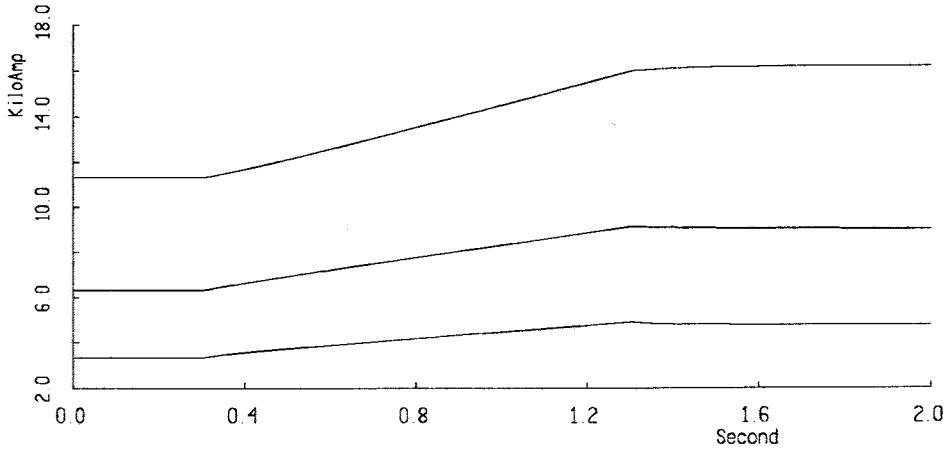

Figure A.5: Example with Unbalanced Rectifier Droops for the System of Figure A.2

resistances of the different rectifiers. The above example had identical rectifiers with identical slopes for their droops. Therefore, the final steady-state current distributions show are the same for each. Figure A.5 shows the results of a simulation where $R_1 = 0.29\Omega, R_2 = 0.155\Omega$ and $R_3 = 0.086\Omega$. Table A.1 shows the rectifier currents for $I_{tot} = 21kA$ at $V_{dc} = 7.5kV$, (rated conditions) and when I_{tot} has been ramped to $30kA$. The rectifier currents computed using equations A.1 and A.2 match those from the simulation. Notice that the rectifier currents in Figure A.5 ramp up to the near their final levels, and then gradually shift to the steady-state values. This is because each rectifier sees a different time constant. Two factors dominate in determining this time constant. One is the 'resistance' presented by the commutation drop. The other comes from the equivalent inductance between the rectifier and location the of the current change. The balance of the dc system needs to be modeled to represent these dynamics. But the steady-state operating points are independent of the layout of the mesh.

A.4.2 Dynamic Control of Voltage Droop

The built-in droop for a large rectifier is quite small. It takes a very large change in current to change the mesh voltage level significantly. This is desirable for normal operation, since it will result in a relatively constant dc voltage level, making it simpler to regulate power at the inverters. However, it also means that a large change in current will cause the generators to approach their MVA limits while not causing a significant change in the mesh voltage. Large changes in the dc voltage can be used to trigger load shedding at the inverters as will be discussed later. In such a case a steeper slope on the droop characteristic would be desirable. This would allow more ability for the inverters to help the system reach a stable point.

The use of the built in droop on each rectifier terminal has some disadvantages. The relative slopes of individual the droop characteristics are fixed by the physical parameters of the generator or transformer connected to each rectifier. This may result in a case where a small rectifier will have flatter characteristics than a large rectifier, and will try to pick up more of current swings than the large one will. This is desirable if large rectifier terminals are treated as the base loading of the system, but this may not be the best scheme.

It is desirable to be able to control the slope of the droop of each of the rectifier terminals. The firing angle of the rectifier can be varied to give the effect of an additional resistance, K_α, appearing as:

$$V_{dc} = V_{do}cos(\alpha_{min}) - K_\alpha * I_{dc} - R_c * I_{dc} \tag{A.3}$$

This is represented schematically in Figure A.6. This provides the ability compute the trajectory of α to give a desired droop. The new firing angle is calculated through the series of steps shown in equations A.4 and A.5, where V_{des} is the desired dc voltage for a given current level, and V_{est} is an equivalent voltage source needed to get the active characteristic to intersect the characteristic of the built- in droop at a selected point. Notice that V_{est} is only used in the control scheme and does not exist on the system. Thus, α can be computed to make the rectifier appear to have a different, or even variable commutation drop.

$$V_{des} = V_{est} - R_c * I_{dc} - K_\alpha * I_{dc} \tag{A.4}$$

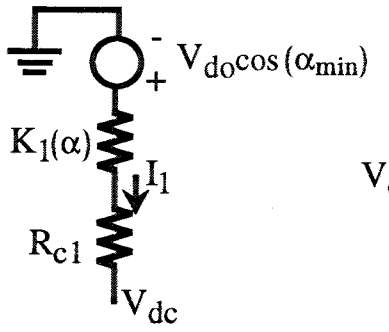

$$V_{dc} = V_{do}\cos(\alpha_{min}) - K_1(\alpha)I_1 - R_{c1}I_1$$

Figure A.6: Active Droop Provided by Variation of Firing Angle

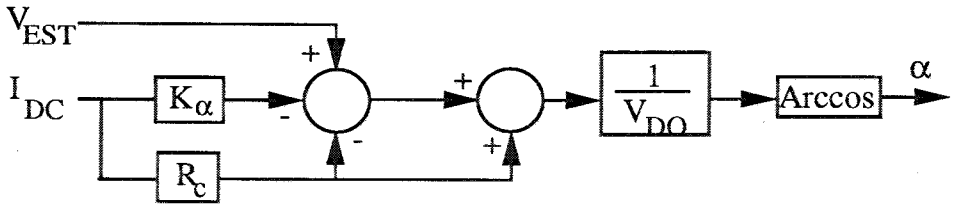

Figure A.7: Block Diagram of Control System for Active Droop

$$cos(\alpha) = \frac{V_{des} + R_C * I_{dc}}{V_{do}} \tag{A.5}$$

A.4.3 Controlling the DC Voltage

Any change in the current supplied by a set of rectifiers operating with voltage droop will result in a change in the steady-state voltage level of the dc mesh. The same thing happens to the frequency on an ac system. However, the ac system uses a slow control loop to restore the frequency to a system wide set point. The droop characteristic eliminates problems with slight errors in the set points of different generators. Similarly the dc voltage level can then be restored once a new steady-state is reached through the use of a slow control loop and a communicated set point. This arrangement will have the ability to respond to transients without communication between the converters. The slow voltage control loop later 'fine tunes' the steady-state operating point. This can either be done by changing the firing angle of each of the rectifiers, changing transformer taps, or increasing the ac voltage output of the generators.

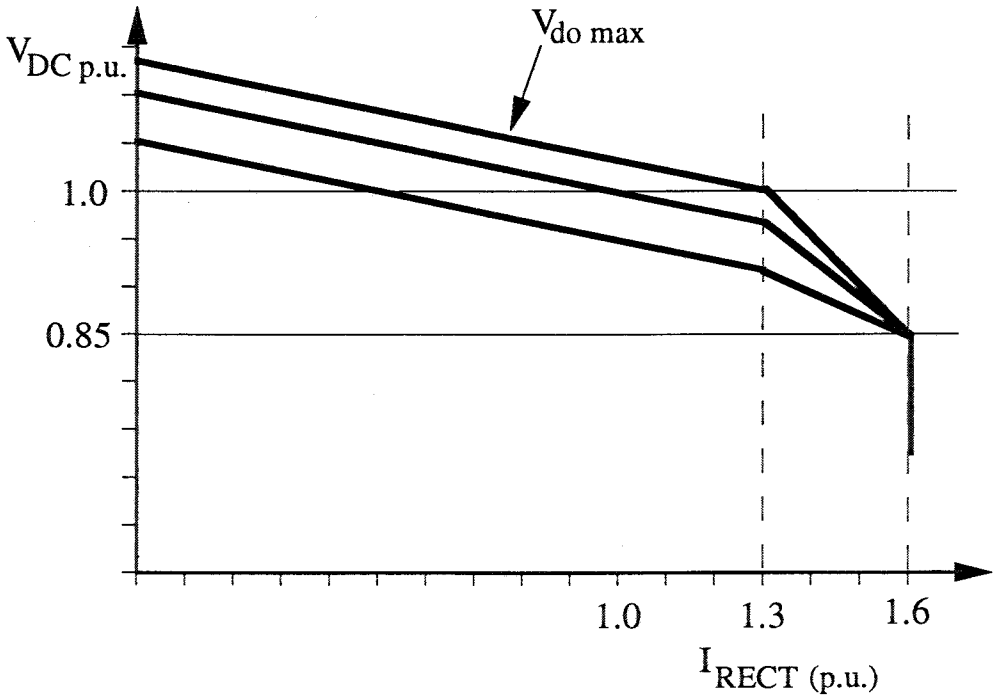

Figure A.8: Effect of Slow Voltage Control on the Droop Characteristic

A full LVDC meshed system will have direct-connected generators that supply no other ac load other than the rectifier and plant apparatus. Therefore, it is possible to use the generator excitation control loop to control the dc voltage level. This has also been discussed as a way to regulate the dc voltage output of diode bridge rectifiers [46]. The generator excitation control provides a slow loop compared to the dynamics of the dc system, achieving the objective of a slow voltage control loop.

The voltage control loop will cause the droop characteristic to slide up and down along the voltage axis, as is shown in Figure A.8. This can be varied to provide a constant mesh voltage level over a wide range of rectifier current. The steady-state voltage level of the dc system can be controlled until rectifier current limits are approached. The scheme shown in Figure A.8 is able to control dc voltage until the rectifier currents reach 1.3 per unit on the rectifier base. The steady-state voltage levels begin to decline beyond this point, as the rectifier approaches its limits.

Figure A.9 shows a simplified model of the voltage generator excitation control and its role in voltage centering. The effects of the controller action are demonstrated in Figure A.10. This

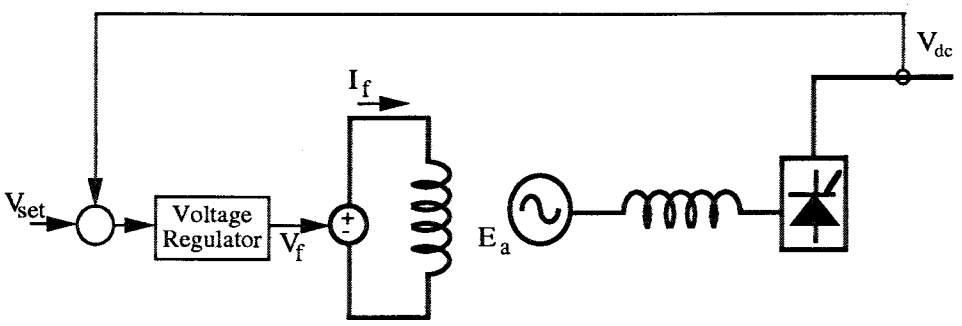

Figure A.9: Simplified Generator Excitation Control Loop

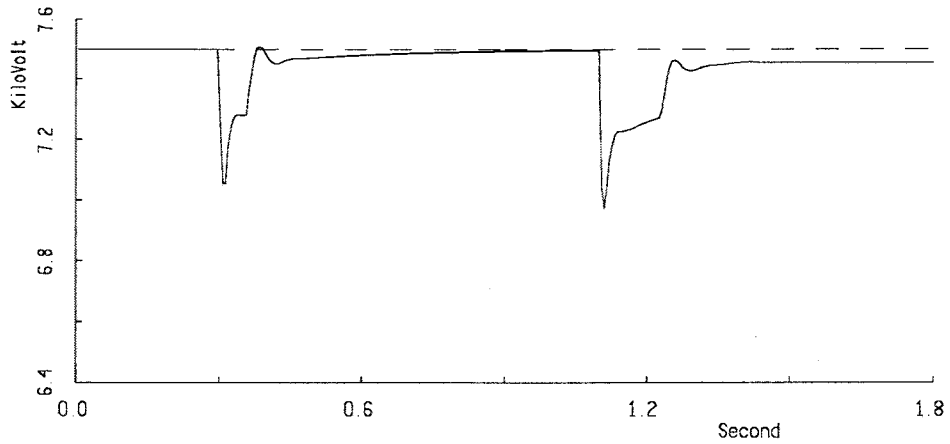

Figure A.10: Demonstration of Slow Voltage Control for A Single Rectifier. Voltage Order (Dashed Line), Compared with DC Voltage (Solid Line)

example uses a faster loop to demonstrate this more clearly. The current is increased twice in this case. The second time the increase is large enough to saturate the excitation control, allowing the voltage to fall below $7.5kV$.

A.4.4 Full Rectifier Control Characteristics

The complete rectifier characteristics will implement all of the features discussed above. The rectifier will operate in an α_{min} mode for much of its normal operating range. However, large increases in current may cause the rectifier to hit the unit-connected generators MVA limits [51], which causes a dramatic change in the behavior of the rectifier. It is better to design a control

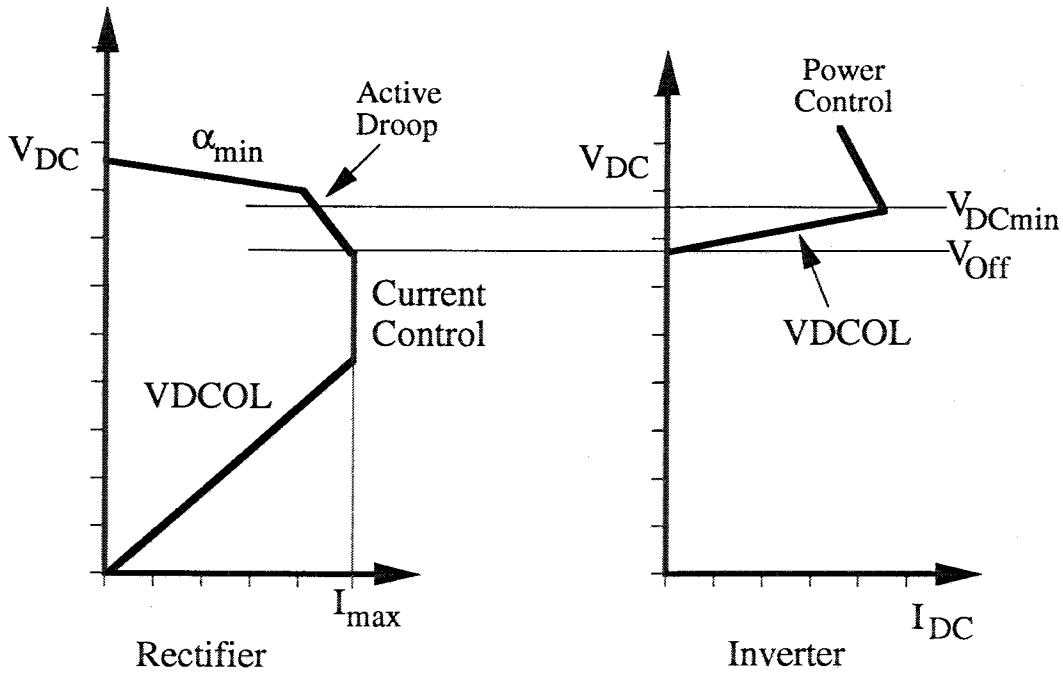

Figure A.11: Complete Rectifier Control Characteristic

scheme to keep the rectifier below the generator limits.

The rectifier will remain at α_{min} until the rectifier current reaches 1.3 per unit (on a rated current level base). At this point it will enter a mode where the slope of the droop characteristic changes. The slope is adjusted so that the dc voltage level will fall to 0.85 per unit (on rated voltage base) when the current reaches 1.6 per unit. The rectifier will then enter a current control mode to maintain the current level at 1.6 per unit. The rectifier will enter a voltage dependent current order limit (VDCOL) mode if the dc voltage level continues to fall, as in the case of a short on the dc system. This will allow the rectifier to starve the fault by increasing its firing angle to 90°. Figure A.11 shows the total control characteristic of the rectifier.

Each of the rectifiers will have similar characteristics. The boundaries where the rectifiers switch modes will be consistent between each of the rectifiers. This scheme will not have difficulties if there are slight errors between the transitions of different rectifiers, since there will still be one of the rectifiers in voltage control mode. If one converter changes modes, it will change the current sharing ratio between the other rectifiers, but the system will remain stable. The inverters will enter a voltage control mode when the rectifiers enter the controlled droop mode. This will be in

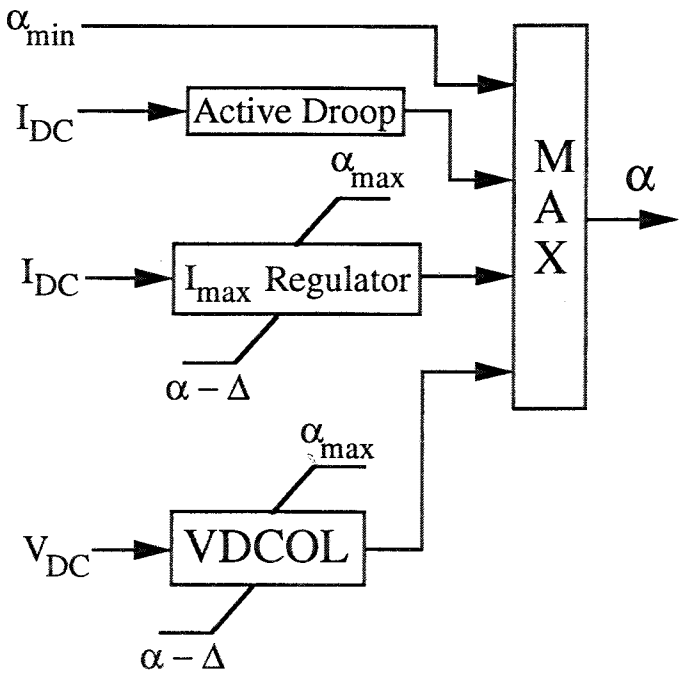

Figure A.12: Rectifier Controller

the form of a voltage dependent current limit as will be discussed below.

This control characteristic requires several mode switches within the rectifier control scheme. A block diagram of the complete rectifier control scheme is shown in Figure A.12. The mode transitions must occur smoothly, without oscillations. The characteristic for the controlled droop portion of the curve will require a firing angle equal to α_{min} at $I_{dc} = 1.3$ per unit. The firing angle will then increase as the current increases further. Therefore this mode switch can be implemented with a simple max function. The steady state firing angles for the operating points in the I_{max} mode are again larger than the firing angles required to continue along the enhanced droop line. So again a max function can be used for this transition.

The minimum α setting given to current regulator for the I_{max} mode presents a bit of a problem. If this is set small enough to avoid interference with the max function, it will require extra time to build up when I_{dc} exceeds the current set point, causing a greater overshoot. If the minimum firing angle is set to be some level, Δ, below the angle at the desired transition point, this overshoot can be reduced.

A slow voltage loop is added as an outer loop for restoring the mesh voltage under normal conditions. This is set to reach its maximum point when the rectifier current reaches 1.3 per unit. This maximum point will be set to provide $V_{dc} = 7500V$ when the rectifier supplies 1.3 per unit current. The mesh voltage will then fall as the current continues to increase. The rectifier current will respond much more quickly than the voltage control loop, so the mode changes must be based on current limits rather than purely on dc voltage levels. However, it is also useful to be able to have the transitions occur at the expected voltage levels. Therefore, the control scheme for the variable droop mode must use the measured value of V_{do} in its computations for the transitions to occur at the proper voltages. This results in a transition from the α_{min} mode to the controlled droop mode to the at 1.3 per unit current, which occurs with V_{dc} above 0.95 per unit so the inverters will not begin shedding load. The transition from controlled droop to current limit control will occur at 1.6 per unit current and 0.85 per unit voltage.

A.4.5 Inverter Control with Voltage Dependent Limits

The control characteristic described above will protect the rectifier from overcurrent conditions. However, it is possible to have a more robust control of the dc system if there is some addition control available at the inverter terminals. The dc voltage level will fall as the current drawn from the rectifiers increases. This is especially true after the rectifier current passes 1.3 per unit (on a rated current base). The inverters will normally operate in either a constant current mode or a constant power mode. The set point for the current control mode will often depend on a some form of power order as well. Therefore, a fall in mesh voltage level will require the inverters to increase their dc current in order to continue to supply constant power to their loads. This increase in current will cause the dc voltage to fall further, and could lead to system collapse. This low voltage condition is especially bad for VSI's that try to regulate reactive power. This is often based on controlling the magnitude of the ac voltage injection.

This problem can be avoided by adding a voltage dependent current limit for the inverters. Figure A.13 shows a typical inverter characteristic with the inverter regulating power for $V_{dc} > 0.95p.u.$ and then entering a VDCOL mode below this voltage. This limit is designed such that the current drawn by the inverter will reach zero at a set level. This could be set at $V_{dc} = 0.85p.u.$ for example. This zero current level would mean a firing angle of 90° for a CSI, and setting the phase angle δ to zero for a VSI. The firing pulses should also be blocked for a VSI. The same droop

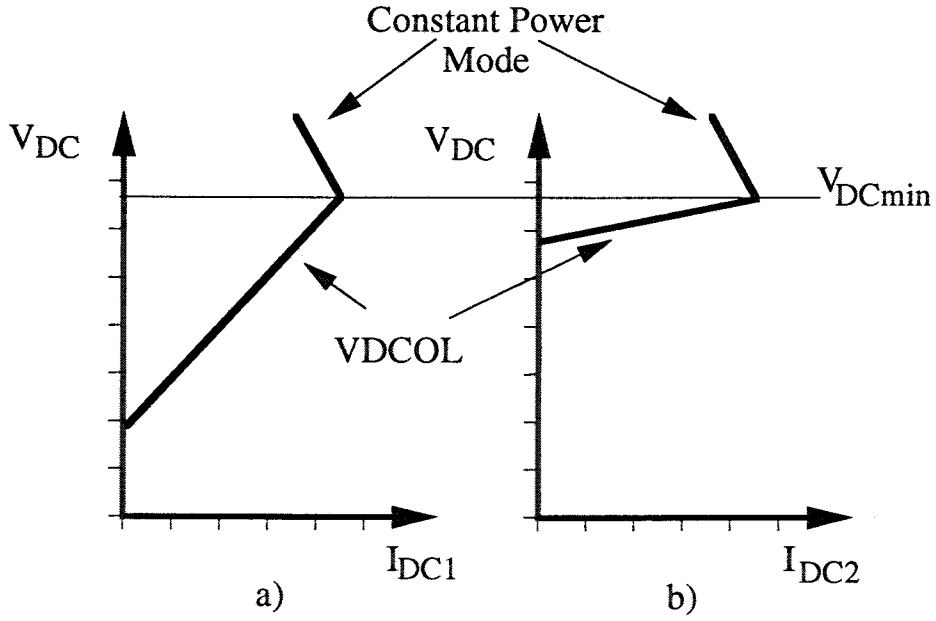

Figure A.13: Inverter Control Characteristics with VDCOL

characteristics can be used for both VSI's and CSI's. The only differences between the controllers for VSI's and CSI's is in how the controller calculates firing angles from the output of the lookup tables.

This control results in the system reaching a new steady state where none of the inverters is able to reach its current or power setpoint, but it does keep the system in operation. This type of forced load shedding on the part of the inverters would allow the system to recover from the loss of a one or more generators or rectifiers without the need for total shut down. It may also be possible to pick up the slack with connections to other ac systems. The set points of the inverters could then be adjusted by the central control using communication until it is possible to resume normal operation. The voltage levels where each inverter will shut down can also be varied. This provides an additional droop characteristic to the system. This one determines the priority of the loads. A high priority load will have little loss in current as the voltage falls, while a low priority load could shutdown after only a small voltage sag. Inverter characteristic a) of Figure A.13 shows a high priority load, while characteristic b) shows a low priority load. The low priority load will shut down with a small change in voltage.

Figure A.14 shows the control scheme for the CSI including the incorporation of the VDCOL.

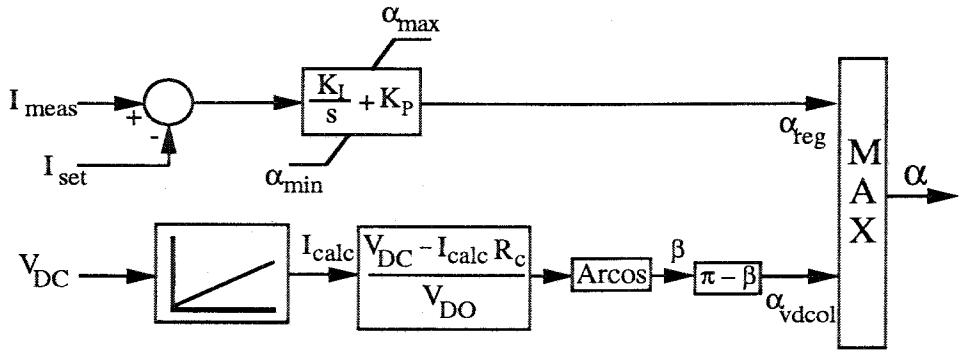

Figure A.14: CSI Current Regulator with Added VDCOL Loop

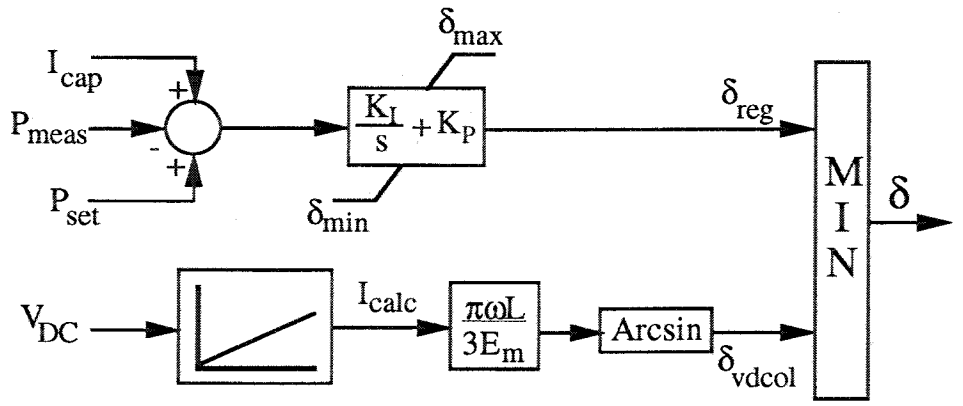

Figure A.15: VSI Power Regulator with Added VDCOL Loop

The inverter will operate in either a current or power regulation mode. The VDCOL utilizes a lookup table approach to determine the firing angle needed to achieve a desired current for a given mesh voltage level. The output of this loop is blocked if the dc voltage is greater than 0.95 per unit. The steady-state value of the firing angle, α, is equal to that of the VDCOL at this point. The output of the two control loops is passed through a max function to determine which one to follow, with the maximum firing angle set at 90°.

Figure A.15 shows the same type of controller for a VSI. Again, the VDCOL computes a desired phase angle, δ, to draw a set current at a given voltage level. This time the output of the two loops are fed through a minimum function to determine the one that is used. There is a control signal to block the firing pulses to the GTO's if the voltage falls lower.

A.5 Application to Systems with Normal Conductors

The control scheme presented here could also be applied to systems with ordinary, resistive conductors. However, the presence of the current dependent voltage drop over each of the lines will complicate the situation. The entire dc system will no longer reach equal steady-state voltage levels. The small resistances associated with splices and switches within the superconducting cables could also have a similar effect, though if these resistances are small they should not cause problems.

The resistive voltage drops in the lines cause two problems:

1. The rectifier terminals no longer reach equal voltages, so they are no longer able to coordinate current sharing in a simple manner. The current sharing will be effected by the system voltages.

2. The inverter terminals will no longer be able to coordinate load shedding based solely on the dc voltage. The voltage at an inverter terminal could fall if all of the terminals in that part of the mesh draw large currents, but the overall load on the rectifiers could still have them far from their limits.

To solve these problems it will be necessary to give the individual converter controllers more information about system state. The available local measurements are the dc voltage, the converter current, and the currents in each of the lines leaving the converter on the dc system. It will be possible to construct observers to determine the system state if the resistances of each of the conductors, as well as the droops of the other rectifiers are known. However, this will be very dependent on the topology of the system, and on the knowledge of this topology. It will depend on having an observable system. This will result in a much more complicated scheme for each converter, and may also require information about line outages as well. A more likely case will be that there won't be enough information available and communication will be needed.

A.6 Simulation Results

The ten terminal system developed earlier is studied using both line commutated current source inverters and voltage source inverters. In addition, a six terminal parallel system and a looped system is studied using line commutated inverters.

The ten terminal study system: models generators, has a multiple rectifier mesh, and can supply passive ac load systems. The study system will operate with a dc voltage level of ± 7.5 kV, with generation totalling $360MVA$.

The superconducting cables used for the study system are based upon a coaxial cable constructed from thin film HTSC superconductors shown in Figure 2.3. The cable used here is rated to carry $50kA$, and has voltage withstand capabilities well in excess of the needs for the present system.

The study system used to test the concepts for operating and controlling a LVDC transmission system must also consist of multiple rectifier terminals feeding a meshed system. The ten terminal system shown in Figure 1.2 was designed to serve as a test bed for developing the concepts of the LVDC mesh. The figure shows the positive pole of the dc system.

This system is supplied by three rectifier terminals, each fed by a 120 MVA direct-connected generator. One of the rectifiers can also supply a superconducting magnetic energy storage coil. The rectifier would then charge the coil during periods of light system loading, and the coil would supply the excess demand during high load periods. The application of SMES coils to LVDC systems is discussed in Chapter 3.

The mesh feeds seven inverter terminals, ranging from 30 MW to 105 MW. The largest inverter feeds a large industrial load, while the smaller inverter terminals feed urban ac distribution systems.

All of the simulations shown here represent the generator as a three phase voltage source with the neutral point grounded through a 700Ω resistor. The generator voltage source is connected directly to the rectifier bridge through an inductance. This inductance represents the subtransient reactance of the generator, and the voltage source represents the subtransient voltage of the generator.

Each of the inverter terminals is connected to an ac system represented by an infinite bus. The

Converter	Power Rating	Current Rating	Rated Firing Angle
Rectifier 1	105 MW	7 kA	$\alpha = 5°$
Rectifier 2	105 MW	7 kA	$\alpha = 5°$
Rectifier 3	105 MW	7 kA	$\alpha = 5°$
Inverter 4	45 MW	3 kA	$\gamma = 20°$
Inverter 5	30 MW	2 kA	$\gamma = 25°$
Inverter 6	30 MW	2 kA	$\gamma = 25°$
Inverter 7	30 MW	2 kA	$\gamma = 25°$
Inverter 8	45 MW	3 kA	$\gamma = 20°$
Inverter 9	30 MW	2 kA	$\gamma = 25°$
Inverter 10	105 MW	7 kA	$\gamma = 25°$

Table A.2: Converter Terminal Ratings for Ten Terminal DC System

inverters are connected to an ideal three phase voltage source through a Y-Y transformer. This is done for both cases with CSI's and VSI's.

A.7 Simulation of Ten Terminal System with CSI's

The system control scheme was tested on the ten terminal mesh connected shown in Figure 1.2. This system operates at a dc voltage of $\pm 7.5kV$, in a monopolar configuration. The system has three rectifiers supplying seven inverters. Details about the ratings of the terminals is shown in Table A.2.

The rectifier control scheme is designed to enter a mode with a steeper droop characteristic when the dc current passes 1.3 per unit. The rectifier will then enter a voltage regulation mode when the current reaches 1.6 per unit, or the dc voltage falls below 0.85 per unit ($6.375kV$). If the voltage falls below below $5kV$, or 0.67 per unit, the rectifiers enter a VDCOL mode. The rectifiers also feature a slow voltage control loop. This is set to keep the mesh voltage at $7.5kV$ for a range of dc current from 0 to 1.3 per unit for each rectifier. The generator excitation control loop will have the generator output voltage at its maximum level at this point.

The inverters each operate in a current regulation mode under normal conditions. The inverters

enter a VDCOL mode when the mesh voltage falls below 0.95 per unit. All of the inverters will shut down when the mesh voltage fall below 0.85 per unit, and only fault conditions will result in the rectifiers entering their current limit control and VDCOL modes.

The inverter connected at Bus 4, as shown in Figure 1.2 will be represented with a detailed switching model. The remainder of the inverters will be represented with averaged models. The differences in response between the averaged and detailed models are negligible for the studies and time scales shown here. The averaged inverter models are connected to the mesh via uni-directional switches to prevent current reversal during dc faults.

A.7.1 Loss of Rectifier Terminal

The first case looks at a simulation where rectifier 1 is shut down and later restarted. The system starts out with each of the inverters drawing rated current. This results in each rectifier supplying $7000A$. Rectifier 1 shuts down 500 milliseconds into the simulation, and turns on after 1.25 seconds. Figure A.16(a) shows the rectifier currents. Rectifiers 2 and 3 increase their currents while rectifier 1 shuts down. Figure A.16(b) shows the current at inverter 4 along with the current order. The inverter is not able to meet its current order in this case. When the remaining rectifiers try to pick up the current that rectifier 1 supplied, they both push their currents beyond 1.3 per unit, and into the enhanced droop region of their characteristics. This in turn pushes the mesh voltage down, as is shown in Figure A.16(c). This fall in the mesh voltage is enough to put the inverters into their VDCOL mode, and reaches a steady-state operating point with each inverter drawing slightly less current than expected. The mesh can be returned to its normal voltage if one or more of the inverters backs off on its current order. This can be done using communication once the initial transient is ended.

The rectifier currents do not return to their original operating states when rectifier 1 turns on again. Rectifier 1 turns on in a minimum firing angle mode, while the other two rectifiers are in the controlled droop mode. Rectifier 1 will increase its current until the mesh voltage reaches $7.5kV$. At this point the voltage centering loop will prevent any other change in the operating state. This results in the case shown where rectifiers 2 and 3 are supplying more current than rectifier 1. This can later be balanced using communication.

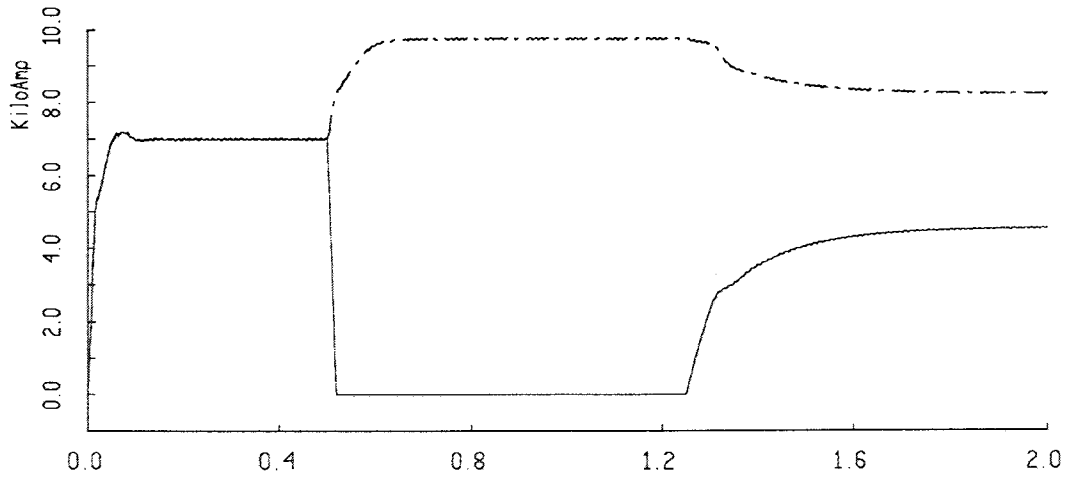

(a) Rectifier Currents

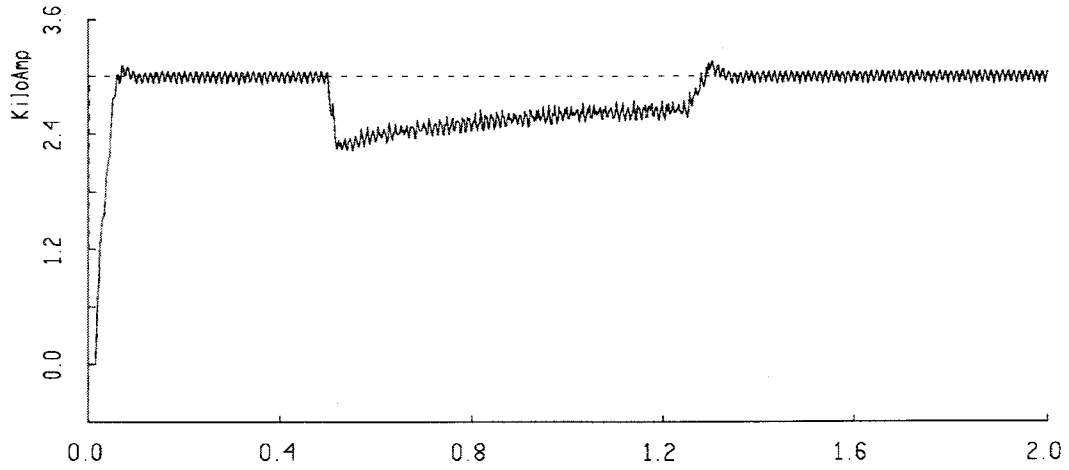

(b) Inverter 4 Current and Current Order

Figure A.16: Ten Terminal Meshed System Supplying Line Commutated CSI's. Case I: Rectifier 1 Shuts Down and Restarts

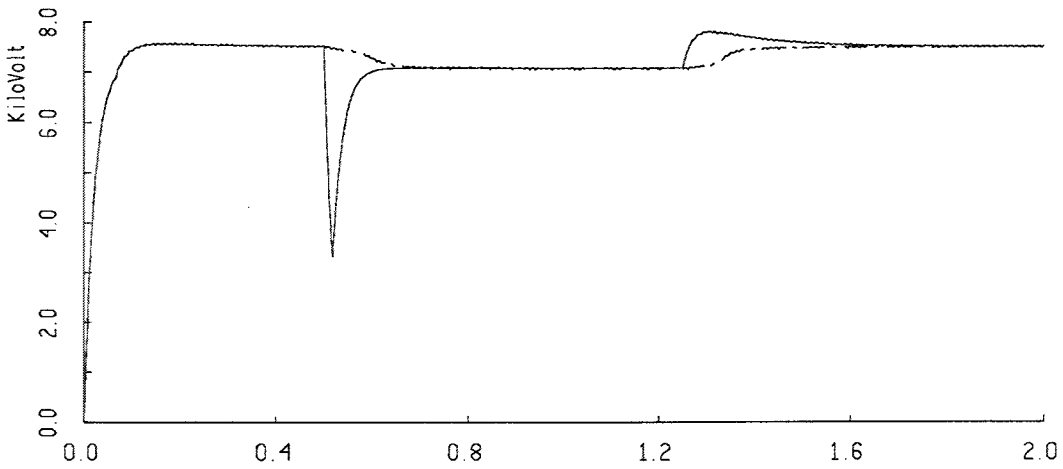

(c) DC Voltage at Rectifier Terminals

Figure A.16: (cont.) Ten Terminal Meshed System Supplying Line Commutated CSI's. Case I: Rectifier 1 Shuts Down and Restarts

There is not a noticeable difference in the dynamics between the three rectifiers. They each show essentially the same response time. This is because the time constant for current variations on each is affected by the RL time constant the droop term each converter sees relative to the source of the current change. The inductive portion of the time constant is dominated by the smoothing reactance of the rectifier, so the effect of the different paths from each rectifier is insignificant on the dynamics in comparison.

A.8 Simulation of the Ten Terminal Meshed System with VSI's

The system shown in Figure 1.2 was next simulated with voltage source inverters used at all seven of the inverter terminals. The terminal power ratings were again set as shown in Table A.2. Each of the inverters is designed to supply rated power at $\delta = 7.4°$.

The settings of the converter controls are set in a manner similar to those used with the current source inverters. The biggest difference is that the inverters now operate in a power control mode rather than current regulation. Inverter 5 shuts down when the dc voltage falls below $7kV$, while inverter 6 will shut down in the voltage reaches $6kV$. The remainder of the inverters shut down at a dc voltage of $6.375kV$ (0.85 p.u.).

The system model for simulation utilizes lumped inductor representations for the cables and assumes strong ac systems. All three rectifiers are represented with detailed switching models. Inverter 4 is represented with a detailed model, while the remainder of the inverters are represented with fundamental component models. The only protective devices added to the system are circuit breakers to prevent current reversal through the inverters during dc faults.

A.8.1 Loss of Rectifier Terminal

The first set of simulations using voltage source inverters looks at a case where rectifier 2 shuts down, and later restarts. This is similar to the case shown above using CSI's, except a different rectifier is shut down. Figure A.17(a) shows the rectifier currents. Again the other two rectifiers pick up additional current due to the shutdown of the other rectifier. Except now the rectifier

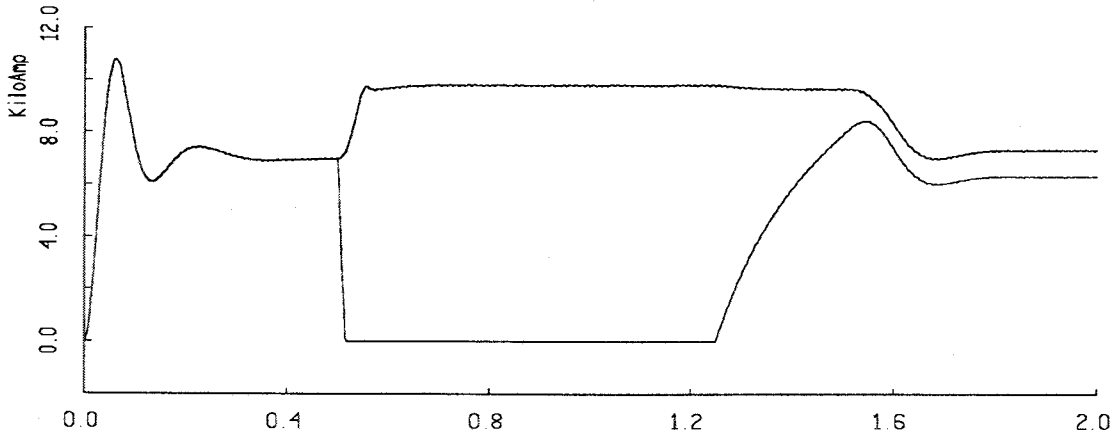

(a) Rectifier Currents

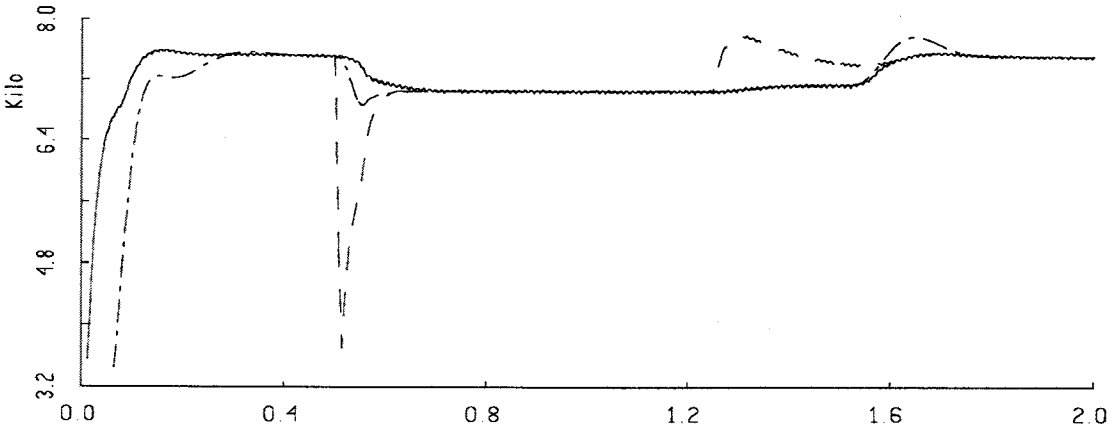

(b) DC Voltage at Rectifier Terminals

Figure A.17: Ten Terminal Meshed System Supplying VSI's. Case I: Rectifier 2 Shuts Down, and then Restarts 0.75 Seconds Later

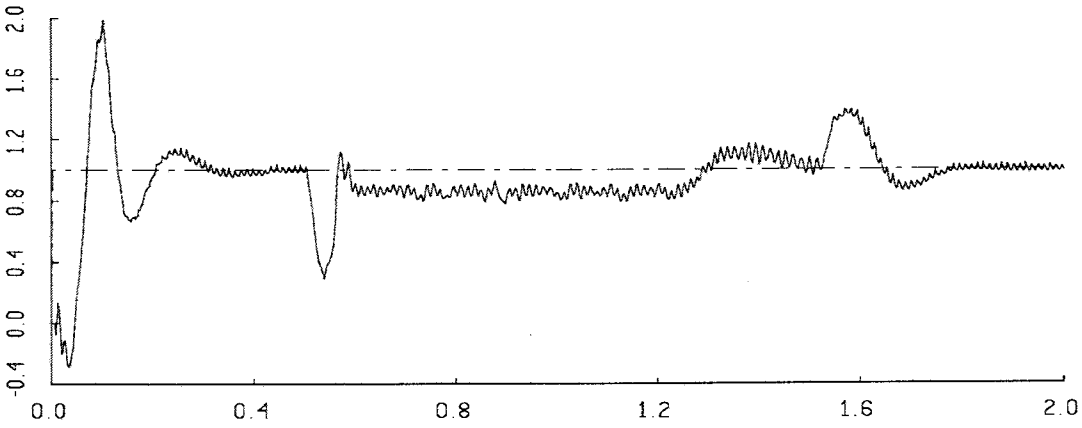

(c) Output Power and Power Order at Inverter 4

Figure A.17: (cont.) Ten Terminal Meshed System Supplying VSI's. Case I: Rectifier 2 Shuts Down, and then Restarts 0.75 Seconds Later

currents come closer to returning to the original operating point when rectifier is restarted. This is because of the different location of this rectifier in the mesh. The new states are affected by a combination of the time constants for the change in currents determined by the equivalent inductance from each location, and the time constant of the voltage centering loop.

Figure A.17(b) shows the mesh voltage at several different locations. The solid line shows the voltage at rectifiers 1 and 3. The dashed line with the largest swings shows the voltage at rectifier 2. The dash-dotted line shows the voltage at inverter 4. Notice that the response in the voltage at inverter 4 lags that of the rectifiers. This is due to the time delay for the change in voltage to travel across the line connecting it to the rectifiers. Figure A.17(c) shows the output power at inverter 4 as compared to the power setpoint. Notice that the inverter is not able to meet its power demand while the rectifier is off, as was the case for the current source inverters as well.

A.9 Simulation of the Six Terminal Parallel System

All three of the rectifiers are represented with detailed switching models. The control settings for the rectifiers keep them in an minimum α mode until the dc current reaches 1.3 per unit. The rectifier then increases its firing angle to represent a steeper droop characteristic. Each rectifier will enter a current limit control mode when the current reaches 1.6 per unit, and the voltage falls below 0.85 per unit. The voltage can also be centered in this case. It is represented as a slow loop identical to that used above for direct-connected generators. This would operate differently for rectifiers supplied by ac systems, where the voltage magnitude control would be provided by tap changing transformers. The rectifiers again enter a VDCOL when the voltage falls below 0.85 per unit.

All of the simulations shown here represent the generator as a three phase voltage source with the neutral point grounded through a 700Ω resistor. The generator voltage source is connected directly to the rectifier bridge through an inductance. This inductance represents the subtransient reactance of the generator, and the voltage source represents the subtransient voltage of the generator.

Each of the inverter terminals is assumed to be connected to an ac system represented by an infinite bus. The inverters are connected to an ideal three phase voltage source through a Y-Y

Line	Length (km)	Inductance (mH)
Rectifier1-Rectifier2	20	0.3482
Rectifier2-Rectifier3	30	0.5222
Rectifier3-Inverter1	60	1.0445
Inverter1-Inverter2	25	0.4352
Inverter2-Inverter3	17	0.2959

Table A.3: Branch Parameters for Six Terminal System

transformer. This is done for both cases with CSI's and VSI's. The line commutated CSI's are all represented by averaged models. The inverters operate in current control mode until the voltage falls below 0.95 per unit. They then enter a VDCOL mode, and shut down when the voltage reaches 0.85 per unit. The mesh is represented using lumped inductor models to represent the cables. Table A.3 gives the parameters for each of the cables in this case. There are no circuit breakers or other protective devices used on the dc system.

A.9.1 Inverter Startup Followed by a Resistive DC Fault

The largest of the three inverters, inverter 3, is started part way into the simulation. This is followed by a resistive fault (with $R_{faul} = 0.1\Omega$) located near inverter 2. Figure A.18(a) shows the rectifier currents. They first increase due to the startup of the inverter. They later increase further, and settle into a new operating point. This is because the rectifiers are in the maximum current mode rather than the VDCOL. Figure A.18(b) shows the inverter currents. The current for inverter 3 increases, and then all of the currents go to zero after the fault. Figure A.18(c) shows the rectifier and inverter voltage levels. The voltage does not go to zero due to the presence of the fault resistance.

A.10 Conclusions

This chapter has introduced a distributed voltage control scheme for parallel and mesh connected dc transmission systems. Each of the rectifier terminals or other power sources on the dc system operate in a shared voltage control mode. The scheme is based on a voltage droop control that

determines the current sharing between the different rectifiers on the system. Such a scheme can be implemented in its simplest form by operating the rectifiers in a constant α_{min} mode by using the rectifier commutation drop to supply the necessary sloping characteristic for the droop. This scheme can be implemented in this simple form when superconducting cables are used on the dc system, because each of the nodes on the mesh will reach the same steady-state voltage. It may be possible to implement such a scheme in a system with normal cable or lines, but it would require the use of observers to maintain a more consistent current sharing between the rectifiers. The presence of current dependent voltage drops in the dc lines complicates the control scheme greatly, and may make it unworkable.

The dual of this scheme, where each of the inverters operates in a distributed voltage control mode while the rectifiers control current is undesirable, as it would require communication to control the inverter output power levels. However, this scheme may work for series connected dc systems. Each inverter would then regulate local voltage to control output power, and the rectifiers would operate in a shared current control mode.

This chapter has also developed control schemes for the rectifiers and inverters to move the system smoothly through major transients without needing to shut the system down entirely in all but the most extreme cases. This is done by adding a VDCOL loop on each of the inverters to cause them to 'back off' on their current demands of the rectifiers as the rectifiers reach their current limits. The rectifiers have loops to limit their current output, as well as a VDCOL to allow them to 'starve' faults to make it easier for protective devices to act, and then bring the system back up rapidly after they do act.

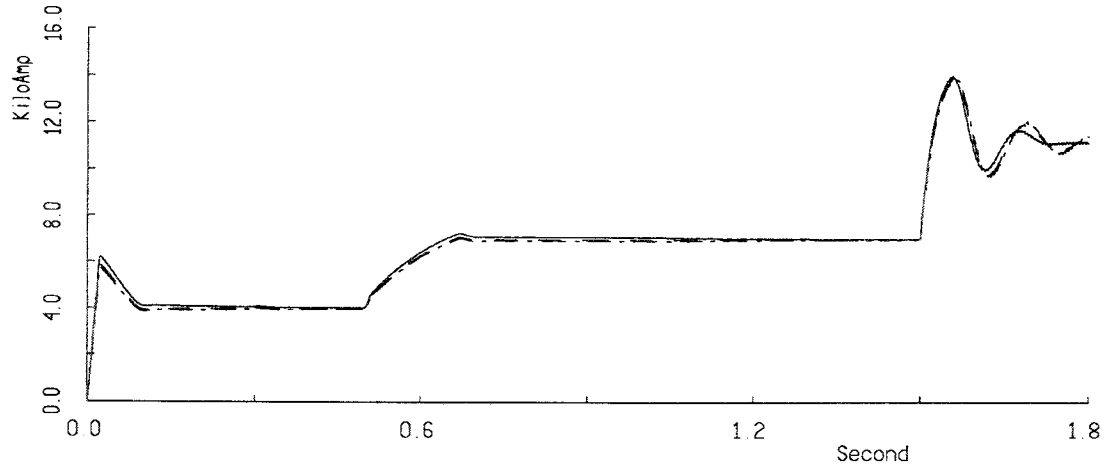

(a) Rectifier Currents

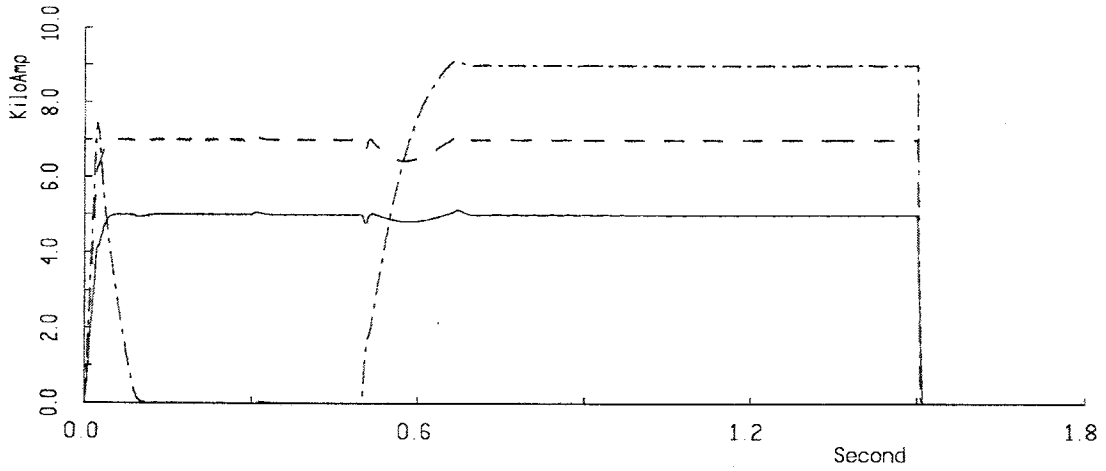

(b) Inverter Currents for Inverters 1, 2, and 3

Figure A.18: Six Terminal Parallel Connected System Supplying Line Commutated CSI's. Case II: Start-up of Inverter 6, then Resistive Fault with $R_{faul} = 0.1\Omega$

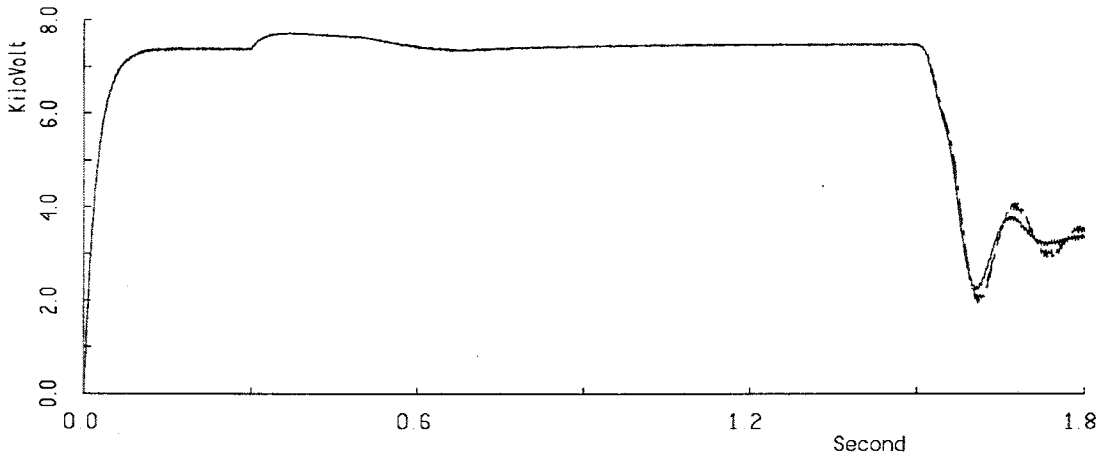

(c) DC Voltage at Rectifier Terminals

Figure A.18: (cont.) Six Terminal Parallel Connected System Supplying Line Commutated CSI's. Case II: Start-up of Inverter 6, then Resistive Fault with $R_{faul} = 0.1\Omega$

Appendix B

Reference Frame Transformation

This section deals with the transformation of three phase electrical quantities from the "natural" $a-b-c$ reference frame to the $d-q-n$ reference frame. The representation in the $d-q-n$ reference frame essentially consists of a vector that has an amplitude and position relative to the $d-q-n$ coordinate axes. It is convenient to represent the transformation using the matrix notation. The following matrices are defined.

$$\mathbf{f}_{abc} = \begin{pmatrix} f_a \\ f_b \\ f_c \end{pmatrix}$$

$$\mathbf{f}_{dqn} = \begin{pmatrix} f_d \\ f_q \\ f_n \end{pmatrix}$$

In these matrices, the quantity f generically denotes a physical quantity such as a current or voltage. The transformation from the $a-b-c$ reference frame to the $d-q-n$ reference frame is given by:

$$\mathbf{f}_{dqn} = \mathbf{T}(\theta) \times \mathbf{f}_{abc}$$

In this equation, $\mathbf{T}(\theta)$ is the transformation matrix. This matrix is defined as:

$$\mathbf{T}(\theta) = \frac{2}{3}\begin{pmatrix} sin(\theta) & sin(\theta - 2\pi/3) & sin(\theta + 2\pi/3) \\ cos(\theta) & cos(\theta - 2\pi/3) & cos(\theta + 2\pi/3) \\ 1/\sqrt{2} & 1/\sqrt{2} & 1/\sqrt{2} \end{pmatrix}$$

where

$$\theta = \omega_r \times t$$

In this equation, ω_r is the rotation frequency of the reference frame, and t is the time. For transformation to the stationary reference frame, $\omega_r = 0$. From the transformation, it is apparent that if $f_a + f_b + f_c = 0$, then $f_n = 0$.

The inverse transformation is given by:

$$\mathbf{f}_{abc} = \mathbf{T}^{-1}(\theta) \times \mathbf{f}_{dqn}$$

In this equation,

$$\mathbf{T}^{-1}(\theta) = \frac{3}{2}\mathbf{T}(\theta) = \begin{pmatrix} sin(\theta) & cos(\theta) & 1/\sqrt{2} \\ sin(\theta - 2\pi/3) & cos(\theta - 2\pi/3) & 1/\sqrt{2} \\ sin(\theta + 2\pi/3) & cos(\theta + 2\pi/3) & 1/\sqrt{2} \end{pmatrix}$$

When $f_n = 0$, the transformation maps the $a - b - c$ quantities onto a plane, with f_d and f_q being components on two orthogonal axes d and q. The quantities f_d and f_q can be considered to be the two components of a vector in the complex plane, as illustrated by Figure B.1.

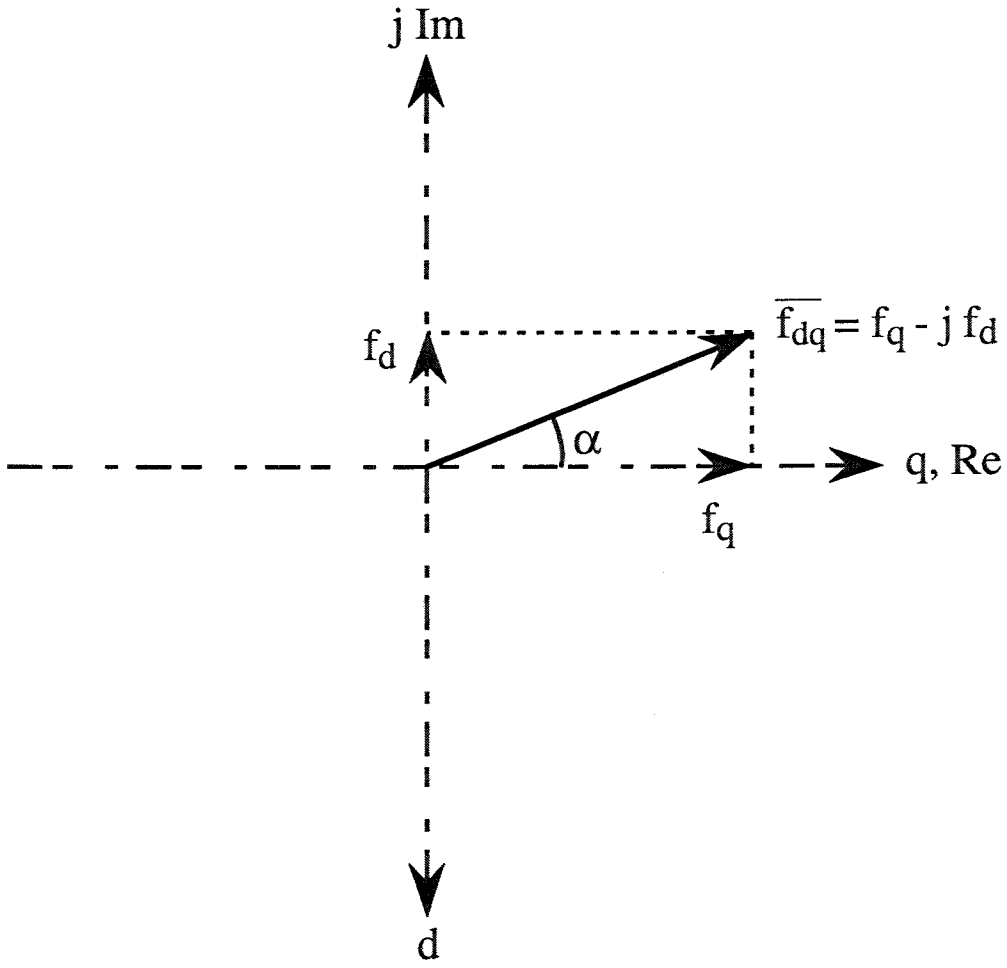

Figure B.1: Vector Representation in the d-q plane

Bibliography

[1] J.G. Bednorz and K.A. Müller, *Possible High T_c Superconductivity in the Ba-La-Cu-O System.* Zeits. Physik, B64, 189, 1986.

[2] Wilson, M. N. *Superconducting Magnets.* Oxford University Press, New York, 1983.

[3] *AC Losses in the New High-Temperature Superconductors.* EPRI Report EL-6277. Palo Alto, California: Electric Power Research Institute, March 1989.

[4] *Energy Applications of High-Temperature Superconductors: A Progress Report.* EPRI, TR-101635, July, 1992.

[5] *Assessment of Higher-Temperature Superconductors for Utility Applications.* EPRI Report ER-6399. Palo Alto, California: Electric Power Research Institute, May 1989.

[6] M. R. Beasley. "A History of Superconductivity," *Advances in Superconductivity. Proceedings of the First International Symposium on Superconductivity (ISS '88).* August 28-31, 1988, Nagoya, Japan. Edited by K. Kitazawa and T. Ishiguro. Tokyo, Japan: Springer-Verlag, 1989.

[7] P. Chowdhuri and H.L. Laquer, "Some Electrical Characteristics of a DC Superconducting Cable," *IEEE Transactions on Power Apparatus and Systems.* Vol.PAS-97, no. 2, pp. 399-408, March/April 1978.

[8] F. Chu and R. Roberge. "Applicability in the Electric Power System: A Canadian Perspective," *Advances in Superconductivity. Proceedings of the First International Symposium on Superconductivity (ISS '88).* August 28-31, 1988, Nagoya, Japan. Edited by K. Kitazawa and T. Ishiguro. Tokyo, Japan: Springer-Verlag, 1989.

[9] *DC Superconducting Power Transmission Line Project at LASL.* Report LA-8323-PR. U. S. Department of Energy, Division of Energy Systems. Compiled by F. J. Edeskuty. Los Alamos, New Mexico: Los Alamos Scientific Laboratory, 1980.

[10] E. B. Forsyth, *The Status of R&D For Suprconducting Power Transmission Systems.* Report BNL-40420. Upton, New York: Brookhaven National Laboratory, 1987.

[11] J.K. Hoffer, E.C. Kerr, and H.L. Laquer, "Stabilizing Superconductors for Power Engineering Applications," *IEEE Transactions on Power Apparatus and Systems.* Vol. PAS-94, no. 6, pp. 2008-2014, November/December 1975.

[12] J. R. Hull and G. F. Berry. "Advantages of High-Temperature Superconductivity in Large-Scale Applications," *Superconductivity Applications and Developments.* Edited by S. M. Shoenung. New York: ASME, 1988.

[13] M. J. Jefferies and K. N. Mathes. "Dielectric Loss and Voltage Breakdown in Liquid Nitrogen and Hydrogen," *IEEE Transactions on Electrical Insulation.* Vol. EI-5, No. 3, pp. 83-91, September 1970.

[14] W. E. Keller. "D. C. Superconducting Cables," *Workshop Proceedings: Public Policy Aspects High Capacity Electric Power Transmission.* EPRI Report WS-79-164. Palo Alto, California: Electric Power Research Institute, 1979.

[15] J. L. Kirtley and F. J. Edeskuty. "Application of Superconductors to Motors, Generators, and Transmission Lines," *Proceedings of the IEEE.* Vol. 77, No. 8, pp. 1143-1154, August 1989.

[16] T. Mitsui. "Application to Electric Power System," *Advances in Superconductivity. Proceedings of the First International Symposium on Superconductivity (ISS '88).* August 28-31, 1988, Nagoya, Japan. Edited by K. Kitazawa and T. Ishiguro. Tokyo, Japan: Springer-Verlag, 1989.

[17] H. L. Saums and W. W. Pendleton. *Materials For Electrical Insulating and Dielectric Functions.* Rochelle Park, New Jersey: Hayden Book Company, Inc., 1973.

[18] T. D. Schlabach. "High-Tc Superconductor Wire Frabrication and Prospects For Use in Large Scale Applications," *Superconductivity Applications and Developments.* Edited by S. M. Shoenung. New York: ASME, 1988.

[19] *Superconductor Materials Science; Metallurgy, Fabrication, and Applications.* Edited by S. Foner and B. B. Schwartz. New York: Plenum Press, 1981.

[20] K. Tachikawa and K. Togano. "Potential Methods For the Fabrication of High-Tc Superconductors for Wires and Cables," *Proceedings of the IEEE.* Vol. 77, No. 8, pp. 1124-1131, August 1989.

[21] T. Tanaka and A. Greenwood. *Advanced Power Cable Technology, Volume I.* Boca Raton, Florida: CRC Press, Inc. 1983.

[22] T. Tanaka and A. Greenwood. *Advanced Power Cable Technology, Volume II.* Boca Raton, Florida: CRC Press, Inc. 1983.

[23] *Underground Power Transmission By Superconducting Cable.* Report BNL-50325. Edited by E. B. Forsyth. Upton, New York: Brookhaven National Laboratory, 1972.

[24] J. E. C. Williams. *Superconductivity and Its Applications.* London: Pion Limited, 1970.

[25] P. Chowdhuri and F.J. Edeskuty, "Bulk Power Transmission By Superconducting DC Cable," *Electric Power Systems Research.* Vol.1, No. 1, pp. 41-49, September 1977.

[26] P.N. Arendt, M.P. Maley, and D.E. Peterson, *Assessment of Higher-Temperature Superconductors for Utility Applications.* EPRI, ER-6399, Final Report, May 1989.

[27] E. Batalla, *Conceptual Design of a Direct Current Superconducting Power Transmission Line (DC SPTL) Using Liquid Nitrogen Coolant.* Madison, Wisconsin: University of Wisconsin-Madison, Department of Electrical and Computer Engineering, December 1989.

[28] Y.Mitani, K.Tsugi, and Y.Murakami, "Fundamental Analysis of Dynamic Stability in Superconductive Power Systems," *IEEE Transactions on Magnetics.* Vol. 27, No. 2, pp. 2349-2352, March 1991.

[29] F.J. Edeskuty, W.F. Stewart, K.D. Williamson, Jr., E.M. Honig, and L.K. Trocki, "High Temperature Superconductors for Power Transmission Applications,"*Proc.Conf. on Electrical Applications of Superconductivity,* Orlando, FL, Sept.21-23,1988, sponsored by the Electric Power Research Institute, Palo Alto, CA.

[30] "Superconductor Development: Tracking and Coordination Network," presentation by R.F. Giese of Argonne National Laboratory, sponsored by EPRI, October 15, 1991, Philadelphia, PA.

[31] G.G. Haselden, "Cryogenic Fundamentals," Academic Press, 1971, New York.

[32] H.L. Laquer, J.W. Dean and P. Chowdhuri, "Electrical, Cryogenic and Systems Design of a DC Superconducting Power Transmission Line," *IEEE Transactions on Magnetics,* Vol. MAGG-13, No.1, January, 1977.

[33] B.K. Johnson, R.H. Lasseter and R. Adapa, "Power Control Applications on a Superconducting LVDC Mesh," *IEEE Transactions on Power Delivery.* Vol. 6, No. 3, pp. 1282-1288, July 1991.

[34] M.C. Chandorkar, D.M. Divan and R. Adapa, "Control of Parallel Connected Inverters in Stand Alone AC Supply Systems," *Presented at the IEEE IAS Annual meeting,* Dearborn, MI, Sept.29-Oct.4, 1991.

[35] B.K. Johnson, R.H. Lasseter, F.L. Alvarado, and R. Adapa, "Expandible Multiterminal DC Systems Based on Voltage Droop," *to be presented at IEEE Power Engineering Society Winter Meeting.* Columbus, Ohio, Jan. 31-Feb. 5, 1993.

[36] J. Arrillaga, *High Voltage Direct Current Transmission.* Peter Peregrinus, London, 1983.

[37] E.W. Kimbark, *Direct Current Transmission: Volume 1.* Wiley Interscience, New York, 1971.

[38] R. Foerst, G. Heyner, K.W. Kanngiesser, and H. Waldmann, "Muliterminal Operation of HVDC Converter Stations," *IEEE Transaction on Power Apparatus and Systems.* Vol. 88, No. 7, pp. 1042-1052, July 1969.

[39] K.W. Kanngiesser, J.P. Bowles, Å. Ekström, J. Reeve, and E. Rumpf, "HVDC Multiterminal Systems," CIGRE, 14-08, 1974. (*ELECTRA.*) August, 1974.

[40] J. Reeve, "Multiterminal HVDC Power Systems," *IEEE Transactions on Power Apparatus and Systems.* Vol. 99, No. 2, pp. 729-737, March/April 1980.

[41] R. Jotten, J.P Bowles, G. Liss, C.J.B. Martin, and E. Rumpf, "Control in HVDC Systems, The State of the Art, Part II: Multiterminal Systems," *CIGRE* 14-07 28th Session Paris, France, 1980.

[42] R.H. Lasseter, K.H. Krüeger, and D. Povh, "Control of Multiterminal D.C. Systems," *MONTECH '86*, Montreal, Canada, Catalog No. THO-154-5, pp. 120-125, 1986.

[43] F. Nozari, C.E. Grund, and R.L. Hauth, "Current Order Coordination in Multiterminal DC Systems," *IEEE Transactions on Power Apparatus and Systems.* Vol. PAS-100, No. 11, pp. 4628-4635, November 1981.

[44] R.H. Lasseter and S.G. Jalali, "Power Conditioning Systems for Superconductive Magnetic Energy Storage," *IEEE Transactions on Enery Conversion.* Vol. 6, No. 3, pp. 381-387, September, 1991.

[45] H. Okada, T. Ezaki, K. Ogawa, H. Koba, M. Takeo, K. Funaki, S. Sato, F. Irie, J. Chikaba, K. Terazono, M. Takamatsu, N. Kawakami, M. Hirano, "Experimental Studies of SMES System with DC Intertie For Power Line Stabilization," *1988 Power Electronic Specialists Conference.* pp. 326-333, paper No. II D-5, April 1988.

[46] J. P. Bowles, "Multiterminal HVDC Transmission Systems Incorporating Diode Rectifier Stations," *IEEE Transactions on Power Apparatus and Systems.* Vol. PAS-100, No. 4, pp. 1674-1678, April 1981.

[47] T.E. Caverly, C.H. Ottaway, and D.H.A. Tufnell, "Concepts of a Unit Generator Converter Transmission System," *IEE Conference on High Voltage DC and AC Transmission.* London, 1973.

[48] M. Hausler and K. W. Kanngiesser, "Generator-Converter Unit Connection with Thyristor and Diode Rectifiers," *DOE Symposium on Incorporating HVDC Power Transmission into System Planning.* Phoenix, Arizona. pp 256-271. 1980.

[49] D. S. Bajawa and R. M. Mathur. "Rerating of Synchronous Generators Supplying HVDC Converters with Special Reference to Unit Connection." *IEEE Canadian Conference on Communications and Power.* Montreal, 1976.

[50] P.C.S. Krishnayya, "Stresses on Generators and Transformers of Block and Double-Block Connections Proposed for HVDC Power Station Infeed," *Proceedings of 1973 IEEE Winter Power Meeting.* pp. 279-286, 1973.

[51] J. Arrillaga, S. Sankar, N.R. Watson, and C.P. Arnold, "Operational Capacity of Generator-HVDC Converter Units," *IEEE Transactions on Power Delivery.* Vol. 6, No. 3, pp. 1171-1176, July 1991.

[52] M. Naidu, and R. M. Mathur. "Unit Connection of a Double Three Phase Generator to HVDC Converters." *IEEE MONTECH '86, Conference on HVDC Power Transmission.* Montreal, pp. 71-74, 1986.

[53] C. Ammann, K. Reichert, and R. Joho. "Converter Fed Synchronous Generator System for Medium and Large Power Plants." *IEEE Transactions on Energy Conversion.* Vol EC-1, No. 2, pp. 75-81, June 1986.

[54] E.F. Fuchs and L. T. Rosenburg, "Analysis of an Alternator with Two Displaced Stator Windings," *IEEE Transactions on Power Apparatus and Systems.* Vol. 93, No. 6, pp. 1776-1786, 1974.

[55] H.W. Weiss, "Power Transmission to Synchronous Machines for Adjustable-Speed Pump and Compressor Drive Systems," *IEEE Transactions on Industry Applications.* Vol. IA-19, No. 6, pp. 996-1002, November/December 1983.

[56] L. Werren, "Synchronous Machine with 2 Three Phase Windings, Spatially Displaced by 30° EL, Commutation Reactance and Model for Converter Performance Simulation," *International Conference on Electrical Machines.* pp. 781-784, Luasanne, Switzerland, September 18-21, 1984.

[57] A.A. Fouad and P.M. Anderson, *Power System Control and Stability Stability.* Ames, Iowa, Iowa State University Press, 1977.

[58] S. Hungsasutra and R.M. Mathur, "Unit Connected Generators with Diode Valve Rectifier Scheme," *IEEE Transactions on Power Systems.* Vol. 4, No. 2, pp. 538-543, May 1989.

[59] F.T. Bennel, "Current Balance in 12-Pulse Rectifiers Comprising Parallel Rectifiers," *Power Electronics, Power Semiconductors and Their Applications.* IEE Conference Series, No. 154, pp. 27-29, September, 1977.

[60] F.T. Bennell, "Current Equalising Transformer For Current Balance in Parallel Connected 12 Pulse Converter," *IEE Proceedings.* Vol. 135, Pt. B, No. 2, pp. 85-90, March 1988.

[61] J.K. Hall, J.G. Kettleborough, A.B.M.J. Razak, "Parallel Operation of Bridge Rectifiers Without An Interbridge Reactor," *IEE Proceedings.* Vol. 137, Pt. B, No. 2, pp. 125-140, March, 1990.

[62] J. Arrillaga and M. Villablanca, "A Modified Parallel HVDC Converter for 24 Pulse Operation," *IEEE Transactions on Power Delivery.* Vol. 6, No. 1, pp. 231-237, January 1991.

[63] F.X. Wang and T.A. Lipo, "Analysis and Steady-State Behavior of an Optimized AC Converter Machine," *IEEE Transactions on Power Apparatus and Systems.* Vol. PAS-102, No. 8, pp 2734-2742, August 1983.

[64] T.A. Lipo and F.X. Wang, "Design and Performance of a Converter Optimized AC Machine," *IEEE Transactions on Industry Applications.* Vol. IA-20, No. 4, pp. 834-844, July/August 1984.

[65] G.W. McLean, J. Chard, and J. Soltani-Zamani, "Design of Rotor Windings to Improve The Performance of Converter Fed Synchronous Machines," *Third International Conference on Electrical Machines and Drives.* IEE Conference Series, No. 282, pp. 135-139, November 16-18, 1987.

[66] W.D. Jackson, W.E. Feero, W.B. Gish, and G.B. Seikel, "Integration of MHD Plants Into Electric Utility Systems," *IEEE Transactions on Enery Conversion.* Vol. EC-1, No. 3, pp. 26-33, September 1986.

[67] B.K. Johnson and M.C. Chandorkar, "Power Conditioning Interfaces for Medium Power Photovoltaic Systems," *Presentated at: International Conference on Electrical Rotating Machines.* January 15-16, 1992, Bombay, India.

[68] R. E. Hein, et al, *Design of a Photovoltaic Central Station (PV-CS).* SAND 82-7147, -7148, -7149, February 1983, prepared by Martin Marietta Corporation for Sandia National Laboratories.

[69] T.S. Key, F.G. Turnbull, "Power Conditioning Options for Central Station Rated Photovoltaic Power Plants," *1985 Photovoltaic Specialists Conference.* pp. 1380-1325, 1985.

[70] P. Seitz, T.S. Key, and F.R. Goodman, *Photovoltaic Power Condition Status and Needs.* Palo Alto, California, Electric Power Research Institute, EPRI GS-7230, June 1991.

[71] J. Ernst "Wind Energy Farm with Synchronous Generators Operating on a Common DC Link," *First European Conference on Power Electronics and Applications.* Vol. 1, pp. 2.1-2.6, Brussels, Belgium, October 16-18, 1985.

[72] A.J. Shi, J. Thorpe, and R.J. Thomas, "An AC/DC/AC Interface Control Strategy to Improve Wind Energy Economics," *IEEE Transactions on Power Apparatus and Systems.* Vol. 104, No. 12, pp. 3428-3434, December 1985.

[73] R.J. Thomas, A.G. Phadke, and C.Pottle, "Operational Characteristics of a Large Wind-Farm Utility System with a Controllable AC/DC/AC/Interface," *IEEE Transactions on Power Systems.* Vol. 3, No. 1, pp. 220-225, February 1988.

[74] K.S.Tam and P. Kuman, "Application of Superconductive Magnetic Energy Storage in an Asynchronous Link Between Power Systems," *IEEE Transactions on Energy Conversion.* Vol. 5, No. 3, pp. 436-444, September 1990.

[75] K.S.Tam and P. Kuman, "Impact of Superconductive Magnetic Energy Storage on Electric Power Transmission," *IEEE Transactions on Energy Conversion.* Vol. 5, No. 3, pp. 501-511, September 1990.

[76] D.K. Reitan, "A Wind-Powered Asynchrounous AC/DC/AC Converter System," *Proceedings of Wind Energy Conversion Systems Conference and Workshop.* Washington,D.C., June 11-13, 1973.

[77] B.T. Merrit, *An Asynchronous AC/DC/AC Link For Wind Power Application.* Madison, Wisconsin, Ph.D. Thesis, University of Wisconsin-Madison, 1977.

[78] *500 kV HVDC Air Blast Circuit Breaker.* BBC, Brown Boveri, and Cie., Final Report, August 1986, EPRI Report, EL-4520, RP-1507-03.

[79] J.P.Bowles and S. Nilsson, "Several Possible Applications of HVDC Circuit Breakers," *DOE Symposium on Incorporating HVDC Power Transmission into System Planning.* Phoenix, Arizona, pp 425-444, 1980.

[80] W.F. Long, "Development and Testing of HVDC Circuit Breakers," *Presented at Spring Conference of Rocky Mountain Electrical League.* Rapid City, S.D., May 6-8, 1984.

[81] V.D. Pham, Y. Lamoud, T. Verhaege, A. Fevrier, M. Collet, and M. Bekhaled, "Towards the Superconducting Fault Current Limiter," *IEEE Transaction on Power Delivery.* Vol. 6, No. 2, pp. 801-808, April 1991.

[82] T. Ishigohka and N. Sasaki, "Fundamental Test of New Superconducting Fault Current Limiter", *IEEE Transactions on Magnetics.* Vol. 27, No. 2, pp. 2341-2344, March 1991.

[83] S.J. Dale, S.M. Wolf, and T.R. Schneider, *Energy Applications of High Temperature Superconductivity Volume 2: Detailed Assessment.* EPRI, ER-6682, Volume 2, pp. 4-1 → 4-34, November 1990.

[84] W. McMurray, *Feasibility of Gate-Turnoff Thyristors in a High-Voltage Direct Current Transmission System.* EPRI Report EL-5332, Project 2443-5 Final Report, August 1987.

[85] L. Lindberg, *Voltage Source Forced Commutated Converters For High Power Applications.* Master's Thesis, Department of High Power Electronics, Royal Institute Of Technology, Stockholm, Sweden, 1990.

[86] J. Holtz, W. Lotzkat, and K.H. Werner, "A High Power Multitransistor-Inverter Uninterruptable Power Supply System," *IEEE Transactions on Power Electronics.* Vol. 3, No. 3, pp. 278-285, July 1988.

[87] K.S. Tam and R.H. Lasseter, *Artificially Commutated Inverters and Hybrid Inverters for HVDC/Weak AC Systems Interconnection.* Madison, Wisconsin: University of Wisconsin-Madison, Department of Electrical and Computer Engineering, ECE-89-4, June 1985.

[88] K.S. Tam and R.H Lasseter, "Implementation of the Hybrid Inverter for HVDC/Weak AC System Interconnection," *IEEE Transactions on Power Delivery.* Vol PWRD-1, No. 4, pp. 259-268, October 1986.

[89] T.A. Lipo and D.W. Novotny, *Dynamics and Control of AC Drives, Course Notes: ECE 711.* University of Wisconsin-Madison, 1991.

[90] N. Kimura, "Dynamic Behavior of HVDC System Using Forced Commutation Converter," *International Power Electronics Conference.* Vol. 2, pp. 1243-1250, April 2-6, 1990.

[91] Y. Tokiwa, K. Suzuki, T. Kawai, and C. Tanaka, "Application of Self-Commutated Converter Using Si-Thyristor on a HVDC Transmission System," *International Power Electronics Conference.* Vol. 2, pp. 1258-1263, April 2-6, 1990.

[92] B.T. Ooi, X. Wang, and J.W. Dixon, "Voltage Source Type HVDC Transmission System," *International Power Electronics Conference.* Vol. 2, pp. 1251-1257, April 2-6, 1990.

[93] X. Wang and B.T. Ooi, "High Voltage Direct Current Transmission Systems Based on Voltage Source Converters," *1990 Power Electronics Specialists Conference.* pp. 325-332, 1990.

[94] B.T. Ooi and X. Wang, "Boost Type PWM HVDC Transmission System," *IEEE Transactions on Power Delivery,*Vol. 6, No.4, pp.1557–1563, 1991.

[95] Y. Sun and R.W. Menzies, "Harmonic Control and Losses of a Current Source GTO Inverter Supplying Load without AC Generation," *IEEE Transactions on Power Delivery,* 1991.

[96] G. Fregien, "Current Monitering in Power Electronic Equipment with GTO Inverters," *Conference Record IEEE Power Electronics Specialists Conference*, pp.417–424, 1986.

[97] T. Kawabata, T. Asaeda, M. Sigenobu and T. Nakamura, "Protection of Voltage Source Inverters," *Conference Record International Power Electronics Conference (IPEC)*, Tokyo, March 27-31, 1983, pp.882–893.

[98] A. Nabae, I. Takahashi and H. Akagi, "A New Neutral Point Clamped Inverter," *IEEE Transactions on IAS*, Vol. IA-17, No.5, pp.518–523, Sept./Oct. 1981.

[99] Westinghouse Transmission and Distribution Reference Book.

[100] N. Cohn, "Control of Generation and Power Flow on Interconnected Systems," John Wiley and Sons, Inc., New York, 1971.

[101] "Synthetic Electric Utility Systems for Evaluating Advanced Technologies," EPRI Report EM-285, February 1977.

[102] N. Engelman, E. Schreurs and B. Drugge, "Field Test Results for a Multi-Shot 12.47 kV Fault Current Limiter," *IEEE Transactions on Power Delivery*, Vol.6, No.3, pp. 1081–1087, July 1991.

[103] W.C. Huening Jr., "Calculating Short Circuit Currents with Contributions from Induction Motors," *IEEE Transactions on Industry Applications Vol IA-18, No.2 March/April 1982*

[104] Oak Ridge National Laboratory, "Comparision of Costs and Benefits for DC and AC Transmission," J.P. Stovall et al., prepared for the U.S. Department of Energy, February, 1987.

[105] Philadelphia Electric Co., "Evaluation of the Economical and Technological Viability of Various Underground Transmission Systems for Long Feeds to Urban Load Areas,"prepared for the U.S. Department of Energy, Division of Electric Energy Systems, December 1977.

[106] R.H. Lasseter, D.M. Demarest, and F.J. Ellert, "Transient Overvoltages on the Neutral Bus of HVDC Transmission Systems," *Presented at IEEE Summer Power Meeting*, Paper No. A 78 607-4, Los Angeles, California, July 16-21, 1978.

[107] K.J.S. Khunkhun, J.L. Koepfinger, and M.V. Haddad, "Resonant Grounding (Ground Fault Neutralizer) of a Unit Connected Generator," *IEEE Transactions on PAS.*, Vol. PAS-96, No. 2, pp. 550-555, March/April 1977.

[108] The Electricity Council, *Power System Protection, Volume 2.* MacDonald & Co. Ltd, London, 1969.

[109] M.D. Robinson, *Power Plant Electrical Reference Series, Volume 5: Grounding and Lightning Protection.* Electric Power Research Institute, Palo Alto, California, 1987.

[110] K.J.S. Khunkhun, *Power Plant Electrical Reference Series, Volume 8: Station Protection.* Electric Power Research Institute, Palo Alto, California, 1987.

[111] J.L. Blackburn (Ed.), *Applied Protective Relaying.* Westinghouse Electric Corporation, Relay-Instrument Division, Newark, NJ, 1976.

[112] S. Jalali, "Current Sharing for Hybrid Current Source Inverter," University of Wisconsin, December 1991.

ABOUT EPRI

The mission of the Electric Power Research Institute is to discover, develop, and deliver high value technological advances through networking and partnership with the electricity industry.

Funded through annual membership dues from some 700 member utilities, EPRI's work covers a wide range of technologies related to the generation, delivery, and use of electricity, with special attention paid to cost-effectiveness and environmental concerns.

At EPRI's headquarters in Palo Alto, California, more than 350 scientists and engineers manage some 1600 ongoing projects throughout the world. Benefits accrue in the form of products, services, and information for direct application by the electric utility industry and its customers.

EPRI—*Leadership in Electrification through Global Collaboration*

Printed with soya inks on recycled paper (50% recycled fiber, including 10% postconsumer waste) in the United States of America.